UTRECHT MICROPALEONTOLOGICAL BULLETINS

R.J.W. VAN LEEUWEN

SEA-FLOOR DISTRIBUTION AND LATE QUATERNARY FAUNAL PATTERNS OF PLANKTONIC AND BENTHIC FORAMINIFERS IN THE ANGOLA BASIN

38

UTRECHT MICROPALEONTOLOGICAL BULLETINS

Editor C. W. Drooger
Department of Stratigraphy and Paleontology
State University of Utrecht
Budapestlaan 4, Postbus 80.021
3508 TA Utrecht, Netherlands

Sales office U.M.B.: Budapestlaan 4, 3584 CD Utrecht, Netherlands
Postal account: 30 28 890, T. van Schaik, Leusden
Bank account: 55 89 855, Algemene Bank Nederland, T. van Schaik, Leusden

After *prepayment* to the sales office on one of the above accounts, the books will be sent by surface mail without further charges. Orders for these books not directly from the purchaser to the sales office may cause much higher costs to the purchaser.

In the series have been published:

Bull. 1. T. FREUDENTHAL – Stratigraphy of Neogene deposits in the Khania Province, Crete, with special reference to foraminifera of the family Planorbulinidae and the genus *Heterostegina*. 208 p., 15 pl., 33 figs. (1969) *f* 32,–
Bull. 2. J.E. MEULENKAMP – Stratigraphy of Neogene deposits in the Rethymnon Province, Crete, with special reference to the phylogeny of uniserial *Uvigerina* from the Mediterranean region. 172 p., 6 pl., 53 figs. (1969) *f* 29,–
Bull. 3. J. G. VERDENIUS – Neogene stratigraphy of the Western Guadalquivir basin, S. Spain. 109 p., 9 pl., 12 figs. (1970) *f* 28,–
Bull. 4. R. C. TJALSMA – Stratigraphy and foraminifera of the Neogene of the Eastern Guadalquivir basin, S. Spain. 161 p., 16 pl., 28 figs. (1971) *f* 44,–
Bull. 5. C. W. DROOGER, P. MARKS, A. PAPP et al. – Smaller radiate *Nummulites* of northwestern Europe. 137 p., 5 pl., 50 figs. (1971) *f* 37,–
Bull. 6. W. SISSINGH – Late Cenozoic Ostracoda of the South Aegan Island arc. 187 p., 12 pl., 44 figs. (1972) *f* 57,–
Bull. 7. author's edition. F. M. GRADSTEIN – Mediterranean Pliocene *Globorotalia*, a biometrical approach. 128 p., 8 pl., 44 figs. (1974) *f* 39,–
Bull. 8. J. A. BROEKMAN – Sedimentation and paleoecology of Pliocene lagoonal-shallow marine deposits on the island of Rhodos (Greece). 148 p., 7 pl., 9 figs. (1974) *f* 47,–
Bull. 9. D. S. N. RAJU – Study of Indian Miogypsinidae. 148 p., 8 pl., 39 figs. (1974) *f* 38,–
Bull. 10. W. A. VAN WAMEL – Conodont biostratigraphy of the Upper Cambrian and Lower Ordovician of north-western Öland, south-eastern Sweden. 128 p., 8 pl., 25 figs. (1974) *f* 40,–
Bull. 11. W. J. ZACHARIASSE – Planktonic foraminiferal biostratigraphy of the Late Neogene of Crete (Greece). 171 p., 17 pl., 23 figs. (1975) *f* 52,–
Bull. 12. J. T. VAN GORSEL – Evolutionary trends and stratigraphic significance of the Late Cretaceous *Helicorbitoides-Lepidorbitoides* lineage. 100 p., 15 pl., 14 figs. (1975) *f* 37,–
Bull. 13. E. F. J. DE MULDER – Microfauna and sedimentary-tectonic history of the Oligo-Miocene of the Ionian Islands and western Epirus (Greece). 140 p., 4 pl., 47 figs. (1975) *f* 45,–
Bull. 14. R. T. E. SCHÜTTENHELM – History and modes of Miocene carbonate deposition in the interior of the Piedmont Basin, NW Italy. 208 p., 5 pl., 54 figs. (1976) *f* 56,–

(continued on back cover)

SEA-FLOOR DISTRIBUTION AND LATE QUATERNARY FAUNAL PATTERNS OF PLANKTONIC AND BENTHIC FORAMINIFERS IN THE ANGOLA BASIN

R.J.W. VAN LEEUWEN

Printed in the Netherlands by Loonzetterij Abé, Hoogeveen and OMI-GB, Utrecht
April 20, 1989

CONTENTS

ABSTRACT

The distribution of planktonic and benthic foraminifers was examined in some hundred core-tops from the Angola Basin, mainly from depths below 2000 metres.

A number of biofacies have been discriminated in the planktonic faunas on the sea-floor and these show a clear relation with the hydrography of the (near-) surface waters. Species distribution can generally be described satisfactorily in terms of surface-water temperature and fertility. However, if the thermocline reaches into the photic zone, faunas different from those of the surface-mixed layer are found at the top of the thermocline. The faunal differences between the top of the thermocline and the surface-water can not simply be attributed to differences in temperature and fertility. We suppose that some species are specifically linked up with a steep thermal gradient, whereas others can flourish in thermally homogeneous water only.

The deep-sea benthic foraminiferal faunas vary primarily with depth. In addition there appear to be differences between the area along the African continent and areas far away from the continent. Faunal contrasts are found also within these areas. The lateral differences must be due to variations in sediment-related parameters and it is suggested that the amount of organic matter at and in the bottom plays a crucial role. Depth-related changes in the faunas are thought to be controlled by vertical gradients in bottom-water temperature and in the amount of organic matter arriving at the bottom. It should be mentioned that our results do not support the widely accepted idea that there is a relation between *Nuttallides umboniferus* and Antarctic Bottom Water. In a more general sense, we contend that fauna/water-mass relations are actually to be reduced to relations between fauna and bottomwater temperature.

Late Quaternary faunal change was studied in five piston-cores from depths between 2000 and 4000 metres in the marginal area of the north-eastern Angola Basin. A climate stratigraphy was established for the last 150,000 years on the basis of regional changes in the planktonic foraminiferal faunas.

The regional changes in the planktonic faunas are thought to be essentially due to variations in cold-water advection by the Benguela Current and in intensity of equatorial divergence processes. These two factors do not only influence the temperature of the surface-water, but also control the degree to which the photic layer is thermally stratified. It is concluded that the primary production of the photic layer was much higher during cold than during warm climatic stages. The influence of the Benguela Current has been stronger during cold than during warm climatic phases and reached a maximum in isotope stage 4.

Equatorial divergence was intense during isotope stages 2 and 3 and weak during stage 4, substage 5e and periods of deglaciation. It is suggested that intensification of the Benguela Current and intensification of equatorial divergence have generally been out of phase. Changes in wind direction could offer an explanation for this inverse relation.

Consistent differences between warm and cold climatic stages show up also in the benthic faunas. In most cores, distinction must be made between an autochthonous and an allochthonous faunal signal. At depths beteen 2700 and 3500 metres in the area north of the Zaire deep-sea fan, the contribution of allochthonous elements reaches maxima in cold climatic stages. This suggests increased down-slope transport during periods of low sea-level stands.

Climate related changes in the frequencies of autochthonous species are recognized at all sites and are to be ascribed primarily to variation in the amount of organic matter at and in the bottom. The amount of organic matter must have been larger in cold than in warm climatic intervals. This is to be attributed mainly to increased primary production of the surface-waters during cold climatic periods. It is further suggested that bottom-water temperatures have varied in the Angola Basin over the past 150,000 years. Variation in bottom-water temperature seems only partially linked up with climatic change. At great depth, bottom waters were colder than today during isotope stages 2 and 4 and the middle of stage 5.

Interpretation of glacial/interglacial differences in benthic deep-sea faunas reported in the literature for the NW Atlantic Ocean and Southern Ocean, indicates that these differences may also be due to variation in the organic matter content of the sediments. Again, increased primary production during cold climatic periods seems likely.

Chapter I

INTRODUCTION

I.1. PURPOSE OF THE INVESTIGATION

It is still a major challenge in earth science to unravel the climatic history of the Quaternary and to understand the interaction between climatic change and oceanic circulation. Over the years, foraminiferal research has produced tools that are widely used to portray changes in the oceanic environment. Planktonic foraminiferal analysis has contributed considerably to our knowledge of variation in the temperature and circulation of surface waters during the Late Quaternary (e.g. Bé et al., 1976; Gardner and Hays, 1976; Ruddiman and McIntyre, 1976). The introduction of the water-mass concept in benthic foraminiferal ecology (Streeter, 1973; Schnitker, 1974) stimulated to employ deep-sea benthic foraminifers as recorders of changes in deep water circulation (e.g. Streeter and Shackleton, 1979; Corliss, 1983a).

The main purpose of the present investigation is to examine the impact of climatic change during the past 150,000 years on the deep water environment in the Angola Basin. In a first attempt to tackle this problem, we studied benthic foraminiferal faunas from a number of piston cores collected in the late nineteen seventies by the Netherlands Institute for Sea Research (N.I.O.Z.) from the area of the Zaire deep-sea fan (Zachariasse et al., 1984). Carbonate dissolution had, unfortunately, largely obliterated the foraminiferal record and we therefore incorporated cores from the continental margin near the Guinea Rise. The eventual selection consists of five piston-cores, which come from depths of between 2000 and 4000 metres.

Because the cores are located in an area, where surface-water conditions have changed drastically during the Late Quaternary (e.g. Gardner and Hays, 1976), we included planktonic foraminifers in our study to portray variation in the surface-water hydrography in the past. The stratigraphic framework of the cores is based on systematic changes in the planktonic foraminiferal faunas.

A thorough understanding of the factors controlling the distribution of foraminifers in the present-day ocean is a prerequisite for interpreting the Late Quaternary faunal record. Our knowledge of the distribution of benthic foraminifers in the modern deep-sea is very inadequate and data were not available for the Angola Basin. Distribution patterns of planktonic foraminifers are better known, but the complex hydrography in the region under considera-

tion hampered interpretation of the Late Quaternary record. We, therefore, analysed a great number of core-top samples to design a conceptual framework for interpreting down core changes in the faunas.

I.2. METHODS

Provenance of samples and sampling procedure

Samples were obtained from deep-sea cores stored in the repositories of the Netherlands Institute for Sea Reasearch (N.I.O.Z.), the Lamont-Doherty Geological Observatory, the Woods Hole Oceanographic Institution, and the Centre Océanologique de Bretagne.

Tops of piston and trigger cores were used to analyse the distribution of foraminiferal species on the ocean floor. Samples were usually taken from the uppermost three cm, but sometimes we sampled from the 0 to 5 cm interval to gather sufficient material.

The five piston cores used for downcore studies were sampled at more or less regularly spaced intervals and usually samples represent two to three centimetre-thick sections. Sample position is possibly inaccurate in RC and VM cores, because it was often uncertain whether the top of the core was still present; shrinkage by desiccation adds to the inaccuracy.

Sample processing and counting procedure

Samples were freeze-dried and subsequently weighed. If sufficient material was available, approximately one gram of sediment was kept aside for measuring the calcium carbonate content. The remainder of the sediment was washed over a set of sieves (595, 63 and 37 μm) and the residues were oven-dried.

For the analysis of benthic foraminifers, we chose to count both the 63-595 μm (total) fraction and the 150-595 μm (large-size) fraction. Different size-fractions are in use in foraminiferal research, and we selected the 150-595 μm fraction because it is most commonly used in deep-sea studies. The total fraction, on the contrary, is seldom investigated, mainly because identification of small-sized species and specimens is difficult. We included the total fraction to get insight in the distribution of small-sized species. Planktonic foraminiferal counts were made only on the large-size fraction.

We aimed to count at least one hundred specimens in each category per sample including broken specimens if more than half of the test was preserved.

We repeatedly subdivided the 63-595 μm fraction using an Otto microsplitter. Subsequently, a small split was strewn over a modified sieve with a mesh-

opening of 150 μm placed on top of a picking tray. After shaking, we started to collect all foraminifers from the sieve (150-595 μm fraction) and all benthic foraminifers from the picking tray (63-150 μm fraction).

The first split was usually sufficiently large to provide the minimum number of planktonic foraminifers, but the procedure had to be repeated until one hundred benthic foraminifers were obtained for both the 150-595 μm fraction and the 150-595 plus 63-150 μm fractions. Specimens were mounted on a Chapman slide, identified and counted.

The proportion of planktonics per total foraminifers in the 150-595 μm fraction, i.e. P/P+B, is based on the split used to obtain the minimum number of specimens in one of the two categories.

In addition, we noted the state of preservation of the foraminifers (fragmentation, etching) and the occurrence of other sediment grains, such as quartz, pyrite, glauconite, pteropods and siliceous fossils.

Mathematical analyses

R-mode analyses were performed on selected quantitative data by using computer program BALANC developed by M.M. Drooger (1982). BALANC calculates correlation coefficients on the basis of the free open covariances model. The correlations were subsequently subjected to DENDRO analysis, a clustering technique based on the unweighted pair group method.

In addition, R-mode principal component analyses were carried out (PCA program; Davis, 1973). In contrast to BALANC, this program does not correct for the closed-sum effect. We decided to use a standardized version in order to give each faunal category equal weight in the analysis (cf. M.M. Drooger, 1982).

Carbonate analysis

The calcium content of the sediment was taken as a measure of the amount of calcium carbonate. Calcium was measured by complexometric titration with EGTA, using a Corning Calcium Analyser. Analyses were performed at the Netherlands Institute for Sea Research, following standard procedures.

Species concept

The species concept used in the present study is basically an assemblage concept (Zachariasse, 1975; Van der Zwaan, 1982). The assemblage concept is essentially a morphological interpretation of the population structure of a species in a biological sense (Mayr, 1976).

A species is defined as a morphologically continuous complex of 'populations', i.e. the assemblages, which are morphologically homogeneous groups of specimens within individual samples.

So defined, a species may grow into a unit which covers a large morphological range and comprises several rather ideal morphologies, the morphotypes. Because we generally considered it disadvantageous to neglect variation in polytypic species, attempts were made to discriminate between morphotypes.

In quantitative research, there are different ways to cope with the problems set by morphological variation in polytypic species. The least reliable procedure is to count morphotypes as separate units, i.e. in a rather typological manner. A more objective approach is to name assemblages after the dominating morphotype. We actually followed both procedures.

Morphotypes should be named on some formal of informal intraspecific level. Our determinations are based on bibliographic reference only, and most of the morphotypes, particularly among the benthic foraminifers, are even in the modern literature identified as different species. A reason for the common use of only binomial taxonomy, is probably that many workers are not confronted with the problem of polytypic variation, because the scope of their studies is geographically limited. Morphological variability is, therefore, generally low and the problem of polytypic variation seldom arises. As a consequence there are far more polytypic species than suggested in the literature. We are well aware that some of the taxa which are given species status in the present study may actually be only morphotypes within a single species. This constraint holds in particular for benthic foraminifers that are restricted to depths of less than 2500 metres (e.g. costate *Bulimina*), because these depths are poorly covered in our material.

An additional problem is that there appears to be a disturbing degree of provincialism in benthic foraminiferal taxonomy. Instead of reviewing the complete literature, we confined ourselves essentially to names of common use in the Atlantic region.

In two cases we refrained from a strict approach and labelled morphotypes as if they were species, viz. *Neogloboquadrina dutertrei* versus *N. pachyderma* and *Uvigerina hispida* versus *U. peregrina* s.l.

I.3. ACKNOWLEDGEMENTS

I would like to express my special gratitude to W.J. Zachariasse for his unflagging interest, his critical reading of the various versions of the manuscript and for the many stimulating discussions.

I am indebted to C.W. Drooger for his comments on the manuscript. Thanks

are extended to A.J. van Bennekom and G.J. van der Zwaan, who read earlier versions of chapters II and IV, respectively.

I am grateful to many workers from the Netherlands Institute for Sea Research (N.I.O.Z.) for their assistance and cooperation and especially to A.J. van Bennekom and J.H.F. Jansen.

I wish to thank T. van Hinte and P. Hoonhout for drafting the figures, W.A. den Hartog and J. Luteyn for making the SEM photographs and the plates, and G.C. Ittmann and G.J. van 't Veld for the preparation of the samples.

Mrs. S.M. McNab is acknowledged for reading the English text of chapter II.

Sample material was provided by the Netherlands Institute for Sea Research, the Centre Océanologique de Bretagne, the Lamont-Doherty Geological Observatory and the Woods Hole Oceanographic Institution.

This research was financially supported by the Netherlands Organization for the Advancement of Pure Research (Z.W.O.). I am indebted to the Director of the Geological Survey of The Netherlands (R.G.D.) for giving me the opportunity to finish my thesis.

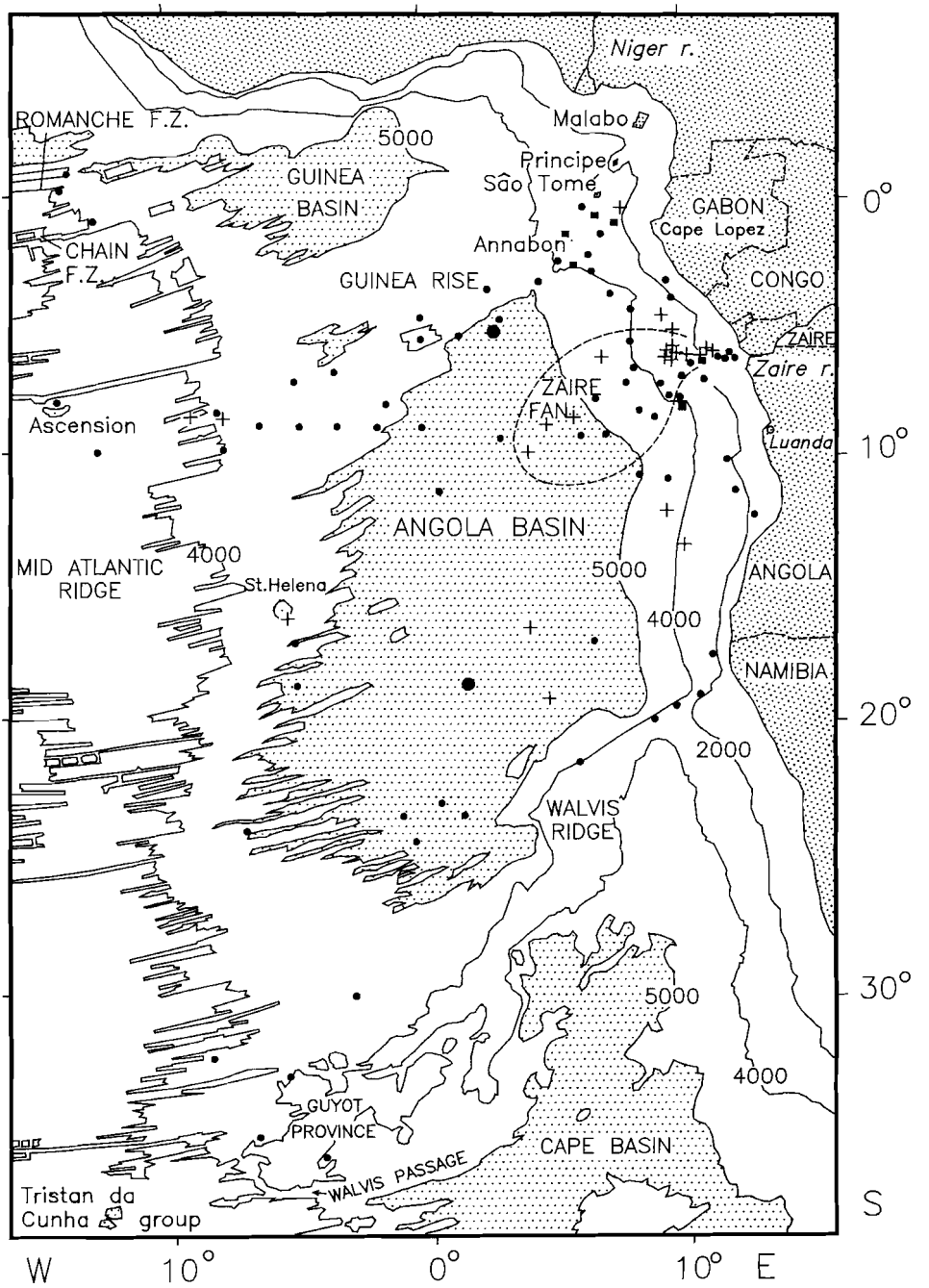

Fig. 1. Physiography of the eastern South Atlantic and location of the cores (■) and tops of cores (.) studied; (+) indicate core-tops that were excluded from the faunal analyses. The 2000, 4000 isobaths are shown and the dotted areas are deeper than 5000 m. Double-sized dots indicate two samples studied from the same locality.

Chapter II

INTRODUCTION TO THE AREA

II.1. PHYSIOGRAPHIC SETTING

The eastern South Atlantic has three basins; these are from north to south the Guinea Basin, the Angola Basin and the Cape Basin. The Angola Basin, which is the deepest and largest, covers most of the study area (fig. 1). It is bounded to the north by the Guinea Rise, to the west by the Mid Atlantic Ridge and to the south by the Walvis Ridge and its eastern edge is the African continent.

The continental shelf adjoining the Angola Basin is generally very narrow. In the south, off Angola it is locally only a few kilometres wide, but north of Luanda it broadens steadily and reaches a maximum width of about 80 kilometres near the mouth of the river Zaire. North of the river, off Congo and Gabon, the shelf is about 50 kilometres wide and the shelf-break is situated at a depth of 120-140 metres (Giresse et al., 1981).

Off the mouth of the river Zaire, the shelf is dissected by the upper part of the Zaire submarine canyon, which is approximately 425 metres deep at the river-mouth. The shelf-channel extends into the estuary and shallows to a depth of 100 metres 30 kilometres inland. The canyon was studied by Heezen et al. (1964) and by Shepard and Emery (1973). Down to a depth of 3600 metres it is distinctly V-shaped and it cuts deeply into the continental slope. The deepest incision is made landwards of a belt of salt diapirs, where the canyon floor is between 400 and 1400 metres below sea bottom. The diapir field extends at least between 13.5°S and 5°S (Emery, 1972) and probably continues northward to Cape Lopez at about 1°S (Bornhold, 1973). It occupies the continental margin between 800 and 3000 metres and produces submarine relief of up to several hundreds of metres. To the west it is marked by the rather steep Angola escarpment.

The deeply incised canyon ends on the Zaire deep-sea fan or Congo Cone, where it continues as a relatively shallow deep-ocean channel. The channel is mainly defined by natural levees and has several ramifications. The deep-sea fan is the most prominent feature of the continental rise and extends from the foot of the continental slope to a depth of more than 5000 metres.

Low hill-like structures, interpreted as relict continental rise hills (Bornhold, 1973), are found in the south-eastern part of the Angola Basin between 4000 and 5000 metres. The deepest part of the basin (5200-6000 m) consists of an essentially flat area, the Angola abyssal plain.

Towards the west the abyssal plain gives way to the rugged topography of the Mid Atlantic Ridge and the adjoining abyssal hills. A few volcanic islands are associated with the ridge: St Helena at approximately 16°S, 5.75°W, the Tristan da Cunha group in the extreme south-west of the area and Ascension, which is actually on the western side of the ridge. Among the numerous fracture zones that cross the Mid Atlantic Ridge, only the Romanche and Chain zones deserve special attention. These zones are located in the northwest of the Guinea Basin and form major gaps in the ridge connecting the abyssal depths of the eastern South Atlantic with those of the western basins.

The Guinea Rise separates the Angola Basin from the Guinea Basin to the north. It is an aseismic ridge, which rises as a broad swell to a depth of approximately 4400 metres. A number of sea-mounts rise from the Guinea Rise and at its eastern end are the volcanic islands of the Cameroon chain (Annabon, Sâo Tomé, Principe, and Malabo).

The southern limit of the Angola Basin is marked by the Walvis Ridge and the Guyot Province. The Walvis Ridge is an approximately NNE-SSW trending aseismic ridge, which varies in width between 50 and 200 kilometres. It extends as a continuous high from the African continent to 1.5°E and 33.5°S. The top is virtually nowhere at a depth of more than 3000 metres and locally at less than 1000 metres. The northern flank is markedly steep where it joins the African continent.

To the south-west the Walvis Ridge joins with the Guyot Province, which is characterized by many flat-topped sea-mounts with rather deep passages in between. The Walvis Passage (about 4000 m depth; Connary and Ewing, 1974) between the Mid Atlantic Ridge and the Guyot Province is the deepest connection between the Cape Basin and the Angola Basin.

II.2. SURFACE-WATER CIRCULATION

The surface waters of the Angola Basin lie almost entirely in the tropical and subtropical region and the current system is dominated by the circulation of the great anticyclonic gyre (fig. 2). The Subtropical Convergence (STC) meets the Angola Basin in the extreme south-west at about 37°S (Van Bennekom and Berger, 1984). The convergence zone marks the hydrographical boundary between the subtropical South Atlantic and the temperate parts of the Southern Ocean. As a consequence, there is a fairly large temperature difference between the surface waters north and south of the convergence (about 4°C, Tchernia, 1980). The circulation is determined by the West Wind Drift (WWD) and the current direction is towards the east and north-east.

Approaching the African continent, the north-easterly components of the

WWD join with waters brought south-west from the Indian Ocean by the Agulhas Current. Under the influence of the prevailing Trade Winds, the water becomes directed towards the north and the anticyclonic circulation continues in the Benguela Current (BC), which skirts the coast of south-western Africa. The width of the current, initially about 180 kilometres, increases toward the north, as the main branch gradually leaves the coast between 23° and 20°S transporting cool waters toward the (north-)west (Bornhold, 1973). Coastal branches reach into the Angola Basin and continue at least to 13°S (Van Bennekom and Berger, 1984). The influence of the BC is clearly recognized on

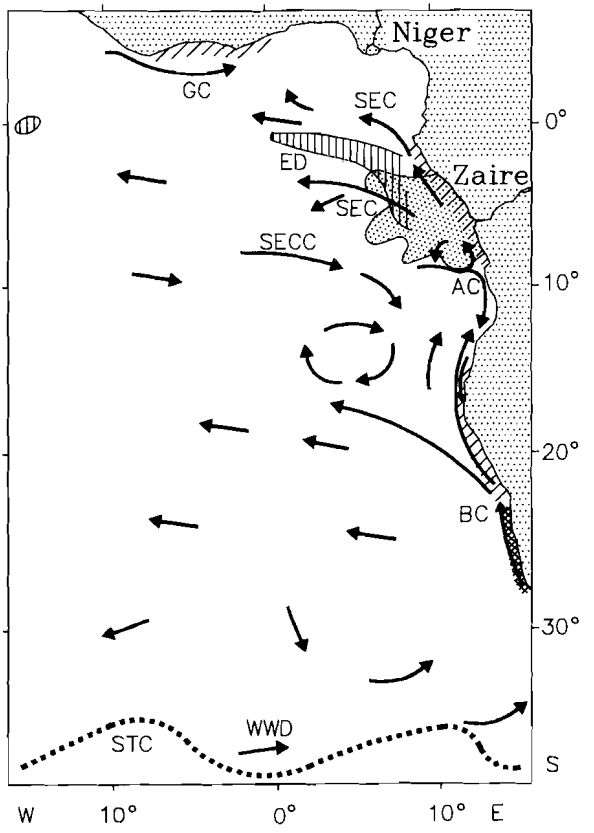

Fig. 2. Main elements of the surface-water circulation in the eastern South Atlantic (for explanation see the text), and regions of seasonal (diagonally hatched) and year-round (double hatched) coastal upwelling. The figure is based on Moroshkin et al. (1972), Bornhold (1973), Tchernia (1980), Herbland et al. (1983), and Van Bennekom and Berger (1984). The region of highest production (80 mgC/m^2.h.) in the Equatorial Divergence (August, 1963; Voituriez and Herbland, 1981) is indicated by vertical hatching and the dotted area delineates the Zaire plume (Van Bennekom and Berger, 1984).

maps that show the distribution of the surface-water temperature (Mazeika, 1968; Mellor et al., 1982). Essentially, the temperature fields are zonally arranged, with maximum values just north of the equator (mean February temperature over 28°C). Minimum values are found south of the STC, where mean summer temperatures are about 14°C (Tchernia, 1980). However, along the coast of southern Africa the isotherms are N-S oriented and annual means as low as 14°C have been registered. The cooling influence of the Benguela Current is intensified by coastal upwelling, which brings even colder water to the surface (10-16°C; Embley and Morley, 1980).

North of 15°S the surface circulation is less simple. Hagen et al. (1981) found that the Benguela Current penetrates along the coast northward to 10°S, but there seems to be no consensus about its continuation further to the north (Van Bennekom and Berger, 1984). The surface circulation is complex in this area, because the system or equatorial countercurrents interacts with the main currents of the subtropical gyre. This results in a complicated pattern with several gyres, fronts and domes, particularly to the west and the south of the river Zaire (Bornhold, 1973; Van Bennekom and Berger, 1984).

Away from the continent, the South Equatorial Counter Current (SECC) transports high salinity waters in a (south-) easterly direction within a broad zone between 5°S and 14°S. In the north the eastward current is detected only in the subsurface, but it reaches the surface at about 10°S. The SECC can be considered as the northern boundary of a quasi stationary cyclonic circulation (Moroshkin et al., 1970), which is centred at approximately 14°S, 4°E. The southern and south-western segments of the cyclonic gyre are formed by the offshore branch of the BC. The north-western boundary has not been defined and is presumably situated west of the area studied by Moroshkin et al. (1970), i.e. west of 4°W. The SECC splits into two branches towards the African coast and the southern branch continues as the Angola Current (AC). The AC marks the eastern boundary of the cyclonic circulation and flows along the coast of Angola south to approximately 16°S (Moroshkin et al., 1970). The northern branch mixes with extensions of the BC (Van Bennekom and Berger, 1984) and forms a small anticyclonic gyre just south of the Zaire plume at 7.5°S, 9.5°E (Moroshkin et al., 1970).

North of the river outflow, the circulation pattern is dominated by the South Equatorial Current (SEC), which runs westward toward South America and represents the northern segment of the great gyre. The SEC is divided into two branches, which are separated by the Equatorial Divergence (ED). North of the Angola Basin, the northern offshoot crosses the equator and continues westward on the northern hemisphere. This current is bounded to the north by the western extension of the North Equatorial Counter Current, here called

the Guinea Current (GC). The southern part meets the SECC at about 10°S in the Tropical Convergence zone.

The third component of the system of equatorial countercurrents, the Equatorial Under Current or Lomonosov Current, transports water towards the east, but mainly in the subsurface. It is usually associated with a salinity maximum and at about 1°S and 4°W its core is at a depth between 50 and 70 metres (Voituriez et al., 1982). Near the African continent, the EUC splits into two parts. The southern branch contributes to the complexity of the circulation in and south of the Zaire plume area. As extensively discussed by Van Bennekom and Berger (1984) the shallow subsurface waters of the plume area can be regarded as a mixture of BC, SECC and EUC waters.

II.3. THE RIVER ZAIRE AND THE SURFACE SALINITY DISTRIBUTION

The river Zaire ranks second among the world's rivers in terms of discharge. The influence of the outflowing fresh water on the surface of the adjacent ocean is accordingly great. The impact was discussed in detail by Eisma and Van Bennekom (1978) and Van Bennekom and Berger (1984). Near the river-mouth a narrow low salinity plume is formed, which broadens offshore as the ejected water loses momentum. Because of the narrowness the residence time of the fresh water in the plume area is very short. The thickness of the low salinity layer varies with the season and increasses towards the west from 5-10 metres near the mouth to 15-30 metres offshore.

Out from the river-mouth salinities of less than 25 per mil prevail over the shelf and shelf-break area. Here, the plume is oriented to WNW, but offshore its main direction changes seasonally under the influence of the prevailing winds. The orientation of the plume generally varies between W and WNW, but was repeatedly found to be towards the southwest during February and March. In front of the river the salinity is usually below 33 per mil up to about 8°E. The plume has its maximum extension in the warm season when waters below 35 per mil are found westward to 5°E and southward to 11°S. During this period, the plume cannot be clearly delineated to the north, because a continuous low salinity surface (less than about 33‰) extends northward along the coast passing into the Gulf of Biafra, which is influenced by the river Niger. In November the northern limit of the plume probably does not extend far north of 3°S.

Mellor et al. (1982) compiled the salinity data for the entire Atlantic Ocean into a map with year-averaged isohalines. West of the plume the salinity rises to about 35.5 per mil at longitude 0° and north of about 15°S the isohalines trend approximately NW-SE. South of 15°S in the land distant part of the

Angola Basin, the isohalines trend NE-SW. The highest salinity (36.5-36.75‰) is found west of about 20°S towards the centre of the subtropical gyre, which is in the western South Atlantic. Near the African continent the salinity is lower, and the Benguela Current is characterized by salinities of approximately 35.4 per mil (Van Bennekom and Berger, 1984).

II.4. PRIMARY PRODUCTION

The surface waters in the eastern South Atlantic are characterized by large differences in fertility, as already shown by Steemann-Nielsen and Aabye-Jensen (1957), who were the first to measure the primary production in the area. The most oligotrophic waters are found towards the centre of the subtropical gyre, whereas areas of high production are situated in the equatorial region and along the African coast.

The tropical region, i.e. the area north of 15°S, has been relatively well studied and the primary production of the offshore waters was systematically mapped during the Equalant expeditions (Corcoran and Mahnken, 1969). Subsequent research on the primary production in the equatorial eastern South Atlantic was performed by Herbland, Voituriez and their co-workers, whose principal results are summarized in Herbland et al. (1983). Their approach is based on the close relationship between primary production and the hydrographic structure of the euphotic zone, which was poorly understood by the earlier workers. In the socalled 'Typical Tropical Situation' (TTS) two layers can be distinguished in the euphotic zone. The upper layer consists of warm water, which is oxygen (super)saturated, nitrate-depleted and low in chlorophyll-a. Production here is low and is essentially governed by recycling of nutrients. In the deeper layer a chlorophyll-a maximum is found. The chlorophyll-a maximum approximately coincides with the top of the nitracline and the depth of the oxycline (Herbland and Voituriez, 1979). The primary production in this deeper layer is called 'new' production, because it uses principally mineral nitrogen originating in deeper water. The new production determines the primary production of the water-column to a large extent. Because the production in the deep maximum is light-limited, the production of the water-column is inversely related to the depth of the nitraclines. When vertical advection is negligible, the depth of the nitracline depends on the depth of the thermocline and the primary production of the water-column is, therefore, high in areas with a shallow mixed layer (Herbland and Voituriez, 1979).

Voituriez and Herbland (1981) estimated the primary production in the offshore tropical region on the basis of oxygen data. Data on the production in

the region of the Zaire plume were summarized by Van Bennekom and Berger (1984). Three centres of high production stand out in the tropical part of the Angola Basin: the Equatorial Divergence, the area of the Zaire plume and the region south of the rivermouth.

During the warm season (January-March), the TTS is established in the area of the Equatorial Divergence. Cool deeper water rises into the euphotic zone forming a subsurface ridge parallel to the equator. The ridge is centred at 2-3°S and can be recognized westward to longitude 20°W. In winter the TTS does not come into existence, because upwelling brings cool water directly to the surface causing a seasonal temperature difference of about 8°C. As a result the primary production is elevated throughout the year over a broad zone, which at longitude 4°W extends between the equator and 5°S. The fertility decreases within this zone from east to west (at least between 6°E and 9°W; Herbland et al., 1983), which parallels an increase in the depth of the thermocline (see also Van Bennekom and Berger, 1984). South of the Equatorial Divergence productivity falls rapidly and oligotrophic conditions prevail away from the continent. Much lower production is also reached just north of the equator, but productivity is high in the coastal waters off Ghana and Ivory Coast where seasonal upwelling occurs.

Voituriez and Herbland (1981) showed that productivity increases towards the area of the Zaire outflow. The plume area is marked by a very shallow thermocline (Van Bennekom and Berger, 1984). In the warm season the mixed layer is less than 20 metres deep between the rivermouth and 5°E and its thickness increases gradually to the west. River induced upwelling brings cool and nutrient rich water to the surface near the river-mouth (Eisma and Van Bennekom, 1978). This process seems to decrease in intensity towards the west, where rising waters do not extend to the surface. The river contributes in another way to the high fertility. The direct input of nutrients produces a distinct surficial chlorophyll-a maximum between 150 and 250 km off the river-mouth (Cadée, 1978; 1984). Directly in front of the river, however, the in situ production is low, probably due to the high turbidity of the surface water (Cadée, 1978). Locally, the situation is even more complex, and cold season upwelling was observed off Pointe Noire, just north of the river-mouth (Van Bennekom et al., 1978; Cadée, 1984). According to Herbland et al. (1983), upwelling might be active on a wider scale along the coasts of Gabon, Congo, and Angola.

Several relatively productive areas have been reported south of the river-plume, in an area marked by a complicated surface circulation (Van Bennekom and Berger, 1984). Most prominent is the Angola Dome, which is centred at approximately 9°E, 10°S. The cyclonic circulation of the South Equatorial

Counter Current causes updoming of deeper waters, which reach into the euphotic zone during the warm season (Herbland et al., 1983).

For the region south of 15°S there is less information on the primary productioin, but an extremely productive zone occurs along the African continent just south of the Angola Basin. Here, a permanent coastal upwelling regime is associated with the Benguela Current. The upwelling rate decreases distinctly north of latitude 23°S (Bornhold, 1973), but seasonal upwelling continues up to 15°S (Hagen et al., 1981). After its main branch has left the coast, the BC seems to remain fairly productive but it is not known how far westward the high production is maintained. From zooplankton biomass data, Steemann-Nielsen and Aabye-Jensen (1957) extrapolated that a bulge of elevated production, centred at 20 S, extends from the BC upwelling area westward to 2°W, but these estimates have been regarded as very inaccurate (Herbland et al., 1983). Dufour and Stretta (1973) found that during November 1971 the primary production was high in the surface waters between 13° and 18°S at 4°W, where the water is derived from the BC. They, however, remarked that it is not clear whether this is a permanent feature. Because of the many uncertainties, we rely on the map of global production compiled by Koblentz-Mishke et al. (1970). The map shows that the high production patch associated with the main branch of the BC does not extend further westward than 2°E; with the exception of that area, the offshore southern part of the eastern South Atlantic is an oligotrophic region.

II.5. HYDROGRAPHY OF THE DEEPER WATERS

The surface waters with their variable characteristics are separated from the more uniform realm of the deep-sea by the thermoclinic layer. The deeper water of this layer is known as the South Atlantic Central Water (Tchernia, 1980). It is thought to be formed by winter cooling of the surface waters in and north of the Subtropical Convergence. The central water is characterized by a quasi linear T-S relation joining T = 6°C, S = 34.5‰ and T = 19°C, S = 36.0‰.

The deep water hydrography of the eastern South Atlantic (fig. 3) was described by Van Bennekom and Berger (1984). Below the South Atlantic Central Water is the Antarctic Intermediate Water (AAIW), which is typified by a salinity minimum. Near the STC, in the extreme south-west of the Angola Basin, this minimum is situated at a depth of 1000 metres (T = 3°C, S = 34.3‰). Further north of its source area at the Antarctic Convergence (about 50°S), AAIW mixes with the overlying central water. As a result both temperature and salinity increase and the salinity minimum gradually shallows (see also Tchernia, 1980). In the area of the Zaire fan the minimum salinity is 34.49 per mil at a depth of 730 metres.

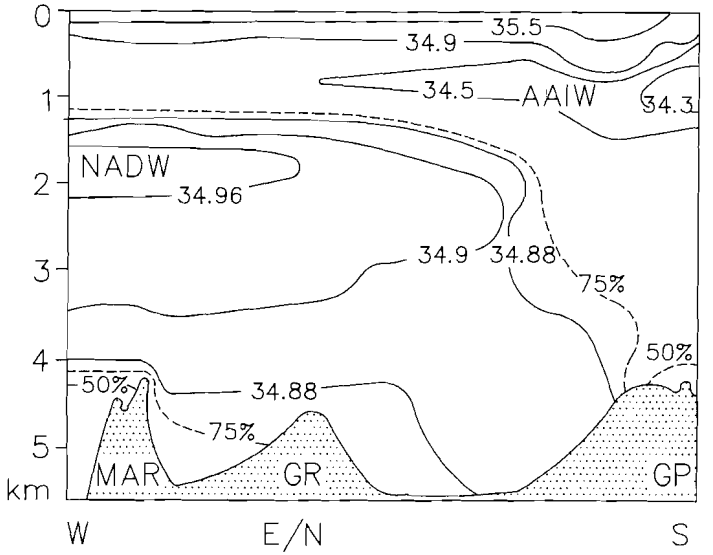

Fig. 3. Salinity section through the Guinea and Angola basins, isolines of 75 % and 50 % North Atlantic Deep Water (NADW) are shown (after Van Bennekom and Berger, 1984). The section runs W-E just north of the equator from the Romanche Fracture Zone to approximately 0° Longitude in the Guinea Basin and from there southward along the axis of the Angola Basin to the Walvis Passage. The following abbreviations are used Mid Atlantic Ridge (MAR), Guinea Rise (GR), Guyot Province (GP), and Antarctic Intermediate water (AAIW).

The AAIW is found on top of the North Atlantic Deep Water (NADW), a complex water-mass composed of several water types. In the entire Atlantic Ocean the NADW is identified by a salinity maximum and its potential temperature (θ) ranges from approximately 2° to 4°C. The major source lies in the northern end of the West Atlantic, where dense waters are formed by the mixing of three different northerly water types (Broecker and Takahashi, 1980). On its way to the south, NADW mixes with the water-masses above and below. NADW enters the eastern South Atlantic from the west through the Romanche Fracture Zone. At the entrance the salinity maximum is found at a depth of 1750 metres (θ = 3.7°C; S = 34,975‰; Tchernia, 1980).

The salinity maximum erodes and deepens towards the south and over the Zaire deep-sea fan the salinity maximum (S = 34.94‰) is found at a depth of 2100 metres (Van Bennekom and Berger, 1984). Actually, the water below 1500 metres is predominantly composed of NADW in the entire eastern South Atlantic. This is in remarkable contrast to the hydrography of the western basins, where an even colder water-mass is present at depths of more than 4000 metres. This water-mass, the Antarctic Bottom Water (AABW), has its major

source in the Weddell Sea from where it spreads northward into the world ocean. In the Atlantic, the main path of AABW is through the western basins. Around latitude 32°S and at a depth of 4000 metres it is characterized by a potential temperature of 0.1°C and a salinity of 34.67‰ (Broecker et al., 1976).

Spreading of AABW into the eastern basins mainly takes place through the Romanche Fracture Zone (Mantyla and Reid, 1983; Van Bennekom and Berger, 1984). The influence of AABW is reflected in lower temperatures, lower salinities, and by a much higher silica content. However, the salinity indicates that only slightly more than 25 per cent of the bottom water of the deepest Guinea Basin is of AABW origin (θ = 1.7°C, S = 34.86‰). The bottom waters of the Angola Basin show little variation in salinity (34.872-34.883‰) and potential temperature (1.89-2°C). From salinity data Van Bennekom and Berger (1984) calculated that between 18 and 22 per cent of the bottom water in this basin is of Antarctic origin.

In the southern part of the Angola Basin the influx of AABW is greatly hindered by the presence of the Walvis Ridge and the adjoining Guyot seamount system. A minor flux, however, passes through the Walvis Passage, where below a depth of 4000 metres the bottom water consists of more than fifty per cent AABW. According to Van Bennekom and Berger (1984), between 25° and 20°S these northward flowing waters meet the AABW that has entered from the Romanche Fracture Zone.

II.6. DISSOLVED OXYGEN DISTRIBUTION

In contrast to the surface layers, which are saturated or slightly supersaturated with oxygen, the deeper waters are oxygen deficient. A pronounced oxygen minimum zone has developed at intermediate depth in the eastern part of the Angola Basin. Here, the lowest oxygen concentrations are found for the entire Atlantic Ocean (Bubnov, 1972; Demaison and Moore, 1980).

Bubnov (op. cit.) described the oxygen distribution in the part of the eastern South Atlantic between 5° and 23°S and east of 5°W, and recognized two distinct minimum layers. The main oxygen minimum layer is located at a depth of between 300 and 600 metres and reaches its shallowest depth in the coastal region. The lowest oxygen concentrations (less than 33 μmol/l) are found between the coastal upwelling area off south-western Africa and approximately 8°S . In the southern part of this area these low values are restricted to the near-coastal waters, but north of 18°S the severely oxygen-depleted waters extend at least to 10°E. The oxygen content generally remains below 67 μmol per litre, but higher concentrations are observed in the west and southwest of the area studied by Bubnov.

A second shallower oxygen minimum layer, is situated in the subsurface waters between 75 and 200 metres. The oxygen concentrations are in general comparable to those of the deeper minimum. The lowest concentrations (less than 22 μmol/l) are found in the coastal upwelling area associated with the Benguela Current, and here the shallow oxygen minimum layer actually merges with the deeper one. The shallow oxygen minimum layer broadens in a north-westerly direction, while the oxygen content steadily increases. Although this layer has a more limited extent than the deeper one, it extends far into the Angola Basin, and oxygen concentrations of less than 67 μmol per litre are observed as far north as 10°S.

Below the main oxygen minimum layer, oxygen concentration gradually increases, but the deep waters tend to have lower oxygen concentrations in the east than in the west of the Angola Basin (Bubnov, 1972). The east-west contrast is also apparent in the bottom waters at depths of more than 3500 metres. According to Mantyla and Reid (1983), the oxygen content of the bottom water is less than 240 μmol/litre in the eastern Angola Basin. Higher values are found towards the west and especially towards the northwest of the Angola Basin. The bottom waters of the eastern South Atlantic have the highest oxygen concentrations near the Romanche Fracture Zone (about 260 μmol/litre)

Van Bennekom and Berger (1984) studied the oxygen distribution over the Zaire deep-sea fan in a section extending westward to 2°E. Offshore, a major oxygen minimum layer is situated at a depth of between 300 and 400 metres with concentrations of less than 50 μmol per litre. These values are slightly lower than those presented by Bubnov (1972). The oxygen minimum intensifies towards the Zaire canyon, and in the upper part of the canyon almost completely anoxic conditions prevail at the bottom (down to 0.5 μmol/litre). The extremely low concentrations are probably caused by in situ mineralization of river-borne organic matter (Cadée, 1984). Down to a depth of 1000 metres the bottom waters of the canyon have clearly lower oxygen concentrations than the deep waters to the west (Van Bennekom et al., 1978). Van Bennekom and Berger (1984) found little variation in the oxygen content of the waters below 2000 metres. In the western part of the section, the oxygen concentration usually varies between 230 and 240 μmol/litre. The bottom waters of the canyon and the deep-sea fan locally contain less than 220 μmol/litre; these low values they also ascribe to in situ processes.

II.7. SEDIMENT DISTRIBUTION

The sediments along the African continental margin are to a large extent derived from the continent. The terrigenous matter is supplied mainly by

rivers, but in the south-eastern Angola Basin aeolian transport is significant as well (Bornhold, 1973).

The most important source of terrestrial debris in the Angola Basin is the river Zaire, which annually transports some twenty million tons of suspended matter directly into the ocean (Eisma and Kalf, 1984). A substantial portion (at least 8 million tons) is deposited on the continental shelf north of the river. This part of the shelf was extensively studied by Giresse, Kouyoumontzakis and others and the main results were summarized in Giresse et al. (1981). Detailed investigations have not been carried out south of the river.

Terrigenous clayey silts and silty clays, which are almost free of carbonate, are deposited near the river-mouth. Towards the north the terrigenous component becomes gradually less important, while the carbonate content increases to some 30 per cent. Much higher carbonate values (over 70%) are found along the shelf-break north of 4.5°S, where relict shell-sands of early Holocene age ('cordon coquiller') are exposed. Quartz sands are of minor importance in the area and they are limited to relatively shallow water. They dominate on the inner shelf off Gabon and off the Congo-Cabinda border. Faecal pellets are a very common constituent of the shelf sediments. Greenish grey pellets made up of relatively unaltered clay, prevail at depths less than 50 metres. On the upper continental slope, between 110 and 300 metres, dark green pellets of essentially glauconitic composition abound.

The major part of the suspended matter brought into the surface water settles in front of the river-mouth on the continental slope and the adjacent ocean floor. The river Zaire contributes in yet another and even more voluminous way to the deep-water sedimentation. Another twenty million tons of suspended load is deposited in the river estuary (Eisma et al., 1978; Eisma and Kalf, 1984). The sediments are stored only temporarily in the mangrove swamps. Ultimately they reach the canyon through which they are transported into the area of the deep-sea fan.

The sediments associated with the deep-sea fan were studied in piston-cores by Heezen et al. (1964), Jansen et al. (1984), and Van Weering and Van Iperen (1984). Both the fan and the adjacent slope are mud-dominated and the sediments generally consist of clays and clayey silts; sands are restricted mainly to the canyon floor. Most sediments of the deep-sea fan area are thought to be deposited either from turbidity currents or by (hemi)pelagic settling. Turbiditic sedimentation is the most important process in the upper fan, whereas (hemi)pelagic sedimentation prevails in the lower part. Debris flow deposits are found in the upper fan near the canyon mouth. They are thought to originate from slumping on the slope and are characterized by mud-clasts in a silty-clayey matrix.

The organic carbon content of the sediments of the deep-sea fan area is generally high. Jansen et al. (1984) found organic carbon contents of more than 3 per cent in surface sediments near the canyon mouth. Surface deposits on the continental slope between 2000 and 4000 metres were reported to contain between 1 and 2 per cent of organic carbon. Van Weering and Van Iperen (1984) showed that the average organic carbon content of the Middle and Late Quaternary sediments decreases from about 3.5 per cent near the canyon mouth to 1 per cent in the outer fan. Both the turbidites and the (hemi)pelagic muds contain very little carbonate, but the opal content (mainly diatoms) is very high (up to 60%; Van der Gaast and Jansen, 1984; Jansen et al., 1984). To the southwest the deposits of the Zaire fan pass into a reddish brown abyssal lutite, which covers the deepest part of the Angola Basin (Heezen et al., 1964). Accor-

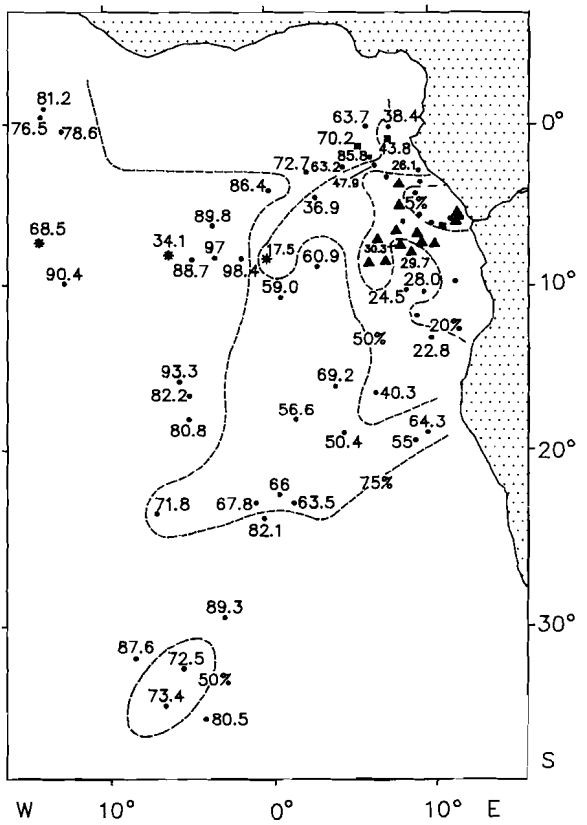

Fig. 4. Distribution of calcium carbonate in surface sediments expressed as percentage; (▲) data from Jansen et al. (1984), (*) samples that deviate from the general pattern.

ding to Bornhold (1973) turbiditic sedimentation is of local significance on the abyssal plain.

Lithofacies maps of the South Atlantic were produced by Ellis and Moore (1973) and by Goll and Bjørklund (1974). Far from the continent and a supply of terrigenous matter, calcareous oozes prevail. In the equatorial region, i.e. north of 10°S, siliceous microfossils are an important element, too. Diatoms are common to abundant in the oozes as well as in the hemipelagic muds of the marginal area. Radiolarians are frequent only on the Guinea Rise and at great depth ouside the area of the Zaire fan.

The distribution of calcium carbonate in a number of core-top samples is shown in fig. 4. The pattern is in accordance with the data presented in the literature (Bornhold, 1973; Ellis and Moore, 1973; Goll and Bjørklund, 1974; Biscaye et al., 1976; Balsam and McCoy, 1987). The highest carbonate values are restricted to relatively shallow depths on oceanic highs. Below 4000 metres the carbonate content steadily decreases towards the centre of the basin. The Zaire deep-sea fan stands out because of its low CaCO3 percentages (see also Jansen et al., 1984). These very low values are attributed primarily to dilution by large amounts of terrigenous sediment. The decrease in carbonate content towards deeper water in the land distant regions is largely the result of carbonate dissolution.

II.8. DISSOLUTION OF CARBONATE

Dissolution of carbonate increases with depth, as higher pressures and lower temperatures enhance the solubility of calcium carbonate. The depth at which the water becomes undersaturated, i.e. where the concentration falls below the critical carbonate content of Broecker and Takahashi (1978), corresponds well to a level of markedly increased dissolution in the sediments (sedimentary lysocline), and in the water-column (hydrographic lysocline) (e.g. Broecker and Takahashi, op. cit.; Broecker and Peng, 1982; Metzler et al., 1982). Below the lysocline the carbonate content of the sediment will gradually decrease until only carbonate-free sediments remain below the Carbonate Compensation Depth (CCD).

A variety of dissolution indices can be derived from sediment data to estimate the position of the lysocline (e.g. Peterson and Prell, 1985). We chose the P/P+B ratio, because in foraminiferal research it can be established on a routine basis. Fig. 5 shows the P/P+B ratios for core-tops from a depth of more than 3000 metres and west of longitude 0°. If a certain degree of diachrony is taken for granted, it seems reasonable to estimate the depth of the lysocline in the western Angola Basin (between latitude 5° and 35°S) somewhere between

4600 and 4900 metres. Well-preserved faunas made up of more than 99 per cent of planktonic foraminifers are absent below 4900 metres, but are common above approximately 4650 metres. Our data suggest that the lysocline rises to about 4200 metres near the Romanche Fracture Zone north of the Angola Basin, and the same depth is attained near the Walvis Passage in the south.

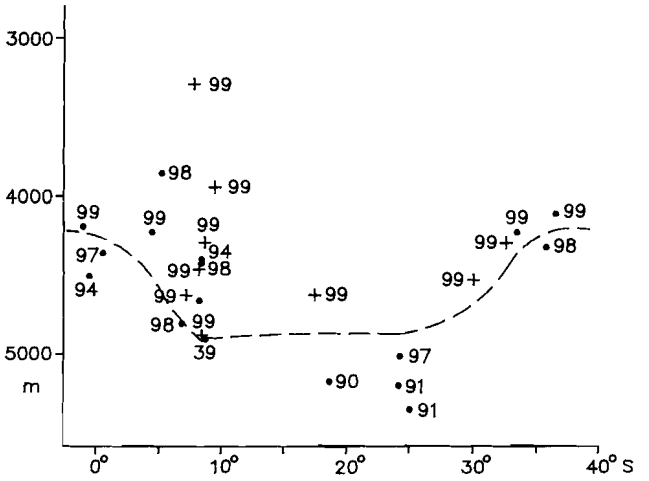

Fig. 5. Depth-latitude diagram showing the P/P+B ratios (x100) and the estimated position of the lysocline in the area west of longitude 0° and deeper than 3000 metres; (+) well-preserved samples.

The inferred position of the lysocline is in agreement with earlier estimates made on the basis of the carbonate content of sediments. Biscaye et al.(1976) reported a depth between 4800 and 5000 metres for the entire basin and Thunell (1982) estimated 4700 to 4900 metres for the western part. The position of the lysocline is much deeper than in the western South Atlantic; this has been attributed to the absence of AABW in the Angola Basin. Antarctic Bottom Water is carbonate-poor compared to NADW, and the lysocline in the western Atlantic tends to coincide with the boundary between both water-masses (e.g. Berger, 1979). This explanation is consistent with our data, which suggest that the lysocline rises in areas where AABW contributes significantly to the bottom waters.

Deep-water properties, however, do not explain all dissolution phenomena in the area under consideration. The P/P+B values show rather a dramatic decrease towards the continent, more specifically in the area of the Zaire deep-sea fan (fig. 6). Since other phenomena, such as etching, fragmentation, and absence of dissolution-prone species, also indicate that preservation greatly

deteriorates, the decrease in P/P+B values must be due to dissolution. In the area bordering the Zaire submarine canyon, severe dissolution was even observed at much shallower depths (see also Zachariasse et al., 1984). Shallow-water dissolution seems to be fairly common in sediments of continental margins (e.g. Berger, 1970, 1979; Diester-Haass and Müller, 1979). It was also observed in the highly productive, pelagic environment of the Gulf of California (Schrader et al., 1983), and Peterson and Prell (1985) found significant dissolution above the lysocline in the Equatorial Indian Ocean.

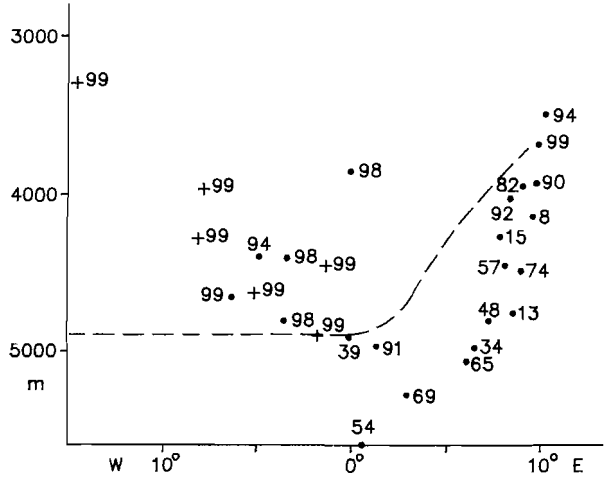

Fig. 6. Depth-longitude diagram showing the P/P+B ratios (x100) and the estimated position of the lysocline in the area between 5° and 15°S and deeper than 3000 metres; (+) well-preserved samples.

It is generally assumed that in sediments above the hydrographic lysocline, the dissolving agent is pore-water carbon dioxide that has been produced by the mineralization of buried organic matter. Emerson and Bender (1981) developed a model for supralysoclinal dissolution in the deep ocean, in which the rain-ratio between organic carbon and carbonate appeared to be the factor controlling carbonate preservation. If this ratio is close to unity, between 40 and 80 per cent of the carbonate will dissolve in the sediment at saturation depth. Broecker and Peng (1982) argued that it would have been more realistic if accumulation rates had been considered. Consequently, in the deep ocean the effect is probably overestimated, because there only a very small percentage of the supplied organic carbon accumulates in the sediment. In regions of rapid sedimentation, however, decomposition of organic matter at the sediment surface is much less effective and more organic carbon will be mineralized in the sediment (Berner,

1982). In these deposits the carbondioxide produced can presumably dissolve calciumcarbonate on a mole equivalent basis (cf. Peterson and Prell, 1985). Solution is of course particularly enhanced by a large input of organic carbon.

The area of the Zaire deep-sea fan is characterized by high sedimentation rates and underlies very productive waters. The flux of organic matter is additionally augmented by the terrestrial organic detritus supplied by the river Zaire. Hence, corrosive pore-waters are the most likely cause of strong dissolution in the fan area. Although we emphasized the anomalously poor preservation of carbonate in the sediments of the Zaire fan area, shallow water dissolution is thought to operate on a much wider scale, although the effects are usually less easily recognized in calcitic fossils. Shallow water dissolution is well exemplified by the complete absence of pteropods (aragonite) in even the shallowest of our surface samples (74 m) from the continental margin (cf. Ganssen and Lutze, 1982).

Because the corrosive effect of carbon dioxide rich pore-waters is not necessarily limited to sediments above the lysocline, the position of the CCD may be influenced as well. Jansen et al. (1984) estimated the depth of the CCD in the fan area at about 5600 metres. Both Ellis and Moore (1973) and Biscaye et al. (1976) found significant carbonate percentages even at a depth of 6000 metres. The latter author extrapolated an ideal value of 6400 metres for the CCD in the Angola Basin. Our data seem to confirm that the figure given by Jansen et al. is of local significance only, because the deepest sample studied (5608 m) still contains 59 per cent calcium carbonate.

It should be noted that high organic carbon levels only affect preservation of carbonate under oxygenated conditions. In anoxic environments mineralization will be governed mainly by sulphate reduction, which increases the alkalinity, resulting in carbonate saturated pore-waters (Berner et al., 1970; Froelich et al., 1979). Under these conditions carbonate preservation is even excellent (e.g. Berger and Soutar, 1970; Phleger and Soutar, 1973; Leventer et al., 1983).

Chapter III

SEA-FLOOR DISTRIBUTION OF PLANKTONIC FORAMINIFERS

III.1. INTRODUCTION

Surface-water data on the distribution of planktonic foraminifers in the eastern South Atlantic are scarce. The most comprehensive set of data was presented by Bé and Tolderlund (1971), but even this classic study on planktonic foraminiferal biogeography poorly covered the area under consideration. In view of the scarcity of surface-water data, we attempted to relate the distribution of planktonic foraminiferal species on the sea-floor to the surface-water hydrography. This is not only a purpose in itself, but insight in surface-sediment distribution of species may also provide a conceptual framework for interpreting downcore changes in planktonic foraminiferal associations. An essentially similar method was applied by Zachariasse et al. (1984) for the area of the Zaire deep-sea fan.

Sample selection

A certain degree of diachrony is inevitable in the study of core-top samples. Samples that were suspected to be pre-Holocene in age were deleted in order to avoid too large time-dependent differences. Absence of *Globorotaloides hexagonus* together with the presence of *Globorotalia menardii* was taken as indicative of a Holocene age (Zachariasse et al., 1984). This criterion is, however, only valid in the (sub)tropical region and age estimates could not be made outside this area.

Since planktonic foraminiferal species vary widely in their susceptibility to dissolution (e.g. Parker and Berger, 1971; Adelseck, 1978), samples showing signs of severe dissolution were excluded from quantitative analysis. As a rule, samples from water deeper than 500 metres showing a P/P+B ratio of less than 0.85 were discarded. Since the ratio is determined by other factors as well, preservational aspects, such as fragmentation and relative abundance of resistent species, were taken into account.

Some samples showed evidence of down-slope contamination (e.g. by the occurrence of quartzsands and shallow-water benthic foraminifers). We excluded these samples as well as those that contain less than one hundred specimens in the 150-595 μm size-fraction. Out of the more than one hundred core-top samples studied, eventually only fifty-one were considered suitable for mapping the distribution of planktonic foraminiferal species on the ocean floor (fig. 7).

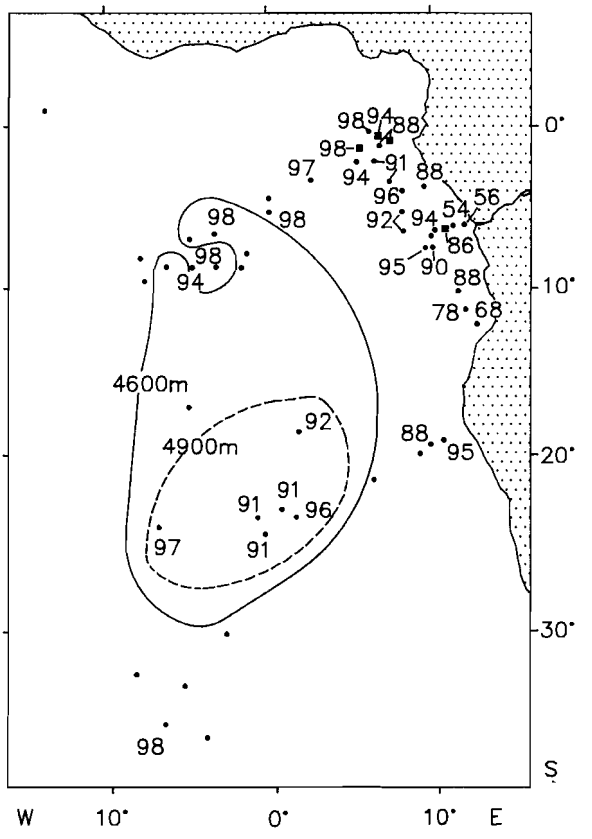

Fig. 7. Location of core-tops selected for the planktonic foraminiferal analysis. P/P+B ratio (x100) is shown if the value is less than 99. Solid and dashed lines encircle samples from below 4600 and 4900 m, respectively.

Foraminiferal number

The planktonic foraminiferal number, defined as the number of specimens per gram of dry sediment, ranges from less than 100 to 36,500 (fig. 8). Major differences in the number of planktonic foraminifers are clearly determined by either dissolution or dilution. Extremely low values, less than 500 per gram, are observed along the continental margin, where the input of terrigenous matter is high. In front of the river Zaire, the effect of dilution is even stronger than is suggested in fig. 8, because only samples containing more than one hundred specimens are shown. All samples that yielded less specimens are from this area.

Within the oceanic realm, differences in the planktonic foraminiferal number seem to be governed mainly by dissolution. High values (more than 10,000 in-

dividuals per gram) are found on physiographic highs above the lysocline. The planktonic foraminiferal number tends to be higher on the Walvis Ridge than on the Guinea Rise, although the P/P+B ratios (fig. 7) indicate no clear preservational differences. The lower values on the Guinea Rise may be explained by dilution with biogenous opal, which contributes considerably to the sediments of the equatorial region. Lowest numbers (less than 2,500) are attained below the lysocline in the deeper parts of the Angola Basin. Comparably low values are also found in two samples from shallower depth located at approximately 5°W, 9°S. P/P+B ratios (see fig. 7) indicate that only one of these samples suffered from dissolution. Dilution with non-terrigenous sediment components is supposed for the other sample, which shows an admixture with dark, presumably iron-manganese components.

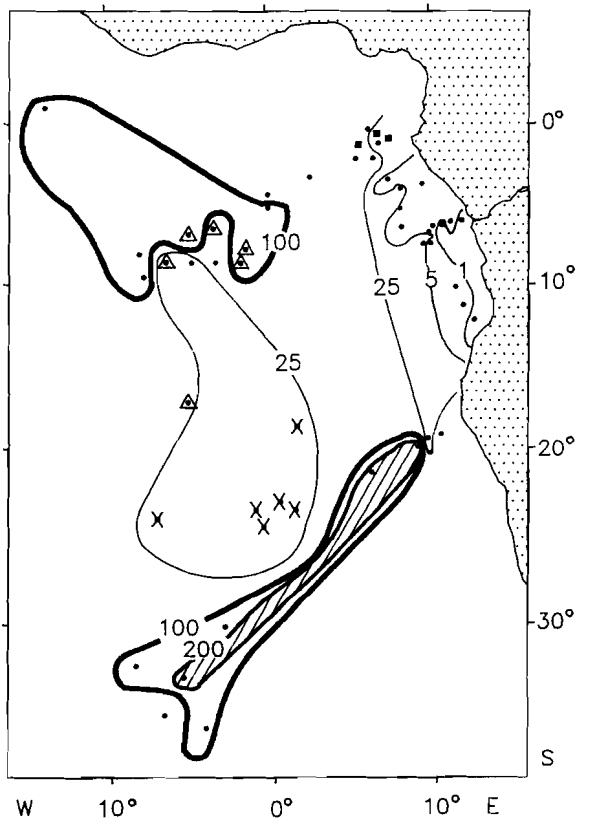

Fig. 8. Contour map of planktonic foramniferal numbers in units of 100 specimens per gram of dry sediment. Crosses indicate samples from deeper than 4900 m and triangles those from between 4600 and 4900 m.

III.2. DISTRIBUTION OF SPECIES

Twenty-six categories were distinguished, amongst which *Candeina nitida, Globigerina quinqueloba,* and *Hastigerina pelagica* were so scarce that they did not show up in the counts. *Globigerina digitata, Globigerinoides conglobatus, G. tenellus, Globorotalia anfracta,* and *Globoturborotalita rubescens* were deleted, because they attain relative frequencies of less than 4.5 per cent. The remaining species will be discussed in approximate order of increasing resistance to dissolution (Parker and Berger, 1971).

Globigerinoides ruber is almost omnipresent and may constitute up to forty two per cent of the fauna (fig. 9a). It seems to avoid the south-western extreme of the Angola Basin and the region overlain by the main branch of the Benguela Current. *G. ruber* gains in importance towards the equator, and north of approximately 15°S it is generally the dominating species making up more than twenty per cent of the association in most samples. Lower abundances are, however, reached in a small area at the Guinea Rise. Two varieties were discriminated, a white form and a pink one. Fig. 9b shows that the proportion of the pink variety per total *G. ruber* is clearly higher in the near-coastal region than in the mid oceanic area.

Globogerinoides trilobus has a more restricted distribution than *G. ruber* (fig. 9c) and is neither present under the Benguela Current, nor in the south-western part of the Angola Basin. Outside these regions, the species is present in all samples, and it tends to become more abundant towards the north. In the tropical region, i.e. north of 15°S, relative frequencies generally exceed ten per cent but it is scarcer in the marginal region between the river Zaire and Cape Lopez. Frequencies of more than twenty per cent are reached in the tropical region both at great distance from the continent and south of the river Zaire.

Globigerina bulloides attains abundances of more than five per cent in three areas: (1) the south-western part of the region, which is the area of maximum frequency, (2) under the Benguela Current and (3) in front of the river Zaire (fig. 9d). Elsewhere this species is rare or absent.

Striking differences in average test size exist between the three high-frequency areas (table 1). *G. bulloides* attains its maximum size in the south-western part of the Angola Basin and the smallest specimens occur in the area of the Zaire deep-sea fan. Size was defined by the largest diameter of the test, corresponding to parameter X1 of Malmgren and Kennett (1977). The differences in mean can be considered significant ($\alpha = 0.01$) on score of the distribution free Wilcoxon test. In the areas, where *G. bulloides* is low-frequent, average test size is even smaller than in the area of the Zaire deep-sea fan, but this difference proved to be not significant.

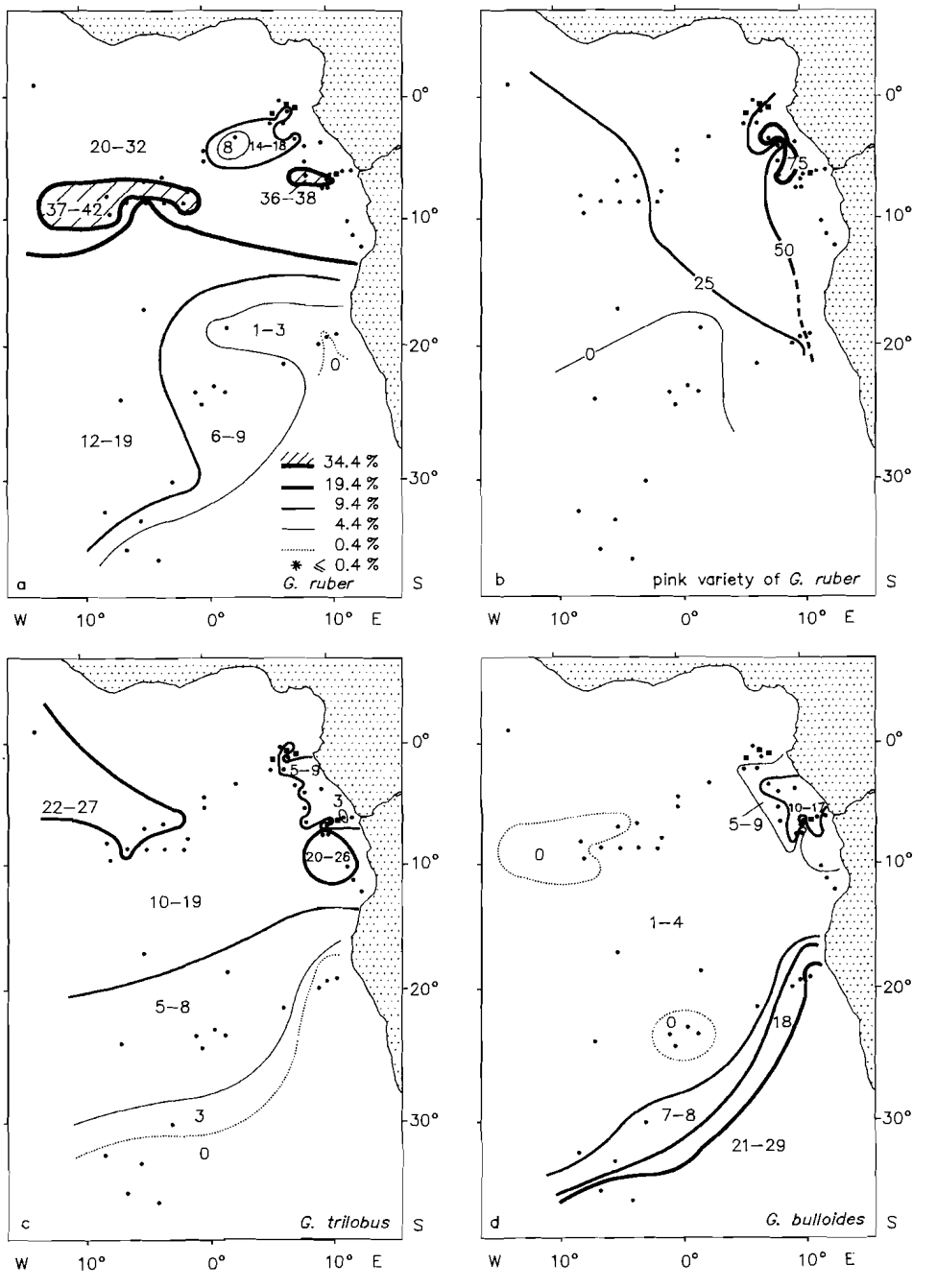

Fig. 9. Percentage distribution of (a) *G. ruber*, (b) pink types per total *G. ruber*, (c) *G. trilobus*, and (d) *G. bulloides*. Contouring is explained in fig. 9a; figures in between the contours refer to the actual range of values.

We may generalize that test size and relative number of *G. bulloides* are positively correlated, which confirms observations of Malmgren and Kennett (1977). A similar relationship holds for many other species, which indicates that planktonic foraminiferal species reach their maximum size in their optimum environment (Hecht, 1976; Keller, 1978; Kahn, 1981).

area	N	range	$\bar{X}$l	SD	chi^2	U
SW Angola Basin	123	200-600	323	93	14.8	
Benguela Current	125	210-425	283	47	5.9	3.03
marginal tropical	178	195-420	258	52	11.6	5.87
central tropical	71	190-430	246	44	16.5	1.89

Table 1. *Globigerina bulloides*. Statistics of size parameter X1 (measurements in μm) in four different areas. The value of the statistical of the Wilcoxon test (U) is given with respect to the next larger mean. The distribution of the size parameter could not be considered normal on score of a Chi-square test (one degree of freedom, α = 0.01).

Globigerina falconensis, which is morphologically very similar to *G. bulloides*, is relatively rare and is only found in appreciable quantities (over 2.5 %) in the southern part of the area (fig. 10a). Frequencies of more than ten per cent are attained in the south-west just north of the samples with abundant *G. bulloides*.

Globigerinella siphonifera is almost ubiquitous (fig. 10b). Although this species seems to be slightly more abundant at relatively low latitudes, its overall distribution is rather diffuse and high frequencies are reached at widely scattered places.

Globigerinita glutinata is present in all but one sample but rarely attains frequencies of more than ten per cent (fig. 10c). It is most abundant in the land distant parts of the Angola Basin. Near the continent and south of 30°S its relative abundance seldom exceeds five per cent.

Orbulina universa (fig. 10d) occurs widespread throughout the area, but generally in low percentages (less than 2 %). High abundances are definitely restricted to the area under the Benguela Current. The distribution seems to be patchy in front of the river Zaire, where frequencies range from zero to seven per cent.

Globorotalia scitula shows a rather non-descript distribution (fig. 11a) and frequencies are generally less than three per cent. Higher abundances are locally reached both in the marginal area and to the south-west of the Angola Basin.

Globorotalia hirsuta has a restricted distribution and occurs only south of latitude 20°S outside the area of the Benguela Current (fig. 11b). Although everywhere scarce, it is slightly more frequent in the southernmost part of the region, where it attains a relative abundance of five to six per cent.

Globorotalia truncatulinoides is split into left- and right-coiling forms and the

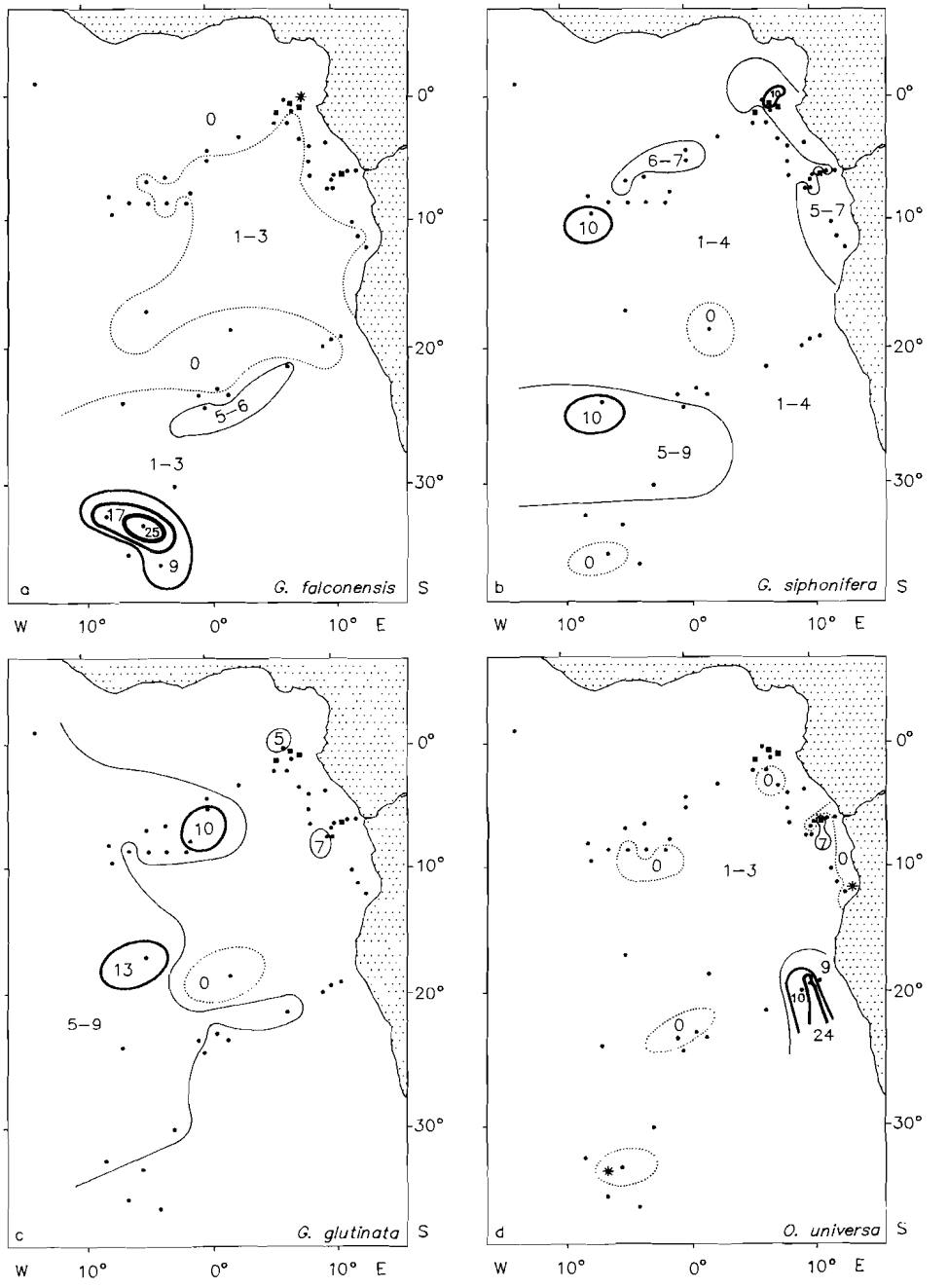

Fig. 10. Percentage distribution of (a) *G. falconensis*, (b) *G. siphonifera*, (c) *G. glutinata*, and (d) *O. universa*. Figure conventions as in fig. 9a.

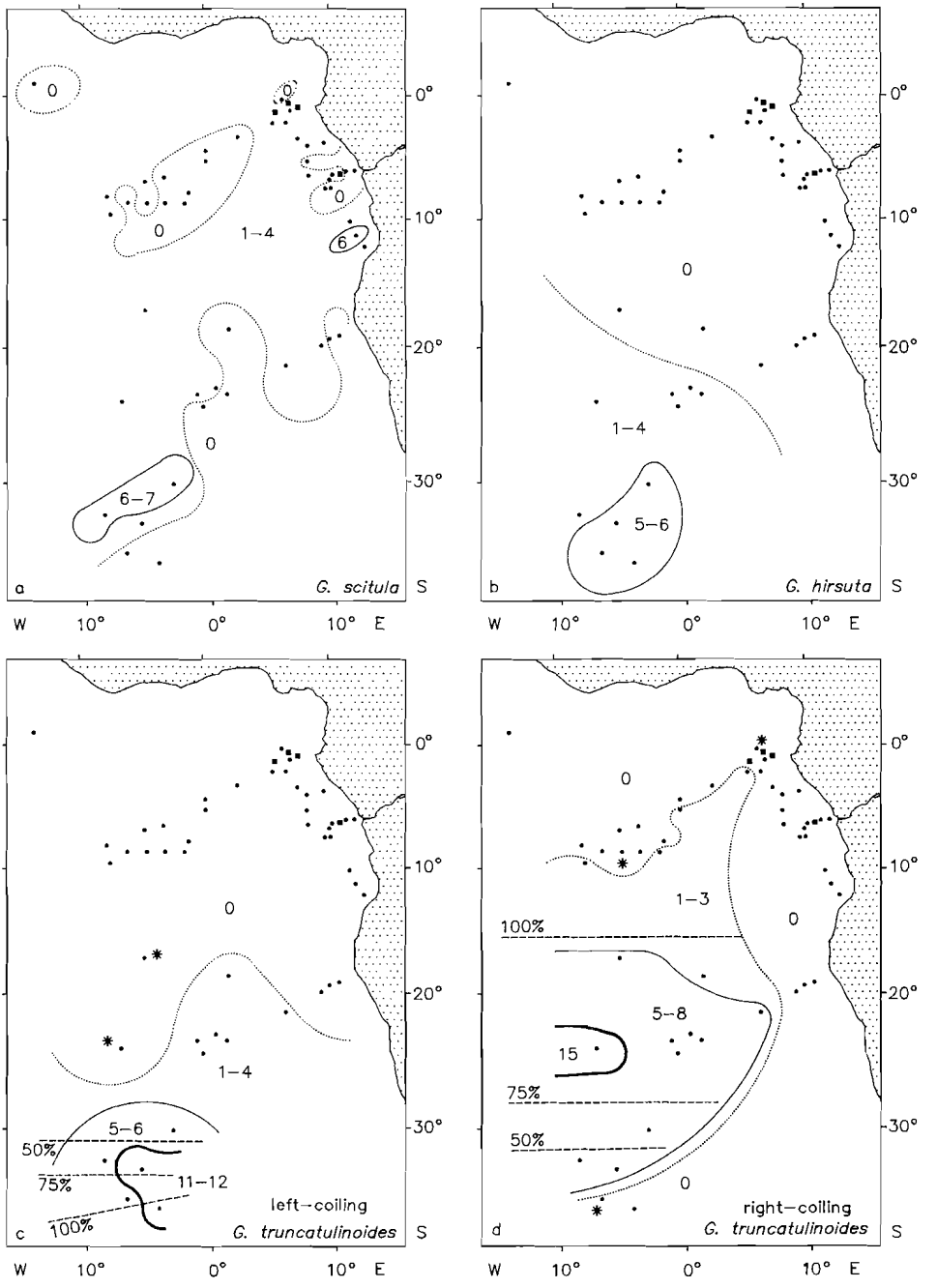

Fig. 11. Percentage distribution of (a) *G. scitula*, (b) *G. hirsuta*, (c) left-coiling *G. truncatulinoides*, and (d) right-coiling *G. truncatulinoides*. Figs. 11c and d also show the proportion of the coiling variety considered per total *G. truncatulinoides*. Figure conventions as in fig. 9a.

distribution of the two types is so different, that they are treated separately. Left-coiling *G. truncatulinoides* is limited to the region south of 15°S but is absent under the Benguela Current (fig. 11c). Relative numbers rarely exceed two per cent between 15° and 30°S. Left-coiling specimens are more abundant at higher latitudes, and their proportion per total *G. truncatulinoides* increases regularly towards the south.

Right-coiling *G. truncatulinoides* (fig. 11d) is locally present at low latitudes, but in percentages of less than two and a half per cent. Frequencies of five per cent and more are generally attained between 15° and 30°S and, just like the left-coiling type, it avoids the Benguela Current region. Right-coiling specimens are virtually absent south of latitude 35°S.

Globorotalia inflata is quantitatively one of the most important species. It is least abundant between 5° and 10°S west of longitude 0° (fig. 12a). Frequencies increase towards the east and the south and *G. inflata* may be the dominating species both in the marginal tropical region and south of 18°S reaching frequencies of more than twenty per cent. Highest abundances are found in the southern part of the Angola Basin around longitude 0°, where it is by far the most abundant species. Considering the depth of these samples, which is below the lysocline (fig. 7), we suppose that these high frequencies partially result from dissolution.

Globorotalia crassaformis is limited to the region north of latitude 30°S but is practically not found in the sediments under the Benguela Current (fig. 12b). High frequencies are clearly associated with the area in front of the river Zaire, where the species makes up more than five per cent of the association. The highest abundance is close to the rivermouth. Outside the fan area, it is a minor faunal constituent, only occasionally attaining frequencies of more than five per cent.

Neogloboquadrinids have been differentiated into two types, viz. a large-sized, loosely coiled form labelled as *Neogloboquadrina dutertrei* and a small-sized, tightly coiled type, which is labelled as *N. pachyderma.*

N. dutertrei is only found north of approximately 18°S and is continuously present here (fig. 12c). This species shows a tendency to higher frequencies towards the north, but frequencies vary strongly between 7° and 18°S, particularly in the western part of the area. *N. dutertrei* exceeds frequencies of ten per cent north of 5°S but may be less frequent near the continent. A coherent area of high abundance is found near the equator at the Guinea Rise, where *N. dutertrei* is the dominating species.

The distribution pattern of *N. pachyderma* seems to be rather non-descript at first sight (fig. 12d). Although this species locally reaches frequencies of more than twenty per cent in the tropical region, it tends to be scarce north of 15°S.

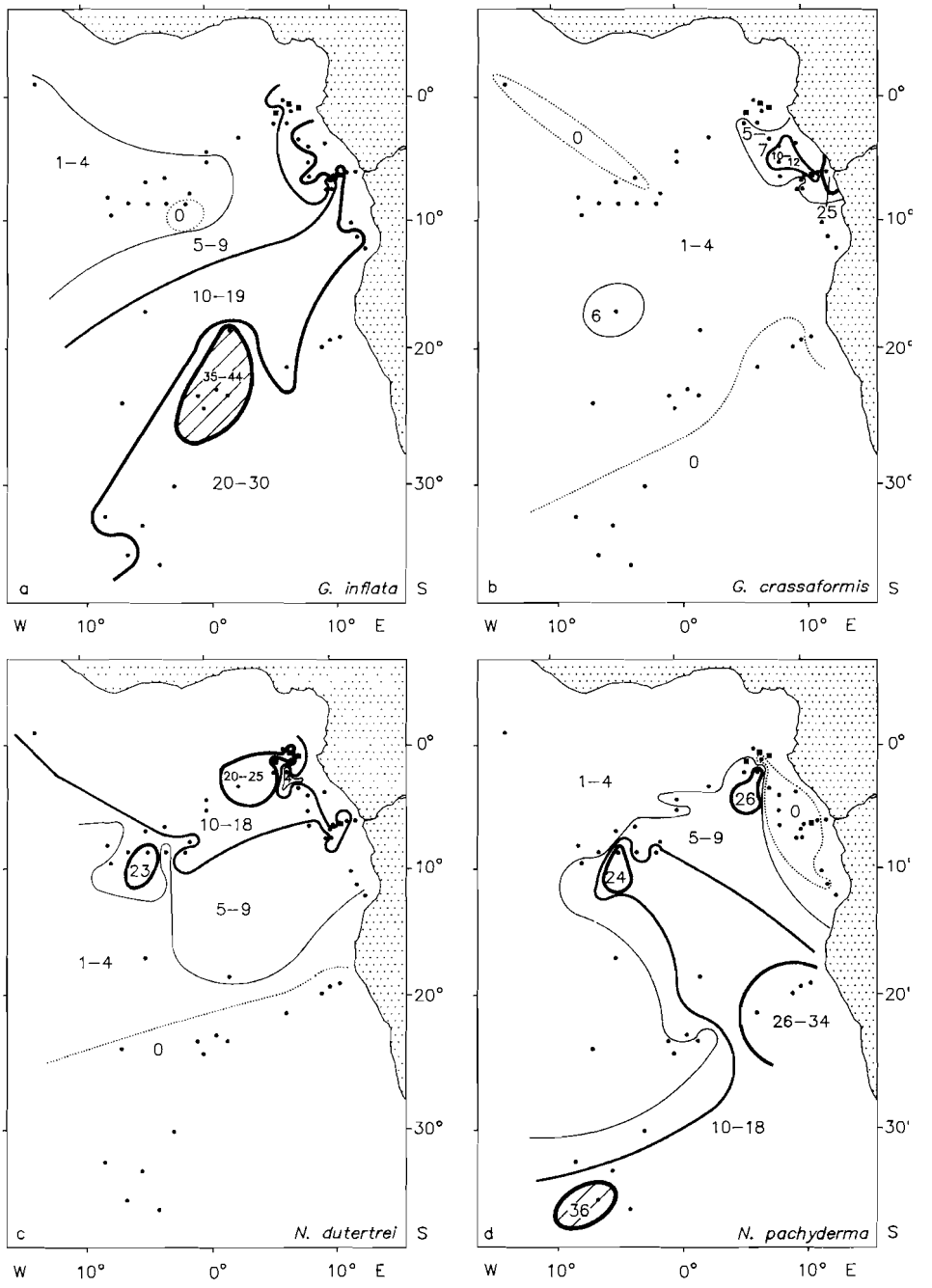

Fig. 12. Percentage distribution of (a) *G. inflata*, (b) *G. crassaformis*, (c) *N. dutertrei*, and (d) *N. pachyderma*. Figure conventions as in fig. 9a.

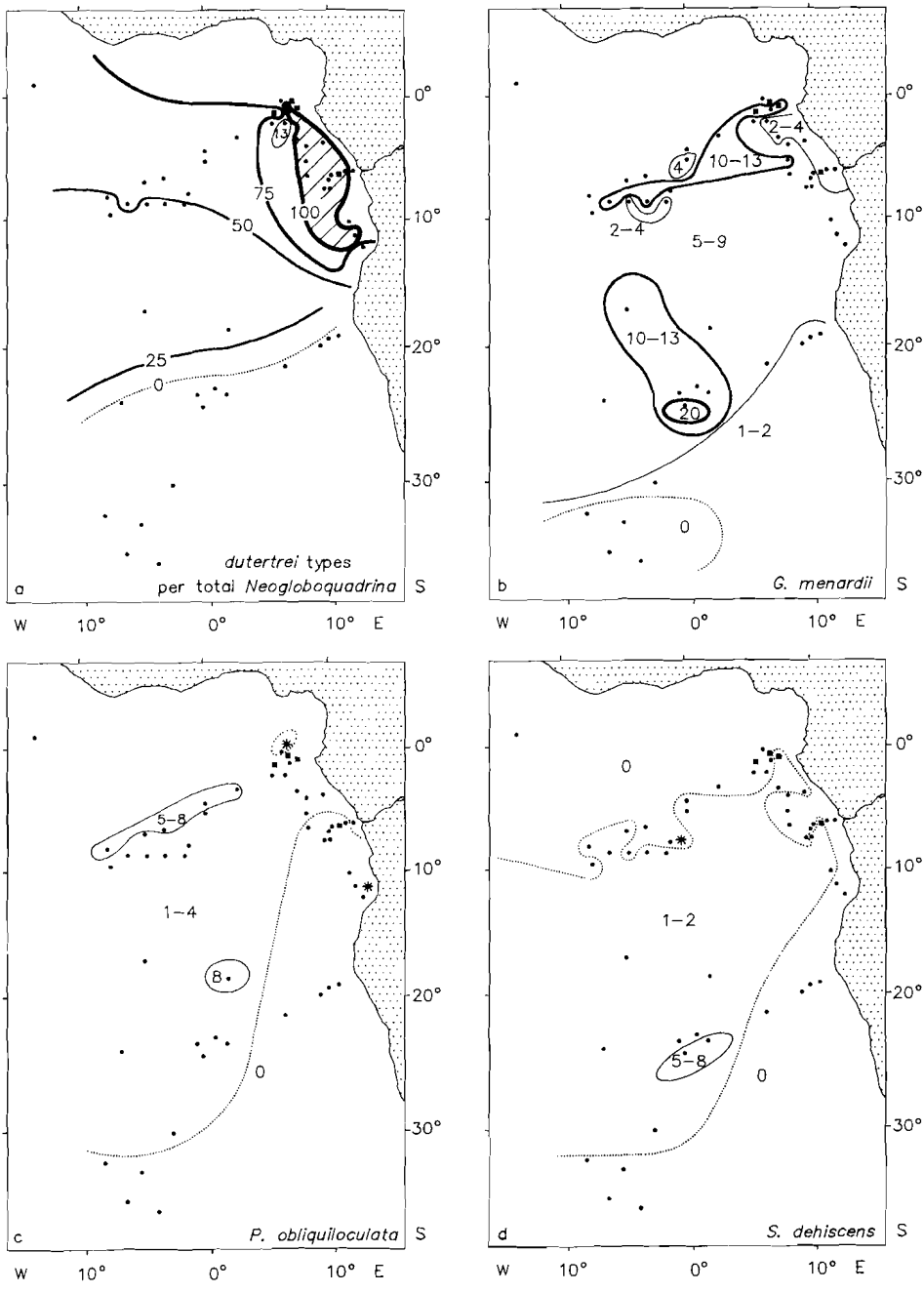

Fig. 13. Percentage distribution of (a) *dutertrei* types per total neogloboquadrinids, (b) *G. menardii*, (c) *P. obliquiloculata*, and (d) *S. dehiscens*. Figure conventions as in fig. 9a.

N. pachyderma is especially rare in the marginal area being completely absent in the region of the Zaire deep-sea fan. At higher latitudes *N. pachyderma* is abundant in both the area under the Benguela Current (26-34 %), and the south-western extreme of the basin (16-36 %). Outside these areas, it is generally as scarce as in the land distant parts of the tropical region. It should be noted that *N. pachyderma* is predominantly right-coiling. Left-coiling types are generally rare and the maximum proportion per total *N. pachyderma* is only 12.5 per cent.

Fig. 13a shows that the proportion of *dutertrei* types per total neogloboquadrinids increases regularly towards the north. The marginal area around the Zaire deep-sea fan stands out because in relation to its latitude it is extremely poor in *pachyderma* types. One sample in the tropical region shows only thirteen per cent of *dutertrei* types and deviates markedly from the general pattern. Inspection of fig. 12d learns that *N. pachyderma* is anomalously abundant here. Since our downcore studies show that *N. pachyderma* was far more frequent at low latitudes in the recent past than it is at present, we surmise an age anomaly for this sample.

Globorotalia menardii is not found in the extreme south-west and is almost missing in the area under the Benguela Current (fig. 13b). Elsewhere, it is generally a rather common constituent of the fauna. Low frequencies are, however, reached in a coherent area along the African continent in front and north of the river Zaire, and locally also at great distance from the continent. In the samples from the deepest part of the Angola Basin, frequencies tend to be higher than elsewhere. Most of these samples also contain markedly abundant *G. inflata,* so that dissolution probably has enriched these faunas with dissolution resistant species.

Pulleniatina obliquiloculata occurs in most of the samples but the maximum frequency is only eight per cent (fig. 13c). South of latitude 5°S, it is absent near the continent, and the species is also missing in the extreme south-western part of the region.

Sphaeroidinella dehiscens is a minor faunal element and its frequency is generally less than three per cent (fig. 13d). This species is absent over large parts of the region, both to the north and to the south, and is almost missing near the continent. Highest relative numbers are found in the centre of the Angola Basin, which again may be due to dissolution.

III.3.1. Overall faunal composition

In order to analyse their covariance, the frequencies of the eighteen most abundant taxa were subjected to an R-mode BALANC program, followed by DENDRO-clusteranalysis. The results of the multivariate analyses are shown in figs. 14 and 15 and suggest the presence of three faunal groups.

A first group of positively correlated species consists of *Globigerinella siphonifera, Globigerinita glutinata, Globigerinoides ruber, G. trilobus, Globorotalia menardii,* and *Neogloboquadrina dutertrei.* These taxa are generally negatively correlated with four other taxa, viz. *Globigerina falconensis, Globorotalia hirsuta, G. inflata,* and left-coiling *G. truncatulinoides.* Three of the latter taxa form a second group of mutually positively correlated elements; *G.*

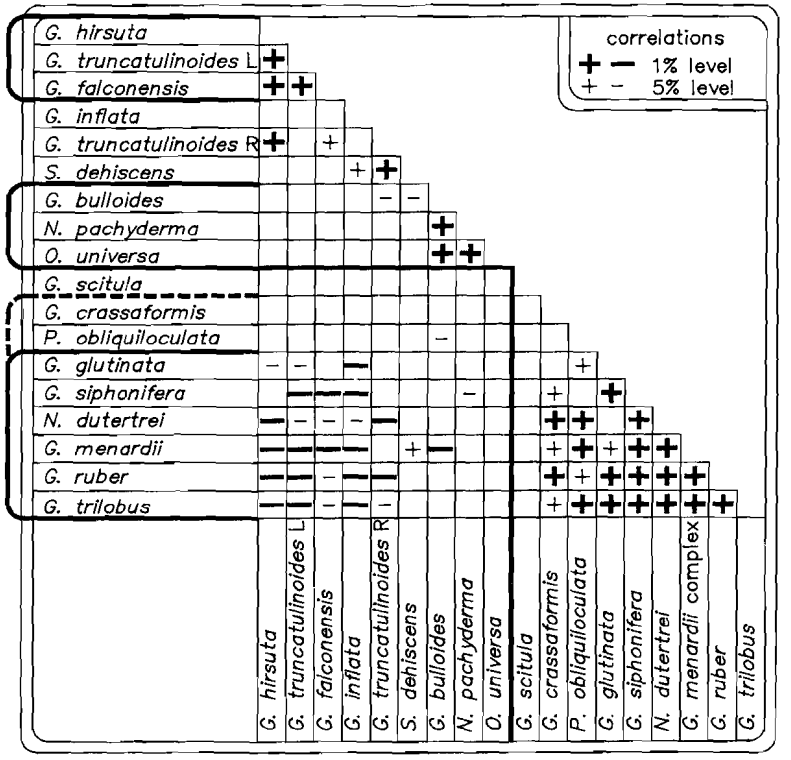

Fig. 14. BALANC correlation matrix based on all core-top data. The heavy line separates the two groups that show the lowest degree of similarity according to the DENDRO analysis.

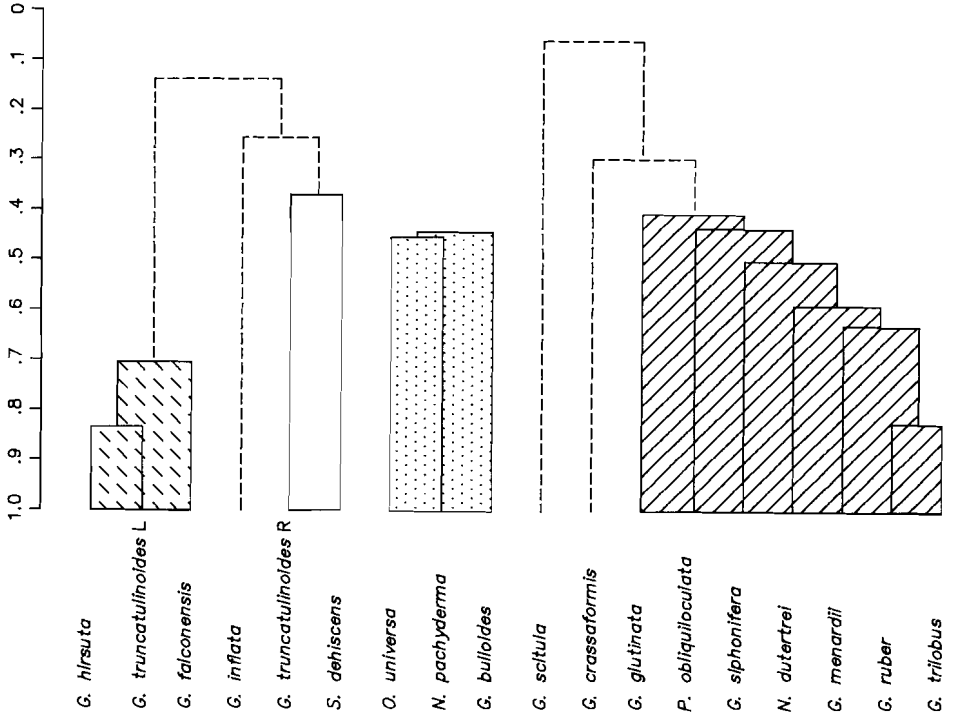

Fig. 15. Dendrogram based on the BALANC correlation matrix of all core-top data showing three major associations. Only positive correlations are shown. Dotted lines indicate correlations which are not significant (α = 0.01).

inflata can not be included in this group, because it lacks positive correlations with the other three taxa.

The first group is composed of species that abound in the tropical region, i.e. the area north of 15°S, and is, therefore, termed the tropical association. *Globorotalia crassaformis* and *Pulleniatina obliquiloculata* may be included in this group, but they lack the negative correlations with the second group. The taxa of the second group jointly make up more than ten per cent of the fauna in the five samples from the south-western extreme of the region and we shall refer to this group as the cool subtropical association.

A third group of positively correlated species consists of *Globigerina bulloides, Neogloboquadrina pachyderma,* and *Orbulina universa.* The first two species have negative correlations with some species of the tropical association. This third group of species is termed the Benguela Current association, because all species reach high abundances in the region under the Benguela Current.

Among the remaining taxa, *Sphaeroidinella dehiscens* has positive correlations with *G. inflata, G. menardii,* and right-coiling *G. truncatulinoides.* We consider it likely that these correlations are in part controlled by dissolution. Finally, right-coiling *G. truncatulinoides* shows positive correlations with members of the cool subtropical association.

Subsequent to the BALANC/DENDRO analysis, we subjected the same data-base to an R-mode principal component analysis in order to visualize the similarity between the samples. The characteristics of the first three components are given in table 2. According to the criterion given by M.M. Drooger (1982), only the first two components can be considered statistically significant.

Species loadings show that the first component roughly represents a polarity between the tropical association and a composite group, which consists of the cool subtropical association plus *G. bulloides* and *G. inflata.* The sample scores on the first component (fig. 16a) show a rather regular pattern with maximum dissimilarity between the northern and the southern part of the area. The samples tend to group in quasi-latitudinally arranged zones, which are deflected

principal component	1	2	3
eigenvalue	5.4	2.7	1.9
variance (%)	29.9	15.1	10.4
species			
G. trilobus	.4	.1	.1
G. ruber	.3	.0	.3
N. dutertrei	.3	-.2	-.1
G. menardii	.2	.3	-.3
P. obliquiloculata	.2	.1	-.3
G. glutinata	.2	.2	.2
G. siphonifera	.2	.2	.2
G. crassaformis	.1	-.2	.0
S. dehiscens	-.0	.3	-.4
G. scitula	-.1	.1	.4
O. universa	-.1	-.3	-.1
G. truncatulinoides R	-.2	.5	-.1
N. pachyderma	-.2	-.3	-.2
G. bulloides	-.3	-.4	.1
G. inflata	-.3	.1	-.3
G. falconensis	-.3	.2	.3
G. truncatulinoides L	-.3	.2	.2
G. hirsuta	-.3	.3	.1

Table 2. Results of a principal component analysis of the frequency distribution of the eighteen most common planktonic foraminiferal species on the ocean floor. Composition of the first three components, eigenvalues, and percentages of total variance.

towards the north near the continent. The marginal area north and in front of the river Zaire deviates from the general pattern and the sample scores suggest similarity to the more southern region.

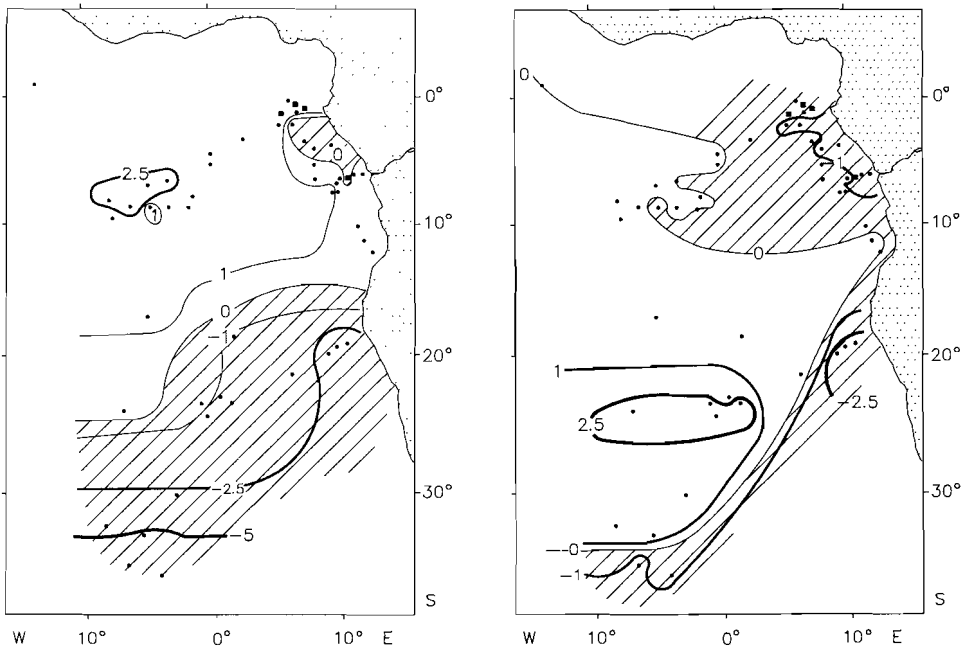

Fig. 16. Contour map of sample scores on (a) the first and (b) the second principal component of the R-mode PC analysis on all core-top data. Hatched area delineates negative values.

The second principal component opposes the Benguela Current association to a non-descript combination of taxa among which right-coiling *G. truncatulinoides*, *G. hirsuta*, *G. menardii*, and *S. dehiscens* show high loadings. Mapping of the sample scores on the second component (fig. 16b) clearly shows, that the axis describes a contrast between the region of the Benguela Current and an area to the west in between 18 and 25°S. An E-W contrast is also evidenced in the tropical region, but the change in faunal composition seems to be more gradual than in the south. Finally, a sigificant change in faunal composition can be identified in the south-western part of the area approximately along 35°S.

A plot of the sample scores on the two significant components (fig. 17) demonstrates that only the samples from the tropical region and those of the Benguela Current area form distinct clusters. We conclude that the tropical region and the Benguela Current area are indeed effectively defined by their respective associations. Although the three cool subtropical taxa group in the

BALANC/DENDRO analysis, their abundances in the south-western part of the Angola Basin are too low and too variable to make these samples form a distinct cluster in principal component analysis. The large scatter shown by these samples (fig. 17), points to a significant faunal difference north and south of 35°S. Fig. 16b shows, that the two southernmost samples bear some resemblance to those from the region of the Benguela Current and figs. 9d and 12d illustrate that this is caused by the high frequencies of *G. bulloides* and *N. pachyderma* in the two areas.

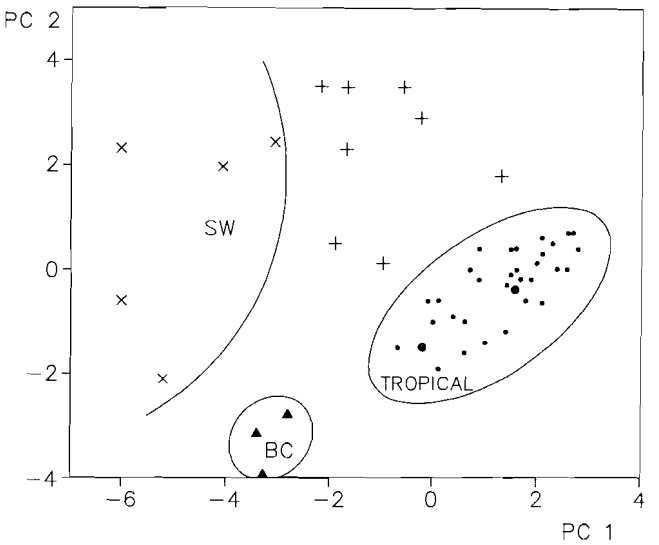

Fig. 17. Plot of the sample scores on the first two principal components of the R-mode PC analysis on all core-top data. Samples from the tropical area, the south-western area and the area under the Benguela Current are marked.

III.3.2. The tropical cluster

Although the samples from the region north of 15°S form a distinct cluster in the principal component analysis, large differences in composition do exist, in particular between the marginal and the more oceanic areas. In order to examine this contrast in greater detail, a new data-base was made, which includes only the thirty-five samples north of 15°. Because *G. hirsuta* and left-coiling *G. truncatulinoides* are absent in the tropical region, the number of species is reduced to sixteen.

The results of the BALANC/DENDRO analysis proved to be difficult to in-

terpret, and we could identify only one group of mutually positively correlated (α =0.01) species. This group consists of *G. bulloides*, *G. crassaformis*, and *G. inflata*. After we eliminated the rare species (less than 2.5%) and split *G. ruber* into two varieties, the structure of the correlation-matrix improved considerably (fig. 18) and two opposite groups are distinguishable. The first group consists of *G. bulloides*, *G. crassaformis*, *G. inflata*, and pink *G. ruber*, to which *G. scitula* may be added. These taxa are all relatively abundant near the continent, more specifically in the area in front of the river Zaire. The other association consists of *G. glutinata*, white *G. ruber*, *G. trilobus*, *G. menardii*, and *P. obliquiloculata* and can be considered characteristic of the open ocean. The remaining four species (*G. siphonifera*, *N. dutertrei*, *N. pachyderma*, and *O. universa*) are rather indifferent.

Principal component analysis seems quite insensitive to the inclusion of rare species, since there proved to be little difference between the analyses of the

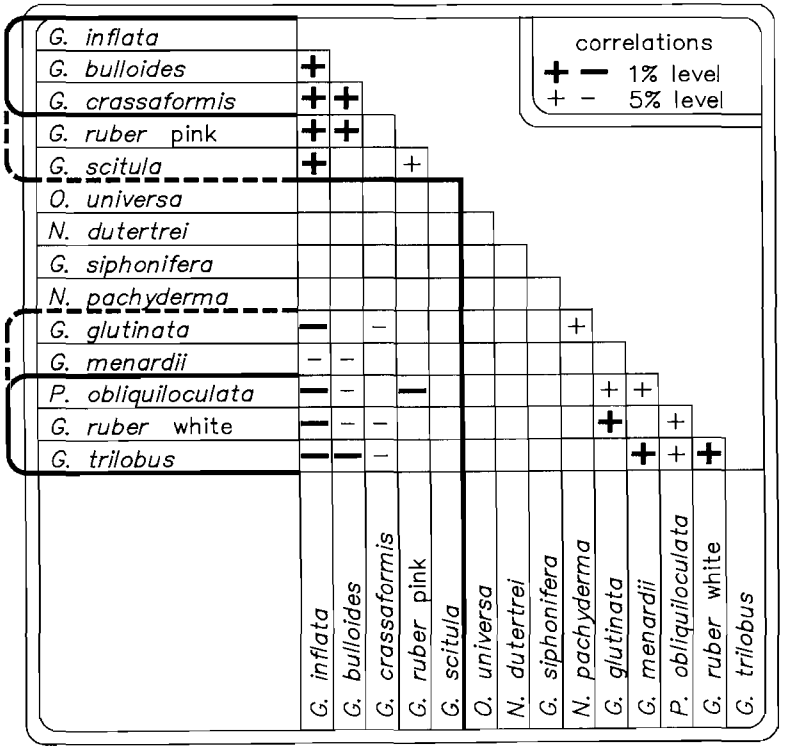

Fig. 18. BALANC correlation matrix based on core-top data from the tropical region. The heavy line separates the two groups that show the lowest degree of similarity according to the DENDRO analysis.

two data-bases. Table 3 gives the characteristics of the analysis of the original matrix, which includes the rare species and total *G. ruber*. Only the first principal component can be considered significant and it describes a similar faunal partitioning as the one based on BALANC/DENDRO analysis. The scores of the samples on the first component are mapped in fig. 19. The resulting pattern clearly illustrates the faunal contrast between the area in front of the river Zaire, or more generally the marginal area, and the land-distant parts of the tropical region.

principal component	1	2	3
eigenvalue	4.3	2.2	2.0
variance (%)	26.8	14.0	12.4
species			
G. trilobus	.3	-.1	-.3
P. obliquiloculata	.3	-.3	.1
G. glutinata	.3	.3	.0
G. ruber	.2	.4	-.2
G. menardii	.2	-.4	-.3
G. truncatulinoides R	.2	.0	.3
N. pachyderma	.2	-.0	.5
S. dehiscens	.2	.2	.1
G. falconensis	.1	.3	.1
G. siphonifera	.1	-.1	-.3
N. dutertrei	.0	-.5	.4
O. universa	-.0	-.3	-.3
G. scitula	-.2	.1	-.3
G. crassaformis	-.3	-.1	.1
G. bulloides	-.4	.1	.1
G. inflata	-.4	.1	-.0

Table 3. Results of a principal component analysis of the frequency distribution of the sixteen most common planktonic foraminiferal species on the ocean floor in the tropical region. Composition of the first three components, eigenvalues, and percentages of total variance.

III.4. SEA-FLOOR DISTRIBUTION AND SURFACE-WATER HYDROGRAPHY

III.4.1. Introduction

The distribution of planktonic foraminiferal species in the surface-water shows a gross relation to surface-water hydrography (e.g. Bradshaw, 1959; Bé and Hamlin, 1967; Berger, 1969; Bé and Tolderlund, 1971; Bé and Hutson, 1977). Bé (1969) and Bé and Tolderlund (1971) were among the first to describe the relation between planktonic foraminiferal zoogeography and gross

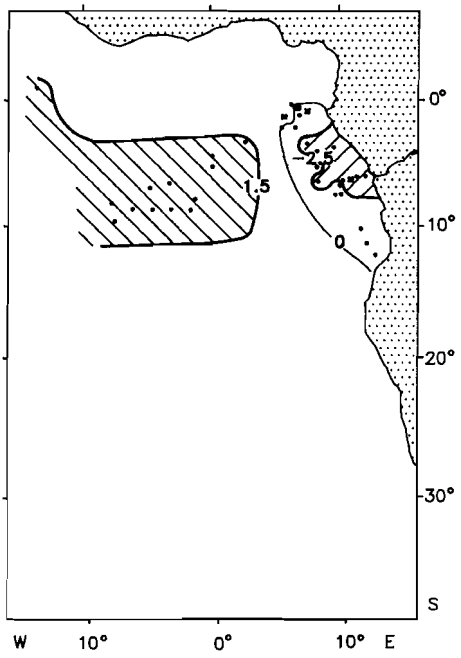

Fig. 19. Contour map of sample scores on the first principal component of the R-mode PC analysis on the core-top data from the tropical region. The faunal contrast between the marginal and mid-oceanic areas is visualized by different hatching.

oceanographic conditions on a global scale and divided the ocean surface-waters into five planktonic foraminiferal provinces, each characterized by a specific association. The provincial boundaries can satisfactorily be described in terms of latitude and circulation and tend to coincide with major oceanic discontinuities.

In order to explain the relationship between faunal patterns and latitude plus circulation, surface-water temperature is commonly assumed to be the most important environmental parameter (e.g. Bé and Tolderlund, 1971; Cifelli, 1971; Parker and Berger, 1971; Bé, 1977; Coulbourn et al., 1980). It is, however, difficult to assess the individual control of a number of other environmental properties (e.g. structure of the watercolumn, general food conditions, seasonal contrast, stability of the system), because they covary with temperature on a global scale, since they are likewise controlled by climate.

Food-supply is generally considered to be another important environmental parameter (e.g. Parker and Berger, 1971; Coulbourn et al., 1980), but again it is difficult if not impossible to separate the effects of surface-water fertility and temperature on the distribution of species from a global point of view. The

significance of surface-water production on the distribution of species is clearly shown in upwelling areas (e.g. Bé and Tolderlund, 1971; Duplessy et al., 1981a; Prell and Curry, 1981; Thiede, 1983) and homothermal water-bodies with a distinct horizontal fertility gradient (e.g. Reiss et al., 1974; Halicz and Reiss, 1981; Almogi-Labin, 1984).

The contention that surface-water temperature and production are of prime importance in the relation between species and environment may seem trivial, but it should be realized that it makes certain considerations rather irrelevant. Any oceanographic feature, which on this general scale is largely defined by temperature and/or fertility, will show a clear correlation with the distribution of species. Interpretation of species distribution in terms of major currents or watermasses seems only meaningful, if the control of temperature and production can be excluded. As a consequence, we reject the faunal parcelling concept of Cifelli and Bénier (1976), which is primarily based on the assumption that the currents determine the distribution of species.

The same restriction holds for salinity, which has often been mentioned as an important environmental parameter (e.g. Bé, 1977; Bé and Hutson, 1977; Thunell, 1978; Loubere, 1981). Although salinity does not covary with temperature and production on a worldwide scale, these factors are generally intimately connected over large parts of the ocean surface. It is, therefore, not surprising that Bé and Hutson (op. cit.) could define a clear salinity range for different species in the Indian Ocean. Subsequent research (e.g. Reiss et al., 1974; Halicz and Reiss, 1981) demonstrated that species can flourish at salinities very different from the values given by Bé and Hutson. Unequivocal evidence of an effect of salinity is, to our opinion, not presented in the literature, and we believe that salinity can control species distribution only under extreme conditions.

A major constraint on the interpretation of planktonic foraminiferal patterns in terms of surface-water characteristics, is that it is well realized that main populations of species may be found in deeper water. Although it is generally accepted that most species grow and calcify in the photic zone (Berger, 1969; Fairbanks et al., 1982), differences in depth habitat have repeatedly been claimed in the literature (e.g. Berger, 1968; Bé, 1977; Duplessy et al., 1981a; Fairbanks et al., 1982; Bé et al., 1985). The studies of Berger (1968) and Bé (1977) even suggest that some species actually prefer depths below the photic layer.

Our knowledge of the vertical distribution of species is, however, still very inadequate. Data are often conflicting and the lack of consistency may be due to (1) seasonal changes in depth habitat (Williams et al., 1981), (2) differences between different hydrographic regions (Fairbanks et al., 1979), and (3) possible sampling errors.

In spite of all this, it has become clear that planktonic foraminifers show large differences in depth habitat in areas with a well-stratified photic layer and a deep chlorophyll maximum (Fairbanks et al., 1979; Fairbanks and Wiebe, 1980; Fairbanks et al., 1982). In the eastern South Atlantic, such a hydrographic setting is found in the Typical Tropical Situation (e.g. Herbland and Voituriez, 1979).

Distribution patterns of planktonic foraminiferal species on the ocean floor differ to some extent from surface-water patterns, but a general relation with the hydrography of the overlying surface-water is usually apparent (e.g. Bé and Hutson, 1977; Coulbourn et al, 1980).

Also in the eastern South Atlantic, surface-water patterns (Bé and Tolderlund, 1971) compare well with patterns on the ocean floor. On the whole, species are, however, dispersed over a larger area on the ocean floor than in the surface-waters. For example, *G. inflata* was not reported from surface-waters north of 15°S and was rare or absent in the surface-waters that overlie the region of maximum abundance on the ocean floor.

The dissimilarity between the two data-sets, stripped of differences in taxonomy, can in part be explained by geographical bias and differences in size-fraction. Bé and Tolderlund used nets with a mesh-opening of 200 μm, while we analysed the 150-595 μm fraction. This difference could for instance explain the apparent absence of the small-sized species *G. scitula* in the surface waters of the eastern South Atlantic. Far more important, however, is the fact that sediment data are fundamentally different from surface-water data. Bé and Tolderlund sampled only the upper ten metres of the water-column and only during certain parts of the year (mainly in May, October and December). By contrast, sea-floor samples provide time-average information on the distribution of species over their complete depth-range, but the original signal can be distorted seriously by post-mortem and post-depositional factors, such as dissolution.

III.4.2. Major faunal patterns on the ocean floor

On the basis of multivariate analyses we discriminated two major sea-floor associations, viz. a tropical and a Benguela Current association, whereas a third, the cool subtropical association showed only up in BALANC/DENDRO analysis.

The tropical association is characterized by *G. glutinata, G. ruber, G. trilobus, G. crassaformis, G. menardii, N. dutertrei,* and *P. obliquiloculata.* The area defined by the tropical association extends as far south as latitude 15°S (fig. 20).

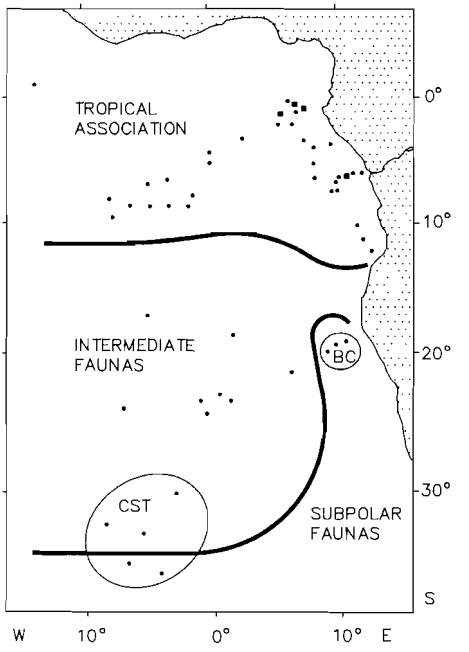

Fig. 20. Major faunal patterns on the ocean floor. BC and CST indicate Benguela Current and Cool Subtropical association, respectively.

Faunas completely different from the tropical association are found in the south-western extreme of the Angola Basin and under the Benguela Current. The faunas in these areas are, however, far from uniform and include two different BALANC/DENDRO associations, a cool subtropical one in the south-west and a Benguela Current association in the south-east. The existence of these two faunal associations suggests that there is a large difference between the SW and the area of the BC, but this is only partly true.

Although the taxa, which define the cool subtropical association, i.e. *G. falconensis, G. hirsuta,* and left-coiling *G. truncatulinoides,* jointly reach relatively high frequencies in the entire south-western area, the overall fauna in this area is far from uniform. This is well exemplified by the results of principal component analysis (see fig. 16b), which show a significant difference between the faunas north and south of 35°S.

In the south-western part of the region, faunas north of 35°S are characterized by high abundances of *G. falconensis* (fig. 10a), whereas *G. bulloides* and *N. pachyderma* (figs. 9d, 12d) flourish south of this latitude. The faunal boundary at 35°S approximately coincides with the position of the Subtropical Con-

vergence, which is centered at 37°S. Considering the fact that the STC is a broad zone, which can vary more than three degrees around its mean position (Tchernia, 1980), the correspondence is altogether satisfactory. The faunal contrast over 35°S, therefore, most likely reflects the surface-water temperature contrast between the cold waters south and the warm waters north of the STC.

Surface-water data of Bé and Tolderlund (1971) show high abundances of *G. bulloides* and *N. pachyderma* south of 40°S, but since they lumped *G. bulloides* and *G. falconensis,* the coherence between the distribution of these two species and the STC can not be ascertained. Sea floor data in the southern Indian Ocean (Malmgren and Kennett, 1977), however, demonstrate a similar change in the frequencies of *G. bulloides* and *G. falconensis* across the STC.

The faunas south of 35°S bear in fact a strong resemblance to those of the Benguela Current area. Both are characterized by high abundances of *G. bulloides* and *N. pachyderma* (see figs. 9d, 12d). This resemblance is readily explained from a similarity in surface-water temperature. An annual mean temperature between 17 and 19°C (Tchernia, 1980; Mellor et al., 1982) seems a fair estimate for both regions.

A similarity between the faunas that occur south of 35°S and in the Benguela Current was also acknowledged by Bé and Tolderlund (1971), who included both areas in their transitional province. Their transitional association consists of a mixture of subtropical and subpolar elements including one indigenous species, viz. *G. inflata.* The distribution of *G. inflata* on the ocean floor (see fig. 13a) is, however, completely different from that in the surface-waters. The sediments under the waters of the transitional province are clearly not exceptionally rich in *G. inflata.* The high frequencies of *G. bulloides* and *N. pachyderma,* actually, indicate that the faunas on the ocean floor are subpolar rather than transitional.

The faunas under the Benguela Current, however, slightly differ from those south of latitude 35°S in the high frequency of *O. universa* and the virtual absence of the elements of the cool subtropical association. As surface-water temperature and salinity are grossly similar (Mellor et al., 1982), the faunal difference is to be attributed to the high fertility associated with the Benguela Current near the African continent. Thus, we surmise that in cold waters high abundances of *O. universa* are indicative of high food levels. This seems in agreement with surface-water data of Bé and Tolderlund (1971), who show that in the Atlantic highest frequencies of *O. universa* are found in the Benguela Current. Furthermore, Bradshaw (1959) observed extremely high frequencies of *O. universa* (over 50 %) in the California Current, which is a similar environment as the Benguela Current.

The distribution of both *G. bulloides* and *N. pachyderma* in cold waters is apparently less affected by the fertility contrast. The virtual absence under the Benguela Current of the elements of the cool subtropical association, viz. *G. falconensis, G. hirsuta* and left-coiling *G. truncatulinoides* (fig. 20), suggests that these species avoid highly productive waters.

We conclude that the faunas south of 35°S and in the Benguela Current area have a predominantly subpolar aspect (fig. 20), which results from the overall low surface-water temperature. The specific character of the BC fauna is due to the high surface-water production.

The part of the Angola Basin in between the tropical region and the areas with a predominantly subpolar aspect (fig. 20), is not characterized by a distinct multispecific association. Principal component analysis clearly suggests that the faunas have an intermediate character (see fig. 17).

Right-coiling *G. truncatulinoides* is the only taxon that is more or less characteristic of the intermediate faunas between 15 and 35°S. The taxa of the cool subtropical association, viz. *G. falconensis, G. hirsuta,* and left-coiling *G. truncatulinoides,* are relatively frequent only in the southern part of this area, which indicates that they abound at overall lower temperatures than right-coiling *G. truncatulinoides.*

Bé and Tolderlund (1971) included *G. hirsuta* and *G. truncatulinoides* in their subtropical association. Their data show that both species reach their highest abundances in the waters directly north of the STC. A connection between *G. hirsuta* and *G. truncatulinoides* and relatively cold subtropical waters is broadly consistent with observations in the Indian Ocean (Bé and Hutson, 1977; Duplessy et al., 1981a). The replacement of right- by left-coiling *G. truncatulinoides* toward higher latitudes is seen in the entire southern hemisphere (Bé and Tolderlund, 1971; Parker, 1971).

A comparison between the faunal patterns on the ocean floor (fig. 20) and surface-water hydrography clearly shows that differences in the areal extent of the major sea-floor associations are maintained by differences in surface-water temperature and fertility. The tropical association underlies the northern segment of the subtropical gyre, where the system of equatorial countercurrents interacts with the South Equatorial Current. Annual mean surface-water temperatures are in excess of 23°C (Mellor et al., 1982).

Faunas with a predominantly subpolar aspect are found in the area of the Benguela Current and south of the STC and essentially reflect the northward extension of cold (17-19°C) waters. The high production associated with the BC is expressed in the faunas by high frequencies of *O. universa.*

Faunas in between the tropical and cold water areas are poorly defined and

display an intermediate signature; they are associated with low surface-water production and intermediate surface-water temperatures. Right-coiling *G. truncatulinoides* is the most characteristic element of the intermediate faunas. *G. hirsuta,* and left-coiling *G. truncatulinoides* are frequent north and south of the STC and *G. falconensis* is, therefore, the only species characteristic of the southernmost intermediate faunas.

The most conspicuous differences between the faunal patterns on the ocean floor and in the surface-water (Bé and Tolderlund, 1971) are (1) the northward displacement of the subpolar faunas on the ocean floor and (2) the absence of a transitional sea-floor association defined by *G. inflata.*

III.4.3. The tropical region

Multivariate analyses on the data-matrix of the tropical region demonstrated a major difference between the faunas in the area off the river Zaire and those from the more central part of the ocean (figs. 18, 19). Faunas off the river Zaire are characterized by a high proportion of pink *G. ruber* and high percentages of *G. bulloides, G. crassaformis,* and *G. inflata.* Pink *G. ruber* and *G. inflata* abound in fact near the continent throughout the tropical region, whereas elevated percentages of *G. bulloides* and *G. crassaformis* are restricted to the outflow-area of the river Zaire. *G. scitula*, which was tentatively added to the marginal association, shows a rather non-descript distribution (cf. Pujol, 1980) and will be excluded from further discussion.

G. bulloides is generally thought to be living near the surface (e.g. Bé et al., 1985). The flourishing of *G. bulloides* in front of the river Zaire suggests a relation with lowered salinities, but literature data support another explanation. In warm water regions, anomalously high frequencies of *G. bulloides* are observed in high-production areas, which are best summarized as (near) coastal upwelling environments (e.g. Cifelli and Smith, 1974; Bé and Hutson, 1977; Coulbourn et al., 1980; Duplessy et al., 1981a; Prell and Curry, 1981; Thiede, 1983; Thunell and Reynolds, 1984; Zhang, 1985) and nutrient-rich marginal basins (Barmawidjaja et al., 1988).

The high frequencies of *G. bulloides* observed in the surface waters off the river Bandana (Ivory Coast) during September (Eckert, 1965), for which an explanation has as yet not been given, must to our opinion also be attributed to coastal upwelling. Coastal upwelling periodically occurs in this region (Voituriez and Herbland, 1981) and is a likely cause for the strikingly low surface-water temperatures reported by Eckert.

Surface-water temperatures in these highly productive waters are extremely variable and can be as high as 29°C (Barmawidjaja et al., 1988), which indicates

that in warm water regions percentages of *G. bulloides* are primarily controlled by food supply. The area of the Zaire river plume is also exceptionally productive. We, therefore, attribute the flourishing of *G. bulloides* in this area to the elevated food levels rather than to lowered salinities. Cooling of the surface waters by ridging of upwelling of deep waters fails to offer an explanation also in this region, because the percentage distribution of *G. bulloides* shows no relation with surface-water isotherms.

Globorotalia crassaformis seems even more distinctly associated with the Zaire outflow than *G. bulloides*. This species attains the highest relative numbers just in front of the river, where the overlying surface-water salinity is below 25 per mil. Again a relation with lowered surface-water salinities may be suggested, were it not that such a low salinity is considered lethal (Boltovskoy and Wright, 1976).

G. crassaformis is in general a minor element of modern faunas and its habitat characteristics are poorly known. Bé and Hamlin (1967) and Bé (1977) considered it to be deep-living (below 100 m). Jones (1967) reported a marked preference for depths between 100 and 250 metres in the area of the Equatorial Under Current, where high abundances of this species seem to coincide with low oxygen concentrations. A possible relation between this species and low oxygen concentrations seems of interest, because a pronounced oxygen minimum layer is present off the rivermouth at a depth of only few hundreds of metres. Oxygen deficiency is particularly marked in the upper part of the canyon near the rivermouth, where oxygen concentrations of less than 75 μmol/l are found below 75 metres depth (Van Bennekom et al., 1978).

A relation with oxygen-poor waters or any parameter covarying with oxygen concentration could explain the sparcity of *G. crasssaformis* in the world ocean. Optimum habitat conditions might be found in warm and oxygen deficient subsurface waters. A very shallow position of the thermocline seems a prerequisite to realize these conditions.

G. inflata is the only species that is found in relatively high numbers (generally over 20 %) all along the African coast from the area of the Benguela Current up to approximately 3°S. Even north of this latitude it is distinctly more frequent near the continent than in the central tropical area.

We consider *G. inflata* a surface-dwelling species, because oxygen isotope data indicate that this species calcifies in the surface mixed-layer only (Fairbanks et al., 1980). The distribution of *G. inflata*, however, shows no relationship with year-averaged surface-water temperatures in the region under consideration.

Coulbourn et al. (1981) and Loubere (1981) suggested that the distribution of this species primarily correlates with the surface-water temperature during the

cold season. Cold-season surface-water temperature data in the Angola Basin (Mazeika, 1968; Hastenrath and Lamb, 1977) indeed suggest that high abundances of *G. inflata* (over 20 %) only occur in regions with surface-water temperatures below 23°C. In spite of this overall relationship, relatively cold waters are not everywhere characterized by high abundances of *G. inflata.* North of 3°S, *G. inflata* reaches higher abundances along the coast than further off-shore, although surface-water temperatures are similar in both areas during the cold season. We, therefore, agree with Loubere (1981), that cold season surface-water temperatures alone can not explain the distribution of this species. Hence, food levels may exert additional control on the distribution of *G. inflata.*

Thiede (1975) suggested that *G. inflata* is anomalously abundant in the upwelling area off NW Africa. The distribution of planktonic foraminiferal species off NW Africa (Bé and Hamlin, 1967; Cifelli, 1974; Thiede, 1975; Cifelli and Bénier, 1976) in relation to coastal upwelling conditions (Wooster et al., 1976), however, indicates that *G. bulloides* and *G. quinqueloba* are the principal upwelling indicators. Elevated percentages of *G. inflata,* on the other hand, fringe the upwelling centres. This suggests that *G. inflata* thrives at intermediate food levels.

The flourishing of *G. inflata* in the near-shore area remains puzzling, because during the cold season cold and nutrient rich waters reach to the surface in the entire equatorial region (0-6°S). As a consequence, surface-water temperature and fertility differences are smoothed out within the equatorial region, unless the upwelling waters in the near-shore and off-shore areas have a different nutrient content.

In the Equatorial Divergence the upwelling water mainly originates from the EUC and Wauthy (1977) suggested that upwelling along the coast is fed by the same current. Van Bennekom and Berger (1984), however, showed that Wauthy overestimated the contribution of the EUC to the shallow subsurface waters along the African coast (1 -13.50°). They suggested a much larger contribution of SECC and BC water mixtures, which have higher nutrient contents than the EUC. In view of their results and because of the possible influence of the Zaire outflow, we can not exclude that during the cold season the coastal surface-waters have higher nutrient contents than the surface-waters in the Equatorial Divergence.

Although we must admit that evidence for a fertility contrast is weak, we assume for the time being that relatively high food levels in combination with lowered surface-water temperature during the cold season determine the high abundances of *G. inflata* in the tropical near-shore area.

The pink variety of *G. ruber* completes the marginal association of the tropical region. *G. ruber* is preeminently a species of warm and nutrient-poor waters (e.g. Almogi-Labin, 1984) and the pink variety is thought to be indicative of higher surface-water temperatures than the white type (e.g. Pujol, 1980). Bé and Hamlin (1967) found only white types in the cool Canary Current and Bé and Tolderlund (1971), as well as Deuser et al. (1981), concluded that pink *ruber* abounds in the North Atlantic only during the warm season. Our observations point in the same direction, because pink *ruber* is virtually absent south of 15°S, where during the warm season surface-water temperatures are below 24°C (Mazeika, 1968).

If the pink variety is indeed virtually restricted to the warm season, we can explain the percentage distribution of the pink variety on the ocean floor to some extent by assuming that *G. ruber* only occurs during the warm season in the marginal tropical area, whereas this species lives troughout the year further off-shore. This assumption seems reasonable, because over a large part of the tropical area cold-season surface-waters temperatures are lower near the continent than in the open ocean. An alternative explanation was given by Orr (1969), who interpreted high abundances of pink specimens in shelf and upper slope sediments as a result of higher sedimentation rates, suggesting that the pink colour fades with time. Neither of the two explanations can, however, account for the fact that high proportions of pink *G. ruber* are also observed in surface-waters near the continent (Bé and Tolderlund, 1971). The only explanation we can think of is that high food levels somehow stimulate pink-coloured specimens.

Multivariate analyses set the marginal tropical association against an off-shore fauna of white *G. ruber, G. trilobus, G. menardii,* and *P. obliquiloculata,* and the rather cosmopolitical *G. glutinata* (figs. 18, 19). All these elements probably avoid the near-shore area, because of the lowering of the surface-water temperatures during the cold season and/or the relatively high fertility. It should be noted that *G. trilobus* and *G. menardii* are particularly scarce in front of the river Zaire (see figs. 9b, 13c). These low frequencies can not be attributed to lowered surface-water temperatures during the cold season.

Another four species that are common in the tropical region, viz. *G. siphonifera, N. dutertrei, N. pachyderma,* and *O. universa,* do not cluster with either the marginal or the off-shore faunal group.

Among these species, *N. dutertrei* shows high abundances (above 10%) in the equatorial zone, reaching maximum percentages (20-25 %) close to the equator not far from the continent (fig. 12c). The abundance pattern suggests a relation between *N. dutertrei* and the year-round high-production zone, which parallels

the equator between 0° and 5 to 6°S. During the warm season, the thermocline is at shallow depth in this area and oceanic upwelling occurs during the cold season. Within the Equatorial Divergence primary production increases from west to east. Percentages of *N. dutertrei* also increase in an eastward direction, which suggests a relation between the abundance of *N. dutertrei* and the level of primary production.

A relation between high abundances of *N. dutertrei* and upwelling is well recognized in the literature (Parker and Berger, 1971; Coulbourn et al., 1980; Duplessy et al., 1981a; Thiede, 1983; Thunell and Reynolds, 1984; Zhang, 1985). In the Panama Basin, Fairbanks et al. (1982) found this species to be associated with the deep chlorophyll maximum. Their findings seem in agreement with the depth distribution of *N. dutertrei* in the equatorial Atlantic (Jones, 1967). Thunell and Reynolds (1984), furthermore, noticed that relative and absolute abundances of *N. dutertrei* considerably increase in the Panama Basin, when the thermocline shallows in response to upwelling. All these observations indicate that abundances of *N. dutertrei* are controlled by the depth of the thermocline and, therefore, correlate with the total production of the photic zone.

Near the continent frequencies of *N. dutertrei* are definitively low, which indicates that the productive near-shore waters west and north of the mouth of the river Zaire are somehow different from the productive waters of the Equatorial Divergence.

There is, in our opinion, little reason to assume that *N. dutertrei* is low-frequent along the continent during the warm season. The deep chlorophyll maximum extends probably from the off-shore waters into the major part of the near-shore tropical area. River-induced upwelling and turbulent mixing of the surface water may locally prevent the development of a well-stratified photic layer, but it seems reasonable to assume that subsurface conditions are in general favourable for *N. dutertrei* near the continent during the warm season. We surmise that the low percentages of *N. dutertrei* along the continent are to be attributed to the absence of this species during the cold season. *N. pachyderma* which, as to be discussed in a subsequent chapter is regarded as merely a low-temperature variant of *N. dutertrei,* is virtually absent too (see fig. 13a). This suggests that cold season conditions near the continent are not favourable for neogloboquadrinids in general. *G. inflata,* on the other hand, flourishes near the continent during the cold season. The inverse relation between *G. inflata* and *N. dutertrei* in the tropical region indicates that the hydrography of the near-coastal waters is fundamentally different from that in the offshore area during the cold season.

The surface-water nutrient enrichment in the off-shore region during the cold season is governed by oceanic upwelling but that of the near-coastal waters is less well-understood. Most authors assume that coastal upwelling takes place along the continent, in particular between the mouth of the river Zaire and 1.50°S (e.g. Wauthy, 1977; Piton et al., 1978). Berrit (1976), however, argued that it is doubtful whether the cooling at the surface is due to classical coastal upwelling caused by Ekman transport. As discussed by Voituriez and Herbland (1982), the cooling may merely result from ridging of deep water without significant vertical water movement.

G. inflata is a mixed layer species, whereas *N. dutertrei* proliferates in the chlorophyll maximum associated with the thermocline. - For clearness' sake, we should point out that the term 'deep chlorophyll maximum' has only signification in the warm season. The chlorophyll maximum associated with the thermocline is during the cold season locally at the surface in the offshore waters (Voituriez et al., 1982). - Because the two species do not have the same habitat, the structure of the photic layer may be different in the offshore and near-coastal waters during the cold season.

Studies by Herbland, Voituriez and their co-workers have shown that the oceanic equatorial system has particular characteristics. Voituriez et al. (1982) found that in spite of the fact that the oceanic equatorial system changes from a Typical Tropical Situation to equatorial upwelling, primary production and zooplankton biomass in the photic layer are not subject to significant seasonal variation. Since upwelling enriches the well-illuminated surface-waters with nutrients, the lack of seasonal contrasts suggests that consumption of nutrients remains low. The low level of nutrient consumption was interpreted in terms of the so-called 'paradox of nutrients' of Walsh (1976), which states that blooming of phytoplankton in response to enhanced nutrient levels is prevented by effective grazing by herbivores. Walsh argued that this implies a certain equilibrium between phytoplankton and zooplankton biomass, which is only possible in a fairly constant physical environment. Referring to the stability of the oceanic equatorial system, Herbland et al. (1983) suggested that the equatorial upwelling ecosystem may be fundamentally different from coastal upwelling and temperate systems, which are both characterized by high-amplitude variations in physical parameters. Voituriez and Herbland (1984) showed that the temperature/nitrate relation is maintained in the photic layer of the equatorial zone, when the system changes from a Typical Tropical Situation to a state of upwelling. They discussed that the deep waters conserve their stability and thermal structure when they rise to the surface during upwelling.

Accordingly, we assume that the inverse relation between *G. inflata* and *N. dutertrei* reflects primarily a difference in ecosytem stability between the near-coastal and offshore equatorial waters.

We suggest that the offshore equatorial system is relatively stable, because the photic layer remains well-stratified throughout the year. Thus, *N. dutertrei* flourishes year-round in the off-shore waters of the equatorial zone, because the waters near the thermocline remain fairly unchanged except for their depth. *G. inflata* may be low frequent in the off-shore region because the food-levels at the surface remain too low, but we surmise that this species can not sustain the large temperature gradient in the waters.

We hypothesize that the coastal 'upwelling' system in the region under consideration is, on the other hand, relatively dynamic and assume that a well-stratified photic layer is absent near the continent during the cold season. Unfortunately, hydrographic profiles are lacking to support this idea but if actual, wind-driven, coastal upwelling occurs in this region, enhanced vertical mixing would prevent a well-defined stratification to develop. A non-stratified photic layer seems less plausible if the cooling of the surface waters near the continent is to be ascribed to ridging of deep waters. However, as a rule vertical and lateral friction significantly increase near continents (Gallardo, 1981) and we may, therefore, assume that even in the case of ridging stratification of the photic layer is less well-developed near the coast than further off-shore.

All things considered, we suggest that *N. dutertrei* is absent along the coast during the cold season, because its specific requirements, viz. relatively high food levels associated with a thermal gradient, are lacking. *G. inflata,* on the other hand, flourishes near the continent during this season because the (near) surface waters are thermally relatively homogeneous, cool and fairly productive.

G.bulloides resembles *G. inflata* in that it is also a surface-dwelling species. Thus, the near-absence of *G. bulloides* in the off-shore equatorial region might likewise be related to the structure of the photic layer. *G. bulloides* is, however, not necessarily restricted to the cold season. We discussed earlier that high abundances of this species primarily reflect the presence of nutrient-rich surface waters, whereas the abundance of *G. inflata* is controlled rather by surface-water temperature. During the warm season, *G. bulloides* must be virtually absent in the off-shore equatorial waters because surface-waters are nutrient depleted. Along the continent and especially in front of the river Zaire, *G. bulloides* may flourish also during the warm season because river run-off and local river-induced upwelling enrich the near-coastal surface-water in nutrients year-round. The area influenced by the river Zaire approximately coincides with the coastal region most strongly influenced by the 'upwelling' processes during winter. It must, therefore, remain uncertain whether the 'upwelling' contributes to the anomalously high abundance of *G. bulloides* in front of the river Zaire.

Note: Discussing seasonal differences in the faunas we simply reasoned in terms of warm and cold season. It should be mentioned that cold season merely stands for peak cold season conditions, i.e. the period of maximum upwelling activity.

Concluding remarks

Evaluation of the downcore frequency patterns of *G. bulloides, G. inflata, G. menardii, N. dutertrei* and *N. pachyderma* provides additional information on the factors controlling the distribution of these taxa. To give an overview, we summarize the habitat characteristics of these taxa.

The closely related taxa *N. dutertrei* and *N. pachyderma* are both living in the chlorophyll maximum which is associated with the top of the thermocline. These taxa flourish only when the photic layer is thermally well-stratified and reach highest frequencies if the thermocline is at shallow depth. The temperature regime at the top of the thermocline determines the ratio between *dutertrei* and *pachyderma* types, with *dutertrei* types predominating at relatively high temperatures.

G. menardii is also linked up with the chlorophyll maximum at the top of the thermocline. Relatively high subsurface temperatures are critical for the presence of this species.

G. inflata flourishes in thermally homogeneous and cool (near-) surface waters with intermediate food levels. This species is considered indicative of a poorly or not stratified photic layer, but is low frequent in areas of intense coastal upwelling. The flourishing of this species in the present-day marginal tropical area is to be attributed to ridging of deep waters in a coastal setting.

G. bulloides abounds in thermally homogeneous (near-) surface waters. In cold water regions this species flourishes at variable food levels, but in warm waters regions only at high food levels. The high abundances of this species in the present-day marginal tropical region are primarily determined by the river input of nutrients.

Chapter IV

SEA-FLOOR DISTRIBUTION OF BENTHIC FORAMINIFERS

IV.1. INTRODUCTION

Quantitative research on the distribution of benthic foraminifers in the deep waters of the Atlantic Ocean was initiated by Schott (1935) and Phleger et al. (1953) and gained renewed interest by the introduction of the water-mass concept in benthic foraminiferal ecology (Streeter, 1973; Schnitker, 1974).

Little research has as yet been done in the eastern South Atlantic. Gofas (1978) analysed a transect over the Walvis Ridge near the African continent between 3300 and 5060 metres depth, but the larger part of the area remained unstudied. The present chapter primarily reports on the distribution of benthos at depths of more than 2000 metres in the Angola Basin. A small number of samples from shallower water have been included, particularly from the area in front of the river Zaire. Shallow-water faunas from this region were earlier studied by Kouyoumontzakis (1979), who analysed associations from the Congolese shelf.

Sample selection

The age of the samples was estimated on the basis of the same criteria as used for the selection of samples for planktonic foraminiferal analysis; samples that were considered of pre-Holocene age were discarded.

The effect of dissolution on the composition of benthic associations is poorly known. Although benthic foraminifers are, as a rule, less easily affected than planktonic species, it is obvious that dissolution is to be of some consequence. Corliss and Honjo (1981) demonstrated that benthic species differ considerably in resistance to dissolution. Unfortunately, only a few species were considered in their experiments and a general ranking in terms of dissolution resistance is not even available for the most common species. A complicating factor is that it is generally assumed that the preservational potential of benthic foraminifers is dependent on their habitat (Adelseck, 1978; Corliss and Honjo, op. cit.). Species that live and die in the sediment are probably less affected by undersaturated bottomwaters than epibenthos. In the absence of sound criteria to evaluate changes brought about by dissolution, we selected the samples (fig. 21) irrespective of their preservational state.

The benthic foraminiferal faunas were analysed in two size fractions, the 63-

595 μm and 150-595 μm fraction. Samples showing evidence of down-slope transport were excluded from the data-base. Occasionally, down-slope contamination seemed restricted to the 63-150 μm fraction. These samples were included in the study of the larger size fraction, if omission would have created an important gap in the data-set.

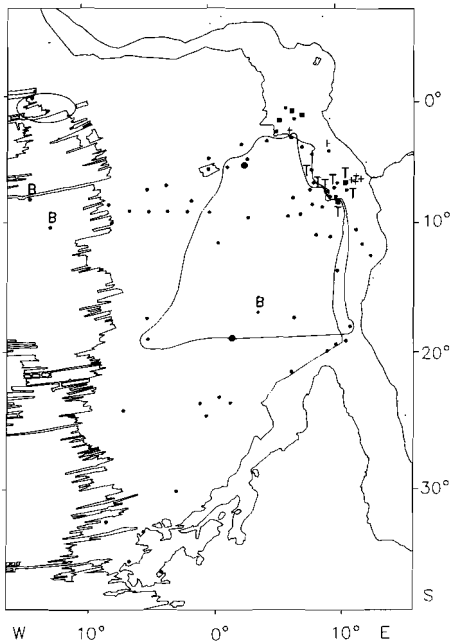

Fig. 21. Location of core-tops selected for benthic foraminiferal analysis. Double-sized dots indicate two samples studied from the same locality. B indicates only 150-595 μm fraction studied, T only 63-595 μm fraction. Crosses mark samples from relatively shallow depth (75-1017 m). Samples showing evidence of severe dissolution are enclosed and the 4000 metres isobath is shown.

We aimed to count at least one hundred specimens in both size-fractions. The size of the samples, however, was not always sufficiently large to reach this number and we had to settle for a minimum of 66 specimens in the 150-595 μm (large-size) fraction and of 99 specimens in the 63-595 μm (total) fraction.

The final selection for the analysis of the total fraction consists of 81 samples, whereas 77 samples were used for the study of the large-size fraction (fig. 22). It should be noted that the selection is unbalanced with respect to depth and geographic distribution.

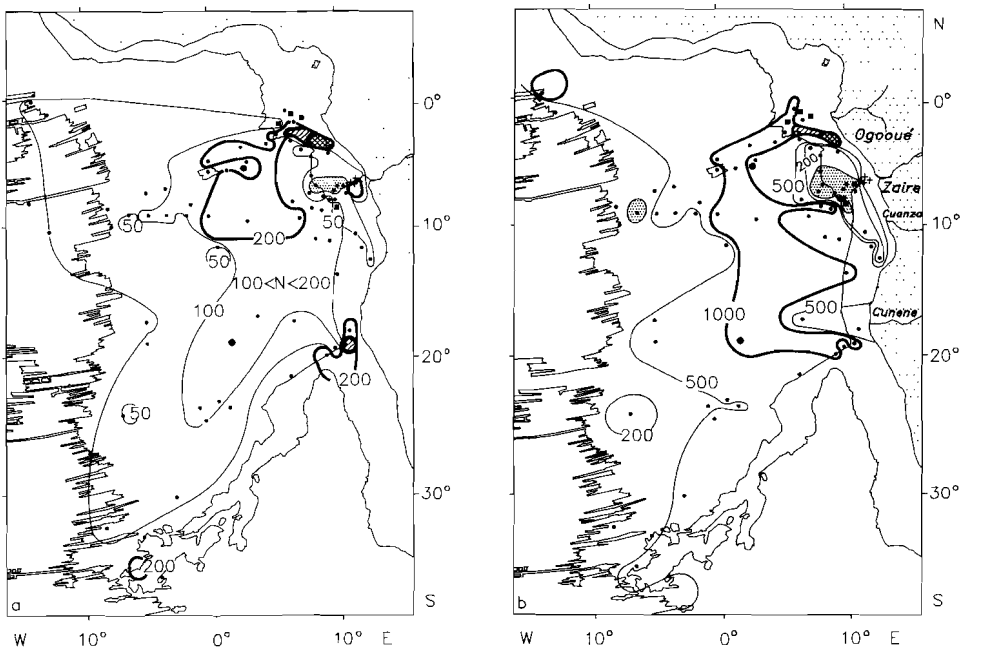

Fig. 22. Contour map of the benthic foraminiferal number (specimens per gram of dry sediment): (a) 150-595 μm fraction. Shading indicates less than 10, hatching more than 500, and double hatching more than 1000 specimens. (b) 63-150 μm fraction. Shading indicates less than 100, hatching more than 5,000, and double hatching more than 10,000 specimens.

Foraminiferal number

The number of benthic foraminifers (excluding agglutinants) in the large-size fraction, standardized to one gram of dry sediment, ranges from seven to 800 (fig. 22a). An exceptionally high number is reached at 719 metres depth north of the river Zaire (VM29-140). Here, the benthic foraminiferal number exceeds 6,500 and the sediment can be classified as a foraminiferal sand.

The lowest densities (less than 50) are reached on the upper part of the Zaire deep-sea fan and in the adjacent area. These low numbers are probably mainly caused by dilution with terrigenous matter, but dissolution may locally be of consequence as well. Although the abundance pattern seems to be rather irregular outside the area of lowest density, the foraminiferal number tends to be lower in the western than in the eastern part of the region. Since dilution with non-carbonate matter can be ruled out as an explanation, this difference must be attributed to either dissolution or standing stock variation. In the eastern area, many samples show signs of severe dissolution (see fig. 21) and it

is , therefore, most likely that preferent dissolution of planktonic foraminifers led to relative enrichment with benthics in these samples. Dissolution can, however, hardly explain the relatively high values (over 200) that are locally reached near the Guinea Rise and in the south-east of the region, because even well-preserved samples have higher numbers here than in the west. We surmise that differences in the standing stock of benthic foraminifers are responsible for this contrast. Large standing stocks may also explain the relatively high numbers in the samples directly in front of the river Zaire.

The 150-595 μm fraction generally makes up between ten and twenty per cent of the total fraction. The benthic foraminiferal number in the 63-150 μm fraction ranges from 11 to more than 10,000. The general pattern (fig. 22b) strongly resembles that of the large-sized benthic foraminifers. The lowest values (10-200) are again reached near the Zaire deep-sea fan (see also Zachariasse et al., 1984), and the numbers are as a rule higher in the eastern than in the western part of the region. The density pattern along the continental margin, seems to reflect variation in dilution with terrigenous matter more clearly than the foraminiferal number in the coarse fraction. Relatively low numbers are not only found in the area of the Zaire deep-sea fan, but also in front of the other major rivers.

Species selection

Six surface samples were analysed from relatively shallow water, i.e. between 75 and 1017 metres. The reason that we included these shelf and upper slope faunas, is to have at least an idea of the bathymetric range of the species that occur at great depth and furthermore to obtain some control over possible down-slope contamination. The overall composition of these shallow-water faunas is very different from our deep-sea faunas and they are only briefly discussed.

The main point of study concerns the distribution of benthic foraminifers in the deep-sea, which in the present study covers the interval between 1760 and 5608 metres. Deep-sea taphocoenoses of benthic foraminifers differ at least in one respect markedly from biocoenoses, viz. agglutinated species generally abound in living associations, whereas they are almost lacking in fossil faunas. According to Douglas and Woodruff (1981), this loss must be explained by the breakdown of organic cements through bacterial and chemical action.

Among the agglutinated foraminifera, *Adercotryma, Cyclammina, Psammosphaera, Reophax,* and *Rhabdammina* species occur in only few deep-sea samples, whereas representatives of *Eggerella, Karreriella,* and *Siphotextularia* are generally present but in low percentages. The latter three genera are, ap-

parently, more resistent to destruction, presumably because the cement of their tests is well-mineralized. The low and variable preservability of this group makes it of little interest from our point of view. As a consequence, we excluded all agglutinated forms from quantitative analysis.

Among the non-agglutinated foraminifera, about seventy species were found to be rather common in the deep-sea samples. Monothalamous and porcellaneous foraminifers (excluding *Pyrgo*) were not determined to the species level. Particularly the monothalamous group shows extensive morphological variation in the deep-sea and comprises numerous species. Although both groups are represented in practically all our samples, individual species are so scarce, that we did not take the trouble to classify them.

We shall only discuss the distribution of deep-sea species, which attain an abundance of more than 4.4 per cent in either of the two size fractions of at least one sample from below 1750 metres depth.

Generally emphasis will be put on their distribution in the large-size fraction, because this is considered the most informative. The distribution in the total fraction mainly reflects the frequency of species in the 63-150 μm fraction, because small specimens largely outnumber the bigger ones. This is rather unfortunate, because (1) the small size fraction is more easily influenced by downslope contamination, (2) determination of small individuals is much more difficult especially if faunas suffered from dissolution, and (3) the 63-150 μm fraction is often dominated by the small-sized *Nuttallides pusillus,* which makes frequencies of larger species to a large extent dependent on the abundance pattern of this species alone.

IV.2. SPECIES DISTRIBUTION ON THE OCEAN FLOOR

IV.2.1. Shelf and upper-slope faunas

There is in general but little similarity between the faunas of the shallow depth-range (75-1017 m). The associations are dominated in the 150-595 μm fraction by species of *Bolivina, Bulimina, Cassidulina, Cibicides,* and *Uvigerina* (table 4). The various species of *Bulimina* are limited to distinct depth-intervals and seem to succeed each other with increasing depth: *B. gibba* (75-267 m), *B. costata* (225-267 m), and *B. aculeata,* which ranges from 267 metres down to more than 2,000 metres depth. *Bolivina* species are virtually restricted to the shallow depth interval. *Nonionella asterizans,* which is the most abundant species at the outer shelf north of the river Zaire (Kouyoumontzakis, 1979), is only found in our samples from 75 and 225 metres depth and in low percentages (maximum 5%).

depth (m) / species	75	225	267	605	719	1017
Bolivina striatula spinata	19	1				
Bulimina marginata	20	14	4			
Cassidulina carinata	7	18	18	10	21	7
Uvigerina peregrina s.s.	6	12	17	15	12	5
Bulimina costata		7	17			
Bolivina dilatata			4	10	24	
Cibicides pseudoungerianus				12	3	1
Bulimina aculeata		1		27	4	2
Cassidulina carapitana						25
Globocassidulina subglobosa					2	10

Table 4. Relative frequencies of the most common species (150-595 μm) in the core-tops taken from relatively shallow water.

depth (m) / species	75	225	267	605	719	1017
Trifarina angulosa pauperata	18	1			1	
Cassidulina minuta	18	9	2	1	4	2
Bulimina marginata	9	16	2		*	
Cassidulina carinata		17	23	3	16	5
Bulimina costata		3	10			
Bolivina dilatata	2	5	4	54	19	
Nuttallides pusillus turgidus		1	2	3	20	

Table 5. Relative frequencies of the most common taxa (63-595 μm) in the core-tops taken from relatively shallow water; (*) less than 0.5 %.

The composition of the associations in the total fraction is completely different (table 5). Species that are too small to be found in the large-size fraction, e.g. *Cassidulina minuta, Nuttallides pusillus turgidus, Trifarina angulosa pauperata,* may dominate the faunas in the total fraction. It is self-evident that large-sized species such as *B. aculeata, Cibicides pseudoungerianus,* and *U. peregrina,* are squeezed to lower frequencies.

IV.2.2. Distribution of common deep-sea species

The species will be treated in order of increasing depth habitat, and polytypic species are treated separately. Unless otherwise indicated, the distribution in the large-size fraction is discussed. The frequency distribution of species is usually shown on maps or in depth-latitude diagrams.

Cassidulina carinata is continuously present from 75 down to 2392 metres ex-

cept in core RC13-225, located at 2078 metres north of the Walvis Ridge (fig. 23a). The samples that cover this depth interval are all on the continental margin. This species occurs down to 2675 metres on the easternmost part of the Walvis Ridge. Abundances of ten per cent and more are found over a large depth-range (225-2392 m) in a geographically coherent area which extends from the Zaire canyon northward to approximately 3°S.

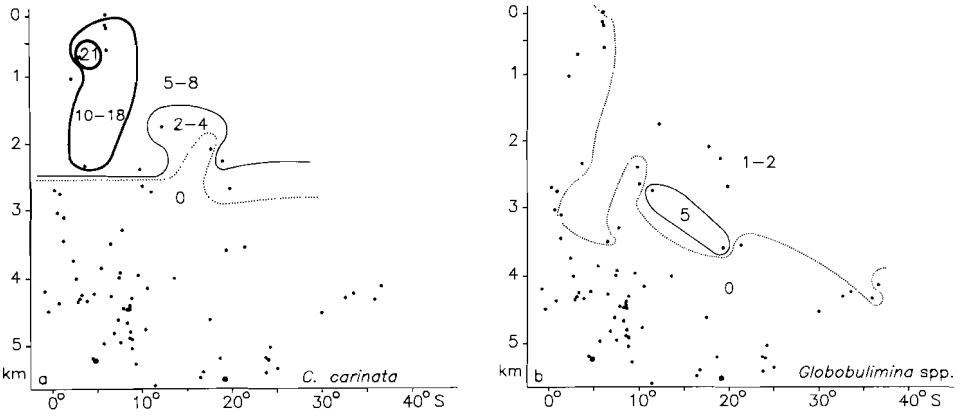

Fig. 23. Depth-latitude diagram showing the percentage distribution of selected species in the 150-595 μm fraction unless otherwise indicated : (a) *C. carinata*, (b) *Globobulimina* spp. Figure conventions as in fig. 9a.

Globobulimina spp. nowhere exceed the five per cent level (fig. 23b). With the exception of the deepest occurrence (4325 m, Walvis Passage), this species category is only found on the continental margin including the easternmost part (east of 8°E) of the Walvis Ridge. South of latitude 9°S, *Globobulimina* spp. are continuously present between 1760 and 3585 metres, but in the north they are only occasionally found and at variable depths (75-348 m).

Bolivinita cincta is virtually restricted to the 63-150 μm fraction. It occurs scattered between 267 and 3585 metres depth and frequencies in the total fraction do not exceed ten per cent (fig. 24a). The samples that cover this depth-interval are all on the continental margin

Bulimina aculeata (fig. 24b) is continuously present between 267 and 2270 metres, except at 2078 metres depth (RC13-225). Again samples from this depth interval are limited to the continental margin. This species is most frequent at 605 metres in the Zaire area, where it dominates the faunas in the large-size fraction.

Hoeglundina elegans occurs locally between 267 and approximately 4000 metres depth (fig. 25a) and a single specimen is found in deeper water (4660 m).

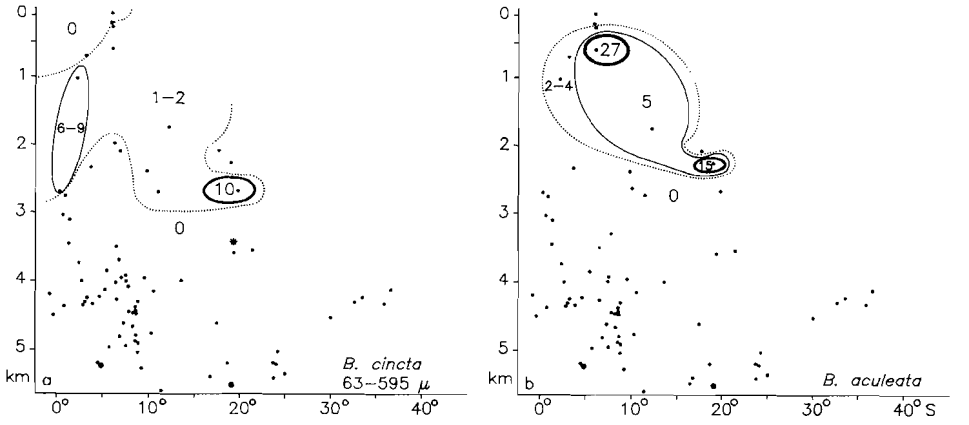

Fig. 24. Depth-latitude diagram showing the percentage distribution of selected species in the 150-595 μm fraction unless otherwise indicated : (a) *Bolivinita cincta* (63-595 μm), and (b) *B. aculeata.* Figure conventions as in fig. 9a.

It is only present in appreciable numbers (3-6 %) between 2000 and 4000 metres depth. These relatively high frequencies are attained both near the continent and in land-distant areas, but this species is completely missing in the area of the Zaire deep-sea fan and in the marginal region between 12.5 and 20°S.

Gavelinopsis translucens is a small species, which reaches the five-per cent level only in the total fraction (fig. 25c). It is strictly limited to depths between 600 and 2400 metres, i.e. on the continental margin, and the highest relative number is attained at 1988 metres in front of the river Zaire.

Uvigerina auberiana occurs in only two samples, viz. at 605 metres depth in front of the river Zaire (4 %) and at 2078 metres depth on the continental margin north of the Walvis Ridge (RC13-225), where it is relatively frequent (23 %).

Bulimina subacuminata is very abundant in core RC13-225 (2078 m) and a single specimen occurs at 719 metres (fig. 25d). This species is morphologically close to *B. inflata* which, although low-frequent, is continuously present on the continental margin between 1760 and 2685 metres depth, except in RC13-225.

Melonis barleeanus occurs from 719 down to 4660 metres, but is not found in all samples (fig. 25b). It is only occasionally present towards the boundaries of its depth range and frequencies of more than five per cent are restricted to depths between 1760 and 3585 metres. These high abundances are reached on the continental margin south of 10°S and in one sample north of the Zaire fan. Elsewhere, i.e. on the Mid Atlantic Ridge, Guinea Rise, and Zaire fan this species is practically absent at comparable depth.

Globocassidulina subglobosa ranges from 719 metres down to the deepest sample studied (fig. 26a). Although it may be rather common at widely scattered places, relative abundances of more than ten per cent are only found in the north-eastern part of the region (2630-4660 m). Highest frequencies are reached between 4000 and 4400 metres near the Romanche Fracture Zone and locally on the Guinea Rise. This species tends to be scarce (below 5 %) both above 2500 metres and below 5000 metres. In the area of the deep-sea fan, it is completely missing between 3900 and 4800 metres depth.

In the total fraction, *Globocassidulina subglobosa* is generally one of the most prominent species and with few exceptions it is present in all samples (fig. 26b). Low frequencies are reached along the continent, in the area of the Zaire deep-sea fan and in the deepest part of the Angola Basin. Abundances of more than twenty per cent are found west of 0° longitude in the north (3950-4850 m) and locally also in the south (4325-4525 m) (fig. 26c). The highest abundance (44 %) occurs near the Romanche Fracture Zone (4195 m).

Bulimina rostrata is the deepest ranging species of *Bulimina* in the coarse size-fraction (fig. 26d). It occurs in low abundances between 1000 and 3000 metres and is found only occasionally in deeper water (down to 5200 m). Frequencies of more than five per cent are found between 2630 and 2770 metres on both the continental margin and the Mid Atlantic Ridge.

Osangularia culter is a rather rare species, which occurs locally at depths between 1000 and 2675 metres on the continental margin (fig. 27a). On the Mid Atlantic Ridge, it is found at 2630 and 3290 metres. This species is most abundant between 1000 and 2000 metres.

Gyroidina polia occurs between 1760 and 4950 metres (fig. 27b). The upper depth limit (UDL) is variable, at least on the continental margin, and in the area of the Zaire deep-sea fan this species is only present between 3990 and 4950 metres. Frequencies of five per cent and more are reached north of 10°S near the Romanche Fracture Zone (4195 and 4505 m) and locally on the continental margin (3096-4356 m).

Pyrgo murrhina is usually present in low numbers in the deep water and its UDL is at 1760 metres (fig. 27c). This species reaches abundances of five per cent and more in some samples from below 3500 metres and the highest relative number is found at 3990 metres in the Zaire fan area.

Astrononion sp. is not found above 2630 metres and occurs only below 3900 metres in the deep-sea fan area (fig. 27d). Throughout the area north of 10°S, it is generally present down to 5215 metres. North of 5°S, frequencies generally exceed five per cent between 3000 and 4600 metres depth. Towards the south, this species is virtually restricted to the marginal area.

Anomalinoides minimus is found only in the 63-150 μm fraction and the UDL

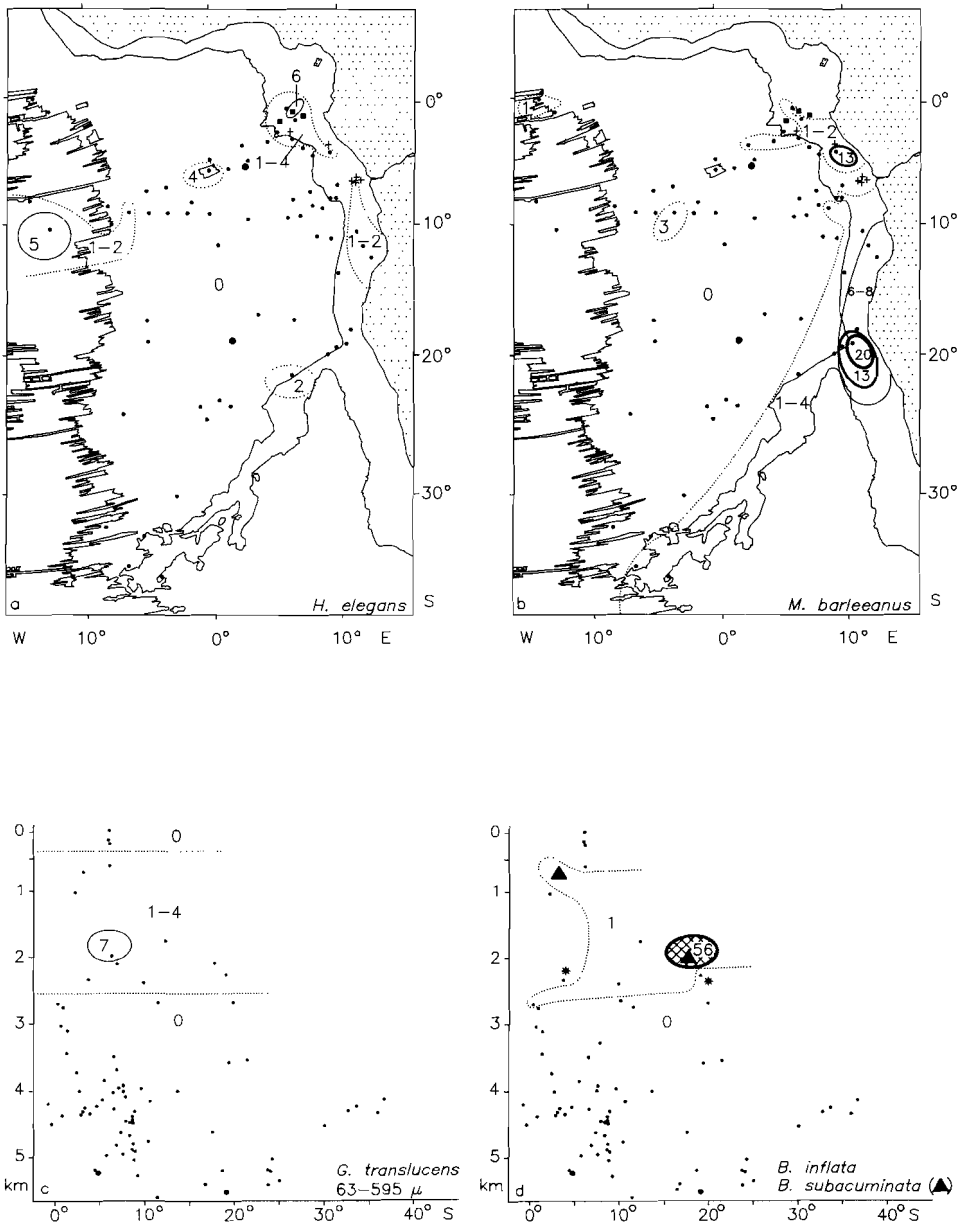

Fig. 25. Percentage distribution of selected species in the 150-595 μm fraction unless otherwise indicated: (a) *H. elegans*, (b) *M. barleeanus*, (c) *G. translucens* (63-595 μm), and (d) *B. inflata* and *B. subacuminata* (▲). Figure conventions as in fig. 9a.

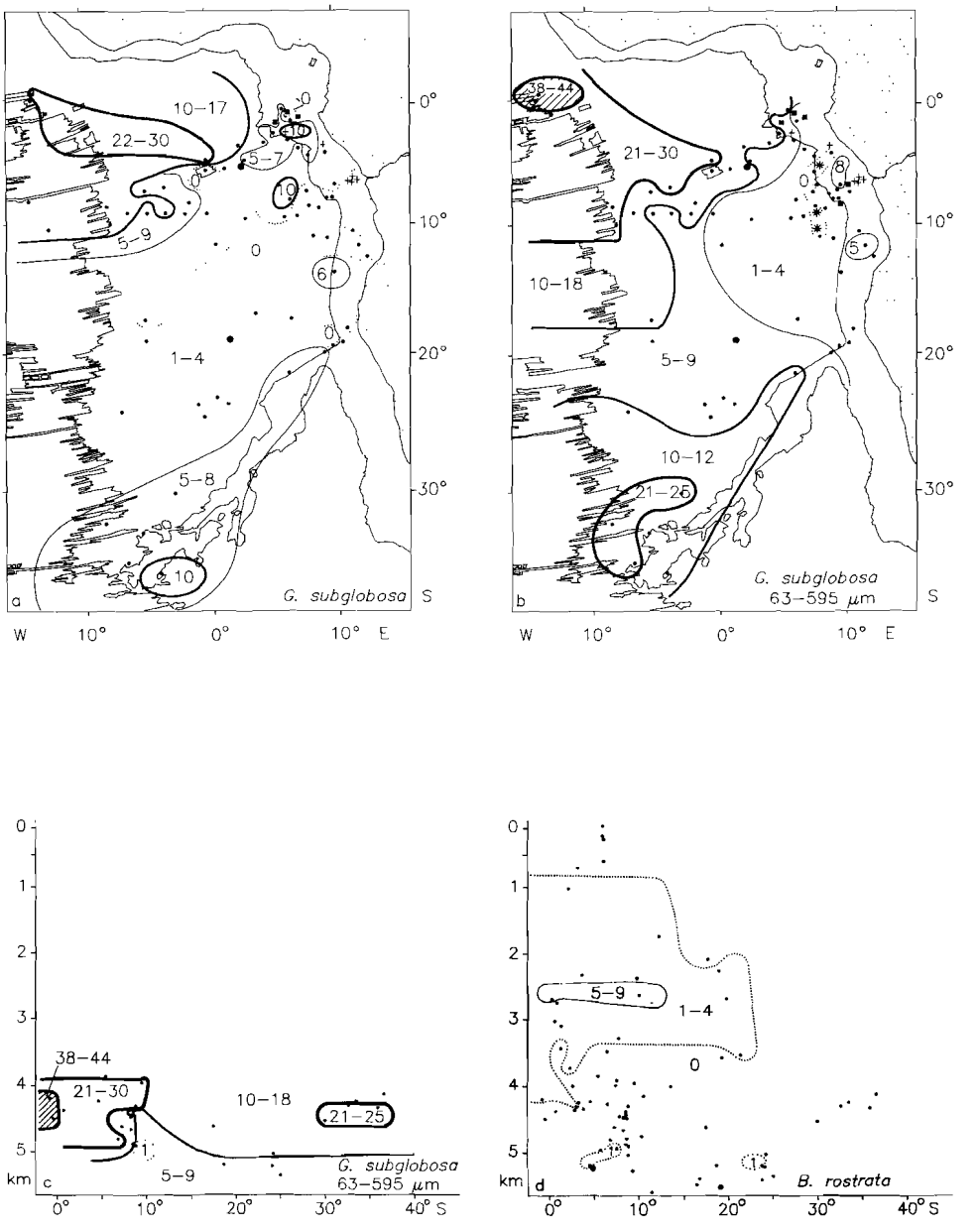

Fig. 26. Percentage distribution of selected species in the 150-595 μm fraction unless otherwise indicated: (a) *G. subglobosa*, (b) *G. subglobosa* (63-595 μm), (c) *G. subglobosa* (63-595 μm) west of latitude 0° and below 4000 metres, and (d) *B. rostrata*. Figure conventions as in fig. 9a.

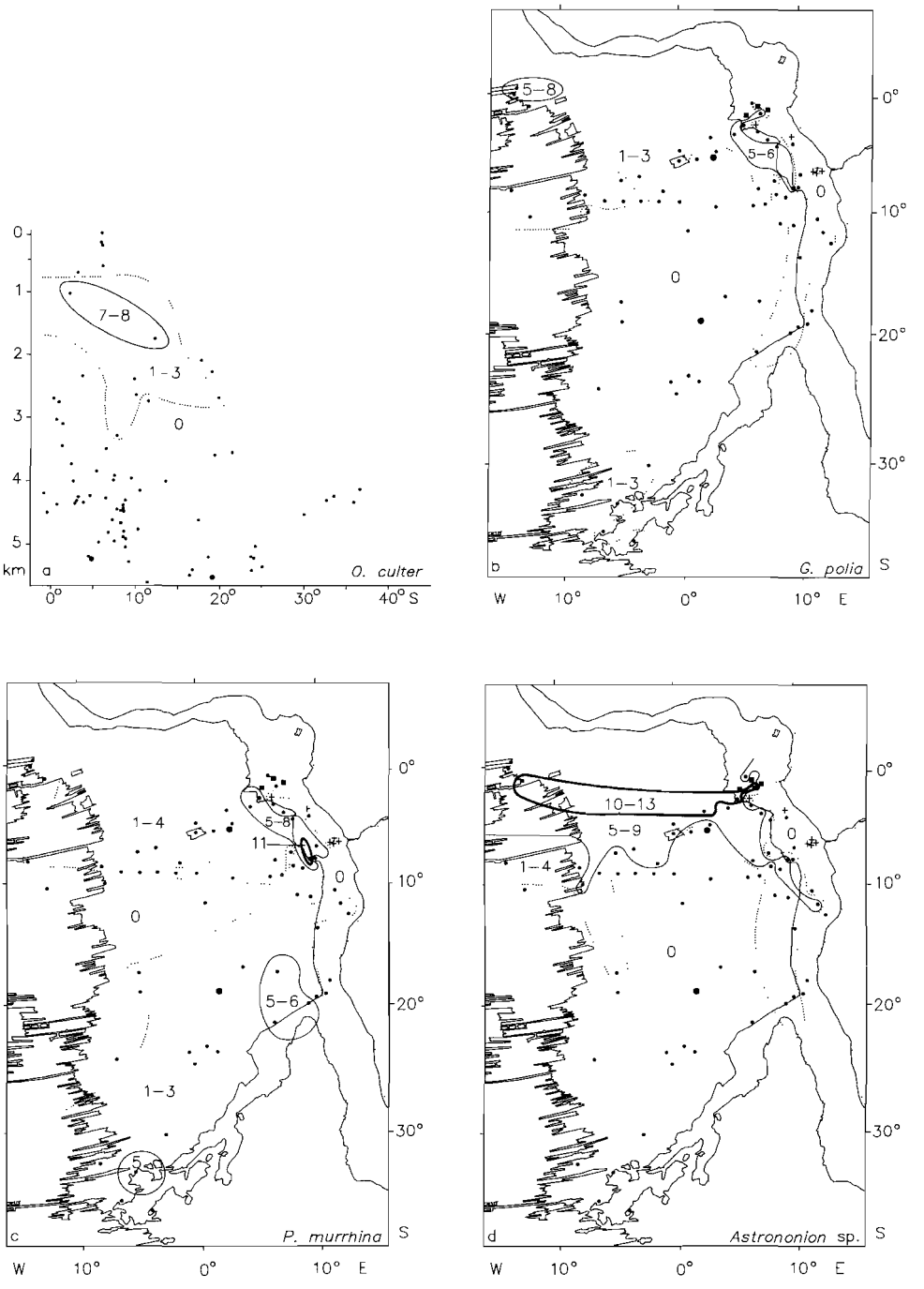

Fig. 27. Percentage distribution of selected species in the 150-595 μm fraction: (a) *O.culter*, (b) *G. polia*, (c) *P. murrhina*, and (d) *Astrononion* sp. Figure conventions as in fig. 9a.

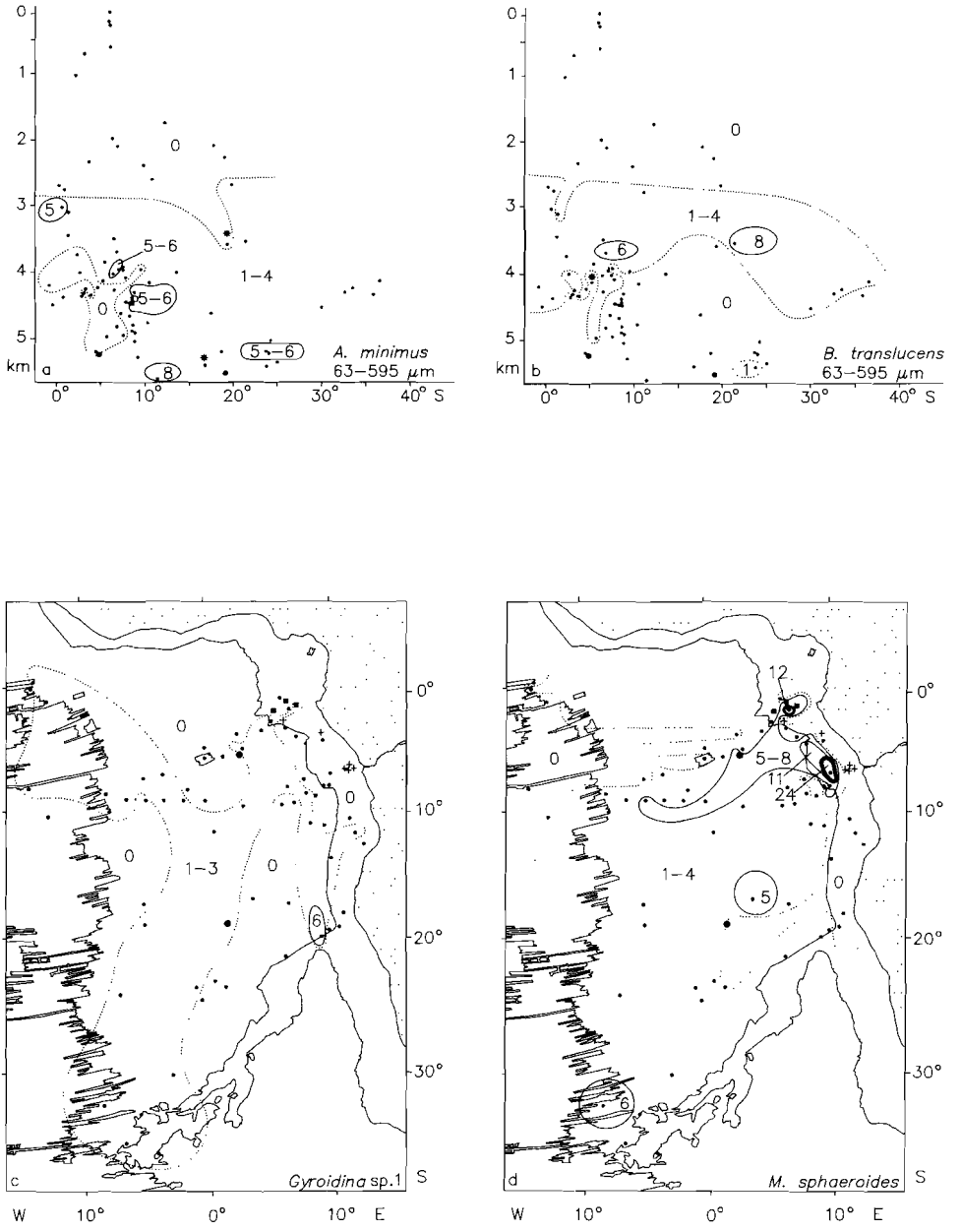

Fig. 28. Percentage distribution of selected species in the 150-595 μm fraction unless otherwise indicated: (a) *A. minimus* (63-595 μm), (b) *B. translucens* (63-595 μm), (c) *Gyroidina* sp. 1, and (d) *M. sphaeroides*. Figure conventions as in fig. 9a.

is at 2675 metres (fig. 28a). South of 10°S it is almost continuously present although in low numbers. This species is not found in a large part of the northern area including the major part of the Guinea Rise.

Gyroidina sp. 1 seems distributed rather at random and is restricted to depths of more than 2675 metres (fig. 28c).

Melonis sphaeroides ranges from 2675 down to the deepest parts of the Angola Basin and is only occasionally absent at great depth (fig. 28d). Abundances exceed ten per cent in three samples, viz. on the Zaire fan (3486, 4330 m) and in the marginal area to the north (3096 m).

Bulimina translucens is hardly ever found in the large-size fraction. In the total fraction (fig. 28b), it is essentially restricted to depths between 2685 and 4525 metres. Although a rare species throughout the region and especially below 3600 metres, *B. translucens* is consistently present in the area of the Zaire deep-sea fan between 3486 and 4260 metres.

Eponides tumidulus is only relatively frequent in the total fraction (fig. 29a). It is not found above 2756 metres and abundances of more than two per cent are reached only outside the deep-sea fan and below 4000 metres.

Cibicides kullenbergi is found in a dozen samples, ranging in depth from 3038 to 4625 metres (fig. 29b). Although dispersed over the entire area, it does not occur on the deep-sea fan. The highest frequency is found at 3537 metres on the Walvis Ridge.

Pullenia sp. 1 occurs only below 3038 metres and is continuously present west of longitude 0°, though in fairly low percentages (fig. 29c). It is generally much sparser in the eastern part of the region. This rather small-sized species appears to be more widespread in the total fraction. With the exception of some sites on the Zaire deep-sea fan and in the marginal area to the south, it is omnipresent and has an UDL of 2770 metres.

Melonis formosus is not found shallower than 3952 metres and its UDL is the deepest of all species (fig. 29d). It is clearly more abundant in the northern part of the region than in the south. Highest relative numbers (5-8 %) are reached north of 6.50°S between 4360 and 5212 metres depth.

Polytypic species

Oridorsalis umbonatus occurs throughout the region at all depths (fig. 30). This species shows conspicuous variation in peripheral characteristics on basis of which two morphotypes were distinguished.

The carinate *O. umbonatus* 1 dominates the assemblages down to 2330 metres and is also the most frequent morphotype at 2630 metres on the Mid Atlantic Ridge (fig. 30a). In the shallowest part of this interval (75-1017 m), *O. umbonatus* seldom reaches abundances of more than two percent. The highest

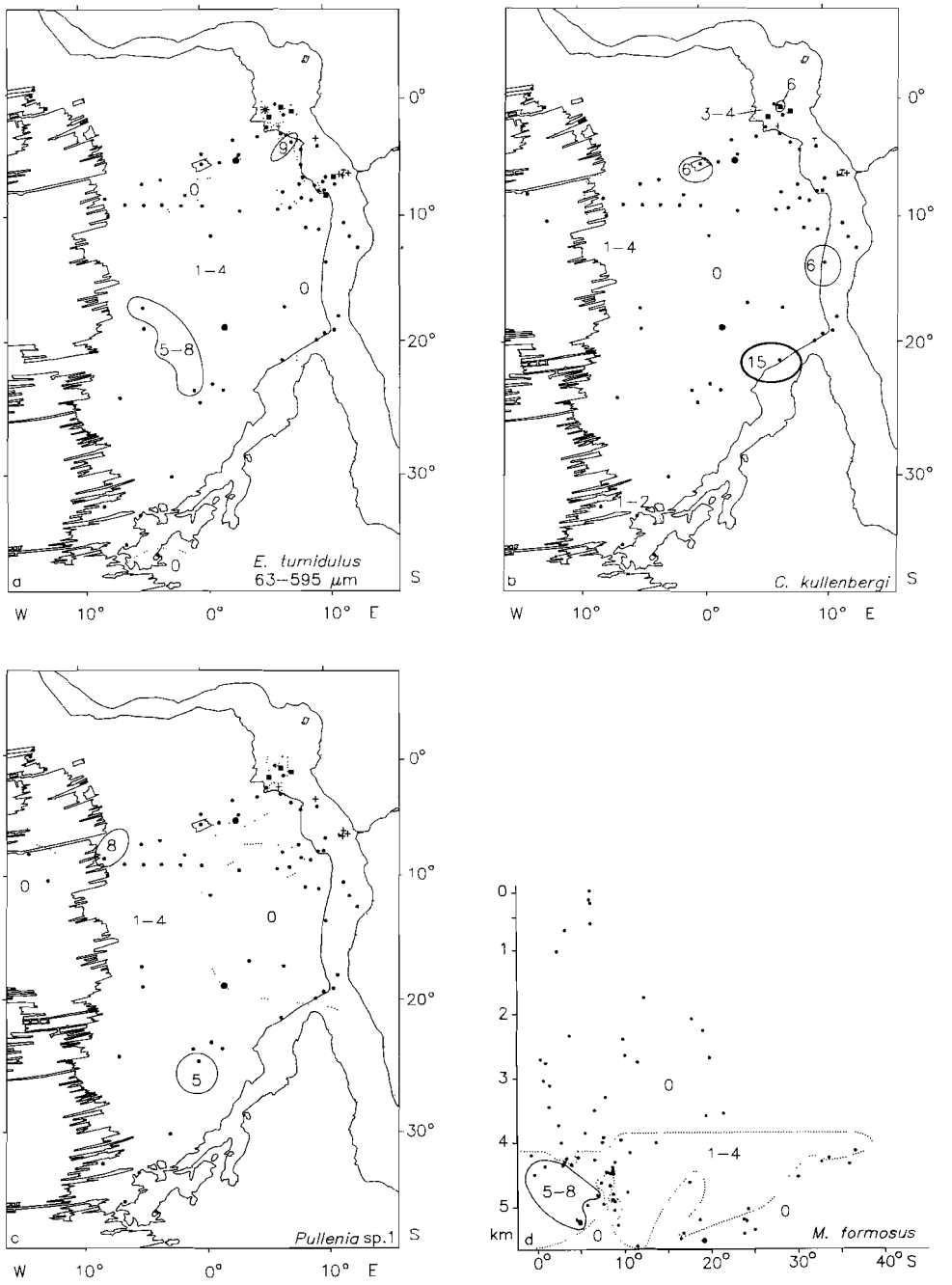

Fig. 29. Percentage distribution of selected species in the 150-595 µm fraction unless otherwise indicated: (a) *E. tumidulus* (63-595 µm), (b) *C. kullenbergi*, (c) *Pullenia* sp. 1, and (d) *M. formosus*. Figure conventions as in fig. 9a.

percentages (12-13 %) of predominantly carinate *O. umbonatus* are attained on the continental margin in the south-eastern part of the region (2078-2270 m).

In deeper water, *O. umbonatus* is almost exclusively represented by the non-carinate type 2, which is a common element in the deep-sea faunas (fig. 30a). Below 3900 metres, abundances usually exceed ten per cent on the Guinea Rise and along the continental margin. Comparable abundances are also found elsewhere, in particular in some samples on the easternmost part of the Guinea Rise (2750-3730 m). Highest percentages occur locally between 3990 and 4790 metres on the deep-sea fan and just north of this area.

In addition to the presence or absence of a keel, *O. umbonatus* displays large variation in the size of the proloculus and three size-classes were distinguished, in order of increasing diameter A, B, and C.

There is little variation in the proloculus size of *O. umbonatus* 1, and type A predominates in all assemblages, except at 2270 metres on the continental slope near the Walvis Ridge. *O. umbonatus* 1 with a large proloculus was not found.

The dominance pattern of the types showing a different proloculus size in the non-carinate assemblages, is given in fig. 30b. Type B is generally the most abundant form in the *O. umbonatus* 2 assemblages, but it should be mentioned that it is almost impossible to distinguish it from type C in the etched faunas from the deepest parts of the basin.

Type C occurs below 2630 metres depth and is the dominant form in a small area on the continental margin near the equator between 3442 and to 4356 metres. Separately counted, type 2C reaches abundances between eight and seventeen per cent in this area. Frequencies of five per cent are only locally reached elsewhere. Little importance can be attached to the occasional predominance of A and C forms in the western part of the region, because *O. umbonatus* 2 is very scarce in these samples (see fig. 30a).

O. umbonatus 2 with a small proloculus is generally rare in the large-size fraction (maximum 5 %) but often abounds in the total fraction. *O. umbonatus* 2 reaches up to twenty per cent in the total fraction, and type A generally dominates the assemblages except at relatively great depth in the area of the Zaire deep-sea fan and at some sites on the continental margin further northward (fig. 30c). Fig. 30d shows that *O. umbonatus* 2A is usually present in abundances of at least five per cent in the land-distant parts of the region and highest percentages are found in the very deep waters west of the deep-sea fan. It is usually sparser near the continent except in the very north.

Nuttallides pusillus is virtually limited to the 63-150 μm fraction and we shall only discuss its distribution in the total fraction (figs. 31a, b). Below 250 metres

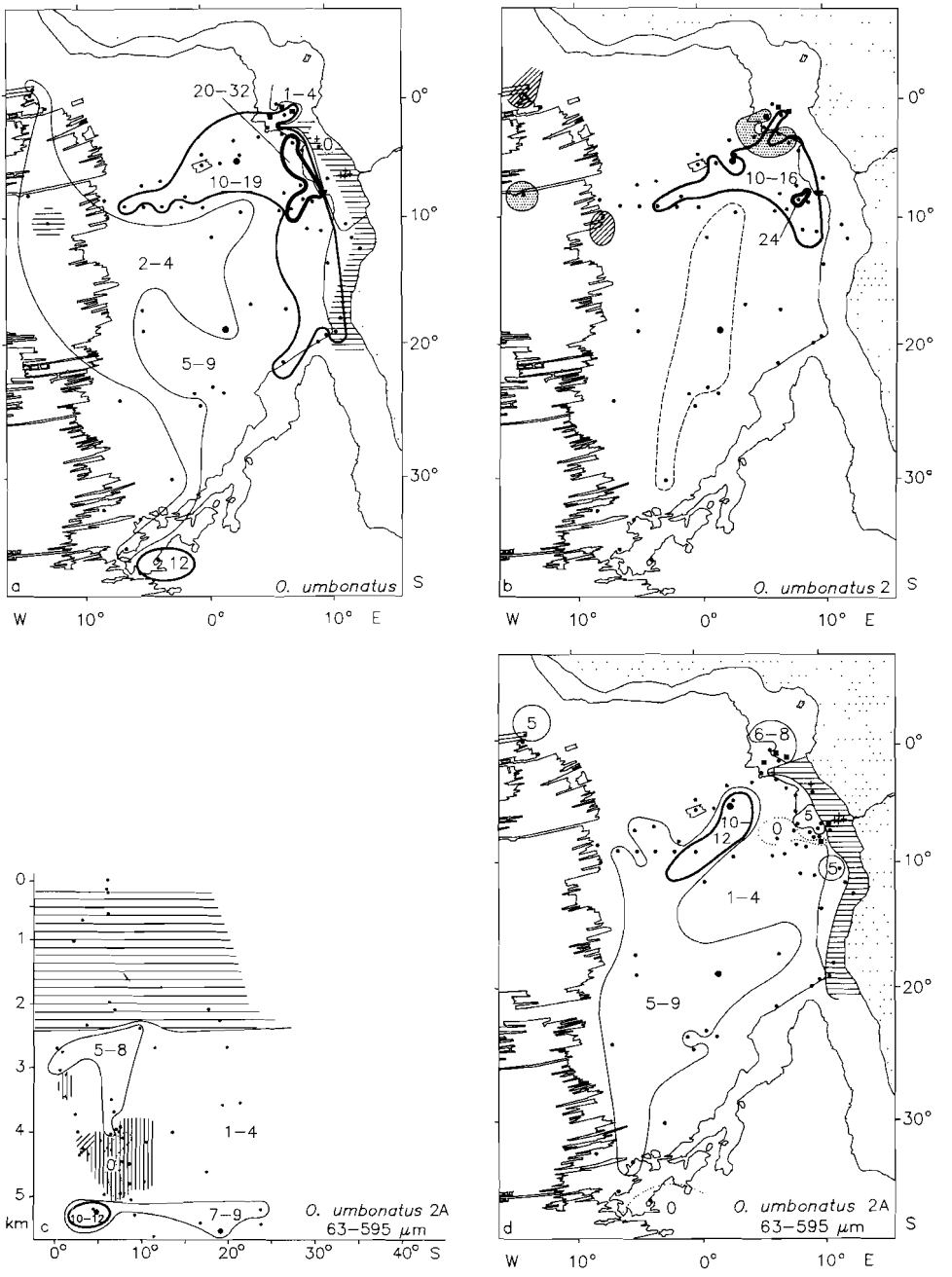

Fig. 30. *O. umbonatus.*
(a) Percentage distribution (150-595 µm); hatching shows dominance of type 1. (b) Dominance pattern of the proloculus types discriminated in *O. umbonatus* 2 (150-595 µm; shading indicates dominance of type C and hatching dominance of type A). Distinction between type B and C is difficult within the dotted line. Area of maximum abundance of type 2B is contoured. Samples with predominantly type 1 not shown. (c) Percentage distribution of type 2A (63-595 µm) and dominance pattern of other types in *O. umbonatus* (63-595 µm): horizontal hatching shows dominance of type 1, vertical hatching type 2B, diagonal hatching type 2C. (d) Percentage distribution of type 2A (63-595 µm). Figure conventions as in fig. 9a.

this species is present in all samples but it is sparse (1-3 %) down to 1000 metres. Higher, though variable percentages (3-30 %) are found between 1000 and 3000 metres. Frequencies exceed twenty per cent between 3000 and 4000 metres, except in the deep-sea fan area where percentages remain relatively low down to 3700 metres. *N. pusillus* is extremely abundant around 4000 metres all along the continental margin south of 3°S and in one sample on the Guinea Rise. Abundances of more than twenty per cent prevail also in deeper waters, but lower frequencies are locally reached at great distance from the continent, notably near the Romanche Fracture Zone and south of approximately 20°S. The morphology of this species changes with depth in that the number of chambers in the final whorl increase towards deeper water, and we distinguished three morphotypes on this basis.

N. pusillus turgidus flourishes in relatively shallow water and is the only morphotype to occur above 1000 metres (fig. 31c). It dominates the assemblages down to a depth of slightly more than 2000 metres, in the area of the deep-sea fan even much deeper (3486 m). The proportion of *turgidus* types per total *N. pusillus* decreases regularly towards deeper water, and this morphotype is virtually absent below 4000 metres.

Deeper water assemblages of *N. pusillus* are dominated by *N. pusillus* s.s., which is subdivided into two morphotypes. The shallowest occurring type is *N. pusillus pusillus* 1, which is found in all samples below 1000 metres. It dominates down to about 4000 metres and is also the most abundant form in the deepest part of the Angola Basin (fig. 31d).

N. pusillus pusillus 2 is the deepest living morphotype, generally dominating the assemblages below 4000 metres. This type is not found above 2675 metres and is restricted to depths of more than 3500 metres in the area of the deep-sea fan (fig. 31d). It should be mentioned that the two types of *N. pusillus* s.s. usually occur in roughly equal percentages in the area of the highest frequencies of *N. pusillus* s.l.

Epistominella exigua was subdivided into two morphotypes, which differ in the degree of rounding of the periphery, viz. a sharp to bluntly angled *exigua* 1 and a broadly rounded *exigua* 2.

The assemblages in the large-size fraction are virtually monotypic and almost exclusively consist of type 1. *E. exigua* 1 occurs almost continuously from 605 metres down to the deepest sample (fig. 32a). Shallower than 4000 metres, *E. exigua* 1 is absent in the two samples on the Mid Atlantic Ridge and frequencies are below ten per cent on the continental margin between the Walvis Ridge and 3°S. North of this latitude and at depths of 3000 to 3500 metres, *E. exigua* 1 is on the contrary very abundant near the continent.

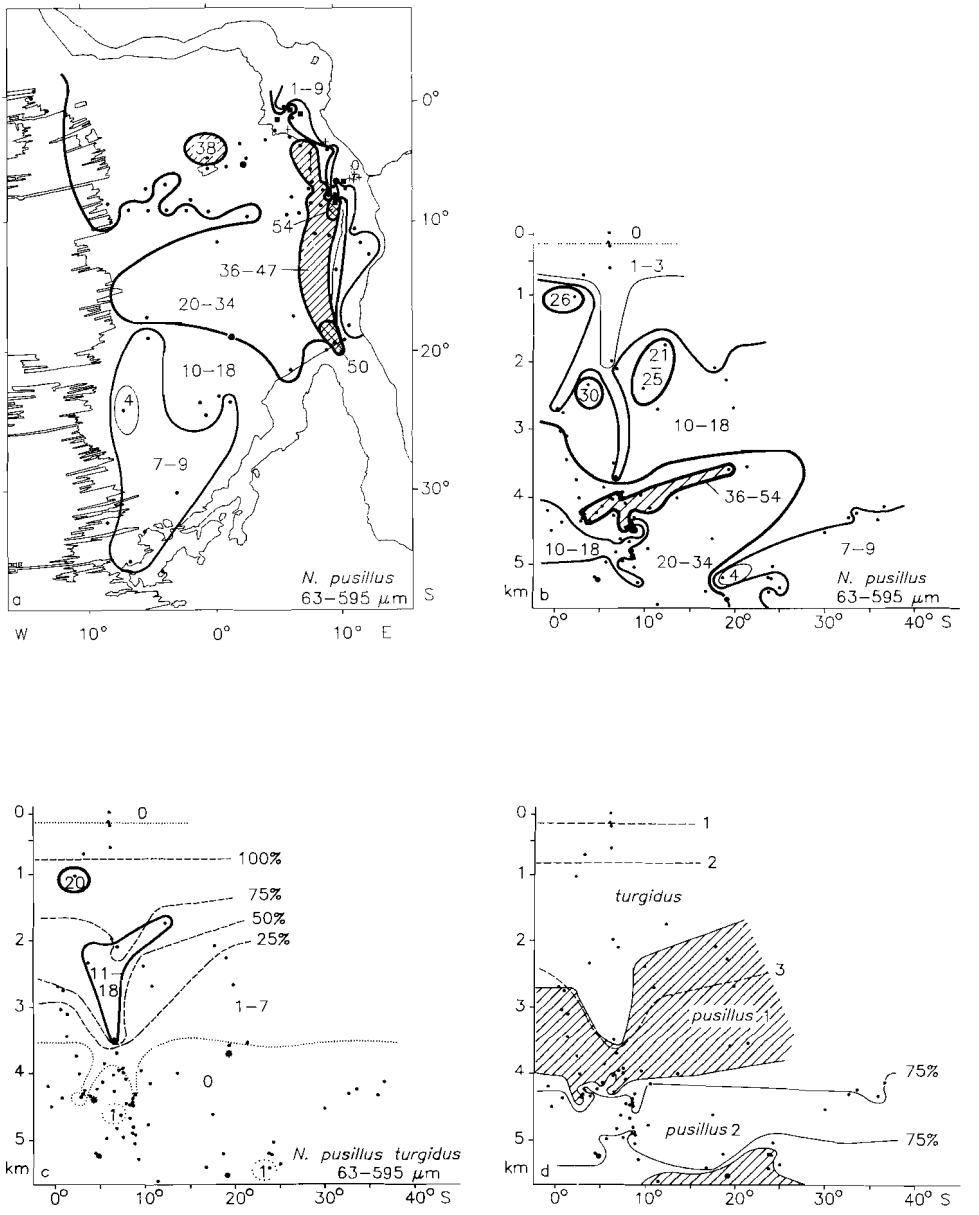

Fig. 31. *N. pusillus* (63-595 µm).
(a, b) Percentage distribution of the species; double hatching indicates frequencies above 50 %. (c) Percentage distribution of the *turgidus* type and its proportion per total *N. pusillus*. (d) Dominance intervals of the three types and their UDL, (1) *turgidus*, (2) *pusillus* 1, and (3) *pusillus* 2. Figure conventions as in fig. 9a.

Below 4000 metres, *E. exigua* 1 generally reaches frequencies of more than ten percent, but it is scarcer in the centre of the Angola Basin and in the western part of the region. At 4505 metres near the Romanche Fracture Zone it is even absent. Highest percentages (20-25 %) in the very deep waters are found at widely scattered places.

In the total fraction, both total *E. exigua* and individual morphotypes show a more irregular distribution (fig. 32b). High abundances (above 35 %) are found at variable depths (1760-5410 m) and in different parts of the region. Very low percentages are again reached near the Romanche Fracture Zone and in some samples at depths between 3500 and 4000 metres on the deep-sea fan.

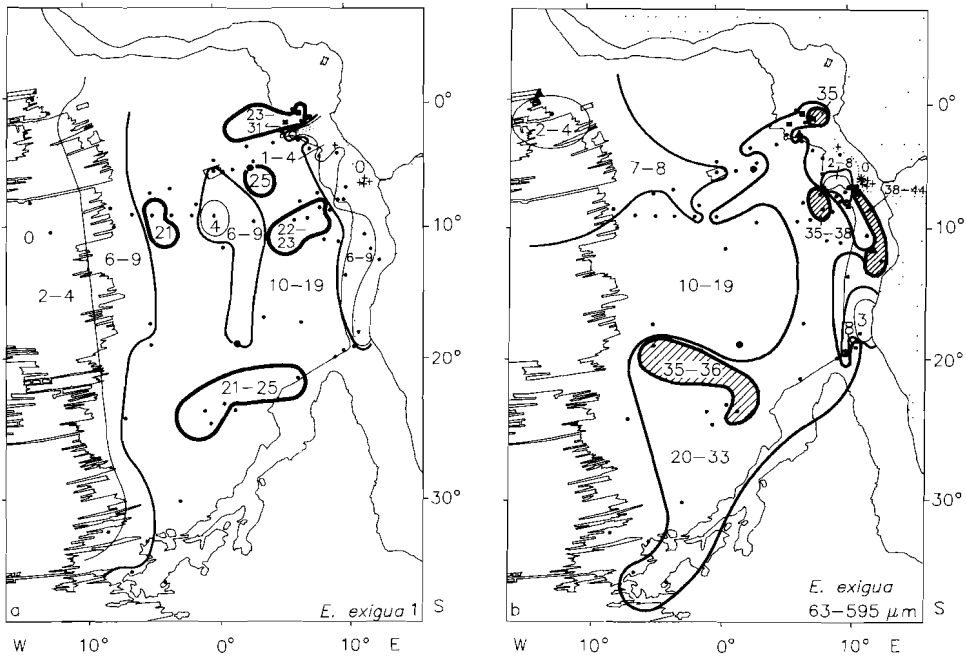

Fig. 32. *E. exigua.*
Percentage distribution of (a) type 1 (150-595 µm); (b) the species in the total fraction. Triangles show dominance of type 2. Figure conventions as in fig. 9a.

E. exigua 2 dominates the assemblages in only four samples, two are located near the Romanche Fracture Zone (4195 and 4505 m) and two on the continental slope (1017 and 2770 m). Except for its occurrence at 1017 metres, this type is absent above 2000 metres and below 5205 metres. In between, *E. exigua* 2 occurs in most of the samples though in low frequencies. Abundances of more than five per cent are locally reached outside the area of the deep-sea fan at

various depths (1017-4625 m). An exceptionally high abundance (29 %) is recorded in a sample from 2770 metres depth.

Two morphotypes were distinguished in *Cibicides robertsonianus*. The *bradyi* type is not found shallower than 1017 metres and is rare in the entire area (fig. 33a). *C.* cf. *robertsonianus* ranges in depth from 2393 to 4813 metres (fig. 33b) but is practically limited to the northern part of the region, where it is found in abundances of up to five percent.

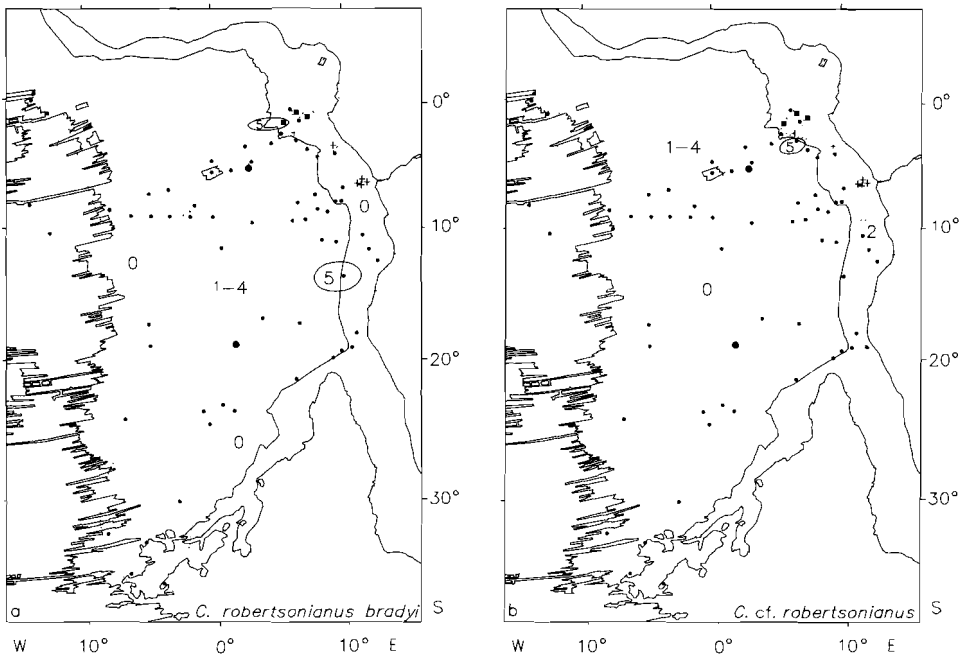

Fig. 33. Percentage distribution in the 150-595 μm fraction of (a) *C. robertsonianus bradyi*, and (b) *C.* cf. *robertsonianus*. Figure conventions as in fig. 9a.

Pullenia bulloides includes two morphotypes. *P. bulloides* s.s. is present in most samples below 600 metres, but generally in low numbers (fig. 34a). With one exception, frequencies of five per cent and more are only reached near the continent. The percentage distribution along the continental margin (fig. 34b), shows that north and south of the fan area abundances of five per cent are attained roughly between 1750 and 3000 metres, whereas in the fan area itself such high values are found between 4000 and 4500 metres.

Pullenia bulloides osloensis is a deeper occurring type with an UDL at 2685 metres. It is generally sparse above 4000 metres (fig. 34c) and frequencies of five

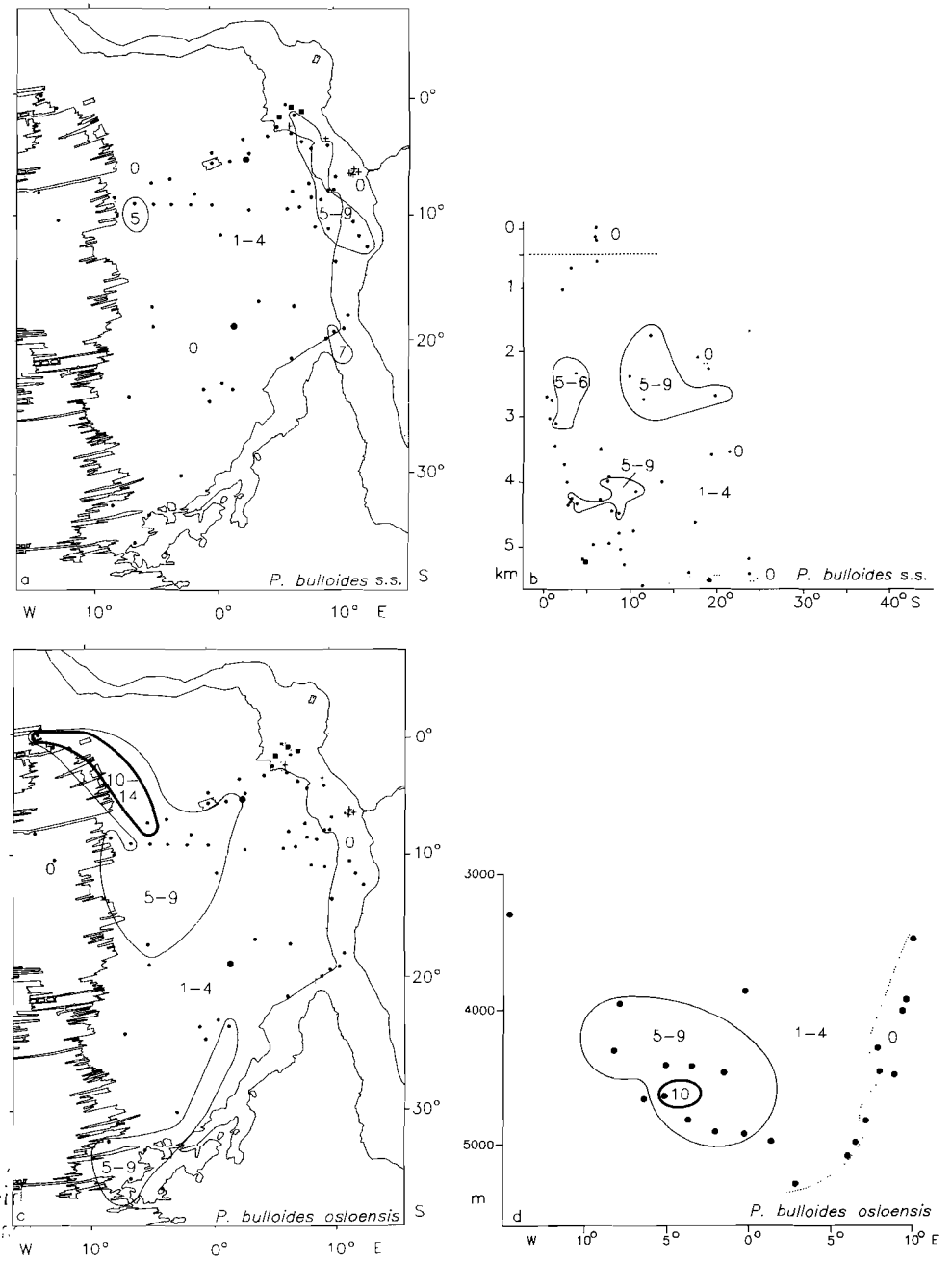

Fig. 34. Percentage distribution of the two types of *P. bulloides* in the 150-595 μm fraction. (a) *bulloides* type; (b) depth distribution of the *bulloides* type east of latitude 0°; (c) *osloensis* type; (d) depth distribution below 3000 metres of the *osloensis* type in between 5° and 10°S. Figure conventions as in fig. 9a.

per cent and more are virtually only reached between 4000 and 5000 metres depth. This morphotype clearly avoids the deep-sea fan and the adjacent continental margin (fig. 34d).

The *Uvigerina peregrina* group includes three morphotypes, the *peregrina*, *dirupta*, and *hispida* types, and the latter was named as a species for convenience' sake. The distribution was discussed in an earlier paper (Van Leeuwen, 1986) and the three types appeared to dominate in different areas (fig. 35).

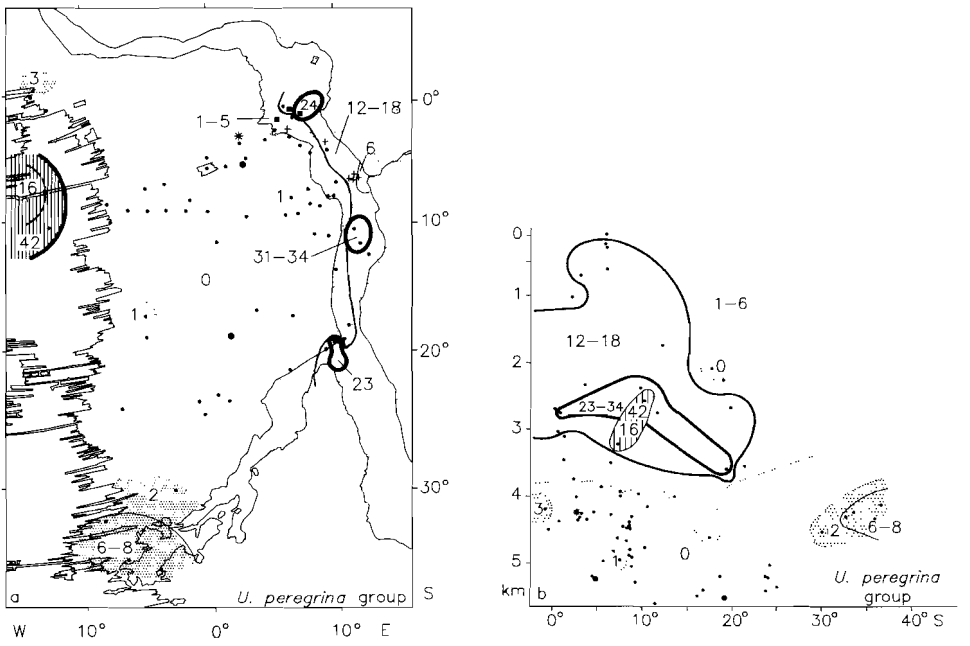

Fig. 35. Percentage distribution of the *U. peregrina* group in the 150-595 μm fraction (modified after Van Leeuwen, 1986). Dominance of *U. hispida* indicated by hatching, dominance of *peregrina dirupta* by dotting. Figure conventions as in fig. 9a.

Along the continental margin, the *U. peregrina* group occurs from 75 down to approximately 4000 metres depth and the assemblages are dominated by the *peregrina* type. Above 3000 metres frequencies are at least five percent, except near the Walvis Ridge. It is scarcer in deeper water, but the Walvis Ridge area is again exceptional, because an abundance of twenty-three per cent is attained at 3600 metres. Highest frequencies (above 30 %) along the continental margin are found south of the deep-sea fan at depths between 2400 and 2800 metres.

Below 4000 metres, the *Uvigerina peregrina* group is almost exclusively found near the Walvis Passage in the south-west (4100-4500 m) and in one site near

the Romanche Fracture Zone in the north-west (4195 m). Frequencies are rather low (2-8 %) and the assemblages are dominated by the *dirupta* type.

Monotypic assemblages of *U. hispida* are found at 2630 and 3290 metres depth on the Mid Atlantic Ridge. This species is very abundant in these samples and dominates the fauna in the shallowest sample.

Nuttallides umboniferus comprises three morphotypes which succeed each other with increasing depth. The shallowest type, *N. umboniferus decoratus,* is restricted to depths between 1760 and 2400 metres, but is absent at comparable depths on the Walvis Ridge (fig. 36a). It is too small to be found in the large-size fraction, but reaches up to six per cent in the total fraction.

N. umboniferus convexus ranges in depth from 2675 down to 4195 metres. In the large-size fraction, frequencies are generally rather low with a maximum of thirteen per cent at 4195 metres near the Romanche Fracture Zone (fig. 36b). Higher numbers are reached in the total fraction, although seldom more than ten per cent (fig. 36a). An exceptionally high abundance of 38 per cent is attained at 2685 metres on the continental margin near the Guinea Rise. Towards deeper water, this form is replaced by *N. umboniferus* s.s., and both types are occasionally found together between 3442 and 4021 metres. Except at 3731 metres on the Guinea Rise, *convexus* types attain the highest numbers in these mixed assemblages.

Below 4000 metres *N. umboniferus* s.s. is generally the only morphotype to occur, except at 4195 metres near the Romanche Fracture Zone. It is large-sized and the distribution is best described in the 150-595 μm fraction (fig. 36b-c). Apart from occasional absence near the continent, it is omnipresent at depths of more than 4000 metres becoming increasingly more abundant towards deeper water. Below 5000 metres it makes up more than 35 per cent of the fauna in southern parts of the region. In the north it tends to be less frequent at all depths (fig. 36c).

Although we distinguished two morphotypes in *Cibicides wuellerstorfi,* only the distribution of *C. wuellerstorfi* s.s. will be discussed. The other morphotype, *wuellerstorfi* var., co-occurs in most samples with *wuellerstorfi* s.s., but is always much less frequent and does not reach the five per cent level.

C. wuellerstorfi s.s. is found from 1760 metres downward and generally attains frequencies between five and fifteen per cent below 3000 metres (fig. 36d). Extremely high abundances (28-42 %) are observed on the Zaire deep-sea fan between 3450 and 4000 metres depth. Although relatively frequent at 3857 metres depth on the Guinea Rise and just north of the fan (4330 m), much lower frequencies are generally reached at other sites within this depth interval.

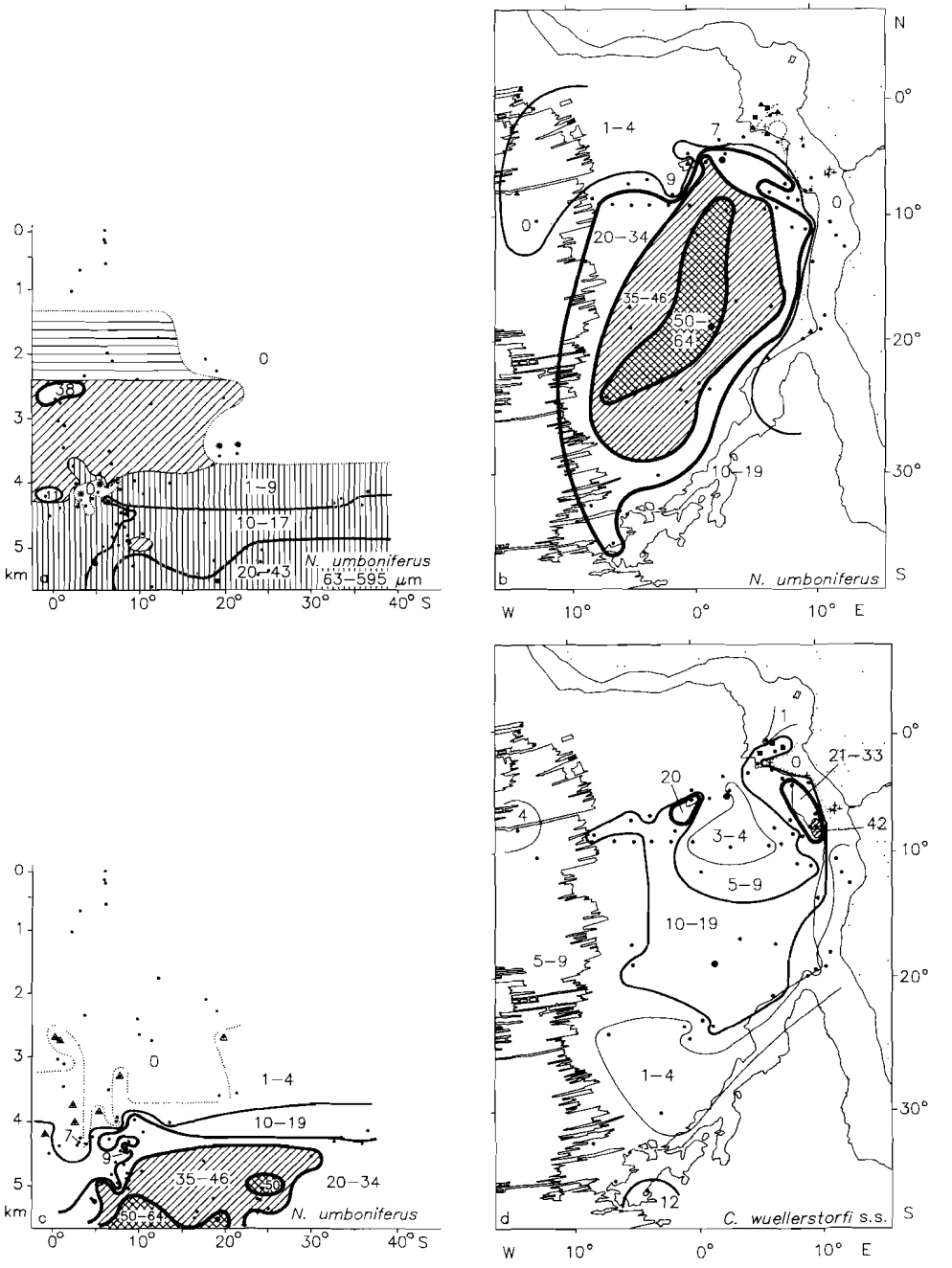

Fig. 36. Percentage distribution of (a) total *N. umboniferus* (63-595 µm) and dominance intervals of the three types; (b, c) *N. umboniferus* (150-595 µm), triangles show dominance of the *convexus* type; (d) *C. wuellerstorfi* s.s. (150-595 µm). Figure conventions as in fig. 9a; double hatching indicates frequencies above 50 %.

IV.3.1. Deep-sea samples

In order to examine the covariance between the common deep-sea taxa and to delineate biofacial patterns, we used the same multivariate techniques as for the analysis of the frequency distribution of the planktonic foraminifera. The presence of polytypic species confronts us with a problem of choice. Various different data-bases can be constructed by splitting species into their morphotypes, or by using lump-categories and arguments could be given in favour of any of the options. We actually did not choose but aimed at structured, well-interpretable output. It should be kept in mind that the statistical behaviour of lump-categories is largely determined by the most common morphotype.

The distribution of thirty-four faunal categories in the samples from below 1750 metres was subjected to BALANC/DENDRO analysis. Polytypic species were split, except for *U. peregrina,* and we differentiated *O. umbonatus* only according to proloculus size. We selected the taxa with a maximum frequency of at least five per cent and added the slightly less frequent *G.* cf. *altiformis*, because it is a typical deep-sea species. Unichambered and porcellaneous taxa (*Pyrgo murrhina* excluded) were lumped into the units 'Monothalamous' and 'Miliolids', respectively.

Three main groups are to be identified in the dendrogram (fig. 37). *B. subacuminata* and *U. auberiana* have a separate position, which is not surprising because both species are almost restricted in their occurrence to core RC13-225 (2078 m).

The first group essentially consists of *B. aculeata, C. carinata, Globobulimina* spp., *M. barleeanus, P. bulloides* s.s., *O. umbonatus* A (predominantly subspecies 1 in this size fraction), *O. culter,* and *U. peregrina* s.l. These taxa generally reach their highest frequencies above 3000 metres and are rare or absent below 4000 metres. Subdivision is possible but hardly warrantable, because depths above 3000 metres are poorly covered in our material. This first group will be termed the bathyal group. However, only one of the localities above 3000 metres is on the Mid Atlantic Ridge, whereas all other samples come from near the continent. In the sample from the MAR, the bathyal group is only represented by *O. culter,* which is in addition rather scarce (3 %). It seems, therefore, equally justified to describe this first unit as a continental slope group.

The second group shows little coherence and consists of *B. rostrata, Cibicides kullenbergi, H. elegans,* and *U. hispida.* Although these species attain their maximum abundance at variable depth, we may generalize that they are frequent between 2000 and 4000 metres and scarce or absent below 4000 metres.

Geographically, their distribution is similar in that they are virtually absent in the area of the deep-sea fan, but notice that depths of less than 3486 metres were not sampled here. The isolate position of *C. kullenbergi* may reflect its absence at intermediate depth (2630 and 3290 m) on the Mid Atlantic Ridge where the other three species are relatively frequent.

All other taxa are united in a fairly heterogeneous third group. Virtually all elements of this group are relatively frequent at depths below 4000 metres and we shall refer to this unit as the abyssal group. Three subgroups can be distinguished. *G.* cf. *altiformis* and *N. rugosus convexus* show a connection with one of the subunits, whereas *C. robertsonianus bradyi* takes a rather isolate position. This taxon occurs sparsely and at random below 1017 metres depth.

The first subgroup comprises *Astrononion* sp., *C.* cf. *robertsonianus, G. subglobosa, G. polia, M. formosus,* and *O. umbonatus* C. The taxa of this unit reach high frequencies between 3600 and 4500 metres depth, but *Astrononion*

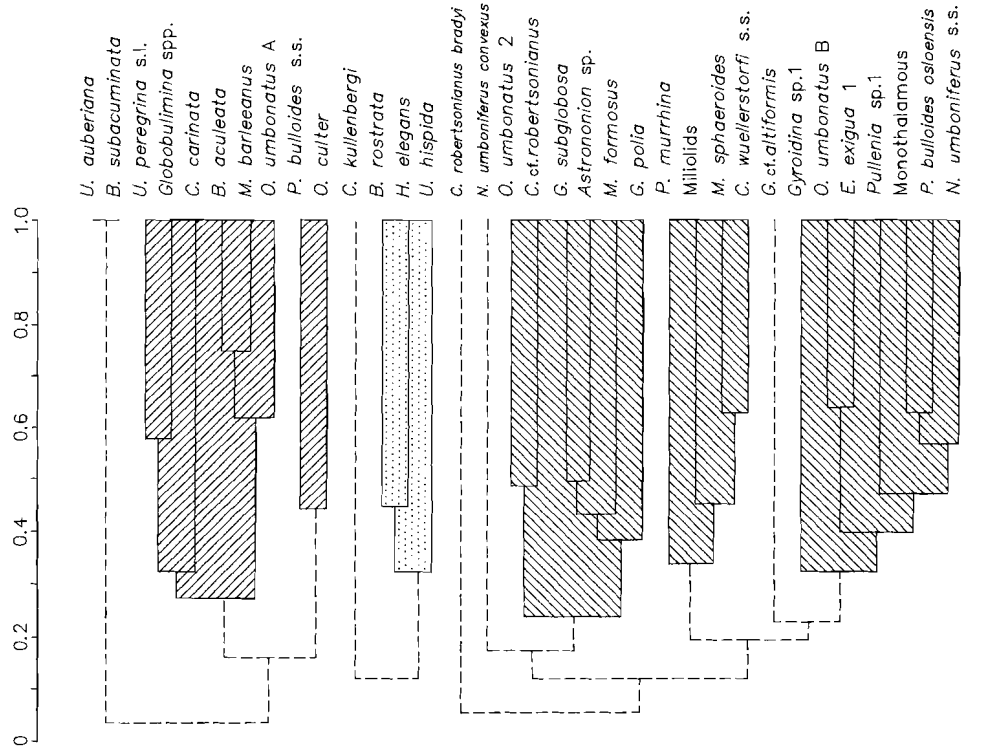

Fig. 37. Dendrogram based on the BALANC correlation matrix of the analysis of 34 taxa (150-595 μm) in all deep-sea samples showing three groups. Only positive correlations are shown. Dotted lines indicate correlations which are not significant (α = 0.05).

sp. and *G. polia* are also frequent in shallower water (up to 3000 m), while high frequecies of *G. subglobosa* and *M. formosus* are also found below 4500 metres. These taxa seem to cluster mainly because their distribution is geographically similar. They all are more abundant in the northern part of the region than in the south. *N. umboniferus convexus*, which only incidentally occurs below 4000 metres, shows a similar preference for the northern area, which explains its connection with this northern abyssal subgroup.

C. wuellerstorfi s.s., *M. sphaeroides*, *P. murrhina*, and the miliolids form a second subunit. The three species reach their highest abundances around 3500 metres in the area of the Zaire deep-sea fan and the adjacent continental margin.

The third subgroup consists of *E. exigua* 1, *Gyroidina* sp. 1, *N. umboniferus* s.s., *O. umbonatus* B, *P. bulloides osloensis*, *Pullenia* sp. 1, and the monothalamous species, to which *G.* cf. *altiformis* may be added. This large subgroup seems to be a restgroup, which comprises the common elements of the faunas below 4000 metres that do not fit in one of the other subgroups.

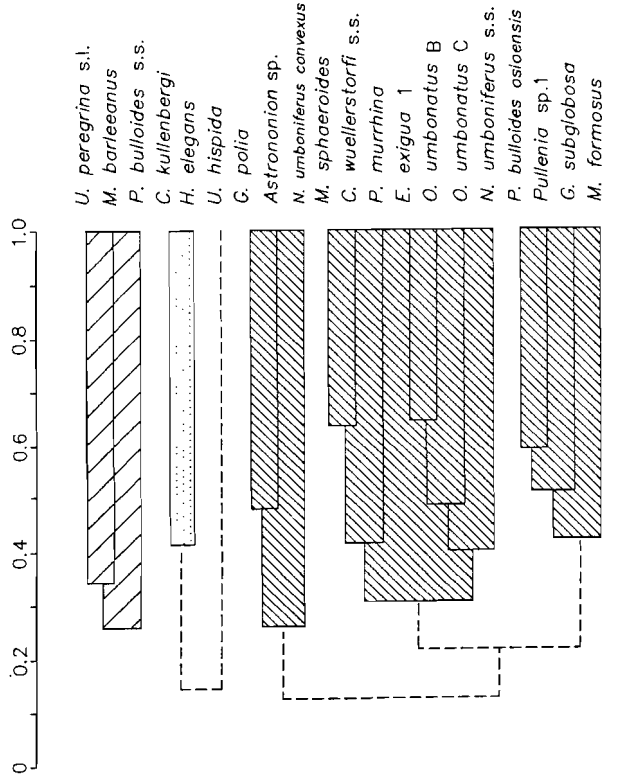

Fig. 38. Simplified version of the dendrogram shown in fig. 37.

A simplified dendrogram based on the same BALANC analysis, is shown in fig. 38. It includes all taxa that exceed the five per cent below 3000 metres but without the lump categories Monothalamous and Miliolids. Again, the three main groups are easily to be identified, but within the abyssal group the taxa are differently arranged. A northern subgroup is still recognizable, but now without *G. subglobosa, M. formosus,* and *O. umbonatus* C. The former two have joined *P. bulloides osloensis* and *Pullenia* sp.1 to form a second subgroup. These four species have low abundances in the area of the Zaire deep-sea fan.

The remaining taxa of the abyssal group are all united in a new restgroup, which consists of the species that occur widespread in the abyssal realm except in the north-west.

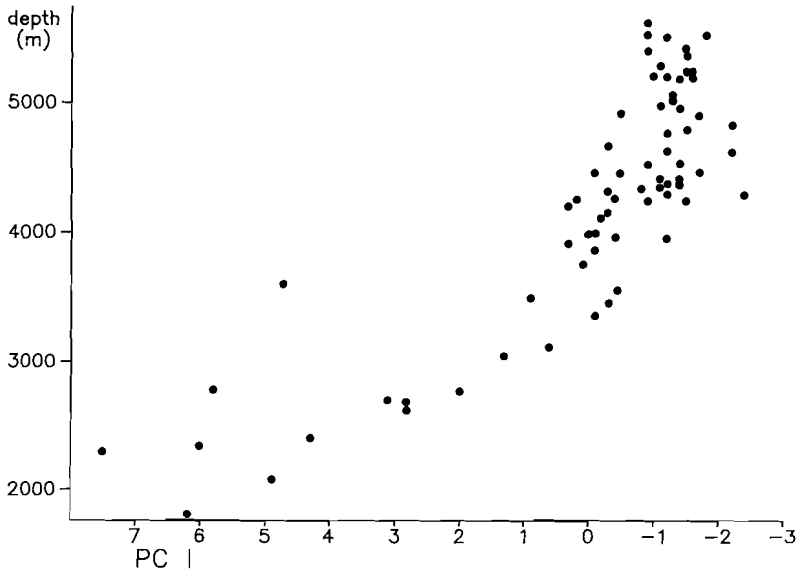

Fig. 39. Sample scores on the first component of the PC analysis of 34 taxa (150-595 μm) in all deep-sea samples plotted versus depth.

The same data-base was subjected to a principal component analysis and the characteristics of the first three components are given in table 6. Only the first component can be considered significant on the basis of the criterion defined by M.M. Drooger (1982). It explains but little of the total variance and the species loadings indicate that it reflects the contrast between the abyssal group and the bathyal group. A plot of the sample scores versus depth (fig. 39) clearly shows that the component expresses depth or some depth-related parameter.

principal component	1	2	3
eigenvalue	4.9	3.6	2.9
variance (%)	14.5	10.6	8.6
species			
M.barleeanus	.4	.1	-.1
C.carinata	.3	.0	.1
Globobulimina spp.	.3	.0	.0
U. peregrina	.3	-.1	.1
B. aculeata	.2	.1	-.1
B. rostrata	.2	-.1	-.0
H. elegans	.2	-.2	.1
O.umbonatus A	.2	.1	-.3
O. culter	.2	-.0	.1
P. bulloides s.s.	.2	-.1	.2
B. subacuminata	.1	.2	-.3
G. polia	.1	-.4	-.2
U. auberiana	.1	.2	-.3
U. hispida	.1	-.1	-.1
C. robertsonianus bradyi	.0	-.1	.1
miliolids	.0	-.1	.1
N. umboniferus convexus	.0	-.2	-.2
Astrononion sp.	-.0	-.4	-.1
C. kullenbergi	-.0	-.1	-.0
C. cf. *robertsonianus*	-.0	-.3	-.0
G. cf. *altiformis*	-.0	-.2	.1
M. sphaeroides	-.0	.0	.3
C. wuellerstorfi s.s.	-.1	-.1	.3
E. exigua 1	-.1	.1	.2
G. subglobosa	-.1	-.3	-.3
Gyroidina sp. 1	-.1	.0	-.0
O. umbonatus B	-.1	-.0	.2
O. umbonatus C	-.1	-.1	.1
P. murrhina	-.1	-.2	.2
M. formosus	-.2	-.1	-.2
monothalamous	-.2	.1	-.0
N. umboniferus s.s.	-.2	.4	.0
P. bulloides osloensis	-.2	-.0	-.3
Pullenia sp. 1	-.2	-.1	-.2

Table 6. Results of a principal component analysis of the frequency distribution of the thirty-four most common benthic foraminiferal species (150-595 μm) in the deep-sea. Eigenvalues, percentages of total variance and composition of the first three components.

IV.3.2. Samples from below 4000 metres

In our total set of deep-sea samples, correlations between taxa of our abyssal group are probably to some extent determined by their covariance in samples from above 4000 metres. In order to examine the relations between the taxa

that are common at great depth on a more appropriate basis, we analysed their distribution in the samples from below 4000 metres. We included only taxa with a maximum frequency of at least five per cent and lumped *N. umboniferus* s.s. and *N. umboniferus convexus.*

The correlation matrix of the BALANC analysis shows the existence of three small units of mutually positively correlated taxa (fig. 40). The first subgroup is composed of *Astrononion* sp., *G. subglobosa,* and *G. polia* and is clearly the equivalent of the northern abyssal subgroup discussed in the preceding section. The three taxa are especially frequent between 4000 and 4500 metres depth. *M. formosus,* which also abounds in the northern area but mainly in deeper water, is only positively correlated with *G. subglobosa.*

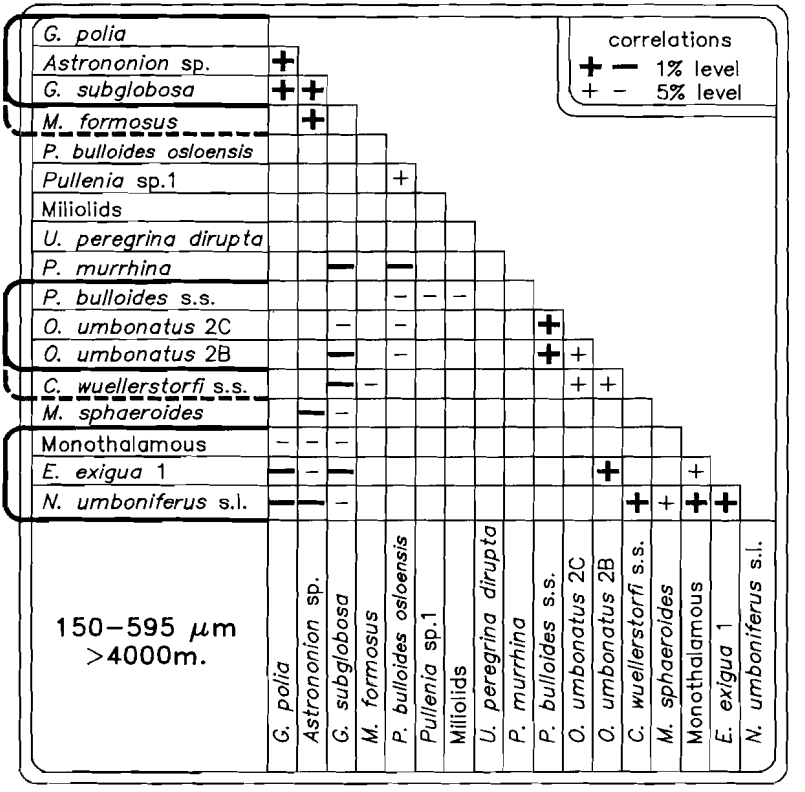

Fig. 40. BALANC correlation matrix based on the analysis of 17 taxa (150-595 µm) in all samples from below 4000 metres. The three most coherent groups recognized in a dendrogram are indicated (uninterrupted lines show species joining each other at α = 0.01).

The northern abyssal subgroup shows overall negative correlations with a second group, which consists of *E. exigua* 1, *N. umboniferus* s.l. and the monothalamous species. These taxa have a more widespread occurrence, but both *E. exigua* 1 and *N. umboniferus* s.s. are scarce in the north-west. *E. exigua* 1 and the monothalamous species do not show a distinct depth preference, but *N. umboniferus* s.l. was seen to abound at depths of more than 5000 metres.

A third subgroup unites *O. umbonatus* 2B, *O. umbonatus* 2C, and *P. bulloides* s.s. *C. wuellerstorfi* s.s. may be added, although it is not positively correlated with *P. bulloides* s.s. Considering their distribution at abyssal depth, we may conclude that these taxa are more abundant near the continent than in the land-distant parts of the region. In the area of the Zaire fan, they jointly reach high frequencies down to a depth of 4800 metres. This subunit shows regular negative correlations with both *G. subglobosa* and *P. bulloides osloensis*, taxa avoiding the deep-sea fan area.

A subsequently performed principal component analysis did not produce a significant axis. We, therefore, created a new abyssal data-matrix, including all taxa with maximum frequencies of more than two and a half per cent and splitting *N. umboniferus* into two morphotypes. The BALANC/DENDRO analysis resulted in essentially the same subgroups, but principal component analysis yielded two significant components (table 7).

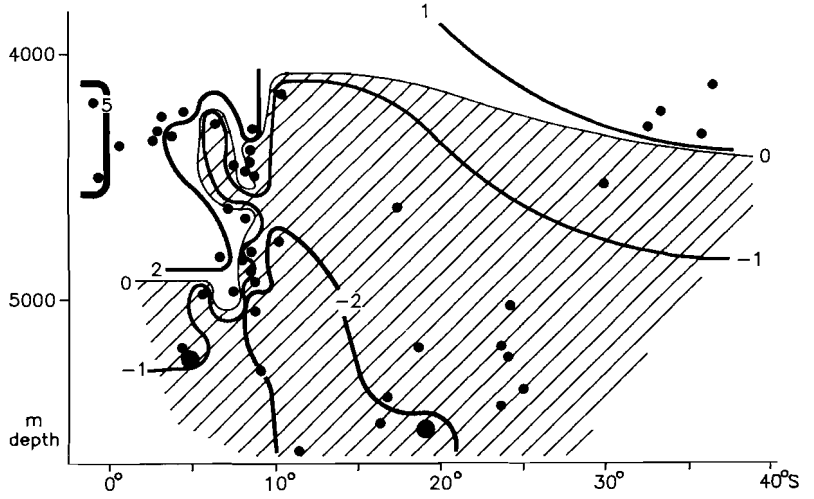

Fig. 41. Depth-latitude diagram showing the sample scores on the first principal component of the PC analysis of 32 taxa (150-595 μm) in all samples from a depth below 4000 metres. Hatching shows negative values (see table 7).

principal component	1	2	3
eigenvalue	5.2	3.9	2.8
variance (%)	16.2	12.2	8.8
species			
Astrononion sp.	.3	.1	.2
G. subglobosa	.3	-.1	.1
G. polia	.3	.1	-.0
Laticarinina pauperata	.3	-.2	-.3
B. rostrata	.2	-.1	-.3
C. cf. *robertsonianus*	.2	.2	.1
M. formosus	.2	.1	.3
miliolids	.2	-.1	-.1
N. umboniferus convexus	.2	-.2	-.4
O.umbonatus A	.2	.1	.0
C. wuellerstorfi s.s.	.1	.2	-.0
Ehrenbergina trigona	.1	-.1	-.2
Fursenkoina bradyi	.1	-.1	.3
G. cf. *altiformis*	.1	-.1	.2
M. barleeanus	.1	1	-.0
O. umbonatus C	.1	.3	-.0
P. bulloides s.s.	.1	.4	-.0
P. bulloides osloensis	.1	-.3	.2
Pullenia sp. 1	.1	-.3	.1
P. murrhina	.1	.2	.1
Sphaeroidina bulloides	.1	-.2	.3
U. peregrina dirupta	.1	-.1	-.2
E. tumidulus	-.0	-.1	-.1
Gyroidina sp. 1	-.0	-.2	.3
O. umbonatus B	-.0	.3	.0
monothalamous	-.0	-.2	.1
Gyroidina spp.	-.0	1	.1
Pullenia sp. 2	-.1	-.2	.2
M. sphaeroides	-.1	.1	-.1
C. robertsonianus bradyi	-.1	-.2	.1
E. exigua 1	-.2	.0	.1
N. umboniferus s.s.	-.4	-.1	-.1

Table 7. Results of a principal component analysis of the frequency distribution of the thirty-two most common benthic foraminiferal species (150-595 μm) at abyssal depth. Eigenvalues, percentages of total variance and composition of the first three components.

The first component opposes *E. exigua* 1 plus *N. umboniferus* s.s. to an equivalent of the northern abyssal subgroup, which now also includes C. cf. *robertsonianus, Laticarinina pauperata, M. formosus,* and *N. umboniferus convexus.* The second component discriminates between the species of the continental margin (plus *P. murrhina*) and those that abound in land-distant areas. The latter group is dominated by *P. bulloides osloensis* and *Pullenia* sp. 1.

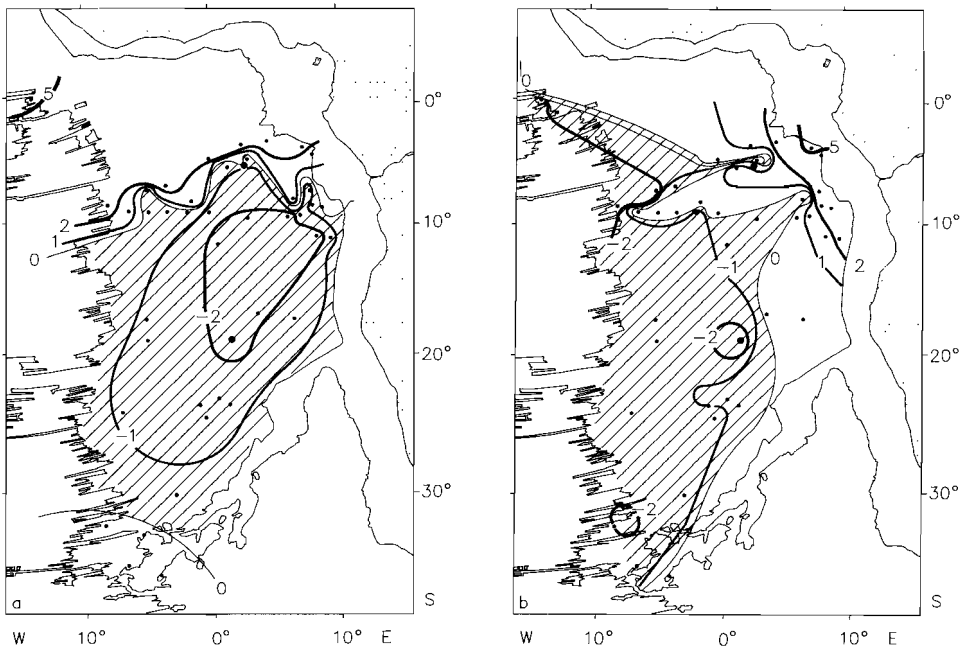

Fig. 42. Contour map of the sample scores on (a) the first and (b) the second principal component of the PC analysis of 32 taxa (150-595 μm) in all samples from a depth below 4000 metres. Hatching shows negative values (see table 7).

A depth-latitude plot of the sample scores on the first axis is shown in fig. 41 and the geographical significance of the two components is illustrated in fig. 42.

IV.4. MULTIVARIATE ANALYSIS OF THE 63-595 μM FRACTION

Multivariate analysis of the fauna in the total fraction hardly gives any new information. It is in general difficult to interpret the results and the BALANC correlation-matrices appear to be poorly structured.

Relevant results are produced by a BALANC/DENDRO analysis of the percentage distribution of the twenty-three most important taxa in samples from more than 4000 metres depth (fig. 43). Three taxa, viz. *B. translucens, G. polia,* and *P. bulloides* s.s., were included, although they do not reach the five per cent level.

Three main groups can be recognized in the correlation matrix shown in fig. 43, but the correlations indicate that the groups are rather heterogeneous. The most coherent one comprises *C. wuellerstorfi* s.s., *N. pusillus* 1 and 2, *O. um-*

bonatus 2B and 2C, and *P. bulloides* s.s. This first group unites taxa that abound along the continental margin and all elements are negatively correlated with *G. subglobosa* and the monothalamous species, categories avoiding the marginal area.

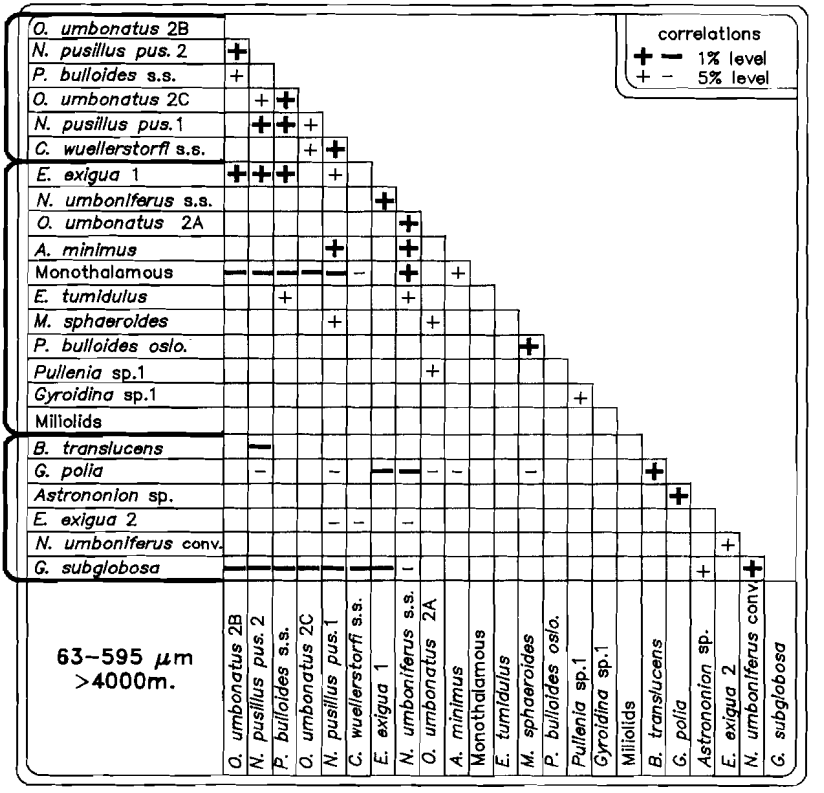

Fig. 43. BALANC correlation matrix based on the analysis of 23 (63-595 µm) taxa in all samples from a depth below 4000 metres. The three main groups identified in the dendrogram are indicated (uninterrupted lines indicate species joining each other at $\alpha = 0.05$).

G. subglobosa is together with *Astrononion sp.*, *B. translucens*, *E. exigua* 2, *G. polia*, and *N. umboniferus convexus*, loosely arranged into a second group. Generalizing, we may conclude from their individual distribution patterns that these taxa all have low frequencies in the deep central part of the Angola Basin.

A third and very heterogeneous group unites the remaining species. Their distribution is not very similar and this group can be considered a rest group. Note that *E. exigua* 1 shows regular positive correlations with the first group.

Principal component analysis does not produce a significant axis. The first component (table 8) essentially discriminates between the first two groups, but

E. exigua 1 has joined the taxa of the continental margin group, while the monothalamous category has similar loadings as the species that avoid the central part of the Angola Basin. These results confirm the heterogeneity of the rest group. A map of the sample scores on the first component shows that this axis defines an overall contrast between the area of the deep-sea fan and the north-western and south-western extremes of the region (fig. 44).

IV.5. RELATION WITH THE ENVIRONMENT

IV.5.1. Introduction

Numerous studies contributing to benthic foraminiferal ecology have shown that a wide array of environmental factors influence species distribution (see for

principal component	1	2	3
eigenvalue	5.2	3.9	2.8
variance (%)	16.2	12.2	8.8
species			
G. subglobosa	.4	-.1	-.0
G. polia	.3	-.3	.1
monothalamous	.3	.2	.1
E. exigua 2	.2	-.2	.0
N. umboniferus convexus	.2	-.1	.2
Astrononion sp.	.2	-.2	-.1
B. translucens	.2	-.2	-.1
P. bulloides osloensis	.2	.0	.0
Pullenia sp. 1	.2	.1	-.3
miliolids	.2	.0	.3
Gyroidina sp. 1	.1	.0	-.3
E. tumidulus	.1	.1	.4
O.umbonatus 2A	.0	.3	-.1
A. minimus	.0	.2	.2
M. sphaeroides	-.0	.1	-.0
O. umbonatus 2C	-.1	-.2	.4
N. umboniferus s.s.	-.1	.4	.1
C. wuellerstorfi s.s.	-.1	-.1	.1
O. umbonatus 2B	-.2	-.3	-.3
N. pusillus pusillus 1	-.2	-.1	.3
N. pusillus pusillus 2	-.2	-.3	-.1
P. bulloides s.s.	-.2	-.3	.2
E. exigua 1	-.3	.1	-.2

Table 8. Results of a principal component analysis of the frequency distribution of the twenty-three most common benthic foraminiferal species (63-595 μm) at abyssal depth. Eigenvalues, percentages of total variance and composition of the first three components.

discussions Phleger, 1960; Murray, 1973; Boltovskoy and Wright, 1976; Van der Zwaan, 1982). Particularly at shallow depth, the number of parameters involved is large and they, moreover, show a high variability both spatially and temporally. Consequently, shallow marine areas are generally characterized by a complex mosaic of biofacies.

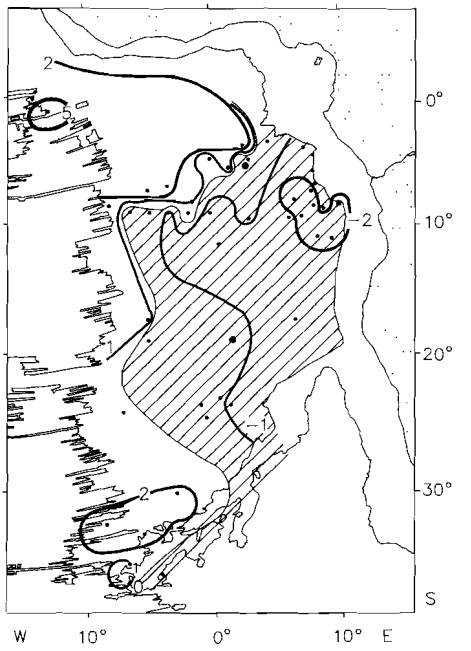

Fig. 44. Contour map of the sample scores on the first principal component of the PC analysis of 23 (63-595 μm) taxa in all samples from a depth below 4000 metres. Hatching shows negative values (see table 8).

As the variability of the physico-chemical variables continuously decreases with increasing depth, deeper water environments tend to be more uniform. Parameters such as salinity, hydrodynamic energy and light penetration, which are of importance in shallow areas, rapidly loose their significance towards deeper water. Deep-water environments, which may include large parts of the continental shelf, are in general more homogeneous in a horizontal than in a vertical direction. This is probably the main reason that many species show a well defined bathymetric distribution over large areas.

The relation between species and bathymetry is of old a major issue in the study of benthic foraminiferal distribution. The initial emphasis on depth distribution is easily understood, because depth used to be the only variable

measured. The reason that many subsequent papers concentrated on bathymetry is that depth-zonations can provide an important tool for estimating paleodepth. Since long it has, however, been realized that depth-zonations are of limited geographic significance. Depth as such is not considered a limiting factor, and is probably only important because other factors are to some extent depth dependent. The only variable, which is directly conditioned by depth, is hydrostatic pressure. Douglas (1979) did not consider it a very influencial parameter, but pressure is known to affect the metabolism of organisms (see Wright and Stephens, 1982).

In environmental studies, particularly those concerning deep-sea foraminifers, interest shifted from waterdepth to water-masses. In his paper on benthic foraminiferal distribution in the deep North Atlantic, Streeter (1973) concluded that the faunal patterns were more effectively described in terms of water-masses than by depth. The water-mass-concept grew very popular and in numerous subsequent studies faunal associations were related to distinct water-masses (e.g. Schnitker, 1974; Gofas, 1978; Lohmann, 1978; Corliss, 1979a; Buzas and Culver, 1980; Culver and Buzas, 1981; Corliss, 1983b; Weston and Murray, 1984). Although fauna/water-mass relations seem to be constant over large areas, different species or combinations of species may characterize a specific water-mass in different parts of the world ocean (Schnitker, 1980; Douglas and Woodruff, 1981).

Schnitker (1980) suggested that discrepancies in fauna/water-mass relations may largely be artificial, caused by the use of different size-fractions. He provided a tentative list of species which if relatively abundant are indicative of a particular water-mass. *N. umboniferus* is an exemplary 'index-species', because it dominates the faunas wherever Antarctic Bottom Water is present. The consistency of this relationship let several authors (e.g. Barker et al., 1981; Peterson and Lohmann, 1982; Troelstra, 1984) to believe that this species is an excellent indicator of AABW.

Douglas and Woodruff (op. cit.), on the other hand, supposed that fauna/water-mass relations differ from one ocean to another, because of variation in non-conservative water properties, notably oxygen content and carbonate concentrations. The significance of oxygen concentrations was already suggested by Streeter and Shackleton (1979), who related high abundances of *Uvigerina peregrina* to waters with low oxygen concentrations (below 220 μmol/l). Subsequent research, however, clearly showed that high abundances of *U. peregrina* are connected with sediments rich in organic carbon rather than with oxygen depleted waters (e.g. Lutze, 1980, Miller and Lohmann, 1982; Corliss, 1983b; Corliss et al., 1986; Lutze, 1986; Van Leeuwen, 1986).

Recent literature, actually, suggests that substrate-related parameters in

general and the organic carbon content of sediments in particular may affect the distribution of benthic foraminiferal species in marginal deep-sea areas to a much larger extent than previously assumed (e.g. Douglas, 1979; Lutze and Coulbourn, 1984; Mackensen et al., 1985).

Comment on the water-mass concept

Although we now know that water-mass configuration can not explain the distribution of deep-sea benthic foraminifers alone, the relation between fauna and water-mass is still a fundamental one in ecologic concepts. Water-masses are, however, generalizations of the environment and like depth this concept leaves us with the question which environmental factors actually control major distribution patterns.

Basic to the water-mass concept is the assumption that water-masses represent unique environments. Physically, a water-mass is a relatively homogeneous body of water, which is described by a characteristic temperature and salinity. Other parameters such as oxygen, carbon dioxide and nutrient concentrations, are less conservative, because they are more dependent on local conditions, and age and history of a body of water. Because even with respect to temperature and salinity, water-masses are only incidentally completely homogeneous, they are usually defined by a particular temperature/salinity curve rather than by a specific value of both parameters.

The water-mass concept, therefore, implies, that the unique environment that a water-mass is supposed to be for benthic foraminifers, is determined by the combination of temperature and salinity rather than by one of the variables alone. In view of the near constancy of salinity in deep waters, this implication is surprising. We fully agree with Bandy (1953), who remarked that variation in salinity probably only affects benthic foraminiferal distribution in near-shore environments. Temperature, on the other hand, is commonly accepted as one of the dominant ecologic factors (e.g. Gevirtz et al., 1971; Murray, 1973; Boltovskoy and Wright, 1976; Lutze, 1980). Bandy (1953) suggested that bathymetric distributions may largely be explained by the regular temperature decrease towards deeper water. Douglas and Woodruff (1981) questioned the importance of temperature in the deep-sea, but their arguments are only valid if temperature would be the only parameter involved.

Reconsidering fauna/water-mass relations in the literature, we may conclude that in all well-documented studies temperature could describe the major faunal patterns equally well. As a matter of fact, Streeter himself concluded that his faunal associations are well related to temperature. Hence, we consider it erroneous to relate major faunal patterns to water-masses and conclude that it seems more appropriate to speak in terms of temperature alone.

It is, of course, conceivable that non-conservative properties have influenced fauna-water-mass relations reported in the literature, because regionally these variables may consistently differ from one water-mass to another. Only two variables are, in our opinion, to be considered as possibly controlling benthic foraminiferal distribution in the deep-sea, viz. oxygen and carbonate concentrations.

As indicated previously, effects of the oxygen content have probably been overestimated in the literature. According to Bandy (1953) and Murray (1973), a direct effect is only to be likely at very low concentrations, i.e. below 23 μmol/l. Such low concentrations are, however, seldom found in the deep-sea.

The degree of carbonate saturation is generally assumed to be a major ecologic factor (e.g. Murray, 1973; Corliss, 1983b; Douglas and Woodruff, 1981). Carbonate undersaturation of bottom-waters offers the most likely explanation for the predominance of non-calcareous species below the CCD. Furthermore, Bremer and Lohmann (1982) showed that the distribution of *N. umboniferus* in the Atlantic is positively correlated with carbonate undersaturation and they suggested that this is at least partially a primary effect (see also Corliss, 1983b).

IV.5.2. Faunal patterns in the deep-sea of the eastern South Atlantic

In our discussion on the faunal patterns in the region under consideration, we shall concentrate on the results of the analysis of the large-size fraction. Constraints on the faunal data such as diachrony, possible down-slope contamination, dissolution and the geographical bias in our set of data, do not permit to interpret our findings in great detail. But even from a general point of view, the faunal information appears fairly complex. Most species and morphotypes occur only within a restricted depth-interval, but lateral differences in upper depth limit and abundance are the rule rather than the exception. However trivial, both depth related and depth independent factors apparently influence the distribution of benthic foraminifers in our samples.

Emphasizing depth-relations, we stated previously that two of the three faunal groups distinguished on the basis of BALANC/DENDRO analyis of the large-size fraction can essentially be described in terms of depth. A bathyal group which combines taxa that abound above 3000 metres and an abyssal one consisting of taxa common at more than 4000 metres depth.

Although the statistical faunal grouping might suggest otherwise, faunal change with depth seems to be rather continuous. Towards deeper water, bathyal taxa successively disappear, whereas typical abyssal taxa are sequentially added to the faunas; some of the abyssal taxa disappear in their turn in the very deep waters. The addition of new elements stops at depths below 4000

metres, be it that *dirupta* types dominate the *U. peregrina* assemblages only at abyssal depth. Many of our abyssal species and morphotypes first appear between 2600 and 2700 metres, which suggests that a significant faunal change takes place within this specific depth interval. The concentration of new arrivals is, however, probably largely artificial, because in various areas the shallowest sample is from this depth interval.

The first principal component of the analysis of the distribution of the large-sized taxa in the deep-sea was interpreted to reflect an overall change in the fauna with depth (see fig. 39). The sample scores indicate a regular change with depth down to approximately 4000 metres, but depth related differences are less pronounced below this depth. Although the larger scatter in the scores at great depth is probably to some extent artificial, it suggests that lateral differences are more significant in the abyssal realm than depth related contrasts. Judging from the distribution patterns of individual species, the most conspicuous change with depth is the fairly continuously increasing percentage of *N. umboniferus* s.s., but even this morphotype clearly shows lateral differences in abundance. Multivariate analyses of the distribution of large-sized foraminifers at abyssal depth corroborate the absence of a clear faunal change with depth. Significant lateral contrasts are, however, well perceptible, viz. a contrast between the marginal region around the Zaire deep-sea fan and the land distant areas and another one between the northern and southern parts of the region.

Although depth-dependent changes do prevail above 4000 metres, lateral differences were shown to exist as well. First of all, the area of the Zaire deep-sea fan has a deviating fauna also at bathyal depth. Within the depth-interval sampled, i.e. between 3500 and 4000 metres, this area is characterized by anomalously high frequencies of a number of species, among which *C. wuellerstorfi* s.s., *M. sphaeroides,* and *P. murrhina* are the most important. Other species, e.g. *B. rostrata, C. kullenbergi,* and *H. elegans,* which belong to the third group discriminated by BALANC/DENDRO analysis (fig. 37), are virtually absent near the deep-sea fan.

Secondly, we noted already that the bathyal species group can be regarded as a continental slope group. Notwithstanding the geographical unbalance in our set of data, it seems justified to emphasize that the bathyal group is virtually absent at 2630 metres on the MAR. The two samples from above 4000 metres on the ridge have an altogether deviating fauna characterized by high frequencies of *U. hispida,* a species which is virtually absent elsewhere.

Additional evidence that the faunas at great distance from the continent significantly differ from those near the continent, can be exemplified by the contrast between cores RC17-034 and VM19-260. These cores are located at comparable depth in the south-eastern part of the region, VM19-260 at 3585

metres near the continent and the other one at 3537 metres far from the continent on the Walvis Ridge. Species of the bathyal group together make up forty-five per cent of fauna near the continent and *U. peregrina* is the most frequent species (23 %). The abyssal group reaches thirty-two per cent and the species of the third group, e.g. *C. kullenbergi* and *H. elegans*, are absent. At the site far away from the continent, the bathyal group is virtually missing (3 %), and the fauna predominantly consists of abyssal elements (65 %), among which *E. exigua* 1 is the most important (23 %). Of the species of the third group, *B. rostrata* and *H. elegans* are present in low abundances and *C. kullenbergi* reaches a frequency of fifteen percent. The absence of these three species in VM19-260, shows that they do not only avoid the area of the Zaire deep-sea fan.

Finally, it should be noted that our data indicate that there are also significant differences on the continental slope at depths of less than 3000 metres. This is nicely illustrated by the occurrence of a peculiar fauna in RC13-225, at a depth of 2078 metres north of the Walvis Ridge. *B. subacuminata* and *U. auberiana* predominate in this sample, whereas these species are hardly found elsewhere. It is obvious that the samples are so arbitrarily dispersed on the continental margin, that it is impossible to define lateral contrasts, but we think that such differences do exist.

Faunal patterns and water-mass distribution

Earlier in this paper, we discussed the deep-water hydrography of the eastern South Atlantic. With the exception of the samples at abyssal depth near the Romanche Fracture Zone and the Walvis Passage, all our deep-sea localities are within the 75 per cent contour of North Atlantic Deep Water (see fig. 3).

Down to approximately 3800 metres, in-situ temperatures decrease regularly, ranging from 3.4° to 2.35°C (Fuglister, 1960). Isotherms are horizontally arranged, but GEOSECS data (Bainbridge, 1976) show that they slightly rise to the south.

Below 4000 metres, bottom waters are very homogeneous in the greater part of the Angola Basin. Temperature varies between 2.35° and 2.5°C and the warmest waters are to be found in the deepest parts of the basin. Slightly lower temperatures are found near both the Walvis Passage and the Romanche Fracture Zone, where AABW contributes substantially to the bottom waters (fig. 45).

Depth related changes in the faunas above 4000 metres depth may to a large extent be determined by the regular temperature decline. It is, however, evident that neither the lateral differences in this interval, nor the overall contrast between the marginal and land-distant faunas at abyssal depth can be explained from water-mass or temperature distribution.

With respect to the north-south contrast that exists in the large-size fraction at abyssal depth, we observed that the most anomalous faunas are found near the Romanche Fracture Zone. Since AABW contributes significantly to the bottom waters here, the faunal anomaly could to some extent be related to low temperatures. Principal component analysis, however, clearly showed that these northern faunas are very different from those near the Walvis Passage, where the influence of AABW results in comparable temperatures.

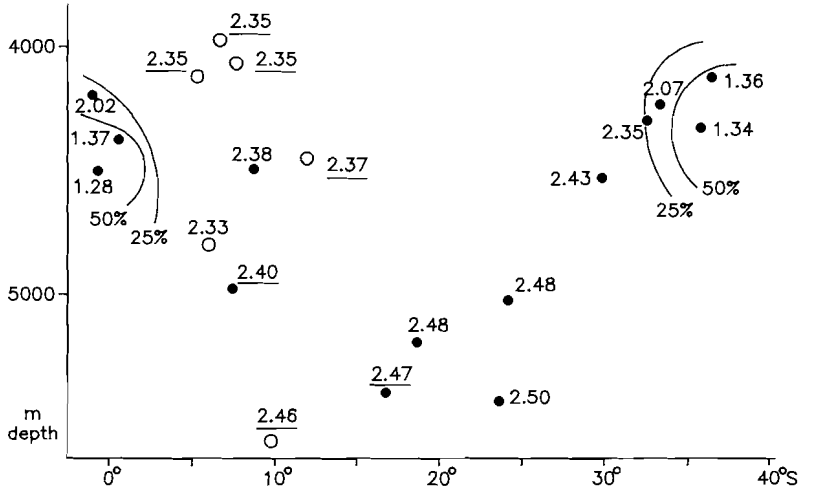

Fig. 45. In-situ bottom-water temperatures at core sites of the 1978 and 1980 NIOZ cruises. Percentage of AABW, based on salinity calculations (see Van Bennekom and Berger, 1984), contoured. Data from Van Bennekom and Berger (underlined) and unpublished data provided by A.J. van Bennekom. Solid circles indicate sites included in the analysis of the benthic foraminiferal (150-595 μm) distribution on the ocean floor.

The northern subgroup which characterizes the faunas near the RFZ consists of *Astrononion* sp., *G. subglobosa*, *G. polia*, *M. formosus* (see fig. 40), and *N. umboniferus convexus* (see fig. 38). With respect to depth, this group is rather heterogeneous because *G. subglobosa* and *M. formosus* show preference for depths below 4000 metres, while the other taxa are also frequent at shallower depth.

Differentiating the northern subgroup accordingly, we plotted the joint frequencies of the taxa to illustrate the north-south contrast once more (fig. 46). We excluded the samples from marginal areas in order to avoid possible blurring of the information. Fig. 46 suggests that the percentage distribution of the taxa of the northern subgroup is much better described by a combination of depth and latitude than by temperature or water-mass distribution. Although

an effect of temperature cannot be excluded, we conclude that the overall distribution of the northern subgroup must essentially be determined by another as yet unknown factor.

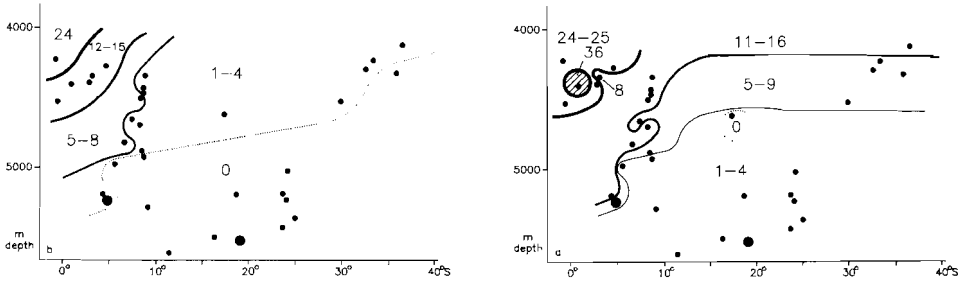

Fig. 46. Depth-latitude diagram showing the summed percentage (150-595 μm) at abyssal depth west of latitude 5°E of (a) *G. subglobosa* and *M. formosus*, and (b) *Astrononion* sp., *G. polia*, and *N. umboniferus convexus*.

Among the other taxa common at abyssal depth in the large-size fraction, only *U. peregrina dirupta* preferently occurs in the areas of inflowing AABW. As discussed in an earlier paper (Van Leeuwen, 1986), we surmise that its distribution is indeed to some extent controlled by temperature. The species *N. umboniferus*, which is so widely accepted as an index species of AABW, is on the other hand not linked up with this water-mass in the region under consideration. The relation between *N. umboniferus* and AABW is actually almost inverse, because this species and the *umboniferus* type in particular, is most abundant where the influence of AABW is weakest. These findings obviously preclude the use of this species as an indicator of AABW.

The first principal component of the analysis of the abyssal total fraction data was seen to reflect a polarity between the fauna of the Zaire deep-sea fan and a group of taxa avoiding the central part of the Angola Basin (see fig. 44). The faunas near the RFZ and the Walvis Passage are positively identified by high abundances of a group of taxa that avoid the central and marginal region at abyssal depth. Again this group is rather heterogeneous and judging from the distribution patterns of the individual taxa, only *G. subglobosa* shows some relation with the areas of inflowing AABW.

The general lack of a relationship between fauna and water-mass distribution may of course be attributed to the small range of temperature differences in the deep-sea under consideration. Since the non-conservative water-mass properties that have been considered of relevance, i.e. carbonate undersaturation and oxygen concentration, are not simply related to water-masses in this region, the

question arises whether variation in these variables could account for the faunal patterns.

The oxygen concentrations of the water below 1750 metres show only little variation and approximately range from 220 to 260 μmol per litre (Bubnov, 1972; Van Bennekom and Berger, 1984; Mantyla and Reid, 1983). The east-west trending oxygen profiles of Bubnov suggest that at 17°S slightly lower values may be found above 2500 metres on the continental slope, which is near the position of RC13-225. Bubnov did not give exact figures, but we may safely assume that even here the oxygen concentration is in the same order of magnitude. Since these concentrations are well above the value that is considered critical for benthic life (Bandy, 1953; Murray, 1973), we may exclude an effect of variation in the oxygen content on species distribution.

As discussed earlier in this paper, the lysocline is situated at a depth between 4600 and 4900 metres in the greater part of the western Angola Basin, shallowing to about 4200 metres in the areas of inflowing AABW. A relation between faunal patterns and the position of the lysocline seems to lack in this area. Considering the distribution of *N. umboniferus*, which according to Bremer and Lohmann (1982) may be controlled by carbonate undersaturation, we must conclude that our data do not support their idea. This species does become more frequent towards deeper water, but carbonate undersaturation of bottom water cannot account for its scarceness in the northern area.

Carbonate dissolution was seen to be a normal phenomenon above the lysocline on the continental margin. Dissolution at shallow depth is, however, governed by pore-water chemistry rather than by water-mass characteristics and we may discard its effects in this context.

All things considered, we conclude that the lateral contrasts in faunal composition cannot be interpreted in terms of water-mass characteristics. This suggests that sediment related parameters must have a profound effect on species distribution.

The Zaire deep-sea fan and the continental margin

The faunal contrast between the marginal and land-distant areas is best documented at depths below 4000 metres, but our data indicate that such a difference exists at shallower depth as well.

The faunas of the Zaire deep-sea fan are in their turn different from those at comparable depth elsewhere on the continental margin. The faunal contrast is most distinctly shown on the upper part of the fan, i.e. between 3500 and 4000 metres. Data are lacking at shallower depth. Although principal component analysis of the 150-595 μm fraction does not indicate a difference between the fan and other marginal areas at greater depth (see fig. 42b), individual species,

such as *E. exigua* 1, *G. subglobosa*, and *P. bulloides osloensis*, do show deviating frequencies on the lower fan and principal component analysis of the total fraction points in the same direction (see fig. 44).

Earlier in this paper, we discussed that the continental margin and the fan area in particular are characterized by a large input of terrigenous matter. Sedimentation rates are high and the sediments predominantly consist of hemipelagic muds containing little carbonate. At greater distance from the continent, deposition is slower and carbonate oozes prevail.

In addition, we may assume that downslope transport processes are more effective along the continental margin than away from the continent. It is, therefore, conceivable that down-slope contamination has affected the composition of the marginal faunas. Although we cannot exclude that allochthonous elements contribute to the faunas, clear evidence of down-slope transport is lacking in our samples. Moreover, since this process can hardly account for the fact that species which are present in the open ocean are missing on the continental margin, we consider the effect of down-slope transport negligible.

Among the substrate-related variables, which control benthic foraminiferal distribution in deep-water environments, the organic carbon content is generally considered of prime importance (e.g. Douglas, 1979; Miller and Lohmann, 1981; Poag, 1981; Lutze and Coulbourn, 1984). Its significance is, in our opinion, self-evident, because the organic carbon available at and in the bottom must directly or indirectly be the food source for benthic foraminifers. Merely quantitative differences may influence species distribution, but nature and origin of the organic carbon should be considered as well. The amount of organic matter is also indirectly of consequence, because it influences interstitial water properties, notably oxygen and carbon dioxide concentrations.

The sediments of the Zaire deep-sea fan and the adjacent continental margin are very rich in organic matter (Jansen et al., 1984; Van Weering and Van Iperen, 1984). Although data are not available for other regions, we can predict regional differences in the organic carbon content to some extent on the basis of general considerations.

The deep-sea ecosystem is almost entirely heterotrophic, because autotrophic organisms (nitrifying bacteria) contribute only a small portion to the organic matter of sediments (Rowe, 1981). As a consequence, practically all the organic carbon at the ocean floor has an allochthonous origin. The amount of organic matter available at the bottom is therefore primarily conditioned by lateral and vertical supply.

The river Zaire supplies an enormous quantity of organic detritus to the area of the deep-sea fan. Eisma and Kalf (1984) estimated that organic matter constitutes between ten and thirty per cent of the suspended matter transported

by the river. It seems reasonable to assume that the lateral flux is lower elsewhere on the continental margin, but generally higher in the marginal areas than away from the continent.

Because it is well-established that the flux of organic matter to the bottom is much higher under highly productive surface-water than in oligotrophic regions (Rowe, 1981; Smith and White, 1982), we may generalize that the vertical flux essentially depends on the primary production in the overlying surface-water. As discussed earlier in this paper, the highest production is found directly in front of the river Zaire and in the area of the Benguela Current. With few exceptions, we may furthermore conclude that the surface waters of the marginal area are in general more productive than those of the open ocean.

Finally, Heath et al. (1977) and Müller and Suess (1979) showed that the concentration of organic carbon in the sediments is directly related to the overall sedimentation rate.

All things considered, it seems plausible that the sediments (including the sediment-water interface) in front of the river Zaire have higher carbon contents than sediments at comparable depth elsewhere on the continental margin. Moreover, we may assume that the marginal sediments contain in their turn more organic matter than sediments deposited in the open ocean. We suggest that these regional differences in the organic carbon content of the sediments essentially control the faunal anomalies discussed above.

Until recently little attention was paid to the effects of substrate related parameters in the deep-sea. It is, therefore, difficult to find evidence in the literature, which supports the interrelation between the abundance of specific taxa and differences in the organic carbon content of sediments. Although we are well aware that comparisons with other areas are hampered by the fact that other variables may be involved, some conspicuous similarities must be mentioned.

Lutze and Coulbourn (1984) showed that along the continental margin off NW Africa, high abundances of *C. kullenbergi* and *H. elegans* are found only in sediments with low organic carbon contents. These observations concur with our data, because these species avoid the area of the Zaire deep-sea fan. The two species are also absent on the continental margin near the Walvis Ridge, i.e. in the sediments that underlie the area of high production associated with the Benguela Current.

According to Poag (1981), high abundances of *C. wuellerstorfi* characterize the faunas on the Mississippi Fan, an area of rapid sedimentation and large supply of terrestrial organic matter. Mackensen et al. (1985) suggested that the abundance of *C. wuellerstorfi* in the marginal area off SW Norway is positively correlated with organic-rich sediments. *C. wuellerstorfi* s.s. is clearly connected

with the Zaire deep-sea fan in our region, and attains its highest relative numbers on the upper fan, which is the area where the bulk of the sediments transported through the canyon is deposited.

A possible interrelation between faunal composition and dissolution has not been discussed. Although we are quite convinced that this factor is of some consequence, a direct effect cannot be evidenced from out findings. The markedly intense dissolution in the area of the deep-sea fan cannot be singled out as a factor, because it is intimately connected with other sediment related parameters. Dissolution might help to accentuate faunal contrasts but is, in our opinion, only of minor importance.

Bathymetric distribution of species and the organic carbon flux

The inferred importance of the concentration of organic matter leads to a relation of general interest. The flux of organic carbon to the bottom is as a rule inversely related to depth (e.g. Honjo et al., 1982). The significance of this relation for benthic macrofaunal abundances was demonstrated by Rowe (1981 and references therein). Rex (1976) thought the gradient of diminishing organic matter even the principal cause of depth-zonations in gastropods.

Whatever the main cause of depth-zonations, it is obvious that the earlier formulated suggestion that depth related changes in the faunas are essentially explained by temperature is too simple and that the flux of organic matter should be considered as well.

If we accept that temperature and the organic matter content of sediments are the major parameters controlling species distribution in deep waters, we would expect that depth-zonations are successful as long as the two variables do not change geographically. If such a change were to occur, species would adjust their depth habitat.

Following this line of reasoning, one could assume that in an area of high organic carbon fluxes, species would tend to occur deeper as long as temperature remained relatively stable.

According to this simplified scenario, one would expect that species tend to have a lower UDL at the continental margin than in the open ocean and that maximum depths are reached in the area of the deep-sea fan.

The geographical unbalance in our set of data, allows to examine only the special position of the Zaire fan on the continental margin. Because a large part of the total depth interval is not covered in the fan area, the distribution of only few species can be compared. Nevertheless, if a difference in depth habitat is observed, it is always in accordance with the model. As an example, the UDL of *E. exigua* 1 is distinctly depressed on the Zaire fan (fig. 47) and the same is suggested for *Astrononion* sp., *G. polia,* and *Pullenia* sp. 1. Even more convinc-

ing are the dominance shifts in the polytypic species *N. pusillus* and *P. bulloides*. In both cases, it is clearly shown that the shallow water morphotypes predominate at much greater depth on the upper fan than elsewhere on the continental margin, while the UDL of the deep-water types is distinctly depressed. This phenomenon is reminiscent of the so-called 'delta-effect' described by Pflum and Frerichs (1976).

We surmise that the interpretation of spatial and temporal variation in the depth-habitat of species may prove to be an important tool in (palaeo)environmental analysis.

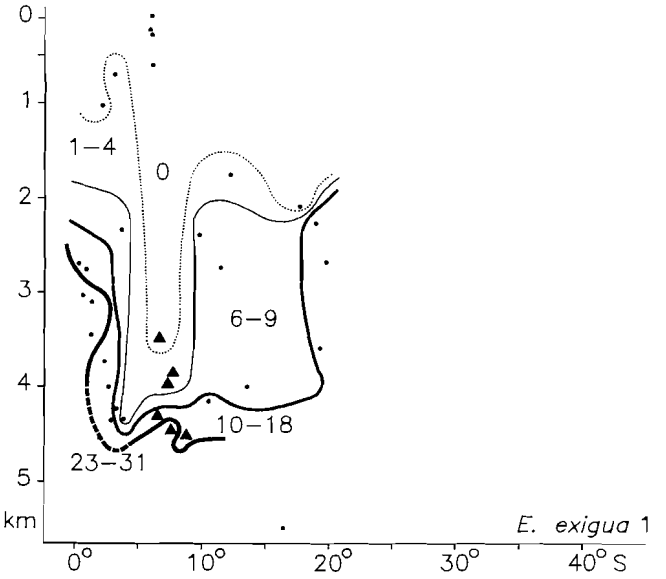

Fig. 47. Depth-latitude diagram showing the percentage distribution of *E. exigua* 1 (150-595 μm) above 4500 metres in the marginal area. Triangles indicate sites on the Zaire deep-sea fan.

The north-south contrast

We have as yet not given a satisfactory explanation for the contrast between the northern and southern abyssal faunas. The north-south gradient (see fig. 42a) cannot simply be related to an overall difference in sedimentary environment, because it crosses the boundaries of the major sedimentary provinces.

The northern region is characterized by relatively high frequencies of *Astrononion* sp., *C.* cf. *robertsonianus, G. subglobosa, G. polia, N. umboniferus convexus,* and *M. formosus,* whereas *E. exigua* 1 and most of all *N. umboniferus* s.s. are more abundant to the south. Because some of the taxa involved, viz. *G.*

subglobosa and *E. exigua* 1, do respond to the contrast between the marginal and land-distant areas, we shall initially only consider the north-south contrast at great distance from the continent, i.e. west of 5°E.

Discussing the relationship with water-masses, we concluded that the distribution of the northern elements should be described by both depth and latitude. Reconsidering their bathymetric distribution (see fig. 46), we may conclude that the taxa become increasingly less frequent towards deeper water irrespective of latitude and that at comparable depth they are more abundant in the north than in the south.

Because an overall effect of temperature can be excluded, we may interpret these general differences in terms of food supply, which in these open ocean area is essentially determined by the vertical flux of organic matter. Thus, the general trend to lower frequencies with increasing depth indicates that the northern elements cannot sustain the low-food levels in the very deep waters. Secondly, the fact that the frequencies of northern elements are higher in the north than at comparable depth in the south suggests that the vertical flux is higher in the north than in the south.

Data on the distribution of *N. umboniferus* s.s. (see fig. 36), show that this taxon follows a reverse pattern, which indicates that it flourishes at low organic carbon levels. The distribution of *E. exigua* 1 does, however, not show a regular relation with temperature and latitude in this area (fig. 32).

The boundary between the northern and southern regions should be situated somewhere between 5° and 10°S. This position approximately coincides with an important boundary in the surface-waters, which separates the highly productive waters of the Equatorial Divergence from the oligotrophic waters to the south. Hence, we suppose that the difference in the benthic faunas primarily reflects a contrast in the production of the overlying surface-water.

Evidence in support of this hypothesis can be inferred from the sediment data provided by Ellis and Moore (1974) and Goll and Bjørklund (1974). They showed that the sediments of the northern region have a much higher content of biogenous opal (mainly diatoms) than those in the southern part of the region.

In the area of Equatorial Divergence, primary production increases towards the continent. If we look at the distribution of the individual northern abyssal taxa in this specific region, we may conclude that *G. subglobosa* becomes less frequent towards the continent. This trend is not only observed in the northern area, but *G. subglobosa* avoids the continental margin in the entire region and is virtually absent in front of the river Zaire. Generalizing, we conclude that at abyssal depth this species actually reaches its highest frequencies at food levels which are intermediate between those of the marginal areas and the oligotrophic region to the south.

The other northern taxa seem more evenly distributed over the equatorial area at abyssal depth. Considering the probable difference in the vertical flux of organic matter, we would expect that these species occupy a deeper habitat near the continent than in the west, but this cannot be confirmed on the basis of the sparse data available. With regard to their overall distribution, little can be said about *M. formosus* and *N. umboniferus convexus*, but *Astrononion* sp., *G. polia*, and *C.* cf. *robertsonianus* show an interpretable pattern. The UDL of the first two species is much deeper in the area of the Zaire deep-sea fan than elsewhere on the continental margin and C. cf. *robertsonianus* is even completely absent in the fan area. Thus. we may assume that these taxa like *G. subglobosa* prefer intermediate food levels. These three species reach their highest relative frequencies at shallower depth than *G. subglobosa*, which indicates that they flourish at slightly higher organic carbon levels than *G. subglobosa*.

Concluding remarks

Summarizing, we conclude that the major faunal patterns in the region under consideration seem determined by variation in water temperature and in organic carbon content of the uppermost sediment layers. Because temperature differences are very small, contrasts in the amount of food are automatically stressed in our set of data.

In the aforegoing sections, we emphasized the quantitative aspects of the organic carbon present at the bottom. We are, however, well aware of the fact that even in essentially homothermal bodies of water, the quantity of food is not the only controlling factor. Pore-water properties and the carbonate flux may be significant as well. Moreover, we fully agree with Poag (1981), who stated that differences in the origin of organic carbon may also influence species distribution.

Many of our taxa do not follow the presumed organic carbon levels in such a regular way as the species on which we extensively commented. As an example, *N. umboniferus* s.s., which is so distinctly connected with the low carbon flux under the oligothrophic open ocean, is not markedly less frequent in the area of the Zaire deep-sea fan than elsewhere at abyssal depth. Yet it is quite probable that the entire fan area is characterized by a comparatively high organic matter content. We cannot explain the relatively high frequencies on the fan, but we would like to point out that it is in general hazardous to compare marginal and land-distant areas. We more or less tacitly assumed that the organic carbon content of the sediment may be considered a measure for the availibity of food. This seems reasonable as long as the vertical flux predominates, but in marginal areas with a considerable contribution of land-derived organic matter, this assumption may be erroneous. The organic detritus

from the continent probably mainly consists of refractory components, which are not readily consumed by organisms. Moreover, there is an important difference in the distribution of organic matter in the upper layers of the sediment. In areas of slow deposition, organic carbon is only available in significant quantities near the sediment-water interface. On the other hand, the higher sedimentation rates along the continental margin favour accumulation of organic matter in the sediments. As a consequence, we consider it likely that a well-developed in-fauna is only to be expected in marginal areas.

Chapter V

LITHOLOGY OF THE CORES

V.1. TIME-STRATIGRAPHIC FRAMEWORK

Glacial/interglacial cycles are well described by the oxygen-isotope record of foraminiferal shells, which registers changes in the isotope composition of the ocean. These changes are considered to reflect primarily global variation in the volume of water that is stored in continental ice-masses (for a discussion, see e.g. Williams, 1984). The isotope-record has been widely accepted as a time-stratigraphic standard for the Quaternary in ocean research. Isotope stages have been defined (e.g. Emiliani, 1955; 1966), which are numbered from recent to past and by convention cold periods have even numbers (fig. 48).

Stages 1 and 5 are basically the equivalents of the Holocene and the last interglacial. Stage 5 has been subdivided into five substages, viz. 5a-e, which represent minor cold and warm intervals (Ninkovitch and Shackleton, 1975). Superimposed on the warm/cold alternation, climate progressively deteriorated toward the end of the last interglacial, for which we take an age of 71,000 yr BP (Imbrie et al., 1984). The oldest substage (5e) represents the only period in the past 150,000 yr, in which there was as little ice as today.

Stages 2 to 4 represent the last glacial and are characterized by an overall larger ice-volume than stages 1 and 5, with a maximum in stage 2 and a mimimum in stage 3.

The stratigraphic framework used here is essentially based on the zonation introduced by Ericson et al. (1961) for the tropical Atlantic Ocean. Zones are based on the presence/absence pattern of *Globorotalia menardii* and lettered Z, Y etc. in order of increasing age. Zones characterized by the presence (absence) of *G. menardii* are thought to correspond to interglacials (glacials).

The zonation has been evaluated to some extent against the isotope record (e.g. Van Donk, 1976; Williams, 1984) and with regard to the Late Quaternary the general concept seems to be essentially correct. The X/Y and Y/Z boundaries are, however, found to be diachronous (e.g. Kennett and Huddlestun, 1972; Berger, 1982; Sarnthein et al., 1982). This holds in particular for the X/Y boundary, which has been correlated with the boundary between isotopic stages 4 and 5 in the central Caribbean (Kennett and Huddlestun, 1972), but which is within stage 5 in the Colombia Basin (Prell and Hays, 1976) and in the Gulf of Mexico (substage 5b; Williams, 1984).

In the eastern South Atlantic, the X/Y boundary defined by the disap-

pearance of *G. menardii* seems to be generally older than the extinction level of *Globorotaloides hexagonus*. Correlations based on carbonate stratigraphy suggest that the temporary extinction of *G. menardii* occurs within stage 5, whereas the Last Occurrence Datum of *G. hexagonus* approximately coincides with the boundary between stages 4 and 5 (Gardner and Hays, 1976; Zachariasse et al., 1984). We, therefore, placed the X/Y boundary in our cores at the Last Occurence Datum of *G. hexagonus* (fig. 49).

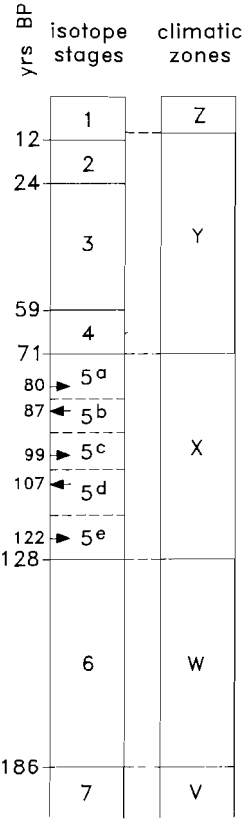

Fig. 48. Correlation scheme showing oxygen-isotope stages and the climatic zonation after Ericson et al. (1961) discussed in the text. Right and left pointing arrows indicate isotope maxima and minima of stage 5, respectively. Age estimates from Imbrie et al. (1984).

The age of the Y/Z boundary is taken to be at about 10,000 yr BP in the area of the Zaire deep-sea fan (see Olausson, 1984; Zachariasse et al., 1984).

Because reworking appeared to be significant in most of the cores, our criteria could not be applied too strictly and we were forced to weigh the stratigraphic

value of the occurrences of *G. menardii* and *G. hexagonus* against the total planktonic signal. It should be noted that the position of the X/Y boundary is very uncertain in KW26.

The studied part of KW25 extends far back into time, but no attempt was made to subdivide the W zone. Clear evidence that the V/W boundary was reached is lacking.

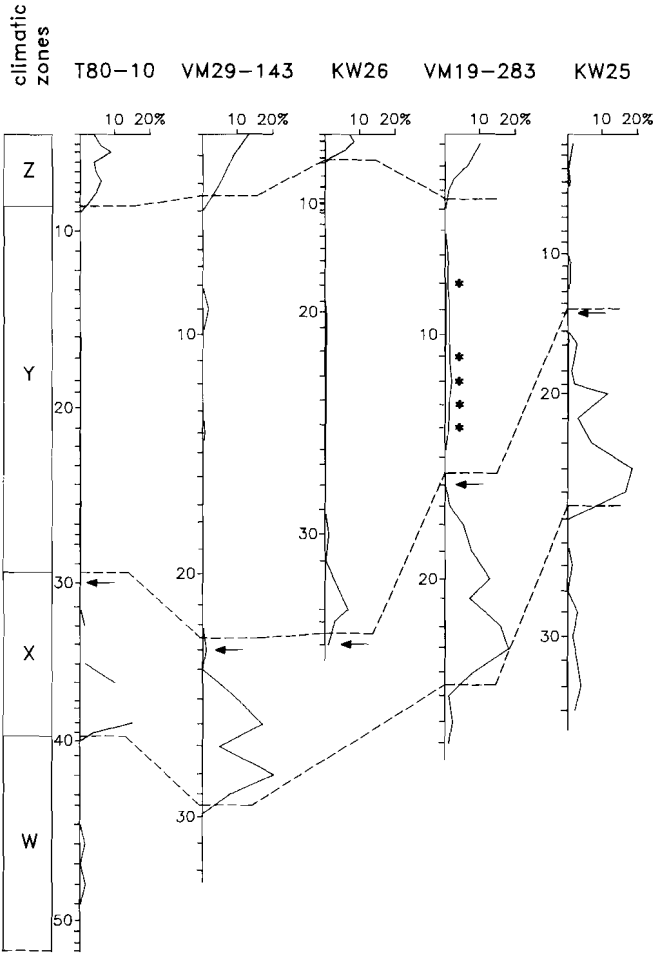

Fig. 49. Time-stratigraphic framework of the cores based on the percentage distribution of *Globorotalia menardii* and the LOD of *Globorotaloides hexagonus* (arrows). Zonation after Ericson et al. (1961) is shown at the left hand side. Asterisks mark occurrences of *G. hexagonus* attributed to reworking. Numbers alongside refer to samples.

V.2. LITHOLOGY

Lithological descriptions were made by different scientists and we slightly modified the original descriptions to eliminate inconsistencies in terminology. The cores were described shortly after opening with the exception of KW26, which was described by the present author long after recovery. The split core was, however, kept sealed and stored under cool conditions. The location of the cores is shown in fig. 50.

Colour codes (fig. 51) are in Munsell notation, based on the Revised Standard Soil Color Charts (Oyama and Takehara, 1970).

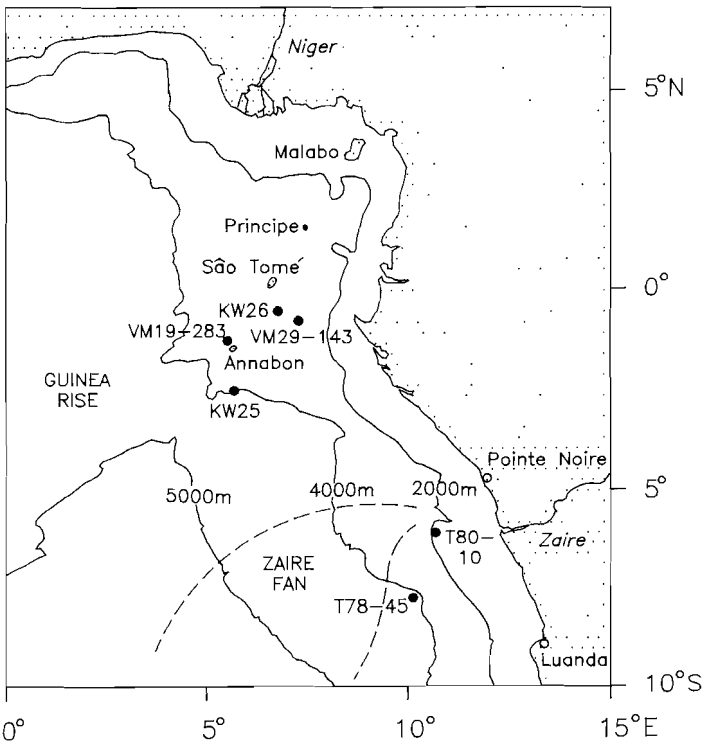

Fig. 50. Location of the cores; included T78-45 studied by Zachariasse et al. (1984).

T80-10 was taken about 180 km west of the river Zaire close to the submarine canyon at 1988 metres depth. The influence of the outflowing river is well reflected in the sediments, which are composed of dark clays. The clays are texturally homogeneous, but as a rule they are distinctly mottled. Large burrows, with a diameter of up to two cm, occur throughout the core. The clay is silty over limited intervals, i.e. between 630 and 780 cm and between 1596 and 1615

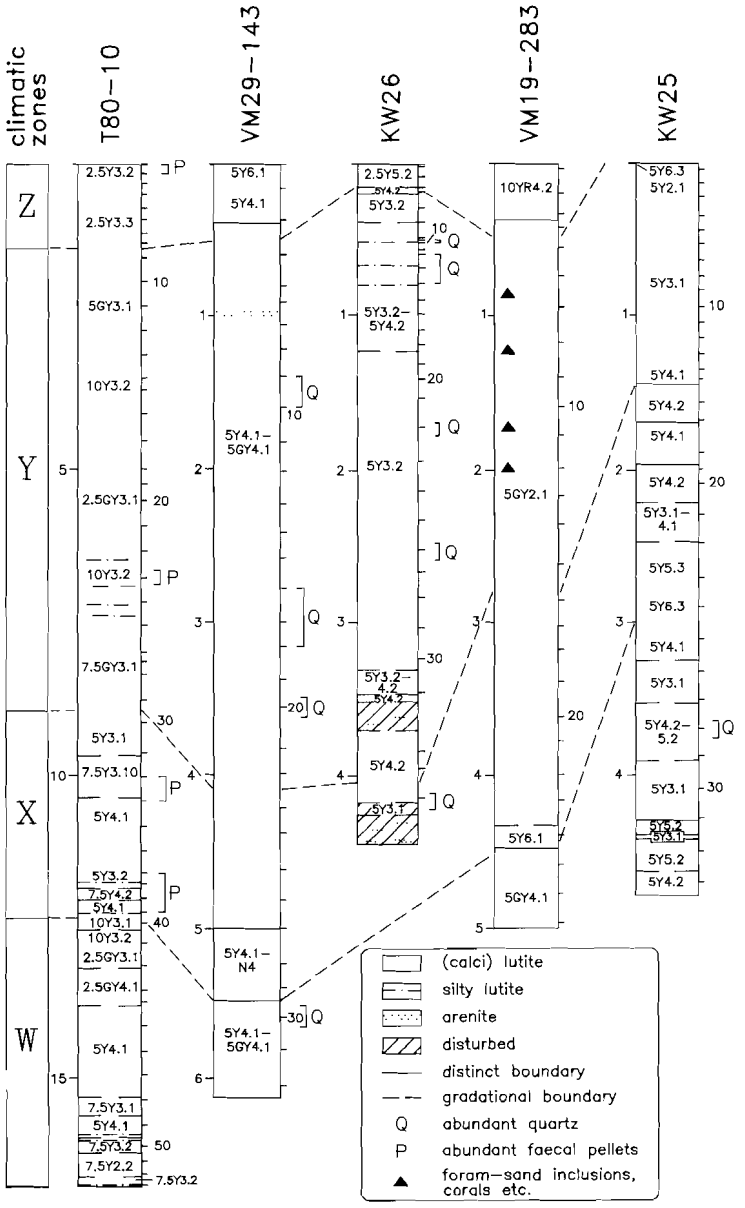

Fig. 51. Lithology of the cores with colours in Munsell notation. The climatic zonation after Ericson et al. (1961) is shown at the left hand side. Correlations are indicated by dashed lines. Sample levels are given to the right and depths (in m) to the left side of the columns. Note the difference in vertical scale for core T80-10.

cm. Silty, laminated layers of about one cm thickness are observed at 1181, 1183, 1227 and 1672 cm (fig. 51).

The sediment varies from greyish olive (7.5Y 2.2; 5Y 4.1) to greyish olive green (7.5GY 3.1) becoming more brownish towards the top (2.5Y 3.2, 2.5Y 3.3).

The content of calcium carbonate (fig. 52) varies from less than one up to seventeen per cent. Faecal pellets are locally frequent and two types can be distinguished, a green one which is particularly abundant is samples 1, 2, 33 and

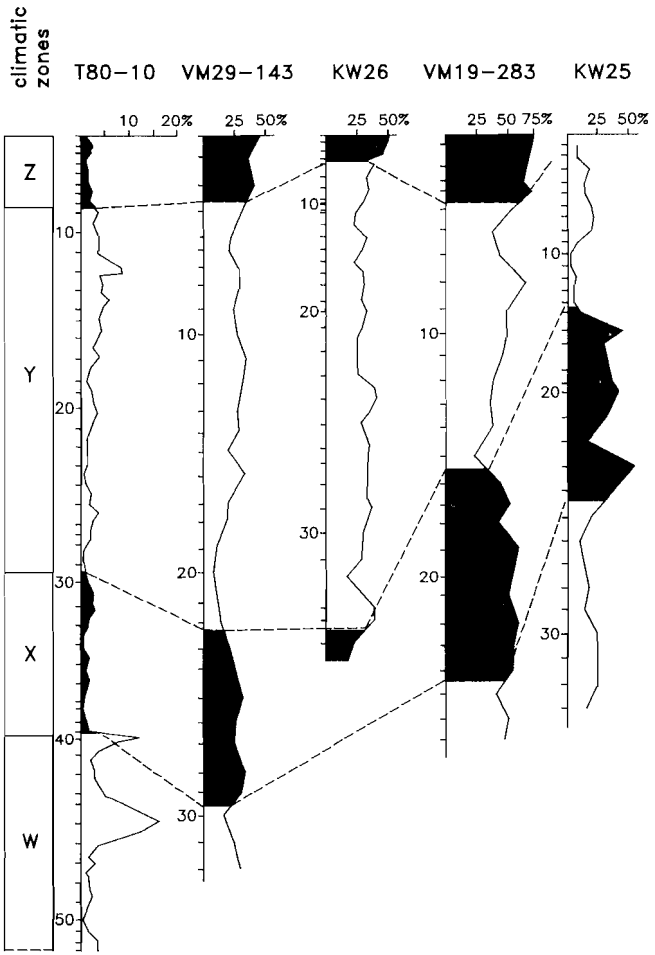

Fig. 52. Calcium carbonate content expressed as weight percentage. The carbonate curve of core T80-10 is from Jansen et al. (1984). The climatic zonation after Ericson et al. (1961) is shown at the left hand side. Interglacials are shaded. Numbers alongside refer to samples.

36-39, and a greyish brown type, which abounds in samples 23 and 32. The number of radiolarians varies greatly, but in a seemingly random way. Pteropods occur in samples 9 and 10 only and quartz grains are extremely rare in the entire core.

VM29-143 comes from a depth of 2756 metres at the continental margin near the Guinea Rise, about 110 km south-east of Sâo Tomé. The core was sampled down to 605 cm and consists of clays, marls and an occasional sandy layer. The sediment is distinctly bioturbated and large burrows occur throughout the interval sampled. Four lithological units can be distinguished.

Down to 40 cm sediments consist of foraminiferal marls. The colour darkens gradually from greyish yellow (5Y 6.1) into greyish olive (5Y 4.1). Carbonate content varies from 36 to 44 per cent (fig. 52). Quartz grains are present in the sand fraction, but in low numbers. The lower boundary is marked by a distinct colour change.

Clays, foraminiferal clays and foraminiferal marls occur between 40 and 500 cm. The colour varies from greyish olive (5Y 4.1) to greyish olive green (5GY 4.1). Carbonate content is generally much lower than in the upper part and varies from 9 to 35 per cent (fig. 52). A layer of quartz sand, with a sharp lower boundary, is found between 97 and 100 cm. In comparison with the upper unit, quartz grains are usually more abundant, especially in samples 9, 10, 16-18 and 20.

A sharp colour change marks the next unit, which extends down to 549 cm. This interval consists of greyish olive (5Y 4.1) to dark medium grey (N4) foraminiferal marls. Carbonate content varies between 29 and 38 per cent (fig. 52). Quartz grains are scarce.

The lower boundary is again sharp and the lowermost unit consists of foraminiferal clays and marls, which are similar to the sediments of the second unit. The carbonate content ranges from 19 to 34 per cent (fig. 52). Quartz grains are abundant in sample 30.

KW26 is located at 3038 metres depth in the northern part of the basin about 60 km south of Sâo Tomé. The core was sampled down to 446 cm and mainly consists of foraminiferal marls with thin silty and sandy intercalations. Carbonate content varies from 21 to 51 per cent with the highest value at the top (fig. 52). The sediment is in general homogeneous and large burrows occur between 100 and 140 cm.

The uppermost sixteen cm consist of greyish olive (2.5Y 5.2) foraminiferal marl. The sand fraction contains radiolarians and rare quartz grains. The lithology remains fairly uniform down to 40 cm, but the colour of the sediment gradually darkens to greyish olive (5Y 3.2) below 22 cm.

Between 40 and 124 cm, greyish olive foraminifal marls alternate with thin, lighter coloured (5Y 4.2) layers of about 1 cm thickness. The thin layers may have the same grain-size as the adjoining sediments (58, 75, 104, 122 cm), but coarser (silty/sandy) horizons occur at 54, 68 and 80 cm; the boundaries are rarely sharp. Quartz is a normal constituent of the sand fraction in this interval. and is particularly abundant in samples 9, 10, and 12-14. Radiolarians are common in samples 6-8 and 12, 13.

Greyish olive (5Y 3.2) foraminiferal marls, similar to the marls between 22 and 40 cm, occur between 124 cm and 329 cm. Quartz grains are locally frequent, notably in samples 22 and 26.

Further downcore again a few lighter horizons (5Y 4.2) are intercalated and this type of sediment prevails between 344 and 352 cm. Flow-in disturbed the original coherence of the sediment between 352 and 377 cm and below 417 cm. The disturbed intervals are composed of a mixture of sand, silt and clay, low in carbonate (less than 25 %); plant remains are locally present.

The interjacent interval consists of greyish olive (5Y 4.2) foraminiferal marls. Quartz grains are abundant only in sample 34 and radiolarians are frequent in samples 30 and 31. A few pteropods were found in sample 30.

VM19-283 is located some 25 km north-west of Annabon, in the northern part of the basin at a depth of 3442 metres. The sediments are rich in carbonate (fig. 52) and strongly bioturbated; large burrows occur throughout the core. Sand-sized quartz grains are missing and radiolarians scarce. Four units have been distinguished in the upper five metres studied.

Greyish brown (10YR 4.2), mottled foraminiferal oozes extend from the top down to 37 cm. Calcium carbonate content varies between 64 and 70 per cent. A distinct colour change marks the lower boundary and dark greyish olive-green foraminiferal marls (5GY 2.1) and foraminiferal oozes are found between 37 and 433 cm. Carbonate content ranges from 26 to 71 per cent. Discontinuous intercalations of foraminiferal sand occur at 79-80, 118-119, and 169-170 cm. Shallow-water carbonate grains (e.g. corals) are abundant in the sand fraction at 118-119 and 198-200 cm. The colour of the sediment becomes lighter towards the base and the boundary with the next unit is gradational.

This next unit covers the interval between 433 and 447 cm and consists of a greyish yellow (5Y 6.1) foraminiferal ooze with a carbonate content of about 60 per cent; the lower boundary is distinct. The lowermost unit down to 500 cm includes greyish olive-green (5GY 4.1) foraminiferal marls and oozes with calcium carbonate values varying between 46 and 63 per cent.

KW 25 was taken from 3994 metres depth some 110 km south of Annabon and is the most land distant site investigated. The core was sampled down to

471 cm and consists of homogeneous clays, foraminiferal clays and foraminiferal marls. The colour varies between dark greyish olive (5Y 2.1) and greyish yellow (5Y 6.3). Many units can be distinguished but these will not be discussed in detail.

There is a general correlation between calcium carbonate content (fig. 52) and colour (fig. 51), the lighter intervals corresponding to sediments rich in carbonate. In comparison with the other cores from the northern part of the region, the carbonate content fluctuates greatly, from 3 to almost 58 per cent. Boundaries between the colour units are usually gradational, but sharp contacts are present as well. The number of radiolarians in the sand-sized fraction varies widely, but is usually high below 320 cm. Quartz grains are only important in sample 28.

V.3. LITHOLOGY AND CLIMATIC STAGES

The lithological differences between the cores primarily reflect a general opposition between the hemipelagic and pelagic realms of sedimentation. Core T80-10 represents the predominantly hemipelagic sedimentation area connected with the river Zaire, whereas core VM19-283 with its high carbonate content characterizes an environment sheltered from the influx of terrigenous debris and dominated by pelagic deposition.

The sand-sized quartz grains that occur in both VM29-143 and KW26 and which are occasionally concentrated into distinct layers, are probably deposited by turbidity currents. An aeolian origin is thought unlikely, because the grains are neither rounded, nor frosted. Deposition under the influence of contour currents can be excluded as well, since fast flowing deep currents are absent in the area (Van Weering and van Iperen, 1984). Resedimentation can account for the local occurrence of plant remains in the levels rich in quartz grains (KW26) as well.

Redeposition by turbidity currents could explain the presence of shallow-water carbonate debris in VM19-283 and the discontinuous layers of foraminiferal sand in this core are likely to have the same origin. The greenish faecal pellets that occur in T80-10 are thought to have their origin in the shelf area (Bornhold, 1973). The occurrence of silty laminated sediments in T80-10 is also attributed to downslope transport.

It appears that mass-transported sediments are confined to glacial intervals in VM29-143 and a similar relationship is suggested for VM19-283. The sedimentary record of KW26 is too incomplete to justify any such conclusion and mass-transported deposits were not clearly recognized in KW25. Redeposition in T80-10 is not correlated with glacial intervals.

Damuth (1975) has described a plausible model to explain climate controlled deposition of turbidites in the western equatorial Atlantic or, in more general terms of terrigenous sediments in the deep-sea. During periods of high sea-level stands, sedimentation of terrigenous debris is largely restricted to shelf areas. The deep-sea is a relatively sediment starved environment and receives silicoclastics mainly through localized submarine channels. During glacials, when the sea level is low, the locus of terrigenous sedimentation is displaced towards the shelf-break and sediments are directly supplied to the deep-sea environment. Redeposition of shallow-water sediments would be another source of allochthonous matter, or in the case of a carbonate environment of shallow water carbonate grains.

This model readily explains the relationship between the climatic stages and type of sedimentation in VM19-283 and VM29-143. T80-10 is located near the Zaire submarine canyon, which has presumably been a major pathway for terrigenous debris during periods of both low and high sea-level stands. A relation between climatic stages and type of sedimentation is, therefore, absent in this core.

Down-core variation in calcium carbonate content

Fig. 52 shows that calcium carbonate percentages in KW25 are much higher in the X zone than in the adjoining glacial intervals. A similar relationship, although less pronounced, is found in VM 19-283. In VM29-143, a relation between climatic zones and carbonate content is less clear, but lowest carbonate percentages are again found in glacial intervals. The poor stratigraphic record of KW26 precludes a well-founded conclusion, but T80-10 is clearly anomalous and shows no such relationship.

A relation between carbonate content and climate is well documented in deep-sea sediments of the Atlantic Ocean. Schott (1935) already observed that Holocene deposits were richer in calcite than those formed during the last glacial period. Over the past decades evidence has accumulated that warm periods are generally characterized by higher percentages of carbonate than cold periods. The pattern is so consistent that carbonate curves are used for correlations in various parts of the Atlantic (e.g. Olausson, 1960; 1965; Hays and Peruzza, 1972; Bornhold, 1973; Damuth, 1975; Gardner, 1975; Bé et al., 1976; Gardner and Hays, 1976; Prell and Hays, 1976).

Jansen et al. (1984) used carbonate stratigraphy for correlations between cores from the deeper parts of the Zaire deep-sea fan. In this area, carbonate percentages are high in the entire Z zone, whereas low carbonate values prevail in the Y zone with distinct minima at the top and base. The X zone shows three major carbonate maxima and two distinct minima. Carbonate content is highest

at the basis of the X zone and the three CaCO3 spikes were thought to be correlatable with the warm substages of isotope stage 5. The W zone shows again low CaCO3 percentages.

The main features of Jansen's carbonate pattern are easy to be recognized in KW25, but the shallower cores show only a superficial resemblance to this pattern. The observation that the carbonate pattern becomes less clear towards shallower depth was made also by Gardner (1975) and Jansen et al. (1984). The anomalous pattern of T80-10 is of course excluded from this comparison; sedimentation is probably dominated by rather local processes here (see also Jansen et al., 1984).

Carbonate content depends on three factors, i.e., (1) input of carbonate, (2) dilution with non-carbonate material, and (3) dissolution. The widespread fluctuations in the CaCO3 content of deep-sea sediments and their overall relation with climatic stages have been explained from one or a combination of these factors.

Carbonate input. The input of carbonate in the deep-sea is usually equalled to the production of calcite secreting pelagic organisms. However, it is highly controversial whether a higher pelagic carbonate production indeed results in a higher carbonate content of the sediment. As discussed by Volat et al. (1980), a simultaneous increase of the input of siliceous remains is likely. Moreover, the flux of organic carbon would probably also be augmented, which might influence the preservation of carbonate (see also chapter two). A proper evaluation of the effect of variation in carbonate input is, therefore, not possible on the basis of our data.

Dissolution. Most authors agree that the fluctuations in carbonate content are strongly influenced by variation in carbonate dissolution, as first suggested by Olausson (1965). Evidence for this relation is inferred from similarities between carbonate curves and curves based on preservation-indices (e.g. Gardner, 1975; Bé et al., 1976; Volat et al., 1980; Zachariasse et al., 1984).

We observed significant differences in the state of preservation of foraminifers. Preservation is particularly poor in T80-10, where some samples yielded only a few and severely damaged specimens.

We used the P/P+B ratio to estimate the degree of carbonate dissolution, under the assumption that other factors controlling the ratio have been constant. Fig. 53 suggests that downcore variation in the degree of dissolution is substantial, but there seems no consistent relation with climatic stages. In VM29-143, strongest dissolution occurs in the X zone but in both KW25 and VM19-283 in the Y zone.

The P/P+B (fig. 53) and the carbonate curves (fig. 52) run parallel only in

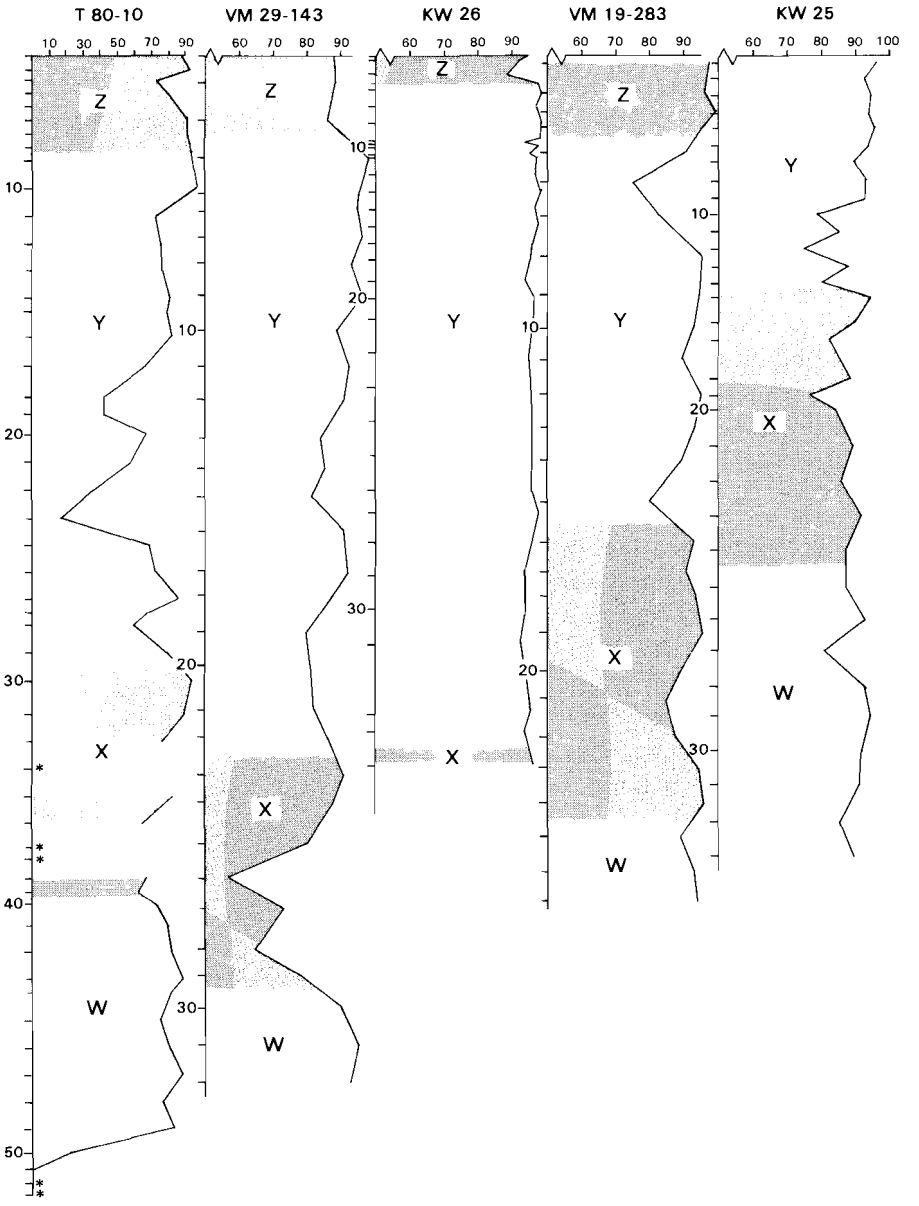

Fig. 53. Proportion of planktonic specimens per total foraminifers in the 150-595 μm fraction (P/P+B x100). Asterisks indicate samples devoid of foraminifers. The climatic zonation after Ericson et al. (1961) is shown and interglacials are shaded. Numbers alongside refer to samples.

VM19-283. The marked glacial/interglacial contrast in the carbonate content of KW25 is clearly not to be attributed to variation in dissolution. The P/P+B ratios indicate that dissolution may, however, have contributed to the very low carbonate content in the lower part of the Y zone in KW25. The lack of an overall coherence between the dissolution proxy and carbonate content, suggests that the glacial/interglacial differences in calcium carbonate content in VM29-143, VM19-283 and KW25 can not primarily be attributed to dissolution.

This conclusion contrasts markedly with the conclusion of Zachariasse et al. (1984). They supposed that the carbonate content of cores from more than about 4,000 metres depth in the area of the deep-sea fan were mainly governed by dissolution. The mutual resemblance of the dissolution patterns appeared so strong, that they established a kind of preservation stratigraphy. Their dissolution events can, however, not be recognized in KW25, which comes from the same depth range. The only exception is the interval directly above the X/Y boundary, which shows evidence of notable dissolution in the area of the deep-sea fan and in KW25 and VM19-283 as well.

The general lack of similarity is in conflict with the suggestion of Zachariasse et al., that the preservation pattern is due to ocean-wide changes in the position of the CCD. We would, instead, suppose that the dissolution is of a more local and, thus, of a supralysoclinal nature. The lower part of the Y zone may represent a period of more widespread dissolution, because elsewhere in the Atlantic (Gardner, 1975; Bé et al., 1976) this interval suffered from severe carbonate dissolution as well.

Dilution. Variation in the input of non-carbonate matter, which is usually equalled to terrigenous material has been considered of influence on the carbonate content by many authors, and some of them even suggested this to be the most important factor in generating the glacial/interglacial carbonate cycles (e.g. Hays and Peruzza, 1972; Dean and Gardner, 1985).

An increased supply of terrigenous matter is a very attractive explanation for the low carbonate content in glacial intervals, because it would fit in with the model of Damuth (1975). In the Angola Basin, glacial/interglacial differences in non-carbonate input are differently appreciated. Bornhold (1973) concluded that there is no overall difference between glacials and interglacials. Jansen et al. (1984), on the other hand, showed that the accumulation rates of both terrigenous matter and opal increased during glacial periods in the area of the deep-sea fan.

If the relatively low carbonate content in the Y zone of KW25, VM19-283 and VM29-143 would be primarily governed by dilution, one would expect to find an increase in bulk accumulation rate, provided that the sedimentary

record is quasi complete. In such a comparison the Z zone should be excluded, because of its presumably higher water content.

As shown in table 9, glacial accumulation rates are indeed higher in VM29-143 and VM19-283. The glacial/interglacial difference in dilution by non-carbonate matter in VM29-143 is of course smaller than the difference in total sedimentation rate, because severe dissolution in the X zone has accentuated the contrast in this core. The opposite holds for VM19-283. The records of KW25 and KW26 preclude a well-founded conclusion. Table 9 suggests a glacial/interglacial contrast in sedimentation rate in T80-10 as well. Jansen et al. (1984), however, demonstrated that it is not that simple in this core. Both the carbonate and non-carbonate accumulation rates are much higher in the upper than in the lower part of the core and the change takes place somewhere in the upper part of isotope stage 3.

core / climatic zone	T80-10	VM29-143	KW26	VM19-283	KW25
Z	14.5	5.0	1.8	5.2*	-
Y	12.4	5.9	6.4	3.7*	2.3
X	5.9	2.4	-	3.1	2.8

Table. 9. Sedimentation rates (cm/10^3yr) calculated for different climatic zones. The age of the Y/Z boundary may be underestimated in VM19-283 (see chapter VI).

All considered, we conclude that the climate-related carbonate pattern in the deeper cores is probably primarily determined by variation in dilution. Dissolution operates as a more random factor, although it may accentuate glacial/interglacial differences in the deeper cores. Sedimentation in T80-10 is to a much larger extent governed by local factors, which are presumably related to its position close to the Zaire submarine canyon.

Chapter VI

THE LATE QUATERNARY RECORD OF PLANKTONIC FORAMINIFERS

VI.1. INTRODUCTION

The presence/absence pattern of *Globorotalia menardii* is a coarse means to delineate changes in the Late Quaternary climate. A useful approach to portray Late Quaternary climatic change in more detail is the analysis of total faunas (e.g. Ruddiman and McIntyre, 1976; Bé et al., 1976).

Species frequencies in the cores under consideration, however, show a rather erratic pattern which certainly stems from local variation in (1) hydrographic conditions, (2) dissolution, and (3) contamination. To reduce local variations and to emphasize the overall pattern of faunal change, we subjected all core data to principal component analysis. This method proved to be helpful in refining the stratigraphy. Principal component analysis, on the other hand, strongly simplifies faunal information and to reconstruct palaeoenvironments we had to rely on the frequency distribution of individual taxa.

Counted numbers and faunal categories

Deletion of the samples with strong evidence of either dissolution or contamination, would have obliterated so much of the essential information, that a quite meaningless database would have remained. We, therefore, included all samples, with the exception of VM19-283/8, in which the coarse fraction benthic fauna is dominated by allochthonous elements.

Most samples yielded sufficiently large numbers of planktonic foraminifers to enable us to count at least a hundred specimens per sample. In T80-10, however, both dilution and dissolution is so strong that a minimum of one hundred could not always be attained. In five samples planktonic foraminifers were even absent. Counts of less than 66 specimens were excluded from mathematical analysis.

The counting results are presented in frequency diagrams (figs. 54-58). All faunal categories reaching frequencies of at least five percent in one of the cores were included. *Pulleniatina obliquiloculata* was added to the selection, because its occurrence has been considered of stratigraphic significance in the equatorial Atlantic (Prell and Damuth, 1978). The pink and white varieties of *Globigerinoides ruber* were lumped. The pink type appeared to predominate in

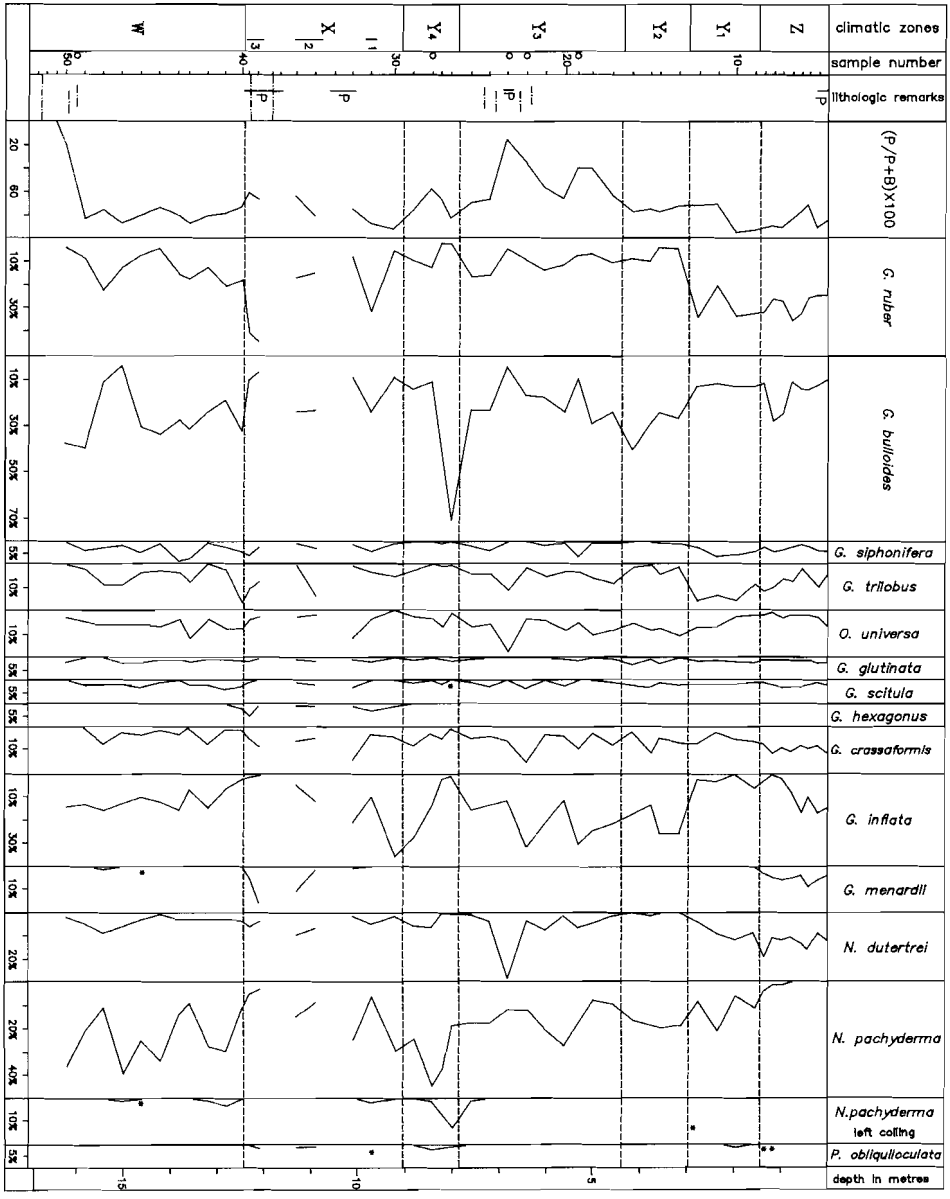

Fig. 54. *Core T80-10.* Percentage distribution of selected planktonic foraminiferal taxa (150-595 μm). Open sections represent intervals without foraminifers, whereas counts of less than 100 specimens are marked by open circles. Frequencies of less than 0.5 % are indicated by asterisks. Major lithologic features are indicated (for legend, see fig. 51). The climatic zonation, which is a refinement of the basic scheme of Ericson et al. (1961) is discussed in the text.

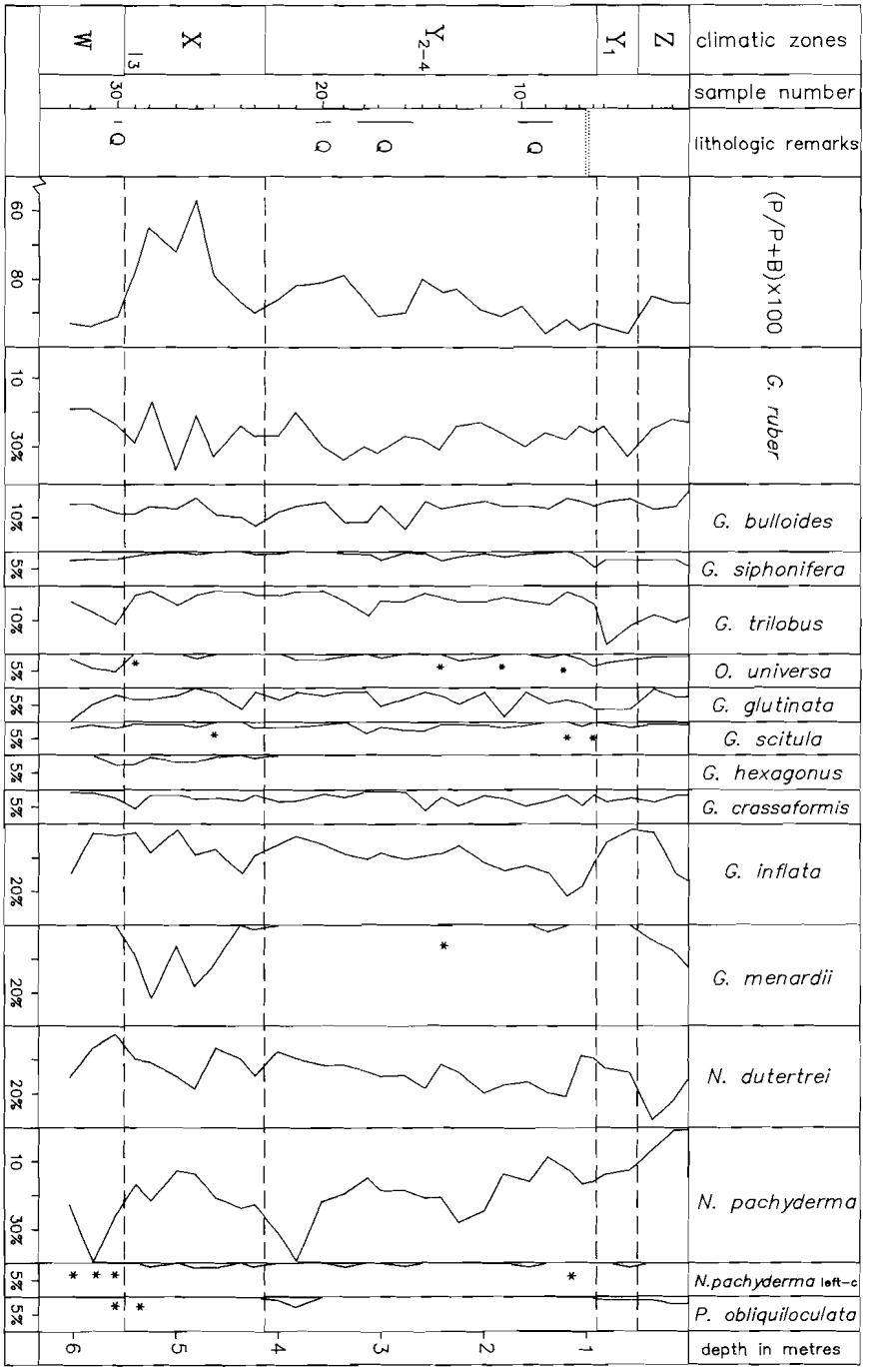

Fig. 55. *Core VM29-143.* Percentage distribution of selected planktonic foraminiferal taxa (150-595 μm). Figure conventions as in fig. 54.

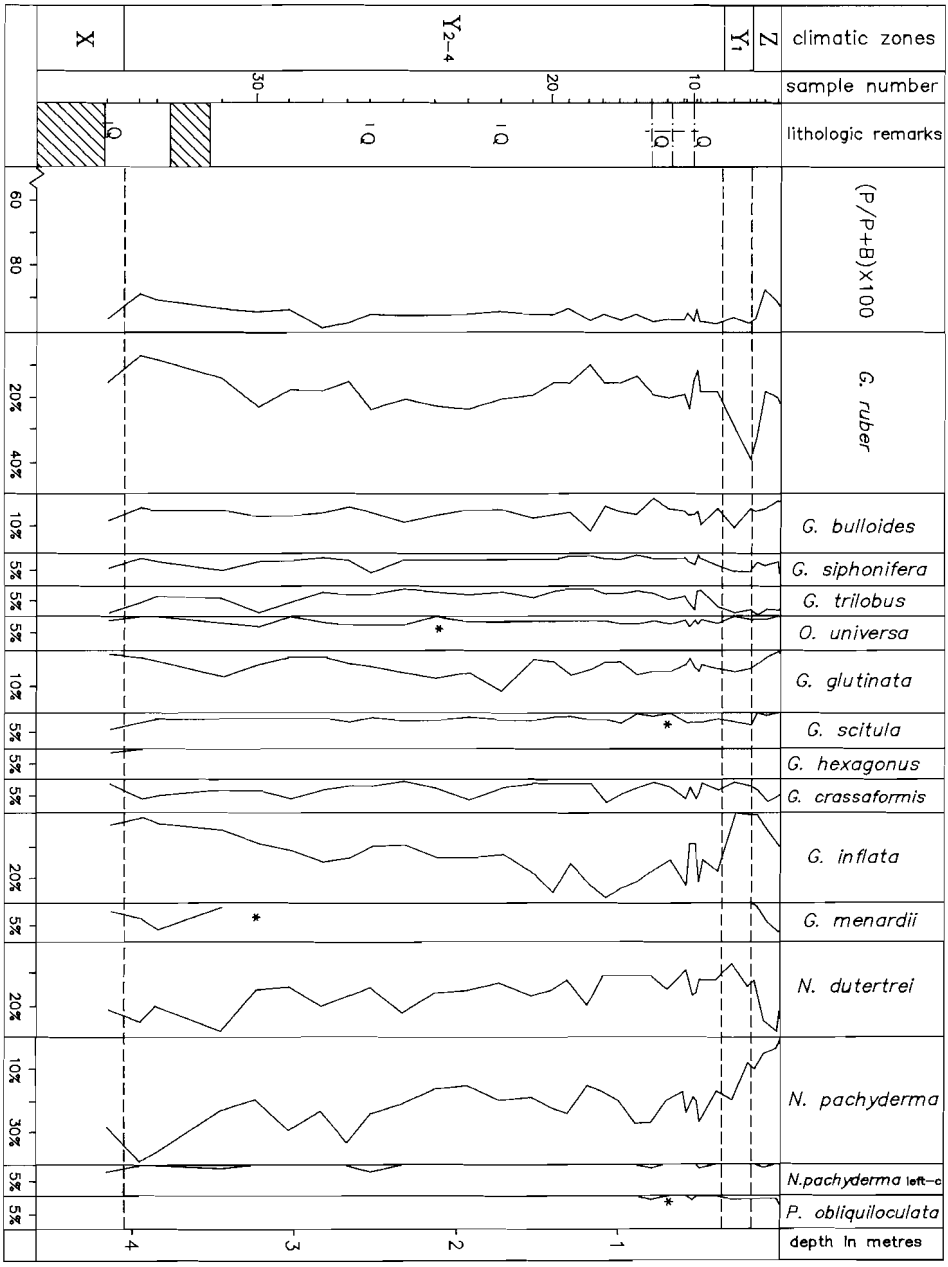

Fig. 56. *Core KW26.* Percentage distribution of selected planktonic foraminiferal taxa (150-595 μm). Figure conventions as in fig. 54.

most of the samples, but variation in the dominance pattern did not show any correlation with our climatic zonation. The distribution of left coiling *Neogloboquadrina pachyderma* is shown in the diagrams as a separate category.

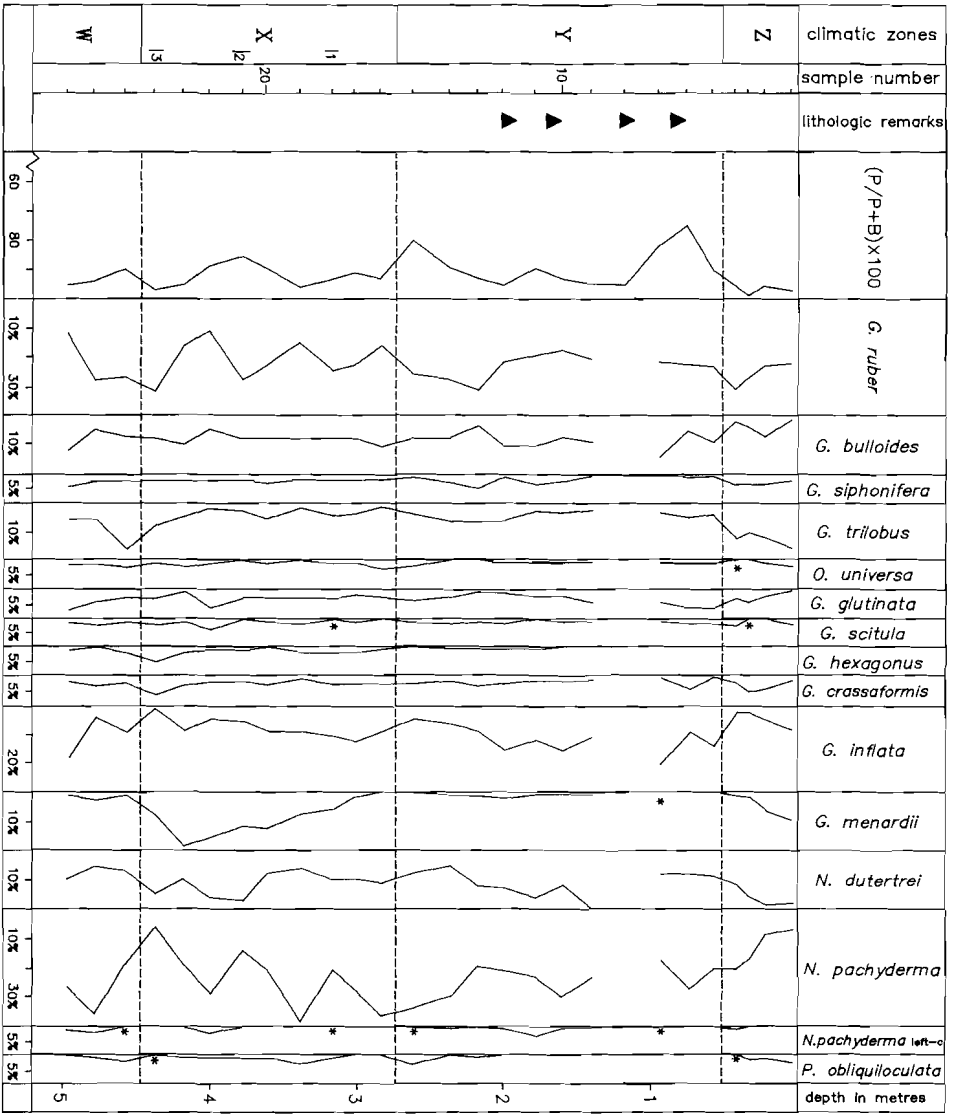

Fig. 57. *Core VM19-283.* Percentage distribution of selected planktonic foraminiferal taxa (150-595 μm). The open section might represent a turbiditic interval and was excluded from faunal analysis. Figure conventions as in fig. 54.

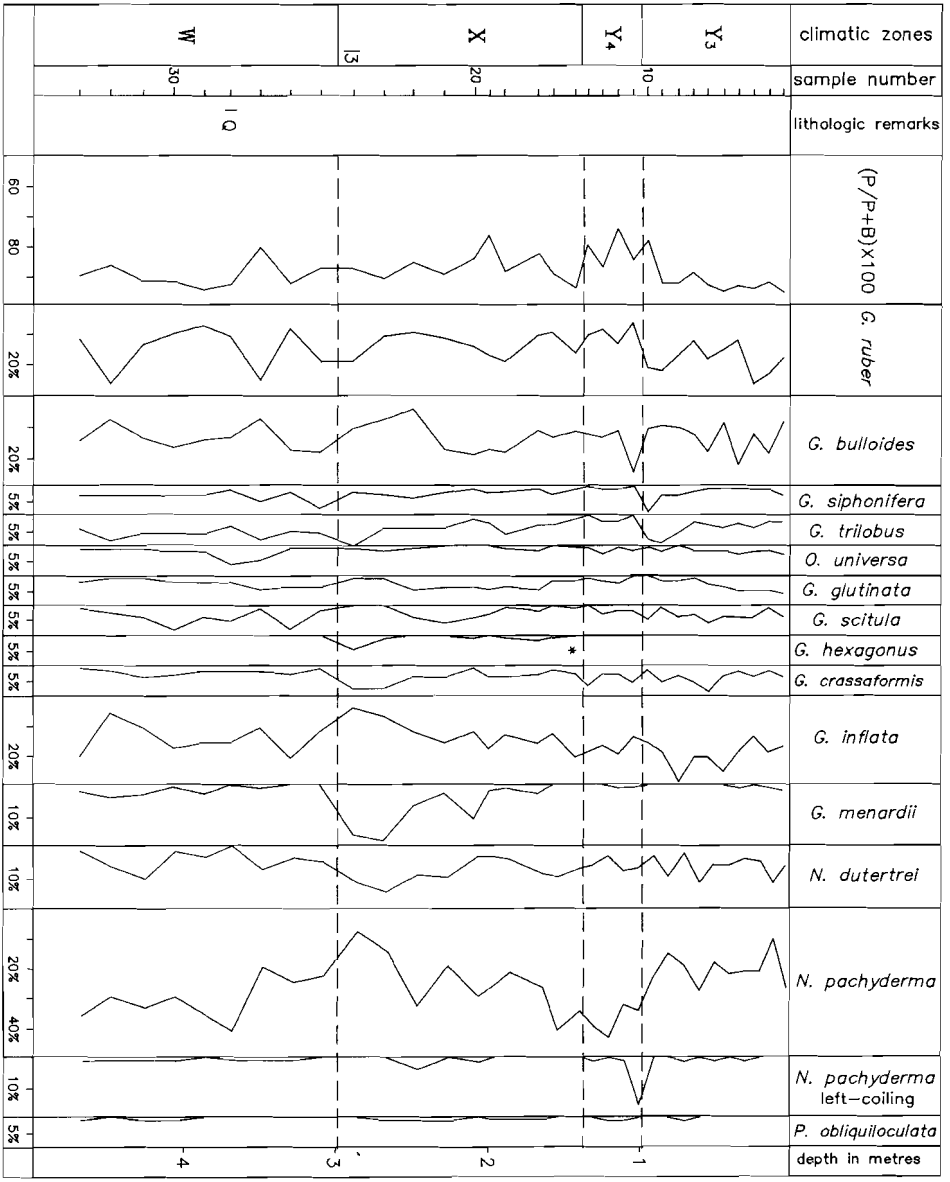

Fig. 58. *Core KW25.* Percentage distribution of selected planktonic foraminiferal taxa (150-595 μm). Figure conventions as in fig. 54.

VI.2.1. BALANC/DENDRO analysis

The frequency diagrams show that there are large differences in faunal composition in each core, which seem independent of dissolution and downslope transport (figs. 54-58).

Faunal change is most pronounced in core T80-10 and although major changes do not always coincide with the boundaries of climatic zones, a general relation to our climatic zonation can be observed (fig. 54). In this core, *Globigerinoides ruber* is usually the most abundant species in the Z zone and high frequencies are also reached at several levels in the X zone. The faunas in the Y and W zones, which represent the on average cooler periods, are general-

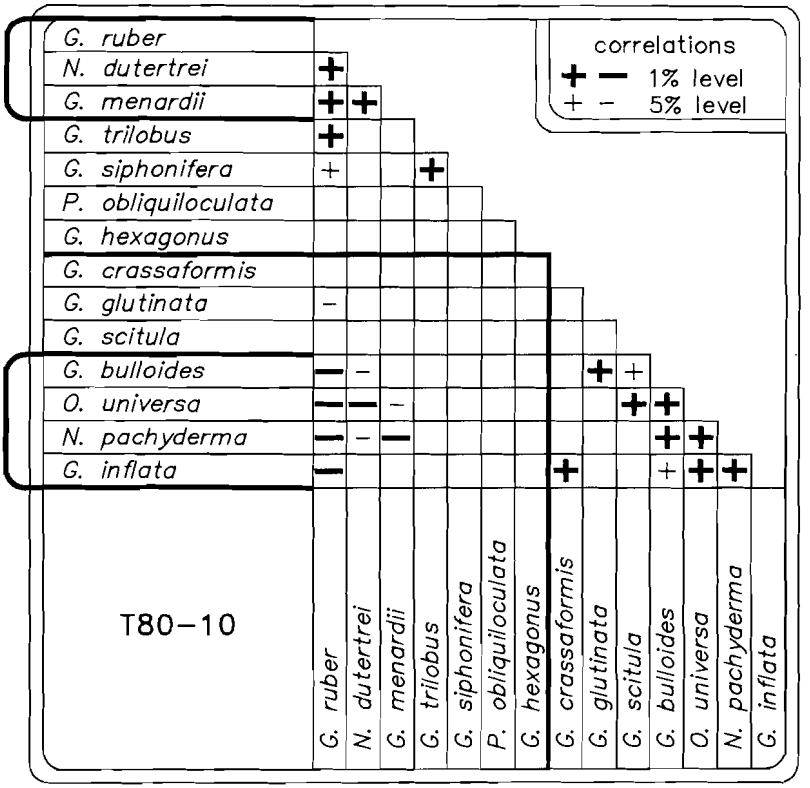

Fig. 59. *Core T80-10.* BALANC correlation-matrix. The heavy line separates the two groups that show the lowest degree of similarity according to the DENDRO analysis.

ly dominated by *Globigerina bulloides*, *Globorotalia inflata*, and *Neogloboquadrina pachyderma*.

The overall faunal contrast between warm and cold climatic periods is well evidenced by a BALANC analysis. The correlation-matrix (fig. 59) shows the presence of two negatively correlated species groups. A first one, termed the glacial group, is composed of *G. inflata*, *G. bulloides*, *N. pachyderma*, and *Orbulina universa*. A second or interglacial group comprises *G. ruber*, *G. menardii*, and *Neogloboquadrina dutertrei*. Two other species, viz. *Globigerinella siphonifera* and *Globigerinoides trilobus* are positively correlated with *G. ruber* but do not show significant correlations with the other species.

Fluctuations in species abundances are less prominent in the four cores from the northern part of the region and a relationship between climatic zones and faunal composition seems to be less clear (see figs. 55-58).

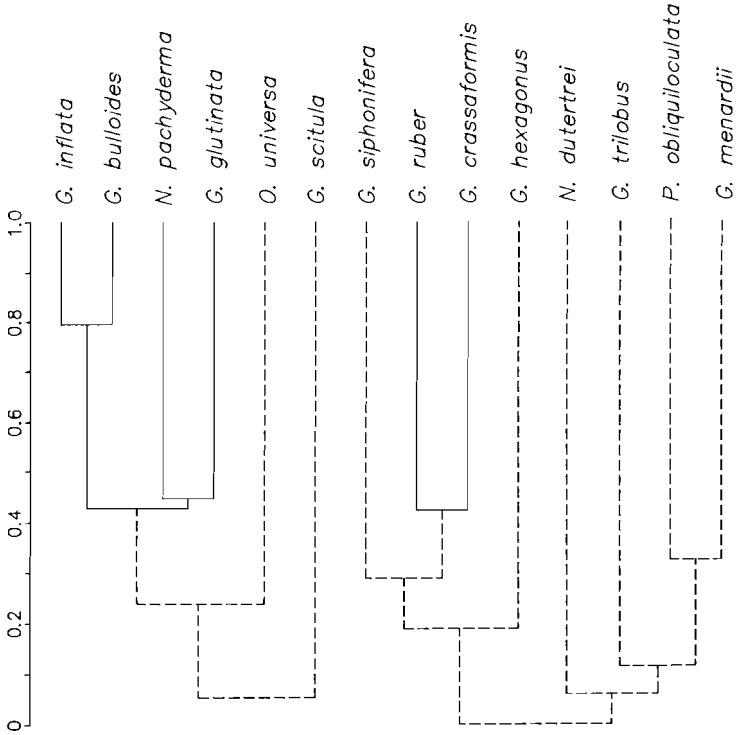

Fig. 60. *Core VM19-283.* Dendrogram based on the BALANC correlation matrix. Only positive correlations are shown. Dotted lines indicate correlations which are not significant ($\alpha = 0.05$).

BALANC analyses on the individual cores give very different results. In both KW25 and VM19-283, the interspecific relations are still comparable to those of T80-10. In KW25, *G. bulloides, G. inflata, Globorotalia scitula,* and *N. pachyderma* are mutually positively correlated (α = .01) and except for *G. scitula* they are negatively correlated with *G. menardii.* Also in VM19-283 there is a general contrast between glacial and interglacial species but the dendrogram (fig. 60) shows that the overall picture is less simple than in T80-10.

BALANC results of KW26 and VM29-143 are even more dissimilar from those of T80-10. Here significant positive correlations (α = .05 and .01 respectively) are evident between *N. dutertrei* and *G. inflata,* and between *G. bulloides* and *G.ruber.* Because the pairs couple two dissolution resistent and two dissolution prone species, respectively, it is suggested that the correlations are determined mainly by dissolution effects.

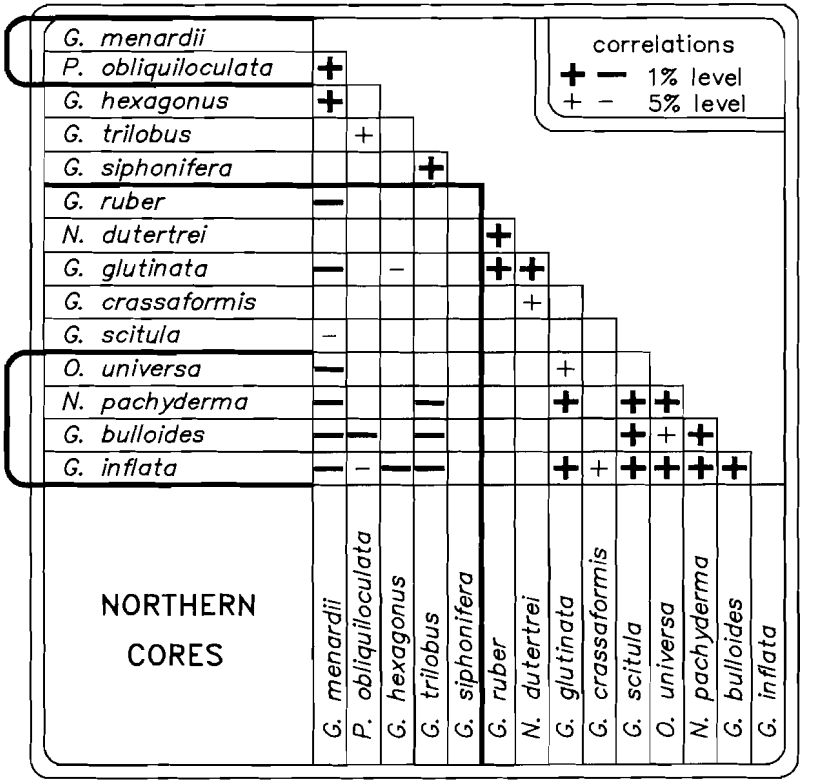

Fig. 61. BALANC correlation-matrix based on the analysis of the four northern cores. The heavy line separates the two groups that show the lowest degree of similarity according to the DENDRO analysis.

As a general relationship between the degree of carbonate dissolution and climatic variation is absent in the cores, we may suppose that dissolution operates rather at random in the total set of cores. Following this line of reasoning, we assume that the effects of dissolution on the interspecific relations lose their impact, if cores VM29-143, KW26, VM19-283, and KW25 are analysed together.

The results are shown in fig. 61 and demonstrate the presence of a coherent group of species consisting of *G. bulloides*, *G. inflata*, *N. pachyderma*, and *O. universa*. *G. scitula* is positively correlated with all these species but *O. universa*. This group is clearly the equivalent of the glacial group recognized in T80-10.

The glacial group in fig. 61 is negatively correlated with *G. menardii* and some elements show negative correlations with *G. trilobus*, *Globorotaloides hexagonus*, and *P. obliquiloculata*. Although these four species do not form a coherent group, their combination may to some extent be considered an equivalent of the interglacial group of T80-10. A third group of mutually positively correlated species consists of *G. ruber*, *Globigerinita glutinata*, and *N. dutertrei*. Just as in T80-10, the low-frequent *G. glutinata* has positive correlations with elements of the glacial group, and negative correlations with elements of the interglacial group. *G. ruber* and *N. dutertrei*, however, belong to the interglacial group of T80-10. These two species lack negative ties with the glacial group of fig. 61 and *G. ruber* is even negatively correlated with *G. menardii*. Figs. 55-57 show that in the northernmost cores, i.e. KW26, VM29-143, and VM19-283, *G. ruber* and *N. dutertrei* tend to be frequent in both glacial and interglacial periods.

VI.2.2. Principal Component Analysis

Principal component analysis on the data from T80-10 yields one significant axis, which opposes the glacial and interglacial groups (table 10). The analysis of the four northern cores also produces one significant axis, which is very similar in composition to the one of T80-10 (table 11a). This suggests that the first component in the northern cores describes the glacial/interglacial contrast sufficiently well and for this reason, we considered it justified to analyse all cores together.

The all core analysis reveals two significant axes (table 11b). The first component has essentially the same composition as the one produced by the analysis of T80-10. The second component cannot be interpreted in simple climatic or palaeoenvironmental terms and will be excluded from further discussion.

Plots of the sample scores on the first component then provides a series of climatic proxy curves (fig. 62), which in combination with the frequency diagrams (figs. 54-58) make it possible to calibrate the stratigraphy of the cores.

principal component	1	2	3
eigenvalue	4.3	1.9	1.7
variance (%)	31.0	13.6	12.1
species			
G. ruber	.4	-.0	-.0
N. dutertrei	.4	.2	-.0
G. siphonifera	.3	-.3	.2
G. trilobus	.3	-.3	.1
G. menardii	.3	.2	-.1
G. crassaformis	.2	.5	.2
P. obliquiloculata	.1	.0	-.5
G. hexagonus	.1	-.2	-.3
G. glutinata	.0	-.4	.0
G. scitula	.0	-.1	.5
O. universa	-.2	-.2	.4
G. bulloides	-.3	-.3	-.1
G. inflata	-.3	.4	.1
N. pachyderma	-.4	.0	-.2

Table 10. Results of a principal component analysis on the frequency distribution of planktonic foraminiferal species in T80-10. Composition of the first three components, eigenvalues, and percentages of total variance.

principal component	1	1	2
eigenvalue	3.3	3.3	2.3
variance (%)	23.4	23.4	16.2
species			
G. ruber	.4	.4	.0
N. dutertrei	.3	.4	-.3
G. trilobus	.3	.3	.3
G. menardii	.2	.3	.1
G. siphonifera	.2	.2	.3
P. obliquiloculata	.2	.2	-.0
G. hexagonus	.2	.2	.2
G. crassaformis	.1	.0	.3
G. glutinata	-.0	.1	-.4
O. universa	-.2	-.2	.4
G. scitula	-.3	-.2	.1
G. bulloides	-.4	-.3	.4
G. inflata	-.4	-.3	-.2
N. pachyderma	-.4	-.3	-.3
	A.	B.	

Table 11. Results of a principal component analysis of the frequency distribution of planktonic foraminiferal species in (A) the four northern cores, and (B) all cores. Composition of the significant components, eigenvalues, and percentages of total variance.

Fig. 62 shows that in T80-10, VM29-143, and KW26 the Y/Z boundary does not coincide with a major faunal change. The most prominent faunal change in the upper part of these cores is well below the zonal boundary. The interval characterized by a predominantly interglacial fauna but without *G. menardii* is termed the Y1 zone. The frequency diagrams (figs. 54-57) show that in the Y1 zone *G. inflata* is almost absent and *N. pachyderma* rather common, which contrasts with their distribution in the Z zone. In VM19-283, the faunal change that characterizes the base of the Y1 unit seems to coincide with the level of reappearance of *G. menardii* (fig. 58). Inspection of the frequency data of VM19-283 further shows that *G. menardii* is very scarce in the basal part of the Z zone and we think that the coincidence is due to bioturbation.

A further subdivision of the Y zone is possible only in T80-10. In this core, two intervals show a pronounced glacial aspect, the Y2 and Y4 units, whereas the interjacent Y3 interval displays a more nterglacial character.

The youngest sediments were not recovered in KW25, which is probably due to the coring process. Not only is the Z zone missing, but judging from the species abundance curves, both the Y1 and Y2 zones are not represented either. The Y3 and Y4 zones can, however, be distinguished in this core. In the upper part of the Y4 unit, a distinct peak in the abundance of sinistrally coiled *N. pachyderma* is observed and high frequencies of *G. bulloides* appear to be associated with this peak. A very similar spike occurs in the upper part of Y4 in T80-10.

The X/Y boundary does not coincide with an overall change in the faunas. *P. obliquiloculata* seems to disappear just above the X/Y boundary in all cores, with the exception of KW26 in which this species is not present in the boundary interval. This contrasts with the suggestion of Prell and Damuth (1978) that the temporary extinction of *P. obliquiloculata* in the eastern South Atlantic coincides with the disappearance of *G. menardii.*

The X zone shows a general trend towards more glacial conditions, but differentiation within this zone is rather difficult. In VM 19-283, we recognize three levels at which interglacial conditions prevail and a similar subdivision is suggested for T80-10. The levels have been termed X1, X2 and X3 in order of increasing age. Stratigraphic resolution is lower in both VM 29-143 and KW25. Here, we can only identify the X3 level, which marks the basal part of the zone. In all relevant cores, the X3 level is characterized by very low abundances of *N. pachyderma* and *G. inflata* (figs. 54-55, 57-58).

The W/X boundary is located within an interval of overall faunal change. The frequency data show that the species of the interglacial group do not all respond at the same stratigraphic level. Abundances of *G. hexagonus* and *G. trilobus* already increase below the W/X boundary in T80-10, VM29-143 and VM19-283.

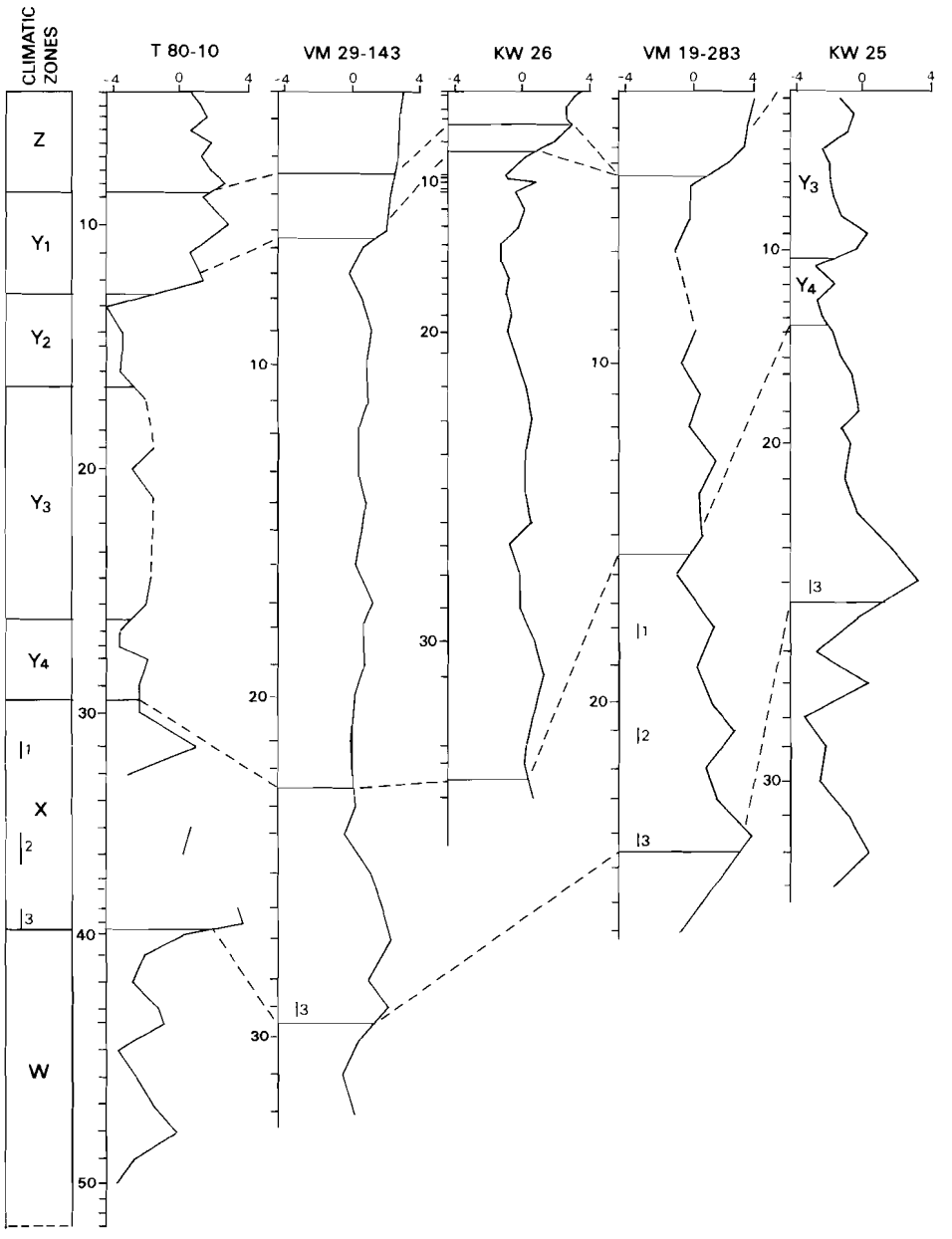

Fig. 62. Climatic-proxy curves and inter-core correlation. The curves are plots of the sample scores on the first principal component of the all core analysis. Intervals excluded from the analysis are dashed. Open sections represent intervals without data. The climatic zonation is shown alongside.

Subdivision of the W zone is not considered relevant for this study, but the climatic proxy curves of T80-10 and KW25 (fig. 62) suggest that glacial and interglacial intervals alternate.

The next step is to correlate the sequence of climatic zones to the main features of the standard oxygen-isotope zonation.

The Z/Y boundary of core T78-46 (Zachariasse et al., 1984), which is located only 65 km south of T80-10, has an estimated age of 10,000 yr BP (Olausson, 1984) and is, therefore time-equivalent with the Pleistocene-Holocene boundary (Berger, 1982; Olausson, 1982). The change from a glacial to interglacial faunal signal, which marks the base of the Y1 zone, thus predates the Holocene. A similar pre-Holocene faunal change in T78-46 (Zachariasse et al. 1984) has an estimated age of 14,000 yr BP (Jansen et al., 1984) and is thought to represent the beginning of a period of rapid deglaciation (Olausson, 1984).

The last deglaciation (Termination I of Broecker and Van Donk, 1970) occurred in two discrete steps, interrupted by a brief pause (Duplessy et al., 1981b). The pause in the deglaciation is probably equivalent to the Younger Dryas, a major cold period on land, which approximately lasted from 11,000 to 10,000 yr BP.

Many authors have corroborated the idea of a two-step deglaciation, but opinions diverge as to the timing of these pulses (Kerr, 1983; Ruddiman and Duplessy, 1985). Berger et al. (1985) established a time-scale for the equatorial Atlantic in which deglaciation starts shortly after 14,000 yr BP with a second step at about 10,000 yr BP (cf. Mix and Ruddiman, 1985).

We suggest that the bases of the Y1 and Z zones are correlative with the two major deglaciation events.

The Y2 interval then corresponds to the full glacial conditions of isotope stage 2. Interval Y3 most likely represents the relatively warm period of isotope stage 3, whereas Y4 correlates with the cold climatic period of isotope stage 4. The progressive deterioration of the climate during isotope-stage 5 is easily recognized in the climatic proxy curves (fig. 62). We suppose that the three warm levels within the X zone are correlative with isotope substages 5a, 5c, and 5e.

VI.3. GLACIAL TO INTERGLACIAL PALAEOENVIRONMENTAL RECONSTRUCTION

VI.3.1. Introductory remarks

Previous studies on Late Quaternary planktonic foraminiferal faunas in the eastern tropical Atlantic were concerned mainly with foraminiferal transfer functions and faunal change was primarily interpreted in terms of surface-water

temperatures. The CLIMAP project workers (1976) mapped differences in August sea-surface water temperatures between 18,000 yr BP and the present. They suggested that at the glacial maximum the surface of the tropical Atlantic was in general between 0° and 2°C cooler than today, but larger deviations (in excess of 4°C) occurred in the mid-ocean region of the eastern tropical Atlantic. A relatively small difference between glacial and interglacial surface temperatures is in agreement with estimates of Broecker (1986), who employed oxygen-isotope data to calculate that surface-water temperatures in the glacial equatorial Atlantic remained within about 2°C of their present value.

Gardner and Hays (1976) concluded that in the mid ocean waters of the eastern equatorial Atlantic glacial cooling was most intense during the cold season and showed that glacial periods have been characterized by higher seasonal contrasts than interglacials over the past 200,000 yr. They estimated that warm season temperatures at 18,000 yr BP were similar to today's, but during the cold season temperatures may have been as much as 8°C lower than at present (see also Mix et al., 1986a, b).

Gardner and Hays attributed the extremely low cold season temperatures at 18,000 yr BP to an equatorial shift of the Benguela Current. They suggested that the BC intensified during the cold season in response to a more vigorous atmospheric circulation. An increased pole-to-equator thermal gradient, caused by the large sea-ice cover of the Antarctic, was held responsible for the strengthened atmospheric circulation. During the glacial warm season, circulation may have relaxed or the system of the BC and SEC changed in position. A northward shift in the position of the BC was also suggested by Zachariasse et al. (1984), who attributed the specific composition of glacial faunas in front of the river Zaire to the influence of the Benguela Current.

Mix et al. (1986b) argued that although the glacial increased sea-ice cover in the Antarctic most likely resulted in an overall more intense circulation, there is little evidence to relate the high seasonal surface-water temperature contrast during glacials to seasonal variation in sea-ice cover. They suggested that the intense winter cooling may have been a response to an increased divergence along the equator. Increased divergence during the glacial cold season could be due to a change in wind direction, from meridional during interglacials to zonal during glacials.

Temperature estimates based on transfer functions should be considered inaccurate. This technique assumes a (quasi-)linear relationship between species (assemblage) abundance and temperature and constancy of surface-water temperature to fertility relations and surface to subsurface temperature gradients. In the present-day region, species distribution is to a large extent deter-

mined by environmental conditions other than surface-water temperature and transfer functions are in our opinion to be considered of little use.

The cores under consideration are located in the marginal part of the tropical region, where the modern associations differ from those more offshore. We suggested that the faunal difference results from higher food-levels near the continent together with a weaker thermocline during the cold season. In addition, surface-water temperatures are locally lower near the continent than further offshore during the cold season.

The complexity of the marginal environment urges the need to discuss Late Quaternary palaeoenvironmental conditions in terms of frequency changes of individual species.

VI.3.2. The north-south gradient

T80-10 is situated in front of the river Zaire, an area within the marginal tropical region characterized by a specific modern fauna, which essentially reflects the extremely high fertility of the surface-water. In addition, surface-water temperatures are slightly lower during the cold season than in the northernmost part of the region.

Comparison between the faunal curves of figs. 54-58 shows that the overall fauna of T80-10 is different from those in the other cores. The majority of the species of the glacial group, i.e. *G. bulloides*, *O. universa*, and to a lesser extent *G. inflata*, reach higher average frequencies in T80-10 than in the northern cores. The contrast is most prominent, if the core is compared with the three northernmost cores, while KW25 occupies a more intermediate position. This indicates that a N-S gradient has almost continuously existed in the marginal tropical region. The presence of the gradient can be explained in two different ways.

Firstly, the associations in the cold climatic stages of T80-10 are very similar to the faunas that are found at present in the area of the Benguela Current (cf. Zachariasse et al., 1984). Hence, we could presume that the gradient reflects primarily a temperature gradient within an area of overall high fertility.

As an alternative, though not mutually exclusive, explanation, we could suggest that the area in front of the river Zaire has always been more fertile than the region to the north.

VI.3.3. Down-core variation in Neogloboquadrina

Associations characterized by high percentages of both *G. ruber* and *N. pachyderma*, as found in the cold climatic stages of the northern cores (figs. 55-58), are not known from the present-day Atlantic. The no-analog composition

of the glacial faunas may be related to a seasonal change in the position of the BC, which concurs with the interpretation of Gardner and Hays (1976). We, however, question whether *N. pachyderma* can be used simply as an indicator of cold surface-water advection by the BC.

In contrast to *G. bulloides, G. inflata,* and *O. universa,* the frequency of *N. pachyderma* is not significantly higher in T80-10 and KW 25 than in the northernmost cores. This suggests that *N. pachyderma* is less sensitive to either temperature or fertility than the other species.

Neither of these interpretations is, however, supported by the distribution of the species of the glacial group on the ocean floor. Along the African continent, *N. pachyderma* is sparse between 10° and 15°S (see fig. 12d), an area still influenced by the BC and of relatively low fertility. *G. inflata* is on the other hand relatively abundant here (see fig. 12a). This suggests that among the species of the glacial group *G. inflata* rather than *N. pachyderma* has the widest tolerance to variation in temperature and fertility.

The distribution of *Neogloboquadrina* in the Y2-Z interval of the relevant cores (figs. 54-57) shows an inverse relation between the abundances of *N. pachyderma* and *N. dutertrei.* We suggest that *N. dutertrei* replaces *N. pachyderma* during post-glacial warming.

In our opinion, there are good reasons to assume that the distribution of both *Neogloboquadrina* species is essentially controlled by temperature. The distinction between *N. dutertrei* and *N. pachyderma* is based on size, and we actually consider them as closely related morphotypes. In the present-day oceans *Neogloboquadrina* displays a continuous variation. Different morphotypes replace each other with changing latitude, which has been interpreted in terms of a latitude-controlled cline (Kennett, 1968; Bé and Tolderlund, 1971; Malmgren and Kennett, 1972). Similar observations were made in the fossil record (Srinivasan and Kennett, 1976; Keller, 1977). Keller (1977) concluded that morphologic variation in *Neogloboquadrina* is controlled by temperature or a parameter directly related to temperature.

High relative numbers of *N. dutertrei* are at present found in the equatorial zone and we discussed that the flourishing in equatorials water is to be related to the fact that *N. dutertrei* lives in the chlorophyll maximum accociated with the thermocline. If different morphotypes of *Neogloboquadrina* replace each other merely as a result of temperature change, then *N. pachyderma* should be also be linked up with this chlorophyll maximum, at least in warm-water regions. Supporting evidence for this assumption is difficult to find in the present-day oceans, because we essentially refer to a situation without a modern analogue. Thunell and Reynolds (1984), however, demonstrated that *N. pachyderma* occurs in equatorial upwelling systems and also showed that the

abundance of this taxon increases with a shallowing of the thermocline. Relating *N. pachyderma* to the chlorophyll maximum associated with the thermocline is, in our opinion, a likely explanation for the fairly high frequencies of this species in the modern tropical region (see fig. 12d). We contend that at least outside the (sub)polar region both *N. dutertrei* and *N. pachyderma* are associated with the chlorophyll maximum at the thermocline. Kellogg et al. (1978) suggested that *N. pachyderma* is a deep-living species at high latitudes, which indicates that *N. pachyderma* could live near the top of the thermocline in (sub) polar regions as well. We do, however, not know if *N. pachyderma* is associated with a deep chlorophyll maximum in those areas.

We, therefore, suggest that the relative abundance of *N. pachyderma* or *N. dutertrei* depends on the temperature regime in the thermocline. Fig. 63 shows the down-core variations in the proportion of *dutertrei* types per total neogloboquadrinids and a comparison with fig. 62 reveals that the curves in fig. 63 correlate well with the climatic proxy curves.

Furthermore, we assume that the total abundance of neogloboquadrinids (fig. 64) is a temperature independent tool to detect changes in the depth of the thermocline and the primary production of the photic layer.

At present neogloboquadrinids proliferate throughout the year only in the offshore waters of the equatorial zone. Near the continent, they are probably present during the warm season, because this is the only period of the year with well-stratified conditions. Down-core variations of neogloboquadrinids may, therefore, be seasonally biased.

VI.3.4. Downcore variation in G. bulloides and G. inflata

We suggested earlier that *G. inflata* reaches high abundances near the continent, because this species requires a not or weakly stratified photic layer, lowered surface-water temperatures and relatively high food-levels. Coastal upwelling has been suggested as one of the possible mechanisms to explain the poor stratification near the continent during the cold season. Because *G. bulloides* primarily responds to high surface-water fertility, coastal upwelling may contribute to the high abundances of *G. bulloides* near the river Zaire. It appeared, however, impossible to discriminate between the effect of coastal upwelling on surface-water fertility and that of river discharge.

Because temperature and nutrient content of the surface-water are both strongly influenced by coastal upwelling, we may expect that, if the distribution of both species is mainly controlled by this process, their down-core abundance patterns are mutually similar. Since the distribution of the two species off NW Africa shows, that *G. bulloides* abounds in the upwelling centres,

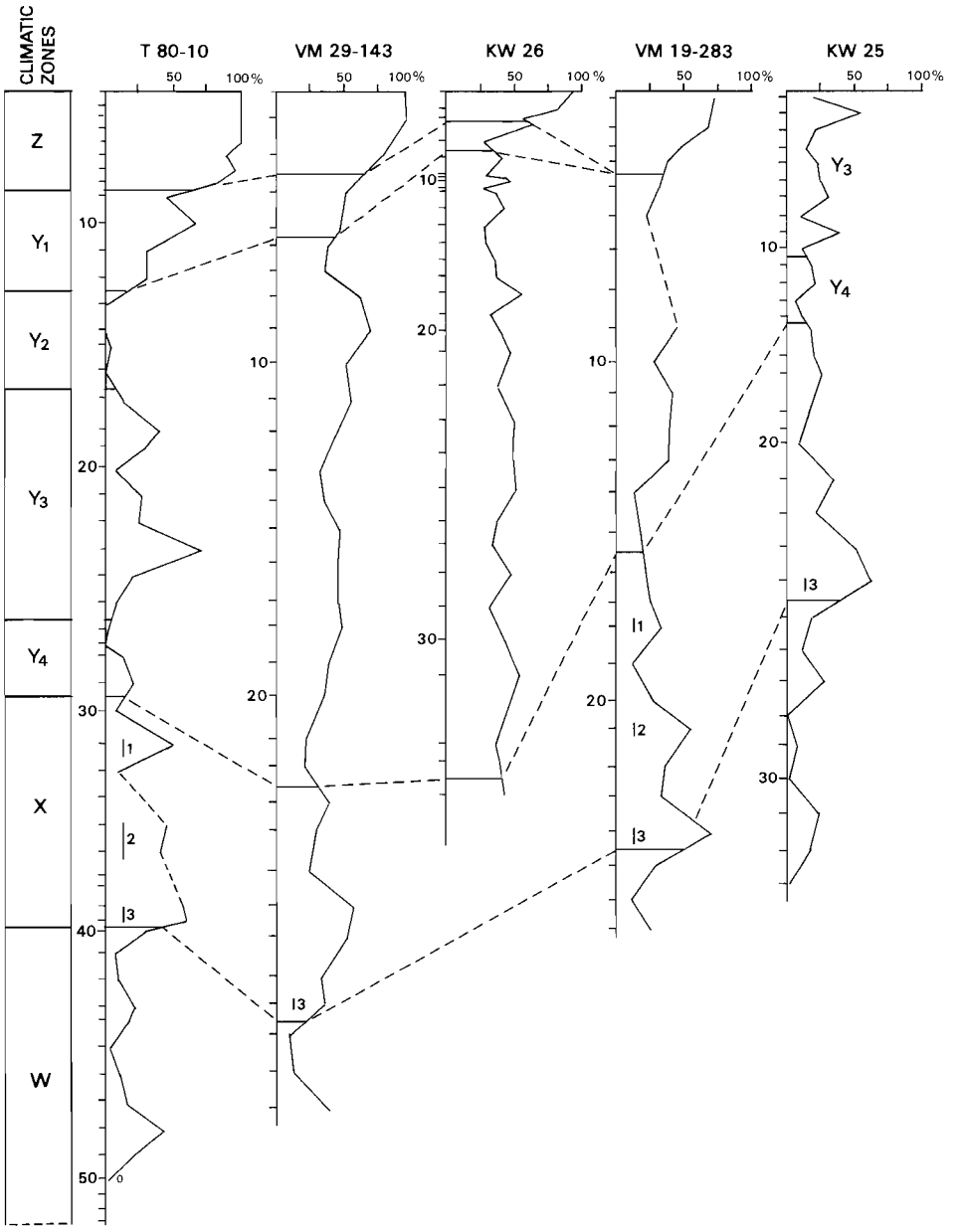

Fig. 63. Proportion of *dutertrei* types per total neogloboquadrinids. The curves are dashed in case of no data.

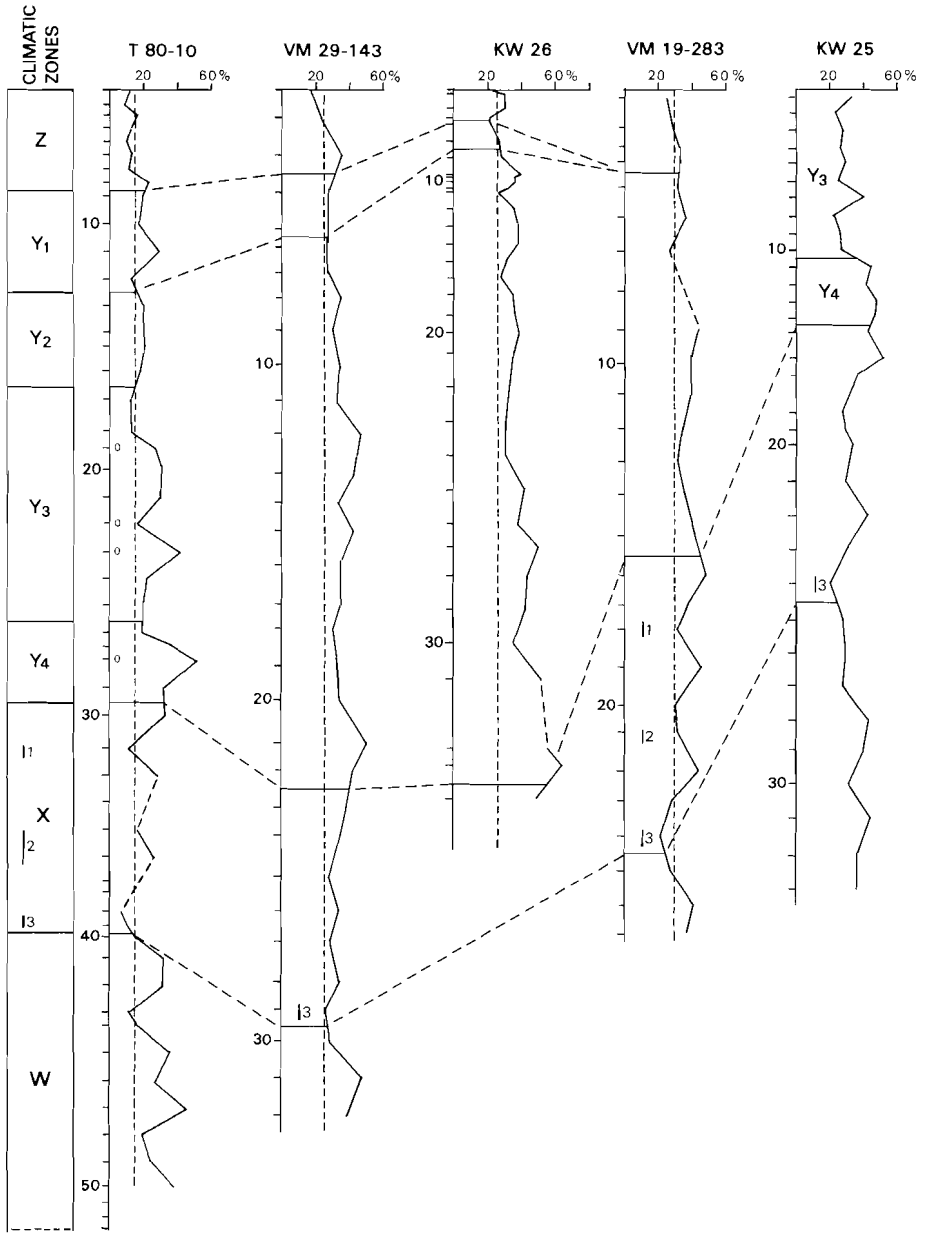

Fig. 64. Percentage distribution of total neogloboquadrinids in the cores. The curves are dashed in case of no data. Dashed vertical lines refer to average percentages in the Z zone. Open circles mark counts of less than 100 specimens.

whereas high frequencies of *G. inflata* fringe these areas, we may further assume that *G. bulloides* reaches lower frequencies than *G. inflata* when upwelling relaxes.

Downcore patterns of both species are, however, generaly dissimilar. In the three northernmost cores, abundances of *G. inflata* vary significantly and in a similar way (fig. 65). Several intervals with low percentages of *G. inflata* can be recognized but, contrary to what we expect, *G. bulloides* does not reach markedly low frequencies in these intervals. Actually, *G. bulloides* shows only minor frequency fluctuations and apart from the fact that this species tends to attain its highest frequencies in cold intervals, down-core variations do not follow a coherent pattern in the northernmost cores (see figs. 55-57).

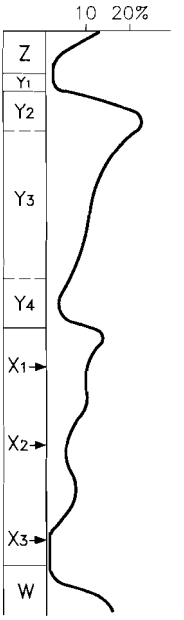

Fig. 65. Idealized percentage distribution of *G. inflata* in the three northernmost cores.

As the obvious differences in the down-core distribution of *G. bulloides* and *G. inflata* can not be ascribed to selective dissolution, they must indicate that variations in surface-water fertility and temperature are not closely related in the northern part of the region. Excluding the possibility that river run-off and coastal upwelling changed simultaneously but in opposite direction, we suggest that the relatively high frequencies of *G. bulloides* in the northern part of the region are essentially due to the input of nutrients by the river Zaire. The low

variability of the down-core percentages of *G. bulloides* in the northernmost cores indicate further that variation in river run-off has had a minor effect in this area.

In KW25 and especially in T80-10, percentages of *G. bulloides* show significant variations, with very high values in the cold climatic stages (figs. 54, 58). A comparison between the down-core patterns of *G. bulloides* and *G. inflata* in T80-10, shows that frequency changes of the two species are concurrent over some intervals but not at other levels. This might suggest that at these sites abundances of *G. bulloides* are influenced by variation in both run-off and upwelling.

Pokras (1987) inferred from diatom data that there have been periods of increased run-off in the subject area and suggested that the associated increased humidity in tropical Africa is connected with an intensification of the African monsoon. Pokras estimated the age of these humid events and comparison with his findings shows that the periods of intense run-off are generally characterized by high abundances of *G. bulloides* in T80-10 (fig. 66). Only the youngest run-off spike, which Pokras tentatively placed near the boundary between isotope stages 1 and 2, seems not associated with high percentages of *G. bulloides* in T80-10. *G. bulloides*, on the other hand, reaches relatively high frequencies in the lower part of the Z zone. Because this interval is characterized by low frequencies of *G. inflata* in all cores (figs. 58-61), the high percentages of *G. bulloides* may result from increased river run-off and we, therefore, assume that this interval is to be correlated with the youngest run-off event of Pokras. As shown in fig. 66, there are additional peaks of *G. bulloides* in T80-10, which might be attributed to increased coastal upwelling.

Core T80-10 shows that percentages of *G. bulloides* in the Y1 zone are similar to those at the top of the Z zone, whereas *G. inflata* is relatively frequent only at the top of the Z zone. This suggests that the relatively high frequencies of *G. bulloides* on the ocean floor in front of the river Zaire (see fig. 9d) are to be attributed essentially to river input of nutrients and river induced upwelling. We, therefore, assume that coastal 'upwelling' processes during the modern cold season have only a minor effect on the overall fertility of the surface water. Consequently, low intensity upwelling processes, including both ridging of deep waters in a coastal setting and low-intensity wind-driven coastal upwelling must be held responsible for the high percentage of *G. inflata* in the modern marginal region.

To structure our reasoning, we made a serious simplification, for it is conceivable that processes other than coastal upwelling control down-core variation in the abundances of *G. bulloides* and *G. inflata.* Increased advection of cold surface-waters could, in our opinion, also prevent the development of a

well-stratified photic layer. It should, however, be realized that this alternative does not alter our discussion on differences in down-core patterns of the two species, because as far as their distribution is determined by temperature, *G. bulloides* tolerates lower surface-water temperatures than *G. inflata.*

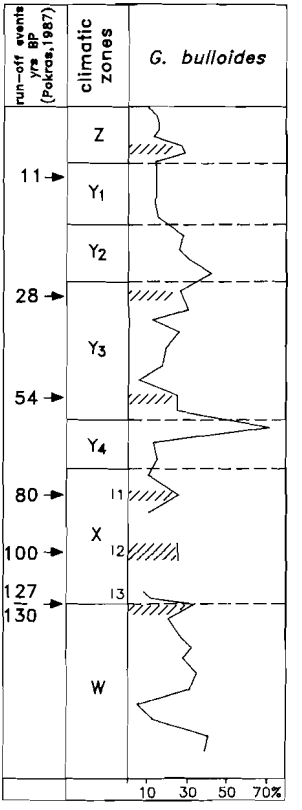

Fig. 66. Percentage distribution of *G. bulloides* in T80-10. Hatched intervals are thought to be associated with increased river run-off and are compared with the sequence and timing of run-off events (arrows) of Pokras (1987).

The habitat definition of *G. bulloides. G. inflata* and neogloboquadrinids, implies that *G. inflata* and neogloboquadrinids are mutually exclusive. *G. bulloides* and neogloboquadrinids may flourish at the same time, but only when the abundance of *G. bulloides* is controlled by river run-off. In the northermost cores neogloboquadrinids are monitors of warm season conditions in intervals with abundant *G. inflata,* whereas they record year round subsurface conditions in intervals with sparse *G. inflata.*

VI.3.5. Palaeoenvironments during Termination I and the Holocene

The end of the last glacial and the onset of deglaciation

Frequencies of *G. siphonifera*, *G. ruber*, and *G. trilobus*, significantly increase at the base of Y1. Coincidentally, abundances of *G. inflata* decrease and this species is low-frequent in the entire Y1 zone (figs. 54-57).

The drop in the abundance of *G. inflata* indicates that the photic layer became permanently stratified during the early phase of deglaciation.

The change in the structure of the photic layer implies that whereas at the end of the last glacial period neogloboquadrinids could flourish only during the warm season, conditions became favourable for them year-round during the early phase of deglaciation. Contrary to what we expect, abundances of neogloboquadrinids slightly decrease over the Y2/Y1 boundary in the northern cores (fig. 64). We, therefore, speculate that the (seasonal) thermocline was at greater depth during deglaciation than during the final stage of the last glacial.

At present the thermocline shallows during the cold season primarily in consequence of increased trade winds in the western Atlantic (Voituriez et al., 1982). By analogy, we may suggest that atmospheric circulation in the western Atlantic was much stronger at the end of the glacial period than during the early phase of deglaciation.

The proportion of *dutertrei* types in the northern cores (fig. 63) shows little change at the onset of deglaciation. Year-average temperatures at the thermocline during the early phase of deglaciation were therefore similar to warm season temperatures during the preceding glacial interval. If subsurface temperatures in the photic layer have always been lower during the cold than the warm season, we suggest that subsurface water temperatures increased during deglaciation. The rise in subsurface temperatures may be attributed to (1) the deepening of the thermocline, (2) reduced lateral advection of cold waters into the region, and (3) global changes in the temperature of the subsurface waters.

During the glacial maximum, *dutertrei* types were much scarcer off the river Zaire than to the north. In front of the river Zaire, the proportion of *dutertrei* types markedly increased at the beginning of deglaciation and the preexisting difference with the northern region diminished. This suggests that there was a subsurface temperature contrast between the region off the river Zaire and the north at the end of the last glacial, which gradually disappeared during the early phase of deglaciation.

The glacial subsurface temperature contrast must have been present at least during the warm season. The N-S subsurface temperature gradient probably

reflects a northward sloping of the thermocline and may be attributed to advection of cold water from the south, presumably by the Benguela Current. The influence of the BC must have weakened at the beginning of deglaciation at about 14,000 yr BP.

In the area off the river Zaire, percentages of *G. bulloides* decreased markedly at the beginning of deglaciation (fig. 66), but there is no clear evidence of a similar decrease in the northern cores, except perhaps in VM19-283 (figs. 55-57). The relatively high frequencies of *G. bulloides* at the end of the glacial in front of the river Zaire can not be attributed to increased river run-off. The glacial abundance of *G. bulloides* in the south and the overall high frequencies of *G. inflata* at the end of the last glacial should therefore be related to the same process. This may be either increased advection of cold waters along the surface during the cold season, or intense coastal upwelling during the cold season in the south and low-intensity coastal upwelling in the north. The first possibility assumes a N-S gradient in surface-water temperature, the second one a fertility gradient. A fertility gradient is probably also to be attributed to advection of cold waters from the south, because this may have caused subsurface isotherms to slope towards the north also during the cold season. Upwelling waters in the south could, therefore, have been colder and their nutrient content higher than in the north, thus contributing to high percentages of *G. bulloides* in T80-10 and high percentages of *G. inflata* in all cores. Because increased advection of BC waters and intense coastal upwelling are both dependent on the strength of coast parallel, i.e. SE to SSE, winds, we surmise that both processes have contributed.

Earlier, we suggested that the thermocline deepened at the beginning of deglaciation, which we attributed to a weakened atmospheric circulation in the western Atlantic. In our opinion, this is not the only possible cause. Before deglaciation began, cold-water penetrated into the region and the thermocline may have coincided with the top of the cold-water body. A decrease in cold-water advection might, therefore, be an alternative explanation for the deepening of the thermocline at the beginning of deglaciation.

In summary, cold BC waters are thought to have penetrated into the area in the final stage of the glacial period, The influence of these cold waters was stronger in the southern than in the northern part of the region.

The thermocline during the warm season was at a shallower depth in the south than in the north. During the cold season, the photic layer was not or poorly stratified and surface-water temperatures were lower in the south than in the north. The absence of a well-stratified photic layer during the cold season at the end of the last glacial may have been brought about by (1) an increase

in atmospheric circulation in the western Atlantic which may have led to an overall shallowing of the thermocline eventually resulting in low-intensity coastal upwelling, and/or (2) increased advection of cold waters from the south.

At the beginning of deglaciation, the overall circulation drastically decreased and the BC gradually retreated from our region. The thermocline deepened in the entire area and trade wind activity in the western Atlantic must have been low. In the entire area the photic layer remained well-stratified throughout the year. Coastal upwelling activity ceased and primary production must, therefore, have been much lower than in the preceding cold period. A lowering of the fertility at 14,000 yr BP was previously suggested for this region by Pokras (1987).

Because upwelling ceased and advection of cold water by the BC reduced, surface-water temperatures during the cold season increased significantly. Temperatures at the thermocline increased likewise, especially in the south.

The increase of *G. ruber*, *G. trilobus* and *G. siphonifera* across the Y2/Y1 boundary should be interpreted against the background of the overall change in circulation. *G. ruber* and *G. trilobus* are both species of the surface-mixed layer (Fairbanks et al. 1982; Thunell and Reynolds, 1984; Bé et al., 1985) and their flourishing at the beginning of deglaciation is triggered by the spreading of warm and nutrient-poor surface waters over most of the area. If true that *G. siphonifera* dwells near the thermocline (e.g. Fairbanks et al., 1982), this species may have responded to the temperature increase in the subsurface.

The Holocene

The base of the Z zone is marked by the reappearance of *G. menardii*. Except for *N. dutertrei*, other species of our tropical sea-floor association do not demonstrate an increase in abundance across the boundary (figs. 54-57).

G. menardii remained present in the Indo-Pacific during glacial periods and probably reentered the Atlantic Ocean from the Indian Ocean. It is, therefore, conceivable that the hydrographic setting around the southern tip of Africa was critical for its reappearance in the Atlantic and thus also in the Angola Basin.

G. inflata is still sparse in the lower part of the Z zone but becomes more frequent towards the top (figs. 58-61). This pattern suggests that Holocene conditions were initially similar to those prevailing during the early phase of deglaciation. In the course of time the photic layer became progressively less well-stratified during the cold season.

Total abundances of neogloboquadrinids are similar below and above the Y/Z boundary (fig. 64). The slightly lower frequencies in the Late Holocene can be attributed to the fact that the photic layer became less well-stratified during the cold season.

The proportion of *dutertrei* types per total neogloboquadrinids is similar in the northern and southern part of the region (fig. 63), which indicates that subsurface temperatures were the same in the entire region. Again this points to a strongly reduced influence of the BC. The absence of a well-stratified photic layer during the late Holocene cold season is, therefore, to be attributed to low intensity coastal upwelling.

G. bulloides is generally low frequent in both the Y1 and Z zone. The prominent peak in the frequency of *G. bulloides* in the lower part of the Z zone of T80-10 is probably associated with increased river discharge (fig. 66).

The increase in the proportion of *dutertrei* types across the Y1/Z boundary in T80-10 and VM29-143 (fig. 63), suggests that temperatures at the thermocline increased in the entire region at the beginning of the Holocene. There is no evidence that the rise in subsurface temperatures is to be attributed to a further weakening of the BC and it could, therefore, be associated with the global climatic amelioration at the beginning of the Holocene.

In summary, the hydrographic conditions during the early Holocene did not deviate much from those prevailing during the early phase of deglaciation. Temperatures at the thermocline, however, significantly increased at the beginning of the Holocene and remained high untill modern times.

In the course of the Holocene, cold-season conditions changed as deep waters reached the surface under the influence of low-intensity coastal upwelling. We suggest that this coastal upwelling is connected with an overall shallowing of the thermocline during the cold season, induced by increased wind activity in the western Atlantic. Cold-season surface-water temperatures are probably lower at present than during the early part of the Holocene. This is in agreement with Mix et al. (1986a,b), who suggested that cold-season surface-temperatures were relatively high in the equatorial eastern South Atlantic between 14,000 and 6,000 yr BP. Increased low intensity coastal upwelling may have resulted in a higher fertility of the surface waters during the Late Holocene. This supports the idea of Pokras (1987) that primary production slightly increased over the past several thousands of years.

Relatively low abundances of *G. ruber* and/or *G. trilobus* in the Z zone of some of the cores (see figs. 54-56), may be attributed to dissolution, but a response to lower cold-season surface-water temperatures can not be excluded. There is no evidence that there was any significant difference in warm-season surface-water temperature between the Holocene and the early phase of deglaciation. *G. menardii* is probably a species living near the thermocline (e.g. Thunell and Reynolds, 1984), and as far as local conditions have been of influence, the reappearance of this species is probably due to the subsurface temperature increase at the beginning of the Holocene.

VI.3.6. Palaeoenvironments during the last glacial

The interpretation of faunal change during the last glacial is seriously hampered by the poor quality of the records. There seems, however, to be a significant difference between the Y4 and Y2 cold climatic stages.

The frequency diagrams of the northernmost cores (figs. 55-57) show that *G. inflata* reaches low percentages in the lower part and high abundances in the upper part of the Y4 to Y2 interval. Although formal subdivision of the Y4-2 interval appeared impossible in these cores, we think that the Y4 and Y2 are characterized by low and high abundances of *G. inflata*, respectively. Intermediate percentages are thought to characterize the interjacent Y3 zone. This pattern (fig. 65) would indicate that the Y4 zone represents the only interval during the last glacial, in which the photic layer was year-round well-stratified in the northern part of the area.

The frequency pattern of *G. inflata* in T80-10 and KW25, indicates that in the southern area the photic layer was poorly stratified during the cold season throughout the last glacial. This species is nearly absent at the top of the Y4 zone in T80-10, but stratification must have been seasonally absent also during this period, because the low percentages of *G. inflata* coincide with very high abundances of *G. bulloides*, which can not be attributed to increased river run-off (see fig. 66).

In the northernmost cores, neogloboquadrinids are exceptionally abundant in the major part of the Y4 zone and show a trend towards much lower percentages in the upper part of the glacial interval (fig. 64). The percentage distribution of neogloboquadrinids tends to mirror the abundance pattern of *G. inflata*.

Frequencies of *G. ruber* do not show a mutually similar pattern in the northernmost cores (figs. 55-57) and it must remain uncertain whether there are systematic differences within the glacial interval. We, therefore, assume that warm season conditions did not change significantly over the last glacial.

The opposite trends in neogloboquadrinids and *G. inflata* suggest that the hydrography of the northern region changed from a system characterized by year-round stratification and a very shallow thermocline during the cold season in stage Y4 to a system which was poorly stratified during the cold season in stage Y2.

If we disregard the peak abundances of *G. bulloides* in the top of the Y4 zone in T80-10 and KW25 (figs. 54, 58), we may generalize that *G. inflata* plus *G. bulloides* reach much higher percentages in stage Y2 than in stage Y4, whereas the curve of total neogloboquadrinids shows the inverse pattern (fig. 64). Percentages of total neogloboquadrinids in the Y3 zone are intermediate be-

tween those in zones Y4 and Y2. This suggests a similar trend in glacial hydrographic conditions as noticed in the northern cores.

Generalizing, we suggest that the length of the period of the year during which the photic layer was well-stratified shortened over the last glacial in the entire area.

Average frequencies of *G. inflata* and *G. bulloides* are higher in the south than in the north, which suggests that cold waters were advected from the south throughout the last glacial. Contrary to what we expect, proportions of *dutertrei* types per total neogloboquadrinids are not consistently lower in T80-10 than in the northernmost cores (fig. 63). There is, however, reason to doubt whether the record of T80-10 can be compared directly with those of the northernmost cores, because well-stratified conditions prevailed during a shorter period of the year in the south than in the north.

Average percentages of total neogloboquadrinids are higher in stage Y4 than in Y1 (fig. 64), which both represent periods with a year-round well-stratified photic layer. Total neogloboquadrinids tend to be more abundant in stages Y3 and Y2 than in the Holocene, both periods during which the photic layer was seasonally poorly stratified. All this suggests that during the relevant season(s) the thermocline was at shallower depth in glacial than in postglacial times.

Left-coiling *pachyderma* types reach highest frequencies in the upper part of zone Y4 in KW25 and T80-10, at the level of maximum abundance of *G. bulloides*. Left-coiling types even outnumber right-coiling types in T80-10. The predominance of left-coiling *pachyderma* types is usually considered indicative of surface-water temperatures below 10°C (Bé and Hamlin, 1967; Kahn, 1981). We suggest that the high frequencies of left-coiling *pachyderma* types at the top of zone Y4 indicate that temperatures at the thermocline were very low in the southern part of the region. Hence, cold water advection from the south was presumably stronger at the end of stage Y4 than in any other period of the last glacial.

Notwithstanding the influence of cold-water advection was at a maximum during late stage Y4, the photic layer seems to have remained well-stratified year-round in the northern part of the region. By contrast, the photic layer in the north was poorly stratified during the cold season in stages Y3 and Y2, while the influence of the BC was less strong than in late stage Y4. This indicates that the two processes, which determine the depth of the thermocline and thus the degree to which the photic layer is well-stratified, - i.e. cold water advection from the south and atmospheric circulation in the western Atlantic - varied independently of each other.

We suggest that during late stage Y4, when the influence of the BC was at a maximum, atmospheric circulation in the western Atlantic was weak. In stages Y3 and Y2, the BC influence decreased whereas atmospheric circulation in the western Atlantic intensified. This may imply that (oceanic) equatorial upwelling processes were insignificant during late stage Y4, whereas they were relatively important in stages Y3 and Y2. On the other hand, if the BC ever transported cold surface waters into the area, it most probably occurred during late stage Y4.

Variation in the influence of the BC should be monitored by changes in the proportion of *dutertrei* types per total neogloboquadrinids (fig. 63). Proportions of *dutertrei* types are generally higher in stage Y3 than in stages Y2 and Y4 in all cores but KW26. Although the difference between stages Y4 and Y3 can not be interpreted unequivocally, because of the seasonal bias in the Y3 signal, relatively high proportions of *dutertrei* types in the Y3 zone are compatible with decreased BC influence.

The high proportions in stage Y3 relative to those in stage Y2 can not be explained from variation in seasonal bias, but clearly indicate that subsurface temperatures were lower during the warm season in stage Y2 than in stage Y3. This suggests that the BC reintensified during stage Y2.

In summary, cold waters were advected from the south throughout the last glacial and their influence was probably particularly strong during the cold season (cf. Gardner and Hays, 1976). The thermocline was at shallower depth than in postglacial times, which suggests that the glacial surface-water circulation was stronger.

This supports the general opinion that atmospheric circulation was more intense in glacials than in interglacials (e.g. Bornhold, 1973; Gardner and Hays, 1976; Van Zinderen Bakker, 1976; Mix et al., 1986a, b; Pokras, 1987) and overall primary production higher (e.g. Bornhold, 1973; Duplessy and Shackleton, 1985; Mix et al., 1986b; Pokras, 1987).

Cold-water advection was at a maximum during late stage Y4. Paradoxically, their effect on surface-water conditions in the northern area was less significant than in the later glacial stages. In our simple model, the discrepancy is to be attributed to an anomalously weak atmospheric circulation in the western Atlantic during late stage Y4. In the northern area, the photic layer was year-round well-stratified and the thermocline was at shallow depth, particularly during the cold season. Cold season surface-water temperatures in the north may have been higher in stage Y4 than in the later glacial stages. The thermocline shallowed towards the south but the photic layer was poorly stratified during most of the year because the BC transported cold (surface) waters into the region.

During stage Y3, the cold season photic layer was poorly stratified in the entire region, although cold water advection decreased. We suggest that the thermocline shallowed during the cold season due to a more vigorous atmospheric circulation in the western Atlantic. The seasonal change from well-stratified to poorly stratified conditions might be ascribed primarily to (low-intensity) equatorial upwelling in a coastal setting. Because subsurface isotherms shallowed towards the south due to cold water penetration, the effects of upwelling were most significant in the south.

During the glacial maximum of stage Y2, the overall hydrographic setting seems to have been roughly similar to that of stage Y3. The supply of cold waters by the BC, however, increased. In the north, poorly stratified conditions prevailed over a longer period of the year than in stage Y3, which may be due to the combined effects of a relatively strong atmospheric circulation in the western Atlantic and increased advection of BC waters. In the south, cold waters were present at the surface during most of the year.

A marked hydrographic difference between stages Y2 and Y4 was also concluded by Pokras (1987). His diatom assemblages from the northern part of our region indicate maximum influence of the BC during isotope stage 2, and strong in situ (read: oceanic) upwelling during stage 4. We come to a completely different interpretation, since we postulate that during late stage Y4 the influence of the BC was at a maximum, whereas equatorial upwelling processes were insignificant.

VI.3.7. Palaeoenvironments during Termination II and the last interglacial

Stage X3 is thought to be correlative with isotope substage 5e, which represents the only period in the last 150,000 yr, during which the ice-volume was as small as today. Oceanic conditions during substage 5e were in general not significantly different from those prevailing today, but surface-water temperatures are thought to have been slightly higher in the eastern South Atlantic (CLIMAP, 1984).

Although a clear-cut equivalent of stage Y1 does not preceed X3, there is some faunal evidence of a climatic warming prior to the reentry of *G. menardii*. *G. inflata* is low frequent in the upper part of the W zone in T80-10 and VM29-143 (figs. 58, 59), which indicates that the photic layer was virtually year-round stratified at the end of the penultimate glacial period. The high frequencies of *G. bulloides* just below the W/X boundary in T80-10 are presumably associated with increased river run-off (fig. 66).

Percentages of total neogloboquadrinids are low in the uppermost part of the W zone (fig. 64), which indicates that the thermocline was at a rather deep posi-

tion throughout the year. Furthermore, *G. trilobus* reaches markedly high percentages just below the W/X boundary in T80-10, VM29-143, and VM19-283 (figs. 54, 55, 57).

All considered, we may conclude that the general hydrographic conditions at the end of the W zone were similar to those between 14,000 and 10,000 yr BP. Again deglaciation may have started before the reentry of *G. menardii.*

Low proportions of *dutertrei* types are found below the W/X boundary, but they significantly increase across the boundary (fig. 63). This corroborates the idea that, as far as local conditions are concerned, temperatures at the thermocline are critical for the reappearance of *G. menardii.*

In stage X3, *G. inflata* reaches minimum frequencies (figs. 54, 58, 65), which together with overall low abundances of total *Neogloboquadrina* (fig. 64), suggests that the thermocline remained year-round at great depth. Percentages of total neogloboquadrinids are similar to those in stage Y1 or even slightly lower, which indicates that primary production was at a minimum.

Although the proportion of *dutertrei* types in stage X3 varies considerably from one core to another (fig. 63), the values are generally high and suggest that temperatures at the thermocline were more or less similar to those at the beginning of the Holocene.

Notwithstanding conditions during stage X3 were in general similar to those prevailing today, low intensity coastal upwelling did not occur, and cold season surface-water temperatures may, therefore, have been higher than at present and primary production slightly lower. There is no evidence that surface-water temperatures were higher during the warm season as well. The absence of coastal upwelling suggests that atmospheric circulation in the western Atlantic was weaker than at present.

The climatic proxy curves (fig. 62) indicate that climate progressively deteriorated from the base of the X zone upward. This trend is well reflected in the abundance pattern of *G. inflata,* which shows increasingly higher percentages towards the top of the zone (figs. 54, 58, 65). Superimposed on this trend is an alternation of relatively cold and warm climatic stages, which is best registered by T80-10 and VM19-283.

Stages X2 and X1

In T80-10, *G. bulloides* reaches high abundances in stages X2 and X1, which is thought to be due to increased run-off (fig. 66).

Percentages of *G. inflata* and total neogloboquadrinids are very similar to those in the upper part of the Z zone but higher than in X3. This indicates that the thermocline was deep during the warm season, whereas during the cold season the photic layer was poorly stratified. The cold season atmospheric cir-

culation in the western Atlantic was probably more intense than in stage X3.

Abundances of *G. inflata* are similar in T80-10 and VM19-283 (figs. 54, 57) and proportions of *dutertrei* types are not significantly lower in T80-10 than in VM19-283 (fig. 63). This suggests that there was no appreciable advection of cold waters from the south. In stage X1, the proportion of *dutertrei* types is even higher in T80-10, but this can not be taken as indicative of higher subsurface temperatures. Total neogloboquadrinids are less frequent in T80-10 than in VM19-283 (fig. 64). This suggests that stratification was periodally disturbed in front of the river Zaire, which in view of the high abundances of *G. bulloides* is most likely due to intense river-induced upwelling.

Variation in the proportion of *dutertrei* types in VM 19-283 (fig. 63) suggests that temperatures at the thermocline were lower during stage X1 than in stage X2. During both periods, subsurface temperatures were lower than in X3 or the Holocene. The progressive lowering of the subsurface temperatures from stage X3 via X2 to X1 is also nicely reflected in the successively lower percentages of *G. menardii.* What process produced the progressive temperature decrease is not clear, but it may reflect a global climatic change.

The cold stages of the X zone and the end of the last interglacial

The cold climatic stages within the X zone are fully documented only in VM19-283.

Percentages of *G. inflata* are similar to those in stages X2 and X1, except at the top of the X zone, where they are higher. This suggests that stratification of the photic layer was seasonally disturbed to a similar degree in these cold and warm climatic stages.

Total neogloboquadrinids and the proportion of *dutertrei* types in VM19-283 (figs. 63, 64), show that the cold climatic intervals are characterized by a shallower thermocline and lower subsurface temperatures than the warm stages of the interglacial.

Proportions of *dutertrei* types per total neogloboquadrinids are relatively high in the cold stage immediately following stage X3 and are very low in the later cold stages. In the two later stages, proportions of *dutertrei* types are even lower than in stage Y3. We think that the scarceness of *dutertrei* types can not be attributed to seasonal differences in the *Neogloboquadrina* signal and suggest that subsurface water temperatures were lower during the warm season than in stage Y3. Thus, we may speculate that cold water penetration from the south was significantly stronger than in stage Y3.

Yet, the percentage distribution of *G. inflata* shows that the cold-season stratification of the photic layer was less severely disrupted than during stage Y3. We may, therefore, speculate that atmospheric circulation in the western

Atlantic was weaker than in stage Y3, though not necessarily as slow as in late stage Y4.

Percentages of *G. inflata* decrease from the top of the X zone to the lower part of zone Y4 in all relevant cores (figs. 54-55, 57-58). They are much higher in T80-10 than in either VM29-143 or VM 19-283, which indicates significant cold water advection from the south. We suggest that trade wind activity in the western Atlantic continued to decrease from the end of the interglacial till late stage Y4. Advection of cold waters, may have remained constant until late stage Y4.

VI.3.8. Concluding remarks

We have based the palaeoenvironmental reconstruction on a simple and essentially actualistic model of the thermocline, which takes into account only two factors, viz. atmospheric circulation in the western Atlantic and cold water penetration from the south. In view of the complex hydrography of the present-day eastern South Atlantic, this may be a serious simplification.

We have suggested that the intensification of the BC and intensification of trade wind activity in the western Atlantic are generally out of phase. Periods of deglaciation, included stage X3, are exceptional because the overall surface-water circulation was at a minimum. It seems somewhat implausible to uncouple trade wind activity in the western Atlantic and the intensity of the eastern boundary current.

We should generalize that any process enhancing equatorial divergence leads to a shallowing of the thermocline. Winds with a strong easterly component at low latitudes could have enhanced equatorial divergence, whereas southerly winds could have acted opposite (cf. Mix et al., 1986a, b). Southerly winds could, on the other hand, have strengthened the eastern boundary current. Changes in wind direction may, therefore, have been involved.

Chapter VII

THE LATE QUATERNARY RECORD OF BENTHIC FORAMINIFERS

VII.1. INTRODUCTION

Early workers on deep-sea cores from the northern and equatorial Atlantic Ocean (Schott, 1935; Phleger et al., 1953) already observed that late glacial benthic foraminiferal faunas are generally different from Holocene ones. Subsequently, Streeter (1973) showed that during the maximum of the last interglacial benthic associations in the North Atlantic deep-sea were similar to modern ones, whereas they were dissimilar during most of the past 150,000 years. Similar results were obtained by Schnitker (1974; 1980), who compared modern faunal patterns in the North Atlantic with those of the last glacial maximum and the last interglacial maximum.

The cores investigated by Streeter and Schnitker are virtually all from the central part of the North Atlantic south of 55°N. A marked contrast between late glacial and Holocene deep-sea faunas is found also in marginal areas at both sides of the North Atlantic (Schnitker, 1979; Haake, 1980; Streeter and Lavery, 1982). Furthermore, Lutze et al. (1979) demonstrated that deep-sea benthic foraminifers on the N.W. African continental margin closely followed climatic change over the past 100,000 years. In that area, the impact of major climatic events on the deep-sea is traceable in the benthic faunas as far back as in the Late Pliocene (Lutze, 1979; see also Lutze, 1977).

Belanger (1982) and Streeter et al. (1982) found that during isotope substage 5e the deep-sea faunas in the Norwegian and Greenland seas were similar to the modern ones. Although benthic faunas changed significantly during the Late Quaternary, these changes do not follow a simple glacial/interglacial pattern.

Within the Caribbean, deep-sea faunas changed drastically over the Y/Z boundary in the Venezuela Basin (Gaby and Sen Gupta, 1985), but in the Grenada Basin there are only subtle differences between faunas of the Y zone and those of the X and Z zones (Sen Gupta et al., 1982).

Late Quaternary deep-sea benthic faunas have as yet been studied less extensively in the South Atlantic. Zachariasse et al. (1984) examined a single core, viz. T78-45, from the Zaire deep-sea fan (see fig. 48) and demonstrated a strong resemblance between the Holocene associations and those from substage 5e, whereas the glacial faunas were very unlike the modern one. Glacial/interglacial differences were found also in the abundance pattern of *Uvigerina*

peregrina in some cores from the Angola Basin (Van Leeuwen, 1986). In the S.W. Atlantic, on the other hand, there is no simple relation between benthic foraminifers and climate (Gofas, 1978; Lohmann, 1978; Peterson and Lohmann, 1982).

In the Southern Ocean adjacent to the south-eastern Indian Ocean, benthic foraminifers closely followed climatic variation during the Late Quaternary (Corliss, 1983b), but such a relation was not found in the south-eastern Indian Ocean (Corliss, 1979).

This summary of literature data suggests that major changes in the Late Quaternary climate are recorded by deep-sea benthic foraminiferal faunas over extensive parts of the world ocean but not everywhere.

Streeter (1973) attributed the climate-related changes in the benthic faunas to changes in deep-water temperature and suggested that deep-water circulation in the North Atlantic changed drastically from glacial to interglacial time. Interpretation of faunal change in terms of deep water-masses has predominated in the literature ever since. Some papers (e.g. Corliss, 1979) suggest that only the areal extent of water-masses has changed in time, but the general opinion is that characteristics of bottom waters may have changed as well.

A distinctive feature of glacial faunas from various parts of the world ocean, is an acme of *Uvigerina* species. Streeter and Shackleton (1979) proposed that high percentages of *U. peregrina* are indicative of low oxygen concentrations. This specific relation has widely been used to reconstruct palaeocirculation in the deep ocean (e.g. Schnitker, 1979; Peterson and Lohmann, 1982; Sen Gupta et al., 1982; Corliss, 1983a).

Lutze (1980) and Miller and Lohmann (1982), however, showed that high abundances of *U. peregrina* correlate primarily with high percentages of organic matter in the sediments. Factors other than watermass properties may, therefore, have a profound effect on the distribution of this species. Another argument against rigidly interpreting benthic foraminiferal change in terms of water-masses, has been provided by Belanger (1982) and Streeter et al. (1982). These authors emphasized that Late Quaternary changes in benthic faunas of the northernmost Atlantic are probably controlled not only by variation in water-mass properties, but also by changes in surface-water production. In addition, Lutze et al. (1986) suggested that faunal changes observed on the continental margin of N.W. Africa are governed by changes in the position of highly productive surface-waters rather than by changes in bottom water.

That variation in surface-water production affects benthic foraminiferal distribution fits in with our contention that the flux of organic carbon exerts

major control on the distribution of benthic foraminifers in the present-day Angola Basin. Interference of local factors, such as surface water production, with the more globally operating system of deep-water circulation may explain why changes in deep-sea faunas not always coincide with global changes in Late Quaternary climate.

Our objectives are, therefore, (1) to establish a Late Quaternary benthic record for the various sites, (2) to find out whether changes in the faunas are linked up with climatic change, and (3) to assess which parameters control possibly climate-related faunal patterns.

VII.2. COUNTED NUMBERS AND FAUNAL CATEGORIES

We aimed to count an approximate minimum of one hundred benthic foraminifers per sample in both size-fractions, but in practice we had to settle for a lower number.

The minimum number of specimens counted in the total fraction is 75. Samples VM19-283/8 and KW26/13, were excluded from quantitative analysis of the total fraction, because of strong down-slope contamination. Sample KW26/13 was, nevertheless, included in the analyses of the large-size fraction, because contaminants are mainly small-sized specimens.

Collecting one hundred of specimens in the large-size fraction proved to be even more difficult. This holds in particular for T80-10, where the total number per sample usually varies between 60 and 100. The topmost sample yielded even less specimens, and the same applies to two samples in KW25; these three samples were excluded from statistical analysis. The minimum number of specimens counted in the large-size fraction is 80 for all other samples.

We generally present frequency curves for the taxa categories that attain relative abundances of at least five percent in one of the samples of a core. Most of the polytypic species were split into their individual morphotypes. Lump categories such as *Pullenia* spp. and *Gyroidina* spp., and the group of indeterminable specimens were discarded. A few additional exceptions were made which are to be mentioned in the presentation of the individual cores.

An important lump category comprises the benthic foraminifers that are of undoubtedly allochthonous origin. This category includes a very large number of species, which are all considered to be virtually limited to the shelf and upper continental slope. Major representatives are *Bolivina albatrossi, B. striatula spinata, Bulimina gibba, B. marginata, Cancris* spp., *Cassidulina minuta, Cibicides lobatulus, Elphidium* spp., *Hanzawaia boueana, Nonion asterizans,* and *Nonionella* spp. Also included are various, very small-sized *Bolivina,* which according to Lutze (1979, 1980) are to be considered as shelf species. The composi-

tion of the allochthonous unit may differ from one core to another, which supposedly reflects differences in source area. In this context, it is interesting to mention that *Amphistegina* occurs repeatedly in VM19-283.

Various data-bases were constructed for statistical analysis. In general all categories shown in the frequency diagrams were included, but a few exceptions were occasionally made.

Foraminiferal number

The number of benthic foraminifers standardized to one gram of dry sediment was estimated separately for the 150-595 μm and the 63-150 μm fractions. The results are included in the graphical representation of the counts, but they will not be discussed in detail, because an interpretable pattern was generally lacking. Numbers tend to be the lowest in T80-10, which presumably reflects the high sedimentation rates in this core (see table 9).

As a rule, small-sized specimens greatly exceed the larger ones in number, but some samples in T80-10 are exceptional. Fig. 67 shows that these are the samples that show signs of severe dissolution. This observation suggests that the smaller individuals are more susceptible to dissolution.

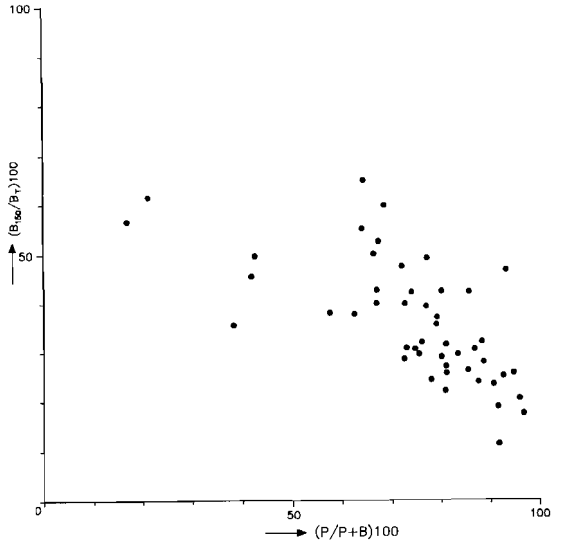

Fig. 67. *Core T80-10.* Diagram showing the relation between the proportion of planktonics in the 150-595 μm fraction (P/P+B x100) and the proportion of large-sized benthics (150-595 μm) in the 63-595 μm fraction (B150/BT).

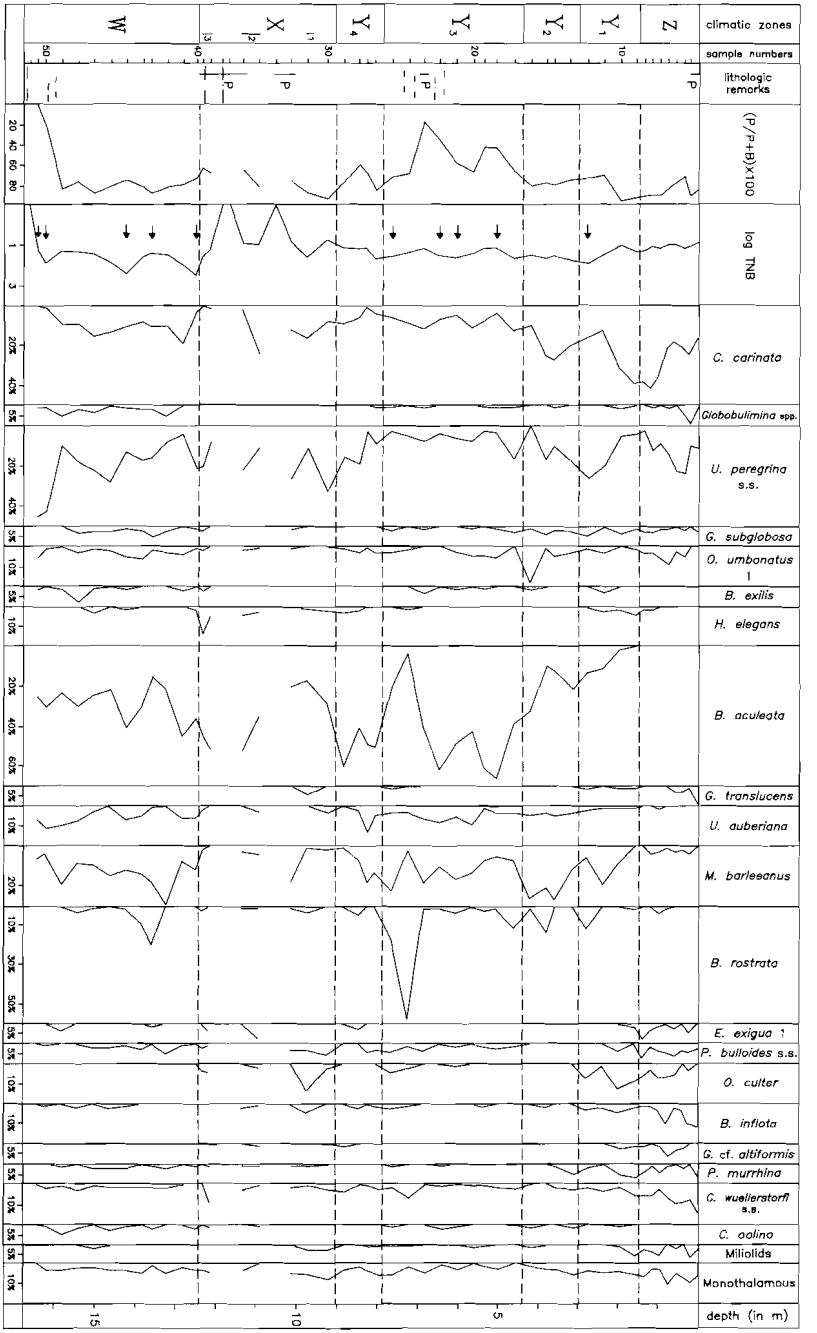

Fig. 68. *Core T80-10 (150-595 µm).* Frequency distribution of the quantitatively most important benthic foraminiferal taxa, excluded *Bulimina subacuminata.* The logarithm of the benthic foraminiferal number (log TNB) and the percentage of planktonics are shown. Arrows indicate counts of more than 100 specimens. Open sections represent intervals without foraminifers.

T80-10 (1988 m)

Large-size fraction (fig. 68).

The composition of the fauna changed drastically over the past 150,000 yr and the changes seem independent of variation in dissolution. The associations are variously dominated by *Cassidulina carinata, Bulimina aculeata, B. rostrata, Melonis barleeanus,* or *Uvigerina peregrina* s.s., but a regular relation between the overall composition of the faunas and variation in climate seems absent.

A closer look at the frequency curves learns that some individual taxa follow climatic change more regularly. *Bulimina inflata, Cibicides wuellerstorfi* s.s., *Epistominella exigua* 1, *Gavelinopsis translucens, Hoeglundina elegans,* and *Osangularia culter* are only occasionally present in cold climatic intervals and

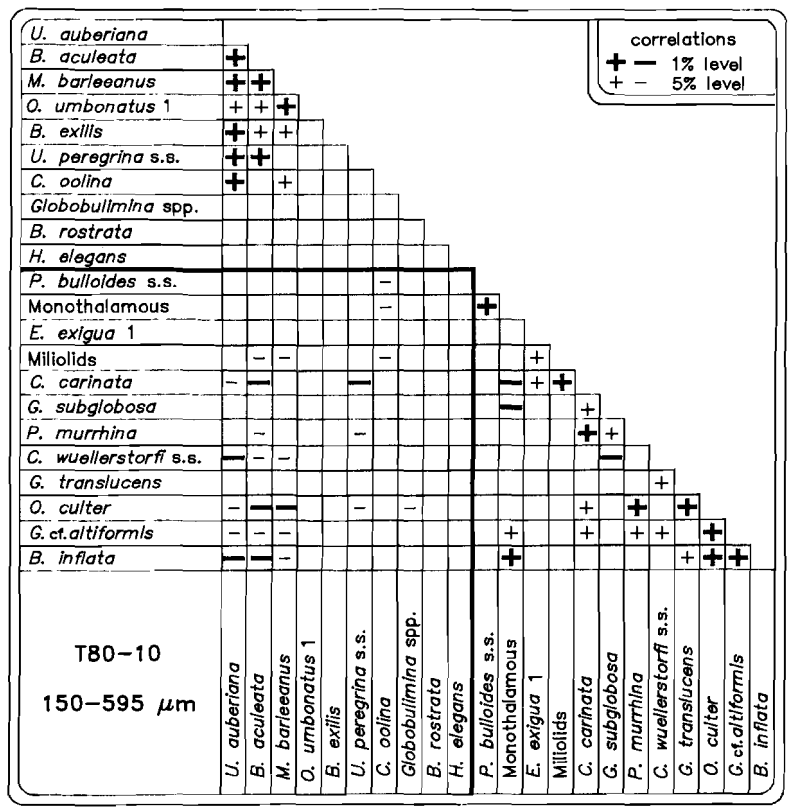

Fig. 69. *Core T80-10 (150-595 µm).* BALANC correlation-matrix. The heavy line separates the two groups that show the lowest degree of similarity according to the DENDRO-analysis.

relatively frequent in some of the warm climatic intervals. A consistent climate related pattern is, however, not shown by any of the taxa. *M. barleeanus* and *Uvigerina auberiana*, on the other hand, show preference for cold climatic intervals. The relation between these two species and cold climatic periods seems to be more regular than that between the other taxa and warm climatic periods.

The BALANC program was used to examine the covariance of the selected categories. The correlation matrix (fig. 69) indicates that there are two small, homogeneous groups, which are mutually negatively correlated.

The first group unifies *B. aculeata, M. barleeanus,* and *U. auberiana. Bulimina exilis* and *O. umbonatus* 1 join at a lower level of significance. This group essentially combines taxa that reach their highest frequencies in the W and the glacial part of the Y zone and that are relatively rare in the Z, the top of the Y1 and the X1 zone. *Chilostomella oolina* and *U. peregrina* s.s. are connected with some of these taxa.

The second group is composed of *B. inflata, Gyroidina* cf. *altiformis,* and *O. culter,* which are all taxa that are relatively frequent in the Z and the top of the Y1 zone. Many other species, which reach their highest frequencies also in warm climatic intervals, have positive correlations with members of this group and some of them have negative ties with the first group (e.g. *C. carinata, C. wuellerstofi* s.s., *Pyrgo murrhina*). However, there seems to be little coherence among the taxa that are most frequent in warm climatic intervals, which indicates that these intervals are not characterized by a specific faunal association.

Total fraction (fig. 70).

Comparison with fig. 68 shows that distribution patterns of large-sized taxa in the total fraction are very similar to those in the large-size fraction. The small-sized *E. exigua* 1 and *G. translucens,* however, show a more consistent relation with warm climatic intervals than in the large-size fraction. Especially *E. exigua* 1 closely follows the climatic proxy curve based on planktonic foraminiferal analysis (see fig. 62).

Other small-sized taxa show distinct distribution patterns as well. *Nuttallides pusillus* abounds in cold climatic intervals, whereas *Nuttallides umboniferus decoratus* is virtually restricted to the warm climatic intervals Z and X3. Percentages of *E. exigua* 2 and *E. smithi* seem to vary independently of climatic change.

A relation between climatic variation and percentage of allochthonous elements seems to be absent, although some down-slope contamination seems to have occurred in the Z zone and in the upper part of the Y1 zone.

The correlation-matrix of the BALANC analysis (fig. 71) shows a polarity, which is similar to the one in the matrix of the large-size fraction. A homogeneous group composed of *B. aculeata, M. barleeanus, N. pusillus, O. um-*

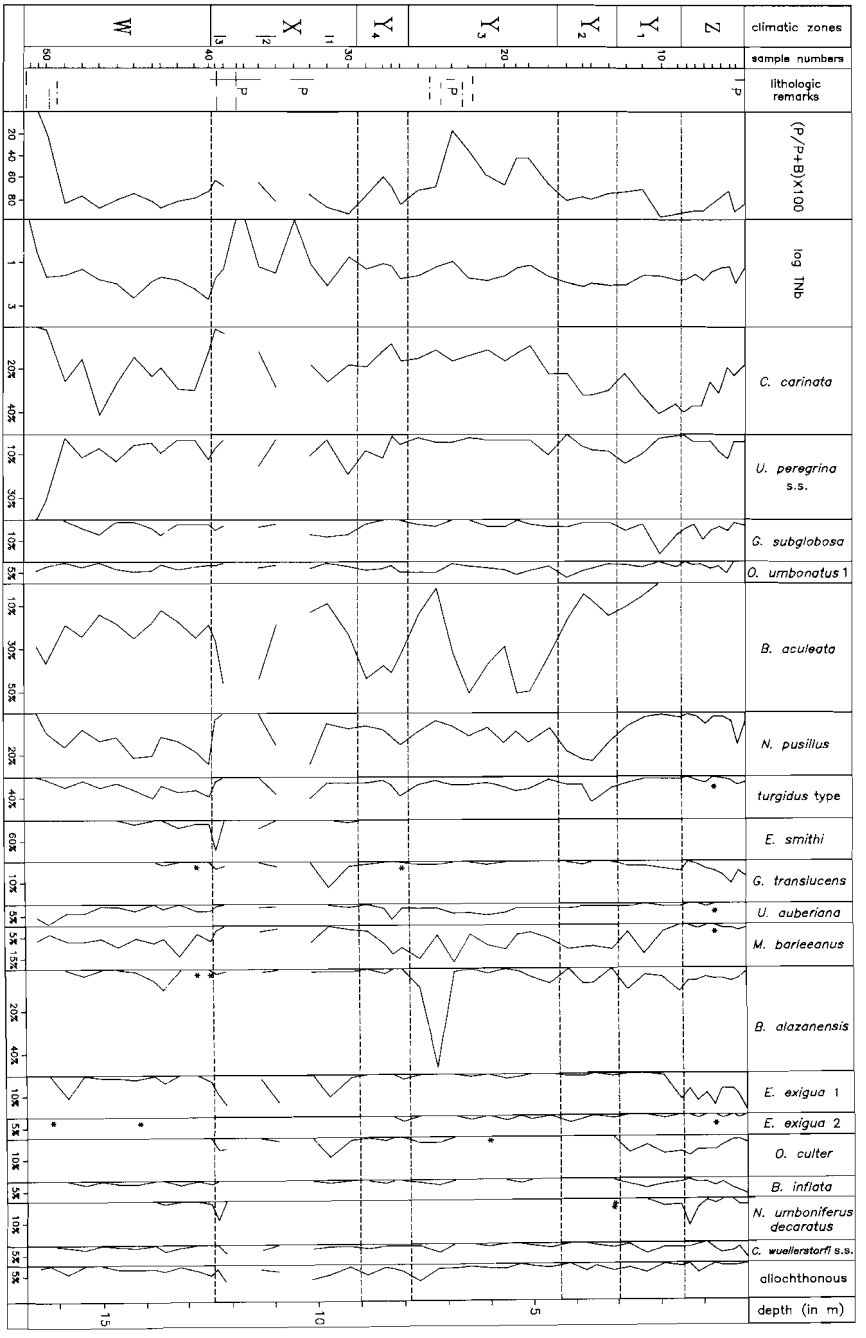

Fig. 70. *Core T80-10 (63-595 μm).* Frequency distribution of the quantitatively most important benthic foraminiferal taxa, included *E. exigua* 2. *H. elegans* and the lump categories Monothalamous and Miliolids have been excluded because their distribution has been depicted satisfactorily in the large-size fraction. The logarithm of the benthic foraminferal number in the 63-150 μm fraction (log TNb) and the percentage of planktonics in the 150-595 μm fraction are shown. Asterisks mark relative frequencies of less than 0.5 %. Open sections represent intervals without foraminifers.

bonatus 1 and *U. auberiana* is clearly the equivalent of the 'cold' group in the large-size fraction. *E. exigua* 2, *U. peregrina* s.s. and the allochthonous elements, are positively correlated with some elements of this group. As a whole, this first group is negatively correlated with *O. culter,* whereas single elements are negatively correlated with *B. inflata, C. wuellerstorfi* s.s., *E. exigua* 1, *G. translucens,* or *N. umboniferus decoratus.*

B. inflata, C. wuellerstorfi s.s., *E. exigua* 1, and *G. translucens* form a coherent second group, which may be regarded as the equivalent of the 'warm' group in the large-size fraction analysis. Remarkably, *O. culter* is only loosely connected with this group, which emphasizes once again that the taxa that are most frequent in warm climatic intervals do not form a uniform association.

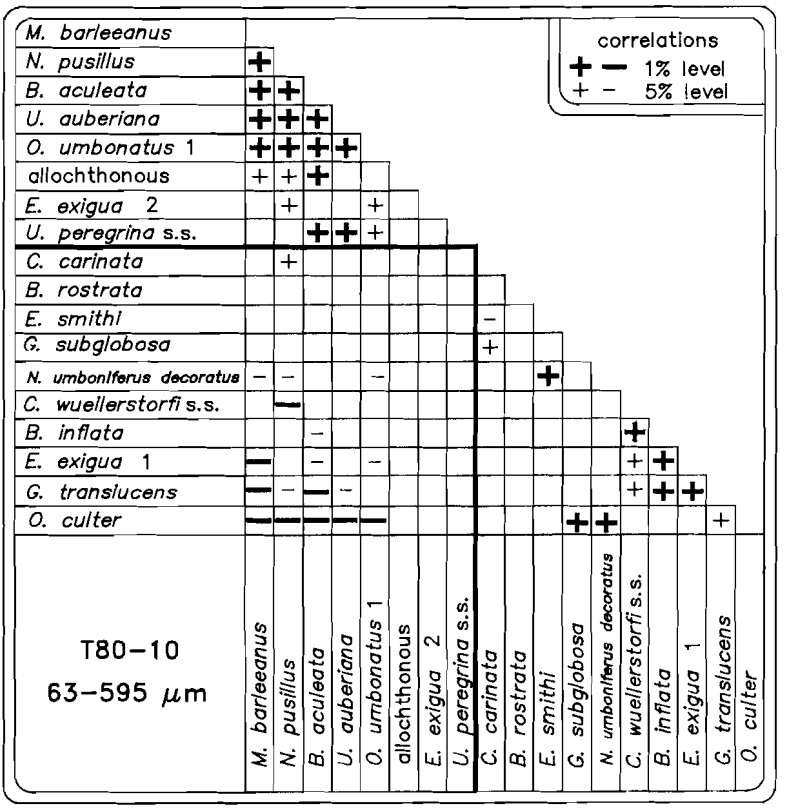

Fig. 71. *Core T80-10 (63-595 µm).* BALANC correlation-matrix. The heavy line separates the two groups that show the lowest degree of similarity according to the DENDRO-analysis.

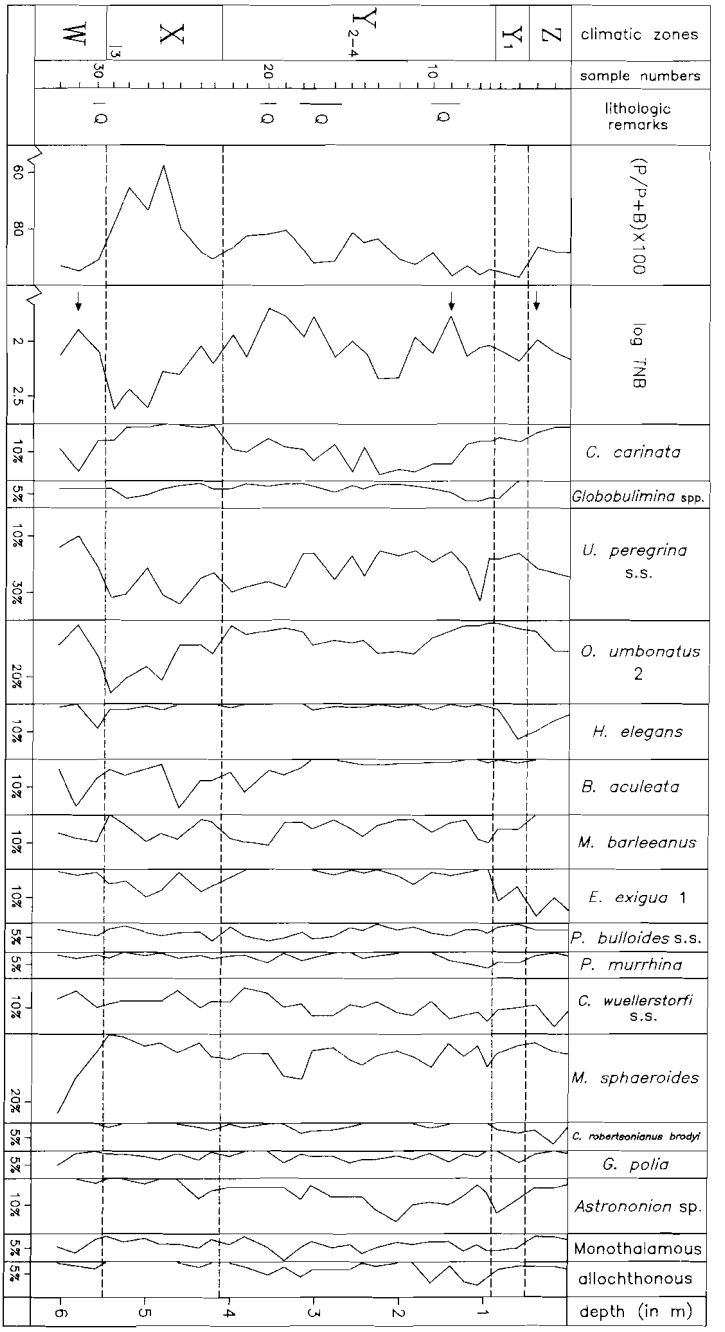

Fig. 72. *VM29-143 (150-595 µm).* Frequency distribution of the quantitatively most important benthic foraminiferal taxa. The logarithm of the benthic foraminiferal number (log TNB) and the percentage of planktonics are shown. Arrows indicate counts of less than 100 specimens.

VM29-143 (2776 m)

Large-size fraction (fig. 72)

Down-slope contamination is negligible in warm climatic intervals, i.e. the Z and X zones and the Y1 zone, but is considerable in the upper and lower part of the glacial Y2-4 interval. These are the intervals that were seen to be influenced by turbiditic deposition as evidenced by high amounts of quartz grains.

A number of taxa show a distinct relationship with climatic variation. *E. exigua* 1 is definitely more frequent in interglacial than in glacial intervals. A similar but more specific relationship may be concluded for *H. elegans*, which reaches highest frequencies just below the Y/Z and the W/X boundaries, i.e. in intervals corresponding to the early phases of deglaciation.

C. carinata attains a maximum frequency in glacials and is rare in interglacial

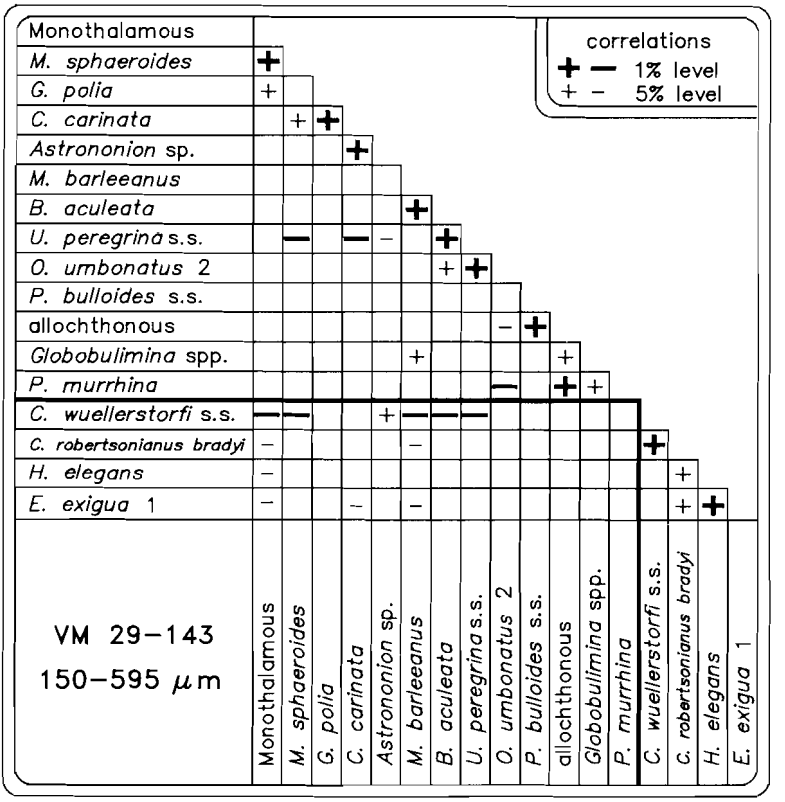

Fig. 73. *VM29-143 (150-595 µm).* BALANC correlation-matrix. The heavy line separates the two groups that show the lowest degree of similarity according to the DENDRO-analysis.

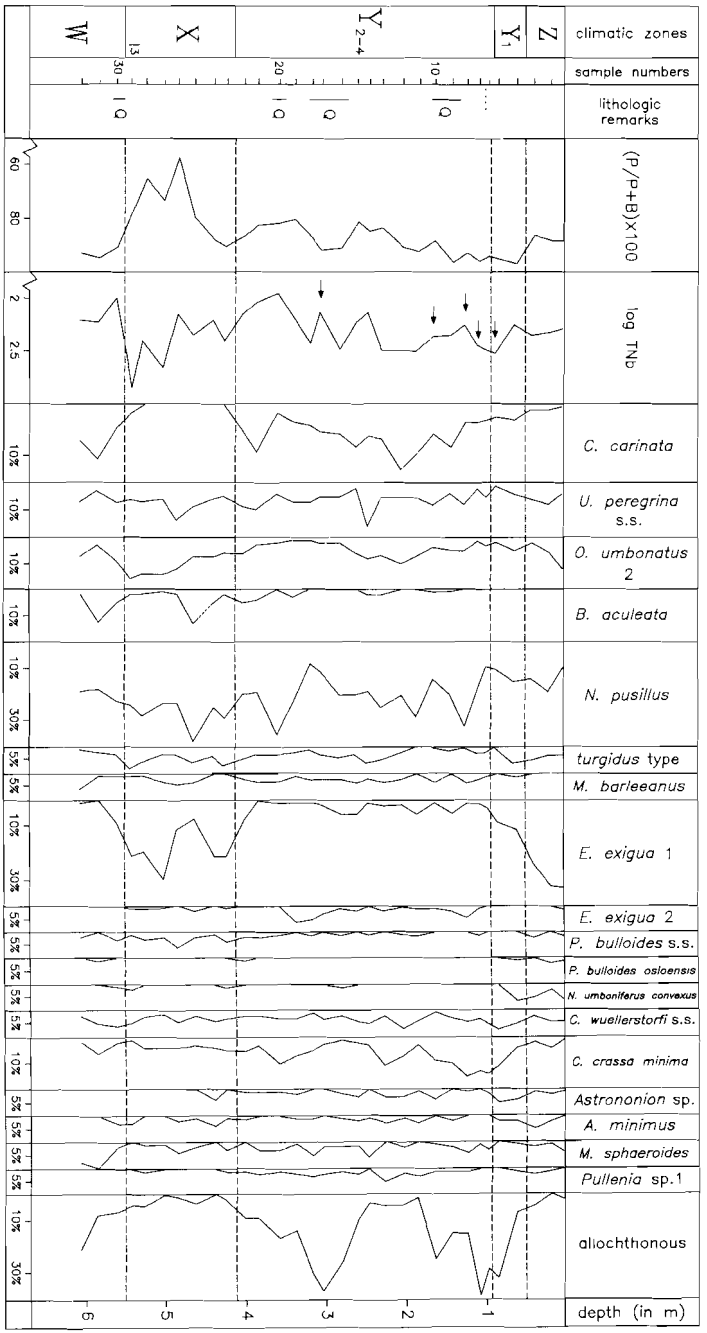

Fig. 74. *VM29-143 (63-595 μm).* Frequency distribution of the quantitatively most important benthic foraminiferal taxa. The monothalamous group has been excluded and *P. bulloides osloensis* included. The logarithm of the benthic foraminiferal number in the 63-150 μm fraction (log TNb) and the percentage of planktonics (150-595 μm) are shown. Arrows indicate counts of less than 100 specimens.

intervals. *M. barleeanus, M. sphaeroides,* and the monothalamous species-group are also more frequent in glacial intervals, but in contrast to *C. carinata* they are rare only in the Z and X3 zone.

The correlation matrix of the BALANC analysis (fig. 73) is not well-structured. *E. exigua* 1, *H. elegans,* and *Cibicides robertsonianus bradyi* seem to form a coherent group. The distribution of the three taxa is similar in the Y and Z zones, but in contrast to the other two taxa, *C. robertsonianus bradyi* is rare in the X zone and this group is, therefore, not uniform.

Among the taxa that tend to be more frequent in the cold than in the warm climatic intervals, there is even less coherence and only few are negatively correlated with *E. exigua* 1 and *H. elegans.*

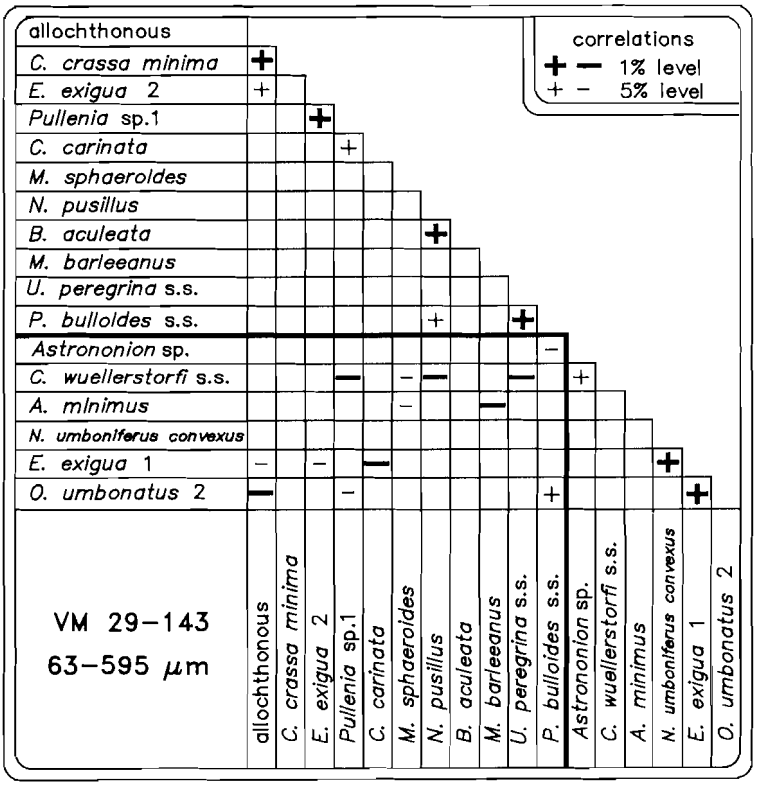

Fig. 75. *VM29-143 (63-595 µm).* BALANC correlation-matrix. The heavy line separates the two groups that show the lowest degree of similarity according to the DENDRO-analysis.

Total fraction (fig. 74)

The allochthonous elements make a larger contribution to the fauna than in the large-size fraction, but the down-core pattern is similar. The frequency distribution of relatively large-sized taxa does not differ from that in the large-size fraction. *E. exigua* 1 is more frequent in the small-size fraction and shows an even more pronounced correlation with warm climatic intervals than in the large-size fraction. A connection with warm climatic intervals is also suggested for *N. umboniferus convexus*. This taxon is, however, clearly more frequent in the Z-Y1 interval than in the X zone.

E. exigua 2, and particularly *C. crassa minima* attain their highest relative numbers in the glacial part of the Y zone. The distribution of the other small-sized taxa, i.e. *N. pusillus*, *Anomalinoides minimus*, *Pullenia* sp. 1, and *P. bulloides osloensis* seems to be rather non-descript.

The correlation-matrix of the BALANC analysis (fig. 75) is even less well-structured than the matrix of the large-size fraction. *O. umbonatus* 2 and *N. umboniferus convexus* are positively correlated with *E. exigua* 1. Little coherence seems to exist among the taxa that show a preference for cold climatic intervals. *E. exigua* 2 and *C. crassa minima* are positively correlated with the allochthonous category.

KW26 (3038 m)

Large-size fraction (fig. 76)

Down-slope contamination is insignificant in the Z-Y1 interval and fluctuates strongly in the glacial part of the Y zone. High percentages of the allochthonous category are clearly limited to intervals that show other signs of down-slope contamination. The lowermost sample also suffered from contamination and it is therefore uncertain whether the X zone is actually represented in our samples.

Three taxa are definitely connected with the Z/Y1 interval, viz. *Cibicides kullenbergi*, *E. exigua* 1, and *H. elegans*. Most of the other taxa attain higher relative numbers in the glacial section and *Fursenkoina bradyi*, *Globobulimina* spp., *M. barleeanus*, and *M. sphaeroides* are clearly correlated with the glacial interval.

The data-base used for BALANC analysis includes *C. robertsonianus* s.l. and the individual morphotypes of *O. umbonatus* 2. The ratio between the number of species and the number of samples (21:34) is far from ideal, but the results are similar to those produced by an analysis of an (18x34) matrix.

The correlation-matrix (fig. 77) shows that a large number of species are opposed to a small and homogeneous group, which combines the taxa that attain

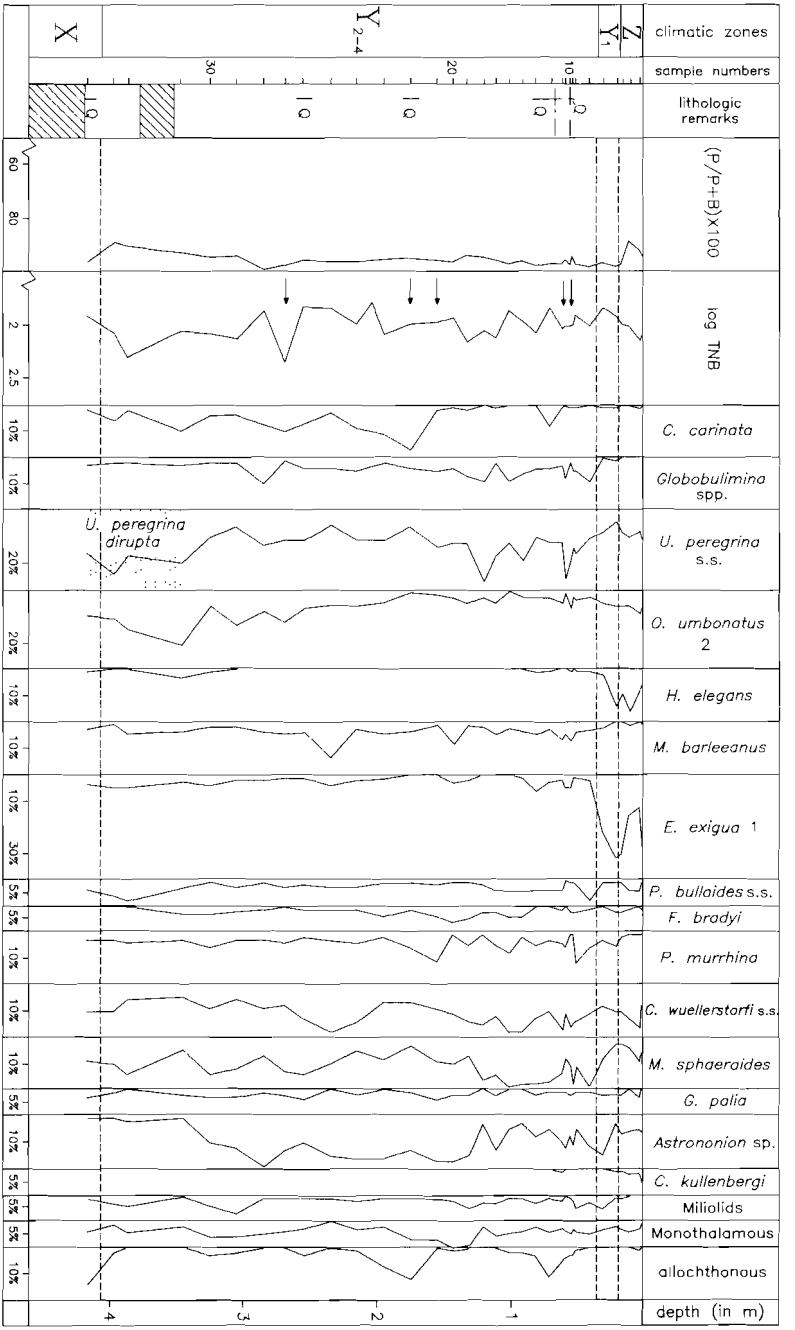

Fig. 76. *KW26 (150-595 µm).* Frequency distribution of the most important benthic foraminiferal taxa, included *G. polia.* Figure conventions as in fig. 72.

high relative numbers in the Z/Y1 interval plus *O. umbonatus* 2C. Five of the taxa that show negative correlations with this group, i.e. *C. wuellerstorfi* s.s., *Globobulimina* spp., *M. barleeanus*, *M. sphaeroides*, and *U. peregrina* s.l. form a second group. The second group might be interpreted as a combination of species that characterizes the glacial interval.

Total fraction (fig. 78).

Almost every sample is to a certain extent influenced by down-slope transport.

The faunas show an overall resemblance to the associations in VM29-143. Again *E. exigua* 1 and *N. umboniferus convexus* are distinctly related to warm climatic intervals. Among the other small-sized species, *E. exigua* 2 and *C. crassa minima* and to a lesser extent also *Pullenia* sp. 1 are relatively frequent in the glacial part of the Y zone.

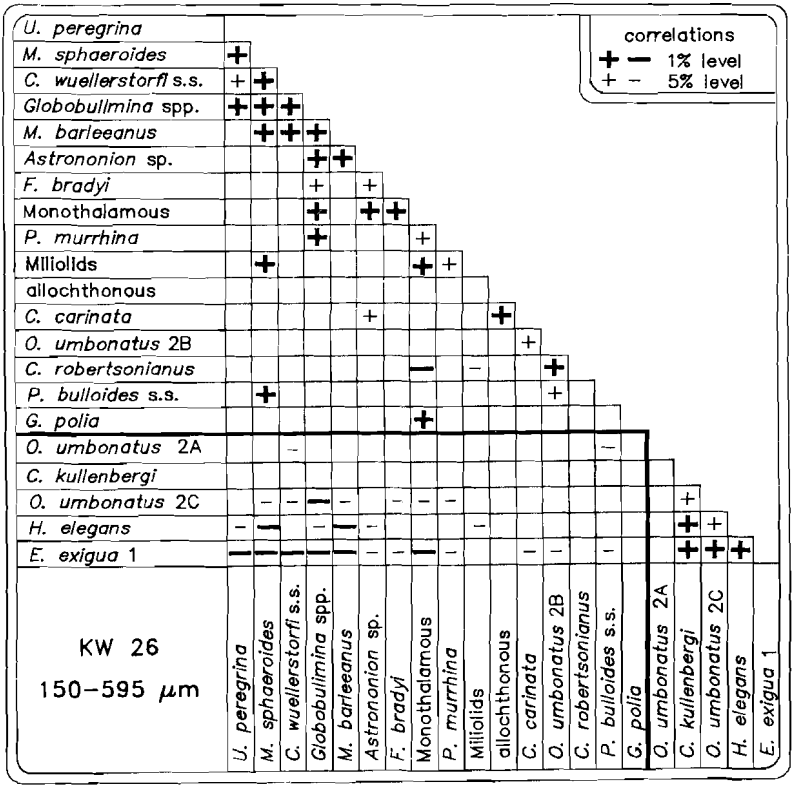

Fig. 77. *KW26 (150-595 µm).* BALANC corelation-matrix. The heavy line separates the two groups that show the lowest degree of similarity according to the DENDRO-analysis.

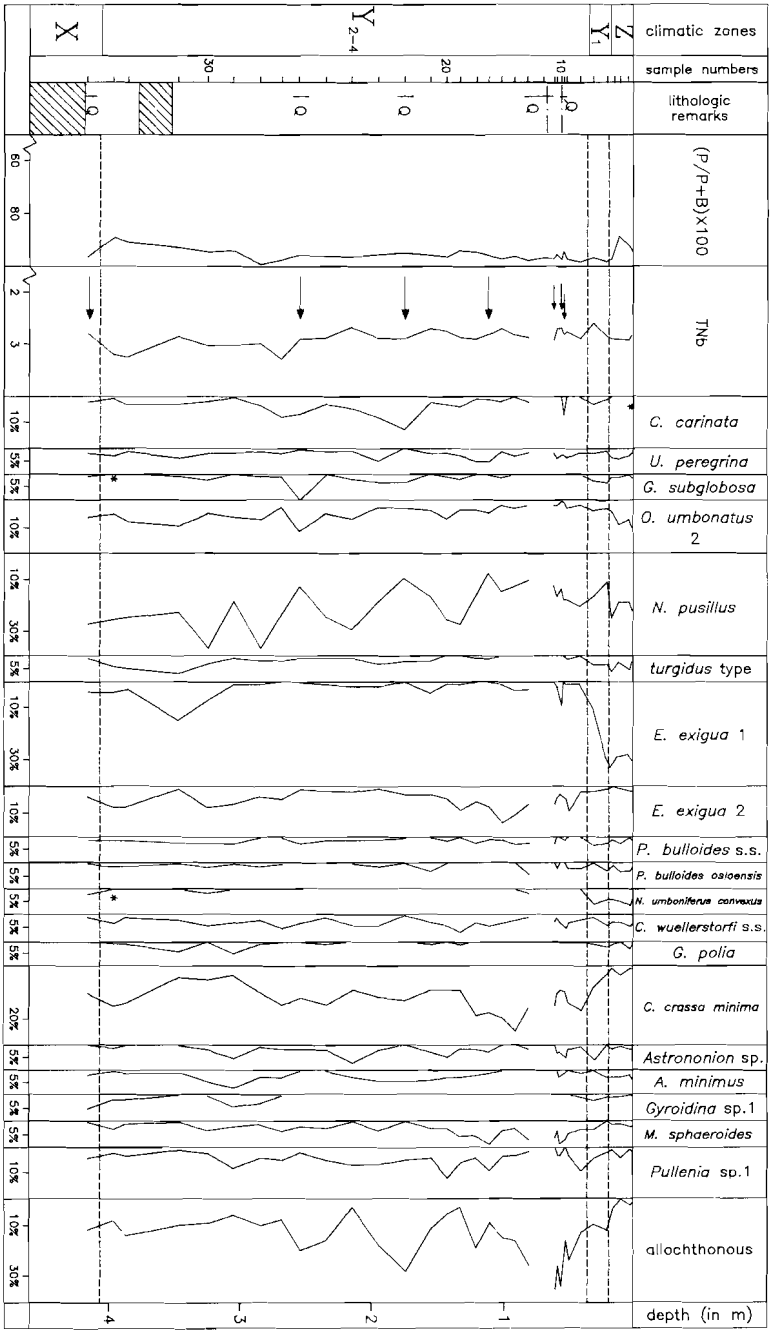

Fig. 78. *KW26 (63-595 µm).* Frequency distribution of the quantitatively most important benthic foraminiferal taxa. *Fursenkoina bradyi*, the miliolids and the monothalamous group have been excluded and *P. bulloides* s.s. and *P. bulloides osloensis* included. Faunal curves are interrupted at the level of considerable down-slope contamination. Figure conventions as in fig. 74.

The glacial/interglacial contrast in the faunas is nicely illustrated in a BALANC correlation-matrix (fig. 79). Just as in VM29-143, both *C. crassa minima* and *E. exigua* 2 are positively correlated with the allochthonous category.

VM19-283 (3442 m)

Large-size fraction (fig. 80).

Down-slope contamination appears to be significant throughout the core, with the exception of the Z zone and the X2 level. Very high percentages of the allochthonous elements are restricted to glacial intervals.

Remarkable fluctuations in abundance are shown by *U. peregrina dirupta.* This taxon dominates the associations in the two intervals that are thought to correspond to intervals Y2 and Y4, whereas lowest abundances are found in

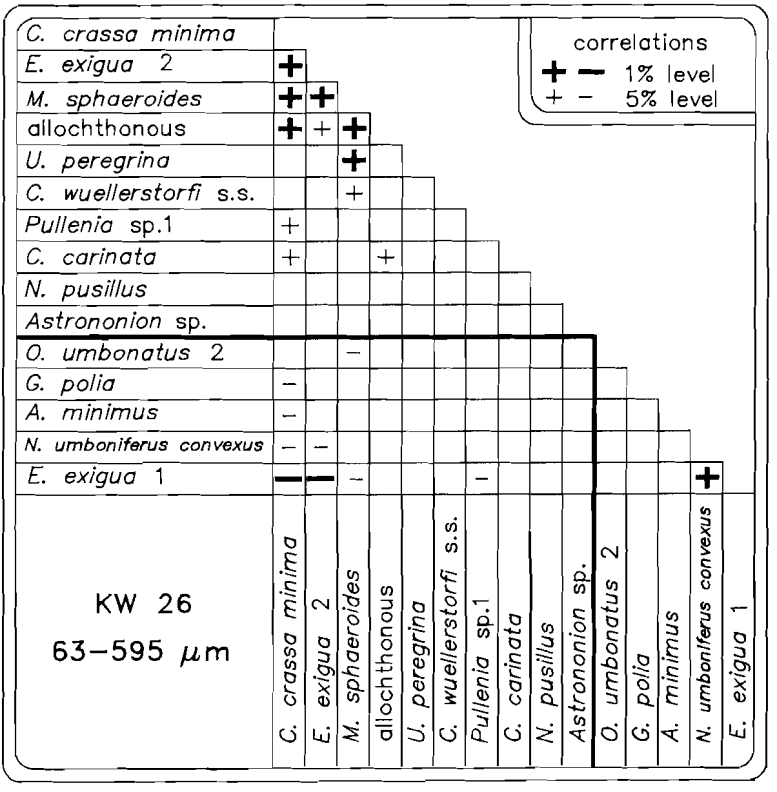

Fig. 79. *KW26 (63-595 µm).* BALANC correlation-matrix. The heavy line separates the two groups that show the lowest degree of similarity according to the DENDRO-analysis.

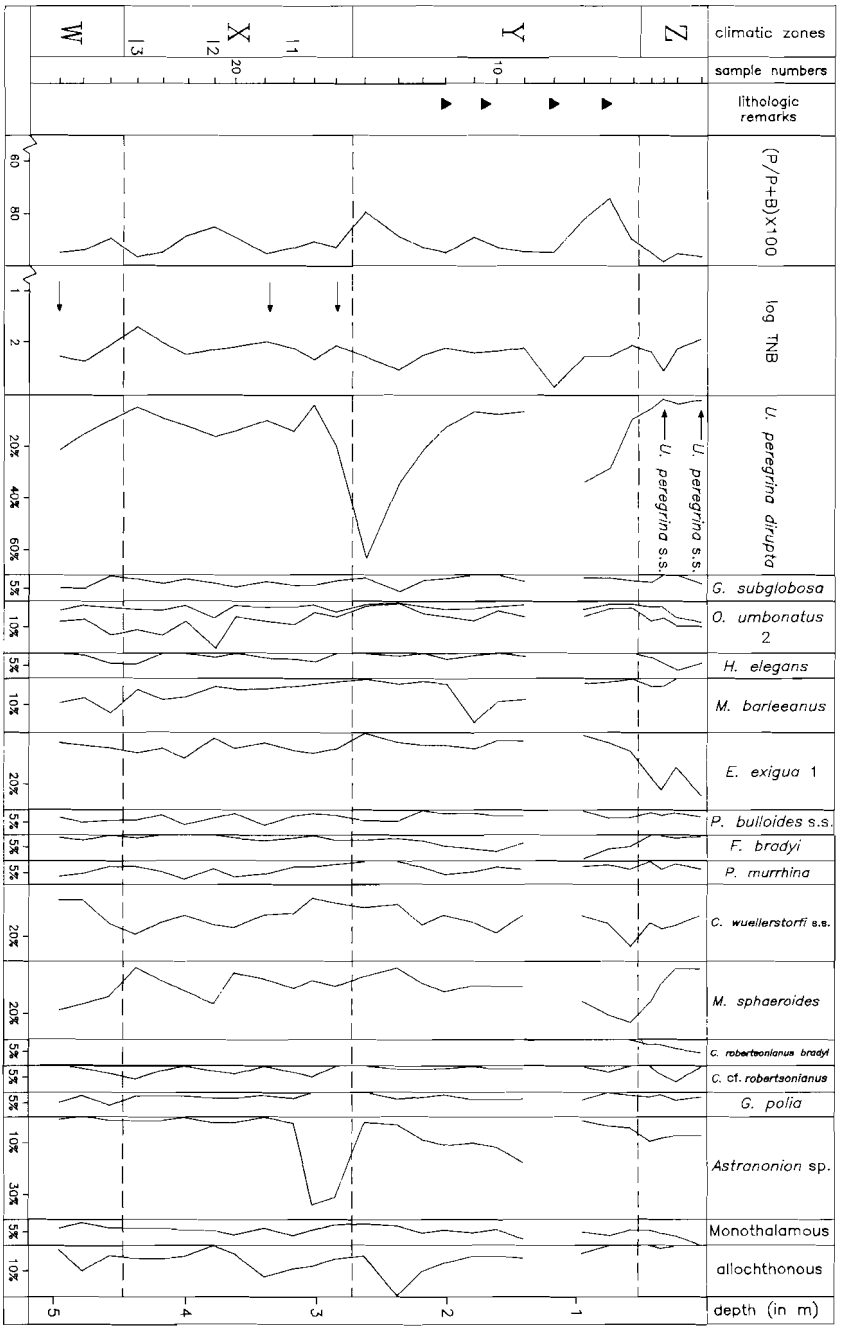

Fig. 80. *VM19-283 (150-595 µm).* Frequency distribution of the quantitatively most important benthic foraminiferal taxa. *Bulimina translucens* and *P. bulloides osloensis* have been included. The second curve under *O. umbonatus* 2 refers to the percentage distribution of type 2C. Faunal curves are interrupted at the level of considerable down-slope contamination. Figure conventions as in fig. 72.

warm climatic intervals, viz. the Z zone and the X1 and X3 intervals. The P/P+B ratios suggest that *U. peregrina dirupta* peaks at levels of strong dissolution, whereas this taxon occurs sparsely in well-preserved samples.

Among the species that showed preference for cold climatic intervals in KW26, *F. bradyi* follows a comparable pattern in this core. The same is suggested for *M. sphaeroides*, which is particularly sparse in the top of the Z zone and in the X3 interval. Although *M. barleeanus* reaches highest abundances in glacial intervals, this species seems to be less consistently connected with cold climatic intervals than in KW26.

C. robertsonianus bradyi, *C.* cf. *robertsonianus*, *E. exigua* 1, *H. elegans*, and *O. umbonatus* 2C reach their maximum frequencies in the Z zone. The latter two taxa are relatively abundant in other warm intervals as well. *E.exigua* 1 does not show a consistent relation with warm climatic intervals, which is remarkable because this taxon closely follows climatic change in the shallower cores.

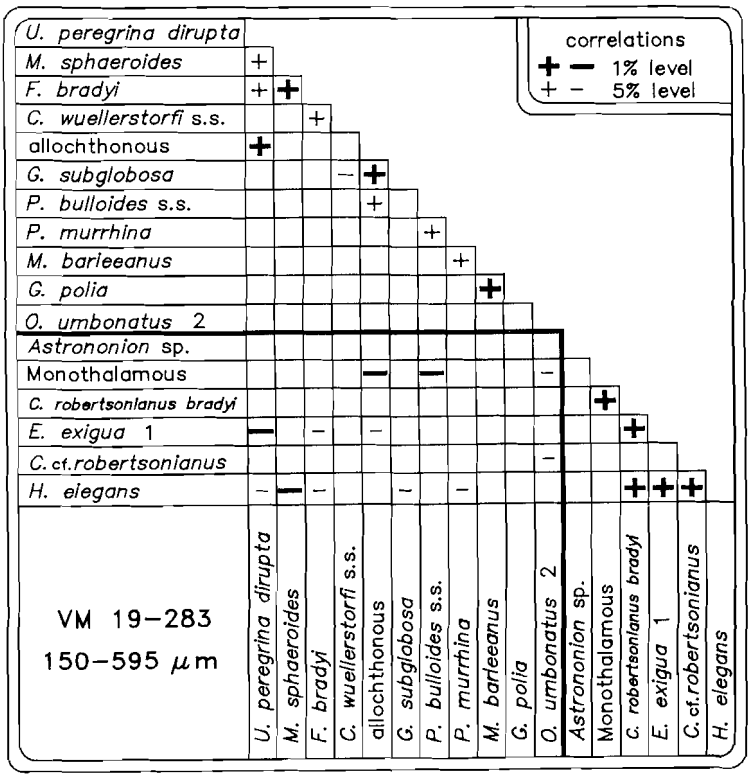

Fig. 81. *VM19-283 (150-595 µm).* BALANC correlation-matrix. The heavy line separates the two groups that show the lowest degree of similarity according to the DENDRO-analysis.

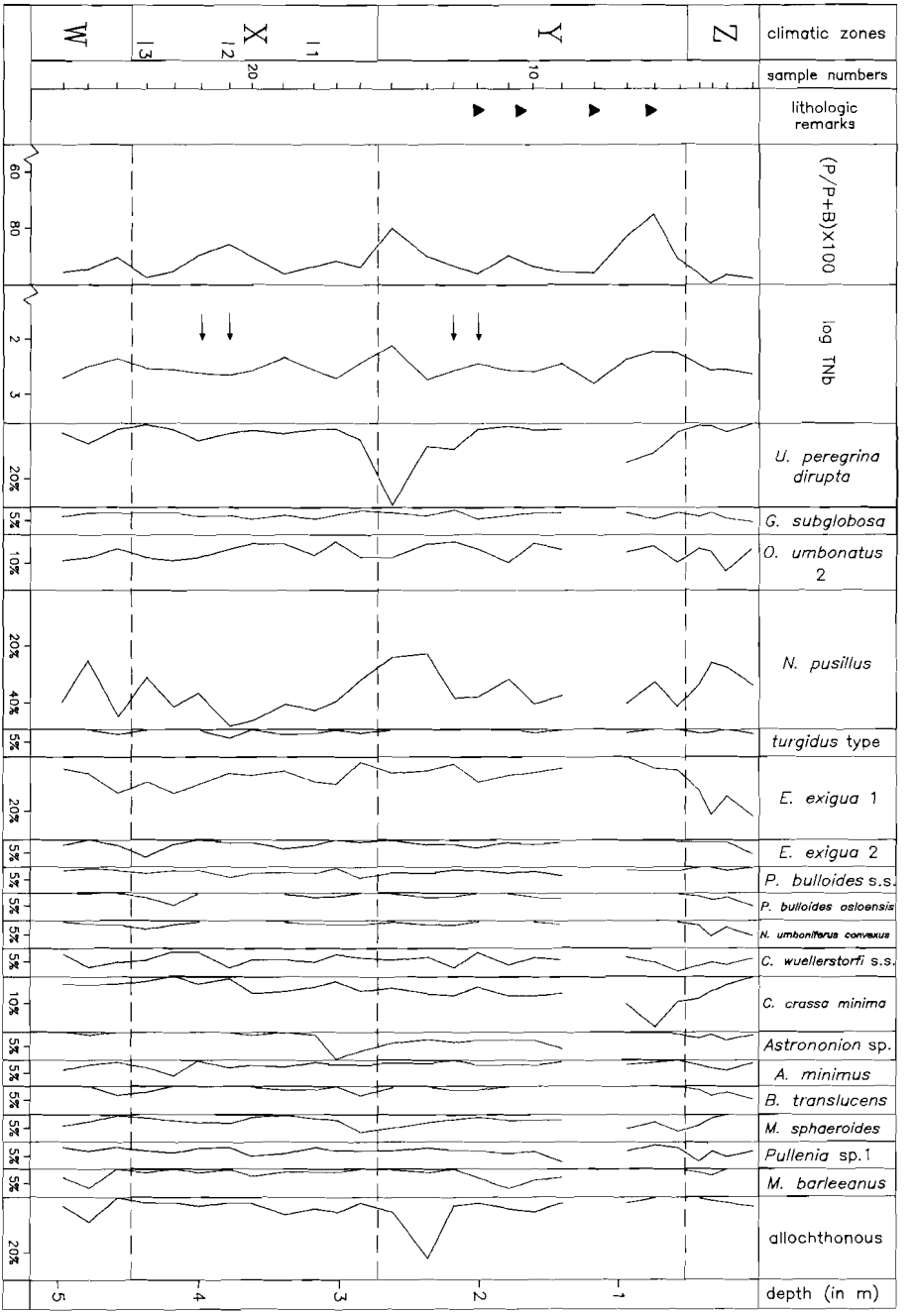

Fig. 82. *VM19-283 (63-595 µm).* Frequency distribution of the quantitatively most important benthic foraminiferal taxa. Faunal curves are interrupted at the level of considerable down-slope contamination. Figure conventions as in fig. 74.

Frequencies of *Astrononion* sp. vary independently of climatic change. This species is only relatively frequent in the upper part of the core, which is similar to what has been observed in VM29-143.

The correlation-matrix of a BALANC analysis is given in fig. 81. The taxa showing a preference for cold climatic intervals, i.e. *F. bradyi, M. sphaeroides,* and *U. peregrina dirupta,* form a small group. This group is negatively correlated with *H. elegans* and some elements display negative correlations with *E. exigua* 1. The species that characterize the Z zone do, however, not form a coherent group. A BALANC analysis of a selection of taxa including the different morphotypes of *O. umbonatus* 2, showed that type C is positively correlated (α = 0.05) with *C.* cf. *robertsonianus* and *H. elegans.*

Total fraction (fig. 82)

The number of displaced specimens is in the same order and follows a similar

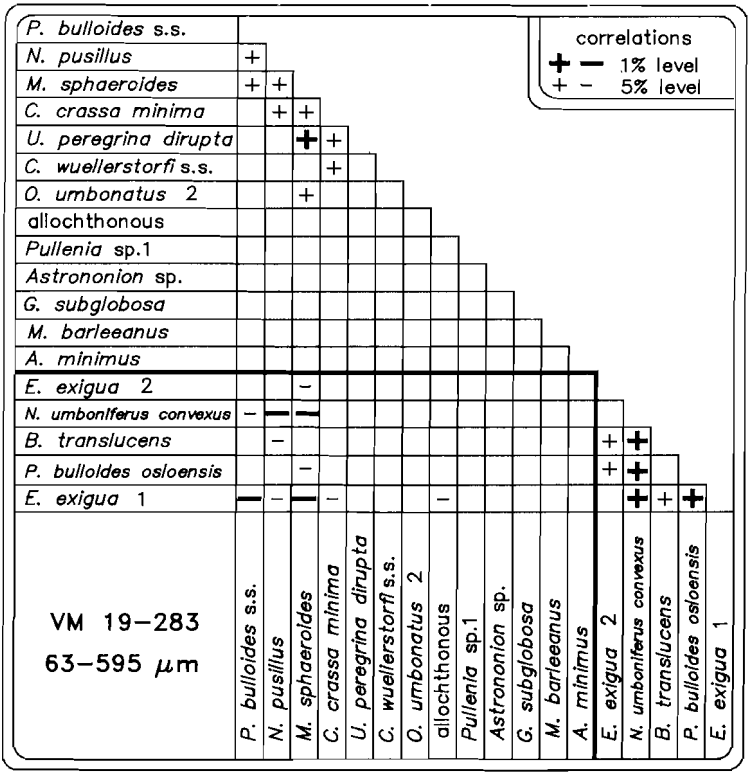

Fig. 83. *VM19-283 (63-595 µm).* BALANC correlation-matrix. The heavy line separates the two groups that show the lowest degree of similarity according to the DENDRO-analysis.

pattern as in the large-size fraction. The associations are invariably dominated by *N. pusillus pusillus.*

The taxa that are most distinctly linked up with warm climatic intervals are *Bulimina translucens, Nuttallides umboniferus convexus,* and *Pullenia bulloides osloensis. E. exigua* 1 reaches highest numbers in the Z zone and is slightly more abundant in the X zone than in the Y2-4 interval. Among the small-sized taxa, only *C. crassa minima* shows a preference for cold climatic intervals. In contrast to what is seen in KW26 and VM29-143, *E. exigua* 2 is most abundant in warm climatic intervals.

The correlation-matrix of the BALANC analysis (fig. 83) shows that the taxa of the warm climatic intervals form a rather coherent group. These taxa have negative correlations with elements of a second group, which essentially consists of *M. sphaeroides, N. pusillus,* and *P. bulloides* s.s. and in which *U. peregrina dirupta* and *C. crassa minima* may be included. The second group can be considered the equivalent of the *F. bradyi* group in the large-size fraction analysis.

KW25 (3994 m)

Large-size fraction (fig. 84)

Three taxa appear to be virtually restricted to parts of the X zone, i.e. *C.* cf. *robertsonianus, Melonis formosus,* and *N. umboniferus* s.s. Both *G. subglobosa* and *P. bulloides osloensis* reach their highest frequency in this zone, but in general frequencies are similar to those in the adjoining glacial intervals. *E. exigua* 1 is not linked up with warm climatic intervals, which contrasts with the distribution of this taxon in the other cores.

Fluctuations in the abundance of *U. peregrina dirupta* are even more salient than in VM19-283, but unlike in that core high abundances are not restricted to glacial intervals. Maximum frequencies are attained just above the X/Y boundary in both cores and the frequency curves resemble each other fairly well higher up in the Y zone as well. Within the X zone, the patterns seem only partially similar. In KW25, frequencies of *U. peregrina dirupta* are low only in the upper and lower parts of the X zone, whereas they are fairly low in the entire X zone of VM19-283.

Other taxa are more consistently connected with the glacial Y and W zones. Particularly *F. bradyi, M. sphaeroides,* and *O. umbonatus* 2 are most frequent in these intervals. Percentages of *Astrononion* sp. vary independently of climatic change and this species is a common faunal constituent from the top of the X zone upward. A similar pattern is present in both VM29-143 and VM19-283.

The correlation matrix of the BALANC analysis (fig. 85) shows that the taxa that correlate with the X zone form a coherent group. The taxa that are typical

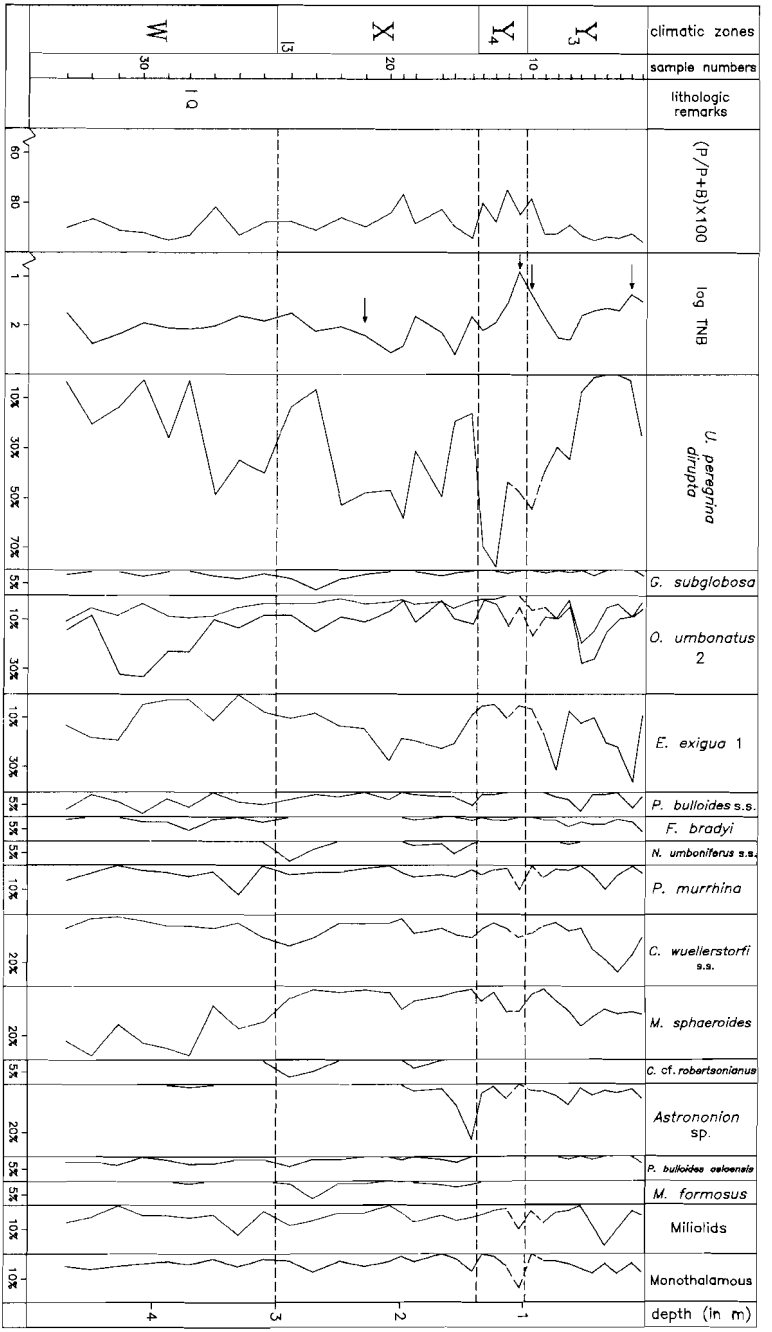

Fig. 84. *KW25 (150-595 μm).* Frequency distribution of the quantitatively most important benthic foraminiferal taxa. *P. bulloides osloensis* has been included and the second curve under *O. umbonatus* 2 refers to the percentage distribution of type 2C. The faunal curves are dashed for counts of less than 75 specimens. Figure conventions as in fig. 72.

of glacial intervals are mutually positively correlated as well and *P. bulloides* s.s. joins with this group. These taxa do, however, not show significant negative correlations with the elements that characterize the X zone.

Total fraction (fig. 86)

The number of displaced specimens is as low as in the large-size fraction.

N. pusillus pusillus is generally the most abundant species and attains highest relative numbers in the W and Y zones. A consistent relation with climatic variation is, however, not perceptible.

Among the small-sized species, *E. tumidulus* tends to be more frequent in the W and Y zones than in the X zone. *E. exigua* 2 and *Pullenia* sp.1 do not display a glacial/interglacial pattern and the same holds for *E. exigua* 1. *C. crassa minima* is a subordinate element of the faunas and occurs only in the upper part of the core. This contrasts with the fairly high percentages of this taxon in the

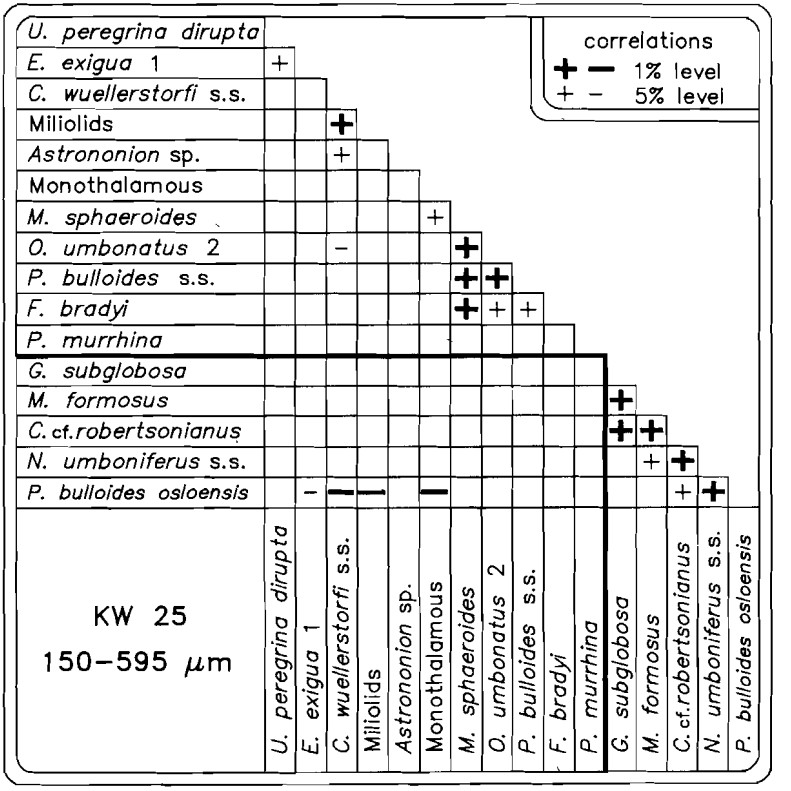

Fig. 85. *KW25 (150-595 µm).* BALANC correlation-matrix. The heavy line separates the two groups that show the lowest degree of similarity according to the DENDRO-analysis.

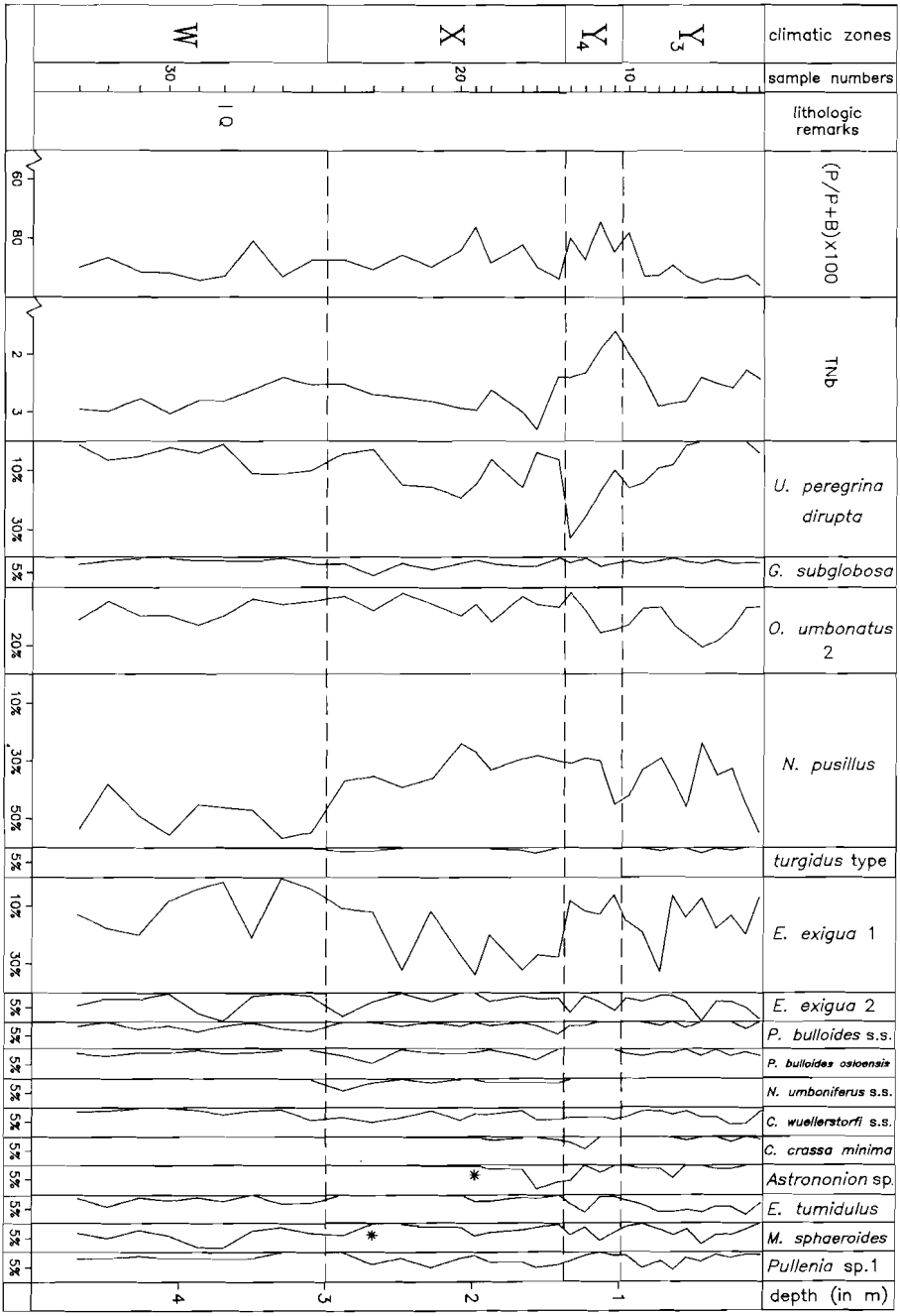

Fig. 86. *KW25 (63-595 μm).* Frequency distribution of the quantitatively most important benthic foraminiferal taxa. *N. umboniferus* s.s., *P. bulloides* s.s., and *P. bulloides osloensis* have been included. and the miliolids excluded. Figure conventions as in fig. 74.

other northern cores. *P. bulloides osloensis* is absent in the Y4 interval and relatively frequent in the X zone.

BALANC analysis indicates that distinct groups are absent (fig. 87). *P. bulloides osloensis* is positively correlated with and *G. subglobosa* and *N. umboniferus* s.s., two taxa which also reach their maximum numbers in the X zone. As in the total fraction of VM19-283 (see fig. 63), *P. bulloides* s.s. is negatively correlated with *P. bulloides osloensis.*

VII.4. CLIMATE RELATED FAUNAL DIFFERENCES

VII.4.1. Principal Component Analysis

Results of principal component analyses are briefly discussed because they illustrate to which extent faunal change follows variations in Late Quaternary

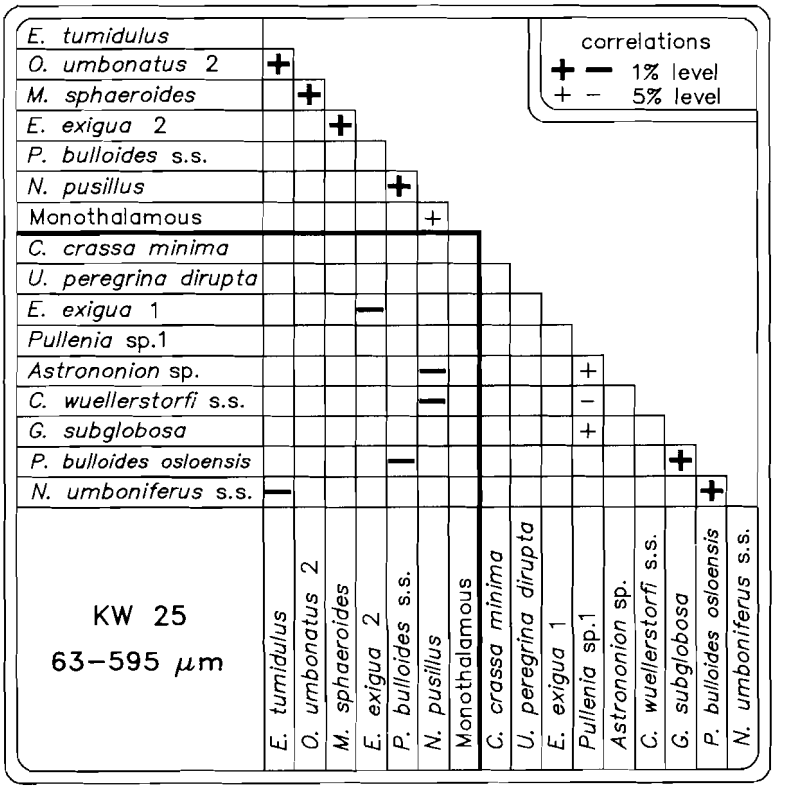

Fig. 87. *KW25 (63-595 µm).* BALANC correlation-matrix. The heavy line separates the two groups that show the lowest degree of similarity according to the DENDRO-analysis.

climate. Analyses were performed on the different size fractions of individual cores and the same data-matrices were used as for the BALANC analyses. Generally, the results of the total fraction analyses proved to be slightly better interpretable than those of the large-size fraction, but the reverse holds for KW25. The analyses generally produced one significant axis, which essentially reflects the polarity between the species that are most frequent in warm climatic intervals and those that abound in cold climatic intervals. The first axis of the analysis on the data from KW25 is, however, not significant.

Plots of sample-scores on the first components (fig. 88) show that there is a to some extent consistent relation between climatic change and overall benthic faunal composition. In all relevant cores, glacial intervals, i.e. the Y2-4 interval and the W zone, are faunistically very different from the Z zone, whereas the Y1 zone clearly displays a transitional aspect.

Within the X zone, the benthic faunal pattern may differ from one core to another, but the curves of VM19-283 and KW25 closely correspond.

In both VM19-283 and KW25, faunas in the lower part of the X zone are very dissimilar from those in the glacial intervals, which indicates that the faunas in this interval strongly resemble those in the Z zone. The middle part of the X zone including the X2 level shows definitely a glacial aspect. Sample scores in the upper part of the X zone, which includes the X1 level, have intermediate values. The overall pattern in these cores is very similar to that of T78-45 (Zachariasse et al., 1984).

In VM29-143, the entire X zone resembles the Z zone. The composition of the planktonic faunas remains also markedly constant within the X zone (see fig. 57) and we, therefore, surmise that the original signal has been blurred in the X zone of VM29-143.

In T80-10, the X1 level shows the strongest similarity to the Z zone. The X2 and X3 levels are less similar to the Z zone, but they are still clearly different from the glacial intervals. A glacial aspect is suggested for the intervals adjoining the X1 level. The relation between fauna and climatic change in stage X is, therefore, clearly different from that in VM19-283 and KW25 and this discrepancy can not be attributed to distortion of an original signal. The frequency diagram of this core (fig. 70) shows that *N. umboniferus decoratus* occurs only at the X3 level. The distibution of the deep-water equivalents, i.e. *N. umboniferus convexus* and *N. umboniferus* s.s., in the X zone of the two other cores is to some extent similar. These morphotypes are found only in the upper and lower part of the zone with maximum frequencies at the X3 level. We attach great significance to the fact that *N. umboniferus* is frequent at the X3 level of all three cores and surmise that the deviating faunal pattern within the X zone of T80-10 is the resultant of local and regional changes in the environment.

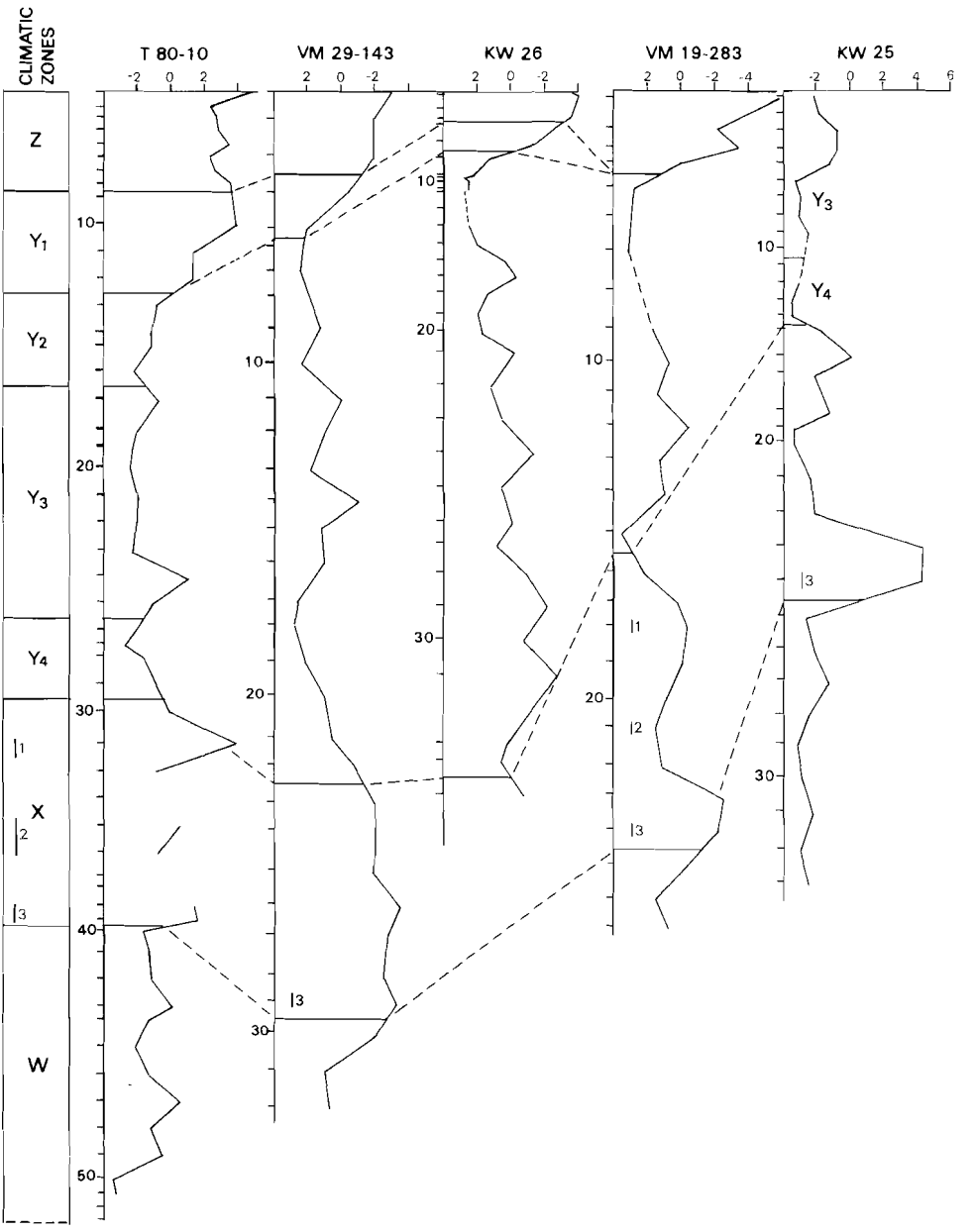

Fig. 88. Plots of the sample scores on the first principal component of PC analyses on the individual cores. Analyses were performed on total fraction data, except for KW25 for which we used large-size fraction data. Open sections represent intervals without foraminifers and the dashed intervals cover samples that were excluded from the analyses.

Combining the information on the distribution of individual species and the results of principal component analysis, we conclude that faunas similar to those in the Z zone are found in the upper part of the Y1 zone and in both the X1 and X3 levels. These intervals will be termed warm climatic intervals for convenient reference. The X2 interval can only be considered a warm interval in T80-10.

VII.4.2. Selected taxa and climate

The results of the countings show faunal differences between warm and cold climatic intervals in all cores, but the species involved are to a varying extent different from core to core. We grouped species characteristic of warm and cold climatic intervals in tables 12 and 14 to obtain an overview of the faunal differences.

In view of the importance of depth or depth-dependent parameters for the distribution of species, attempt will be made to reconstruct changes in the relative frequency of individual taxa over the entire depth-interval. Because the stratigraphic resolution is poor, such reconstructions are necessarily a severe simplification. We shall confine ourselves to the species that show a systematic relation with climate in at least one of the cores. But even then, we can only make an educated guess of the species frequencies in cold and warm climatic intervals.

T80-10 (1988 m)	VM29-143 (2756 m)	KW26 (3038 m)	VM19-283 (3442 m)	KW25 (3994 m)
G. translucens	-	-	-	-
O. culter	-	-	-	-
C. wuellerstorfi s.s.				
E. exigua 1	*E. exigua* 1	*E. exigua* 1		
H. elegans	*H. elegans*	*H. elegans*	*H. elegans*	*H. elegans*
N. umboniferus decoratus	*N. umboniferus convexus*	*N. umboniferus convexus*	*N. umboniferus convexus*	*N. umboniferus* s.s.
-	*O. umbonatus* 2C	*O. umbonatus* 2C		
-	*P. bulloides osloensis*	*P. bulloides osloensis*	*P. bulloides osloensis*	
-		*C. kullenbergi*	*C. kullenbergi*	-
-			*C.* cf. *robertsonianus*	*C.* cf. *robertsonianus*
			B. translucens	
			E. exigua 2	
-	-	-	-	*M. formosus*

Table. 12. Survey of the taxa that show a regular relation with the warm climatic intervals. The absence of a taxon is indicated by a dash.

Most of the climate-related species occur in low numbers only, and the change in frequency is often a change from absence to presence. Whenever possible, the distribution of a species in T78-45 (4070 m) will be included. This core was examined by Zachariasse et al. (1984) but their data have not all been published.

Taxa characteristic of warm climatic intervals (table 12)

N. umboniferus is relatively frequent in warm climatic intervals in all cores, T78-45 included. In VM29-143, KW26, VM19-263 and KW25, this species is occasionally present in cold intervals. When present, the morphotypes display the same distribution versus depth as at present.

H. elegans is a rather common species in the warm intervals between 2756 and 3442 metres depth. Highest abundances are observed in VM29-143 and KW26. Although its frequency does not exceed two per cent in KW25, a preference for warm climatic intervals is suggested here as well, because *H. elegans* occurs only in the X zone. *H. elegans* is virtually absent in T78-45.

C. kullenbergi reaches the five per cent level only in KW26. It has not been found in T80-10, nor in KW25 and is a minor faunal element in both VM29-143 and VM19-283. In VM29-143 it is occasionally found in the Z/Y1 interval. In VM19-283, *C. kullenbergi* is limited to the Z zone and the X3 level. This species does not occur in T78-45.

E. exigua 1 is relatively abundant in warm climatic intervals at depths between 1988 and 3038 metres. In deeper water the distribution is more erratic, although it abounds in the Z zone of VM19-283. *E. exigua* 1 is clearly related to warm intervals in T78-45.

C. cf. *robertsonianus* reaches the five per cent level only in the warm climatic intervals of VM19-283 and KW 25. In the cold intervals, it is absent in KW25 and rare in VM19-283. This species becomes increasingly less frequent toward shallower water. Single specimens occur in VM29-143 and this species is absent in T80-10 and T78-45.

O. umbonatus 2C is low-frequent and virtually restricted to the warm climatic intervals in both VM29-143 and KW26. This type is almost continuously present in VM19-283 but reaches the five per cent level only in the Z zone and the X2 interval. Maximum frequencies are found in KW25, but here it is only common in the glacial zones.

Pullenia bulloides osloensis is absent in T80-10 and sparse in the deeper cores. As discrimination between *P. bulloides* s.s. and *P. bulloides osloensis* is easier in the large-size fraction, we shall only discuss the distribution of the large-sized specimens. In VM19-283, this taxon is almost limited to warm intervals. Large-sized specimens are relatively frequent in the Z/Y1 interval of both VM29-143

and KW26. Although *P. bulloides osloensis* reaches its maximum frequency in the basal part of the X zone in KW25, it does not show a clear preference for warm climatic intervals in this core. In sum, we suggest that *P. bulloides osloensis* displays a slight preference for warm intervals at depths between 2776 and 3994 metres. In glacial intervals, large-sized specimens are virtually absent in the upper part of this depth-interval, but they are still found in the deep-water environment of KW25.

The frequency distribution of the taxa that are characteristic of warm climatic intervals in more than one core is plotted versus depth in fig. 89. *E.exigua* 1, *O.umbonatus* 2C, and *P. bulloides osloensis* clearly show a shallower UDL in warm than in cold climatic intervals, whereas their frequencies change only slightly at great depth. The other species essentially show a change from absence in cold to presence in warm intervals.

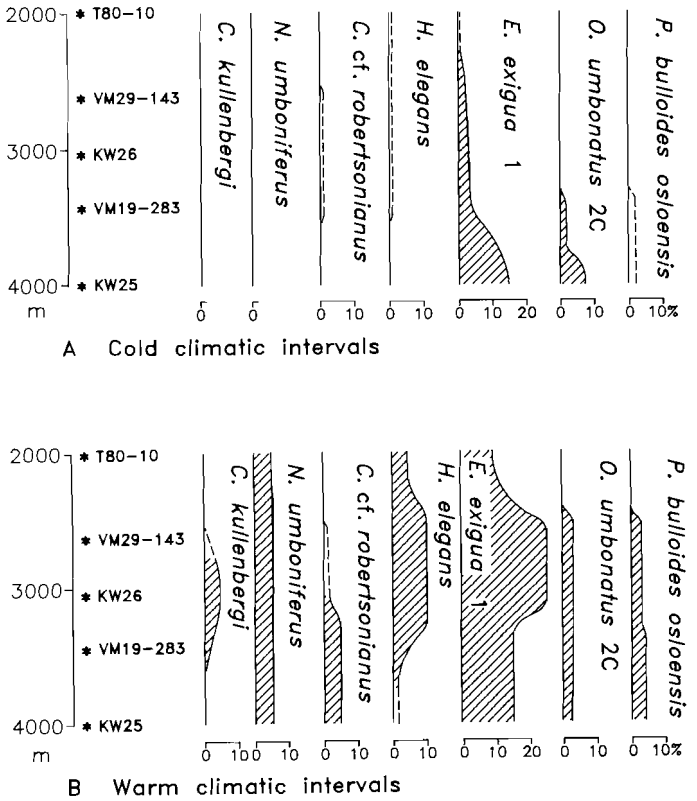

Fig. 89. Idealized depth/distribution diagram for a selection of species displaying a distinct preference for warm climatic intervals. The percentage distribution in (A) cold intervals, and (B) warm intervals. Dashed curves indicate that the species is only intermittently present. Asterisks mark the position of the cores.

Most of the other taxa listed in table 12 are virtually restricted in their occurrence to one core and will be excluded from further discussion. *C. wuellerstorfi* s.s. and *E. exigua* 2 show, however, a wider distribution. The latter taxon will be discussed in the following section. *C. wuellerstorfi* s.s. shows a slight preference for warm climatic intervals in T80-10, but follows a non-descript pattern in the other cores. BALANC analysis even suggests that *C. wuellerstorfi* s.s. is related to cold climatic intervals is KW26.

Taxa characteristic of cold climatic intervals (table 14)

Allochthonous taxa

The first category to be discussed is that of the allochthonous elements. Down-slope contamination seems negligible in KW25 but transported elements are almost continuously present in the other cores. Although this suggests that down-slope processes operate quasi permanently above 3500 metres, a (periodic) intensification during glacial periods is evident in VM29-143, KW26 and VM19-283. Increased down-slope transport during glacial periods agrees with the previously described model of Damuth (1975). Contamination is also significant in the (lower part of the) Y1 zone in both VM29-143 and KW26. This indicates that sea-level was still relatively low during the early phase of deglaciation.

In T80-10, transported elements are relatively abundant in both warm and cold intervals, which is probably due to its position near the submarine canyon.

VM19-283 is the only core in which down-slope contamination seems to be more prominent in the large-size than in the total fraction, which suggests a rather near-by source area. The nature of the transported elements (e.g. corals, *Amphistegina*) points to an origin from a shallow carbonate environment. Such an environment is likely to be found around the island of Annabon, which is in the vicinity of the site.

Considering the local importance of down-slope contamination, one may wonder if there are displaced elements among the taxa hitherto considered autochthonous. The taxa that are positively correlated with the allochthonous category are listed in table 13.

Although positively correlated with the allochthonous category, it seems highly unlikely that notorious deep-water taxa, such as *G. subglobosa, M. sphaeroides, P. bulloides* s.s., *P. murrhina,* and *U. peregrina dirupta,* are displaced. *B. aculeata, Globobulimina* spp., and *M. barleeanus* can not be considered typical deep-water taxa. However, their positive correlation with the allochthonous group seems to be incidental, because they are also present in deeper cores for which such a relation is not found.

T80-10	VM29-143	KW26	VM19-283
B. aculeata	*C. crassa minima*	*C. crassa minima*	*G. subglobosa*
M. barleeanus	*E. exigua 2*	*E. exigua 2*	*P. bulloides* s.s.
N. pusillus	*Globobulimina* spp.	*C. carinata*	*U. peregrina dirupta*
	P. bulloides s.s.	*M. sphaeroides*	
	P. murrhina		

Table 13. The taxa that are positively correlated (α = 0.05) with the allochthonous category. A significant contribution of displaced specimens was not recognized in KW25.

C. carinata is assumed to be autochthonous in KW26, although an allochthonous origin can be advocated since this species has its deepest occurrence at this site.

There is no need to consider *N. pusillus* a transported element in T80-10. Assemblages of *N. pusillus* are, indeed, frequently dominated by the shallow-water *turgidus* type (see fig. 70), but this does not conflict with the present-day distribution. Moreover, an allochthonous origin would not explain the perfect correlation in this core between the distribution of the *turgidus* type and *N. pusillus* as a whole (see fig. 70).

C. crassa minima and *E. exigua* 2 are more consistently correlated with downslope contamination. Both species are very small and therefore easily transported. *C. crassa minima* is extremely sparse in the present-day region, but rather frequent in two tops of cores from the MAR. These two samples (VM22-174, VM22-177) were excluded from faunal analysis because considerable contamination was evident. This observation strongly supports a shallow-water origin. The fact that *C. crassa minima* has not been found in T80-10, indicates to our opinion that this species avoids a shallow-water environment dominated by terrigenous sedimentation.

Data are less conclusive with regard to *E. exigua* 2. On the ocean floor, this morphotype occurs at random between 1017 and 5205 metres. High abundances are locally reached at the continental margin at rather variable depths. It is also markedly frequent in sample VM22-177 from the MAR, which suggests displacement.

A displaced origin could, however, not explain the relatively high frequencies of *E. exigua* 2 at the X3 level in KW25 and VM19-283. The BALANC correlation matrices show that *E. exigua* 2 is negatively correlated with *E. exigua* 1 in three cores, viz. VM29-143, KW26 and KW25. Unlike *E. exigua* 1, *E. exigua* 2 is always low frequent downcore and we may, therefore, assume that type 2 replaces type 1 when environmental condition become unfavourable for the species as a whole.

T80-10 (1988 m)	VM29-143 (2756 m)	KW26 (3038 m)	VM19-283 (3442 m)	KW25 (3994 m)
N. pusillus				
O. umbonatus 1	-	-	-	-
U. auberiana	-	-	-	-
M. barleeanus	*M. barleeanus*	*M. barleeanus*		
	C. carinata	*C. carinata*		-
-	*C. crassa minima*	*C. crassa minima*	*C. crassa minima*	
	E. exigua 2	*E. exigua* 2		
	allochthonous	allochthonous	allochthonous	
-	*M. sphaeroides*	*M. sphaeroides*	*M. sphaeroides*	*M. sphaeroides*
	F. bradyi	*F. bradyi*	*F. bradyi*	*F. bradyi*
-	-		*U. peregrina dirupta*	*U. peregrina dirupta*
-				*E. tumidulus*

Table 14. Survey of the taxa that show a regular relation with cold climatic intervals. The absence of a taxon is indicated by a dash.

Autochthonous taxa

Melonis barleeanus proliferates in cold intervals between 1988 and 3038 metres depth. In the deeper cores VM19-283 and KW25, *M. barleeanus* is discontinuously present in both cold and warm climatic intervals, but in VM19-283 maximum frequencies are found in cold periods. The five per cent level is not attained in KW25 and *M. barleeanus* is even scarcer in T78-45, in which it is more consistently found in warm than in cold intervals.

Melonis sphaeroides is absent in T80-10 but common in the deeper cores. Frequencies vary around five per cent in warm climatic intervals and are higher in glacial intervals. This species follows a non-descript pattern in T78-45.

Fursenkoina bradyi is a rare species especially at shallow depth. It has not been found in the large-size fraction of T80-10, but small specimens occur in glacial intervals. In VM29-143, *F. bradyi* is generally absent in the warm climatic intervals and frequencies do not exceed two and a half per cent in cold intervals. This species is most frequent in the cold climatic intervals of the deeper cores, occcasionally, reaching the five per cent level. In warm periods, *F. bradyi* is rare also at great depth. This species is a subordinate faunal element in T78-45 and restricted to cold intervals.

Cassidulina carinata is, in general, a common faunal constituent in the cold climatic intervals of T80-10, but frequencies vary considerably in the different warm climatic intervals of this core. A clear correlation with cold climatic intervals is shown in both VM29-143 and KW26. This species is very rare in VM19-283 and a relation to climate is not recorded here. It has neither been found in KW25, nor in T78-45.

The distribution of *Uvigerina peregrina dirupta* was discussed by Van

Leeuwen (1986). This type is virtually absent in T80-10 and VM29-143 and generally a rare element within the assemblages of *U. peregrina* in KW26. Except in the upper part of the Z zone in VM19-283, *Uvigerina peregrina dirupta* predominates in the deeper cores and in T78-45 as well. In these cores this type is clearly connected with cold climatic intervals, included the middle part of the X zone in both KW25 and T78-45. Frequencies, however, are low in the middle of the Y zone. A correlation between frequency and dissolution is suggested in VM19-283, but not in the other cores.

Eponides tumidulus is generally rare showing maximum frequencies in KW25. In that core *E. tumidulus* is correlated with cold climatic intervals, but a relation with warm intervals is suggested in VM29-143 and KW26. This species occurs intermittently in VM19-283, attaining a maximum abundance at the X3 level, but a consistent relation to warm climatic intervals is not apparent here. *E. tumidulus* was not found in T78-45.

Nuttallides pusillus is intermittently present in the warm intervals and common in the cold climatic intervals of T80-10. Relative frequencies increase toward greater depth in both warm and cold intervals. BALANC analysis suggests that it is linked up with cold climatic intervals in VM19-283 (see fig. 83). Frequencies are relatively low in the Z-Y1 interval of both VM29-143 and KW26, but a consistent relation with climatic variation can not be concluded for the other cores.

Morphologic changes in *N. pusillus* were obvious in all cores, but a clear relation to climatic variation seems absent. The only possible exception is that the *turgidus* type shows a slight preference for warm climatic intervals in VM29-143.

The modern distribution of the various morphotypes is related to depth in the region. Averaging the abundances of the various types in the assemblages per core strongly suggests that the succession of morphotypes with depth has remained the same over the past 150,000 yr. (fig. 90).

N. pusillus is in general the most frequent species in the total fraction of T78-45.

The frequency distribution of the species characteristic of cold climatic intervals is plotted versus depth in fig. 91. Abundances of *F. bradyi, M. sphaeroides,* and *U. peregrina dirupta* increased during glacial periods but the depth-ranges of these taxa remained unchanged.

U. auberiana and *O. umbonatus* 1, which are also listed in table 14, are clearly related to cold climatic intervals in T80-10, but they are absent in the deeper cores. Not included in table 13 are the taxa that are linked up with cold climatic intervals only in KW26, i.e. *C. wuellerstorfi* s.s., *Globobulimina* spp., and *U. peregrina.* The assemblages of *U. peregrina* are not uniform in this core. *U.*

peregrina s.s. usually dominates in this core, but *U. peregrina dirupta* is the dominant type in the four lowermost samples. *Globobulimina* spp. is not discussed, because the distribution in VM29-143 suggests that this category is not only relatively frequent in the Y but also in the X zone.

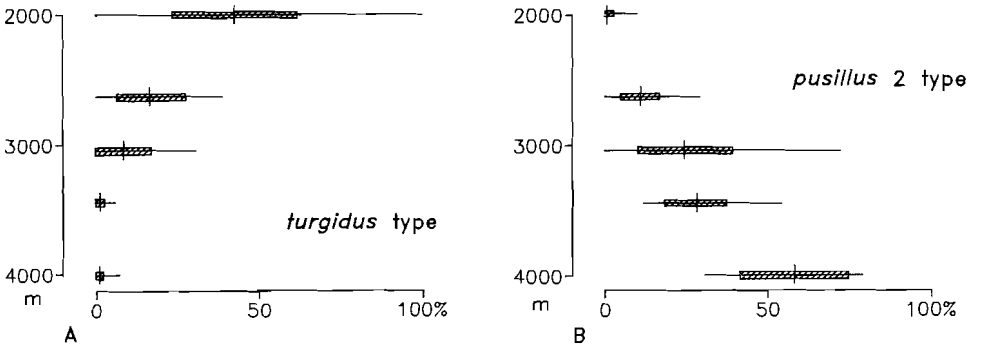

Fig. 90. *Nuttallides pusillus.* Diagram illustrating the relation between the depth and the distribution of the individual morphotypes. Average proportions of morphotypes per core. Mean, standard deviation, and range of the proportions of two morphotypes are shown: (A) *turgidus* type, and (B) *pusillus* 2 type.

VII.5. CLIMATE RELATED CHANGES IN THE DEEP-WATER ENVIRONMENT

Among the taxa characteristic of warm climatic intervals, *E. exigua* 1, *P. bulloides osloensis* and *O. umbonatus* 2C were shown to occupy a habitat that was deeper in cold than in warm intervals. According to the simplified scenario outlined in chapter four, a shift toward deeper water can be explained by an increase in either temperature or food supply or both.

The present-day distribution of *E. exigua* 1 and *P. bulloides osloensis* suggests that these taxa are very sensitive to differences in the organic carbon content of the sediment, because their UDL is depressed in the area of the Zaire deep-sea fan. There is no evidence that the UDL of *O. umbonatus* 2C is also lower in the fan area than elsewhere, but this taxon attains maximum frequencies to the north of the fan area and seems to be replaced by type B at the fan itself. Because these taxa clearly respond to variation in the food-supply at present, we hypothesize that the organic carbon content of the sediment was higher in cold than in warm climatic intervals.

Fig. 89 shows that the other taxa that are connected with warm climatic intervals did not simply change their depth habitat during cold climatic periods. *C.* cf. *robertsonianus* and *H. elegans* are extremely rare in cold intervals and become

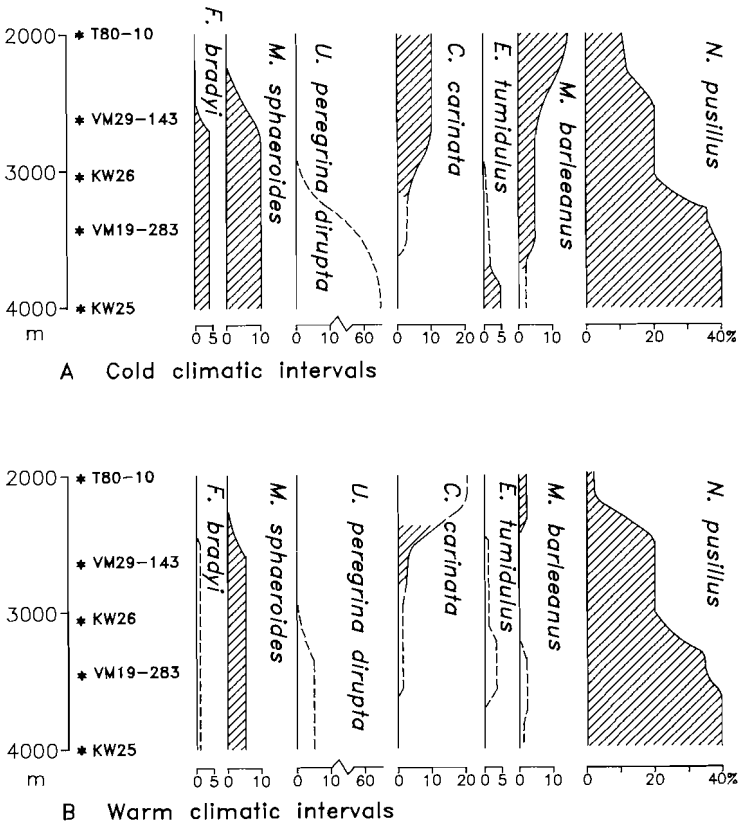

Fig. 91. Idealized depth/distribution diagram for a selection of species displaying a distinct preference for cold climatic intervals. The percentage distribution in (A) cold climatic intervals, and (B) warm climatic intervals. Dashed curves indicate that the species is only intermittently present. Asterisks mark the position of the cores.

relatively frequent over the greater part of their depth range in warm intervals, during which they also invade the deep-water environment of KW25. *C. kullenbergi* is even absent in cold climatic intervals at all depths.

Sea-floor data show that the distribution of *C. kullenbergi, C.* cf. *robertsonianus* and *H. elegans* is also to a large extent controlled by variation in food supply. All three species are absent in the area of the deep-sea fan and in the marginal region adjacent to the Benguela Current upwelling area. The (near) absence of these species at intermediate depth during cold climatic periods can, therefore, be attributed to increased organic carbon levels in the sediment. The fact that these species did not descend towards to the deep-water environment of KW25 is less anomalous than it seems, because in contrast to *E. exigua* 1 and

P. bulloides osloensis, these three species are not found at great depth in the present-day area of the Zaire deep-sea fan. This indicates that the glacial environment at site KW25 was in some respects similar to the present-day environment of the Zaire deep-sea fan area.

One might suggest that the organic carbon levels were still too high for these taxa at depths around 4000 metres during cold climatic periods. However, it is well conceivable, that other factors are involved as well, because species can only adjust their depth habitat in response to raised food-levels if other environmental parameters remain within certain limits. These parameters may include sediment-related factors other than the organic carbon content (e.g. carbonate supply), but the absence of *H. elegans* could be influenced by temperature as well. This species is at present only frequent between 2000 and 4000 metres with maximum abundance between 2500 and 3000 metres. The depth distribution indicates that *H. elegans* does not occur at temperatures below 2.5°C. It may, therefore, be suggested that temperatures were too low for this species to survive during cold climatic periods at great depth.

N. umboniferus includes three morphotypes, which all flourish in warm climatic intervals. The shallowest type, viz. *N. umboniferus decoratus* seems absent in cold climatic intervals, whereas the other two are nearly absent. It is remarkable that the individual types do not descend toward deeper water during cold climatic periods and the question arises whether the individual morphotypes are to be considered as genetic entities or as part of a coherent genepool.

Firstly, let us consider the morphotypes as separate units. Unfortunately, the depth ranges of *N. umboniferus decoratus* and *N. umboniferus convexus* are poorly covered by the sea-floor data, which hampers evaluation of the parameters controlling their distribution. Yet, we may conclude that *N. umboniferus decoratus* avoids very high organic carbon levels, because of its absence in the marginal region near the BC upwelling area (see fig. 36a). There is no evidence that *N. umboniferus convexus* shows a similar response to high food levels. The depth at which *N. umboniferus convexus* replaces *N. umboniferus decoratus* is the same in the entire area (see fig. 36a), which suggests that this level is primarily temperature controlled.

As a consequence it seems likely that the (near) absence of the deeper living *N. umboniferus convexus* in cold climatic periods results from a temperature change in the deep-water. Higher temperatures during cold climatic periods could account for the absence of *N. umboniferus convexus,* but as to be discussed further in this chapter, it is more likely that temperatures were lower during cold climatic periods. It is difficult to see how the (near) absence of *N. um-*

boniferus convexus at all depths is to be attributed to a drop in deep-water temperature.

In our opinion, the changes in the distribution of *N. umboniferus* are more easily understood if the *decoratus* and *convexus* types represent marginal populations of *N. umboniferus* s.s. It is intuitively felt, that when optimum conditions are realized for a species at a certain depth, it will tend to occupy a larger depth-range than under less favourable conditions. If the size of the central population is severely reduced, chances increase that the peripheral populations become isolated, which may lead to local extinction. Following this line of reasoning, the presence/absence of the *decoratus* and *convexus* types may be primarily controlled by environmental changes which affect the main population, i.e. *N. umboniferus* s.s. Because *N. umboniferus* s.s. abounds in the region of the lowest organic carbon fluxes, we may attribute the (near) absence of all *N. umboniferus* types in cold climatic intervals to an increase in the carbon content of the sediments.

Among the species that characterize cold climatic intervals, *C. carinata* and *M. barleeanus* are at present restricted to relatively shallow water. *M. barleeanus* (see fig. 25b) is rare below 2500 metres, except in the marginal region influenced by the high production of the Benguela Current, where it flourishes down to 3600 metres. *C. carinata* (fig. 23a) does not occur below 2400 metres, again with the exception of the BC region where it extends down to 2675 metres. The distribution of both species indicates that they abound where carbon fluxes are high. In cold intervals they occur at greater depth than in warm intervals, which clearly suggests that the carbon content of the sediments increased from warm to cold climatic intervals.

U. peregrina dirupta is intermittently very abundant in the cold intervals of the deepest cores and almost absent in the warm climatic intervals at all depths. In the present-day region *U. peregrina dirupta* is only relatively frequent in the areas of inflowing AABW, indicating that this taxon proliferates at low temperatures (Van Leeuwen, 1986). This strongly suggests that bottom-water temperatures at great depth were periodically significantly lower in cold than in warm climatic intervals.

However, *U. peregrina dirupta* reaches much higher percentages in the cold climatic intervals of the deepest cores than at present in the areas of inflowing AABW. In our opinion, the anomalously high frequencies in the cold intervals are to be attributed to a combination of low bottom-water temperatures and high food levels in the sediment. Admittedly, this specific combination can not explain why at present *U. peregrina dirupta* is more abundant near the Walvis Passage than near the Romanche Fracture Zone. Yet, a combination of low bottom-water temperature and high food levels may offer an explanation for

the distribution of *U. peregrina* at abyssal depth in the Atlantic Ocean. At present, *U. peregrina* is a rare species below 4000 metres in the Atlantic (e.g. Streeter, 1973; Schnitker, 1984; Lohmann, 1978), except in the marginal area of the Cape Basin, directly south of the Walvis Ridge (Gofas, 1978). That area adjoins the region, in which coastal upwelling associated with the Benguela Current is most intense. This strongly suggests that *U. peregrina* is only frequent at low bottom-water temperatures if the flux of organic carbon is high.

Fursenkoina bradyi and *Melonis sphaeroides* are relatively frequent in cold intervals below 2500 metres. *F. bradyi* is a very rare species in the modern area and downcore changes in frequency can not be explained readily from its present-day distribution. *M. sphaeroides* is, on the other hand, common in the present-day area and reaches maximum abundances in the area of the Zaire deep-sea fan (3486 m). This strongly suggests that *M. sphaeroides* flourishes at high carbon levels, but we should point out that this species is relatively rare at comparable depths in the marginal region influenced by the high production of the BC (see fig. 28d). Since deep-water conditions are similar, sediment-related parameters other than the organic carbon content may be of influence as well.

Eponides tumidulus is characteristic of cold climatic intervals only in KW25. The distribution in the shallower cores, on the other hand, indicates that *E. tumidulus* has a shallower UDL in warm than in cold climatic intervals. At present, *E. tumidulus* is low-frequent at abyssal depth and avoids the deep-sea fan area. Its descent toward deeper water in cold intervals can therefore be attributed to an increase in organic carbon content of the sediment. This explanation is in line with the continuous absence of *E. tumidulus* in T78-45 but does not satisfy for the relatively high frequencies in the cold intervals of KW25.

Nuttallides pusillus is indicative of cold climatic intervals in T80-10 and possibly in VM19-283, but not in the other cores. The assemblages in T80-10 are frequently dominated by the *turgidus* type. This type is of minor significance in the deeper cores, but seems more frequent in warm than in cold climatic intervals in VM29-143. *N. pusillus turgidus* is the shallowest morphotype of *N. pusillus.* Shallow depths, however, are poorly covered and the present-day distribution of this type is poorly known. We can, therefore, not give a sound interpretation of the down-core frequency changes of this species.

Summarizing, we conclude that the faunal differences between cold and warm climatic intervals primarily reflect variation in the organic carbon content of the sediments with higher values in cold than in warm intervals at all depths. Because some species of the cold intervals are at present specifically connected with the Zaire deep-sea fan area (e.g. *M. sphaeroides*), whereas some of the species of the warm intervals are at present absent in that area (e.g. *C.*

kullenbergi, *C.* cf. *robertsonianus*) sediment-related parameters other than the organic carbon content may have changed as well.

The distribution of *U. peregrina dirupta* suggests that bottom-waters were periodically colder in cold than in warm climatic intervals. This seems in line with oxygen isotope data, which suggest that deep-waters temperatures in the (North) Atlantic were lower in glacials than in interglacials (Streeter and Shackleton, 1979; Duplessy et al. 1980; Shackleton et al., 1983b; Chappell and Shackleton, 1986). We may speculate that the influence of cold bottom waters in the Angola Basin was most intense in the Y4 zone and weak in the middle part of the X zone. The distribution of *U. peregrina dirupta* indicates that the temperature of the bottom waters and the organic carbon content of the sediments may have varied independently of each other.

We recall in mind that the benthic faunas suggest that the Z and Y1 zones and the X1 and X3 levels are to be considered in all cores as warm climatic intervals. A warm faunal aspect for the X2 level is found only in T80-10. Because *U. peregrina dirupta* is an abundant element in the middle part of the X zone in KW25 and T78-45, the question arises whether the cold climatic aspect of the X2 interval in the deepest cores, including VM19-283, is primarily due to lower bottom water temperatures or to increased food levels. This question can not be solved satisfactorily, because some of the taxa related to warm climatic intervals are absent in this interval, whereas others are present.

As both the carbon content of the sediment and bottom water temperatures have varied, overall conditions during cold climatic intervals at given depth were markedly different at times from those prevailing at present. This may be the reason that some species of which the modern distribution is to a large extent controlled by variation in food supply (e.g. *Astrononion* sp., *C. wuellerstorfi* s.s., *G. polia*, *P. murrhina*), do not or not consistently respond to climatic change. The interaction between variation in food-supply and water temperature may also account for the fact that species such as *F. bradyi* are more frequent in cold intervals than anywhere in the modern region.

Remarkably, there are systematic faunal differences between KW25 and T78-45, although both sites are at similar depth. *C.* cf. *robertsonianus* and *E. tumidulus* are both absent in T78-45. In addition, down-core abundance patterns of *E. exigua* 1 are different. In cold climatic intervals, this taxon is virtually absent in T78-45 but relatively frequent in KW25. These faunal differences suggest that organic carbon levels have been continuously higher in the Zaire deep-sea fan area than in the area to the north of the fan.

VII.6.1. The organic carbon content

Unfortunately, we have no data on the organic carbon content of the cores so that we have to employ published data from other cores to verify whether down-dore changes in the faunas are indeed controlled by changes in the organic carbon content.

Bornhold (1973) measured the organic carbon content in a number of cores from the Angola Basin, including VM19-280 and VM19-281, which are located in the northern part of the region near KW25. Glacial sediments were shown to be characterized by significantly higher organic carbon levels than interglacial sediments. The average difference in weight percentage ranges from 0.8 to 1.4. The glacial/interglacial difference in organic carbon content was attributed to changes in surface-water production.

Jansen et al. (1984) recorded a similar relationship between climatic stages and organic carbon content in cores from the area of the deep-sea fan including T78-45 and T78-46. The latter site is located near T80-10. They found an exponential relationship between carbon burial rate and total sedimentation rate and suggested that variations in the organic carbon content were essentially determined by sedimentation processes.

These data indicate that there are indeed systematic differences in organic carbon content between glacial and interglacial sediments in the region under consideration. The organic carbon record of T78-45 (Jansen et al., 1984) is of particular interest, because this core has been studied for benthic foraminifers as well. Lowest organic carbon values are shown for the Z zone, the upper part of the Y1 zone and the X3 level, which perfectly fits in with our estimates based on the benthic record. The organic carbon content of both the X2 and X1 levels is slightly higher but still much lower than in the cold stages. The low organic carbon content at the X2 level strongly suggests that the cold aspect of the benthic faunas in the middle part of the X zone in VM19-283, KW25 and T78-45 must be attributed to low bottom-water temperatures rather than to increased organic carbon levels.

VII.6.2. Lateral flux of organic carbon and sedimentation rate

A relation between organic carbon content and sedimentation rate (Jansen et al., 1984) is understandable, because the more rapidly the organic carbon is buried, the less it will be affected by decompositional processes (e.g. Heath et al., 1977).

The cores are located at or near the continental margin, where organic carbon reaches the ocean-floor by both vertical and lateral supply. The amount that arrives by lateral transport is thought to be related to the extent to which down-slope processes redistribute the organic matter that was stored on the shelf and upper continental slope. It is, therefore, conceivable that the lateral flux of organic carbon covaries with sedimentation rate.

The question arises whether the overall faunal contrast between cold and warm climatic intervals merely results from variation in sedimentation rate and/or lateral flux of organic matter or that changes in the vertical flux (Bornhold, 1973) are involved as well.

Sedimentation rates are higher in glacial than in interglacial intervals in most cores, but not in T80-10 (see chapter V). In that core, sedimentation rates are higher in the upper part than in the lower part and the change seems to occur in the upper part of isotope stage 3 (Jansen et al., 1984).

In addition, the lateral supply of organic carbon may have been high periodically in cold intervals in VM29-143, KW26, and VM19-283, because down-slope processes intensified during glacial periods. However, T80-10 is again anomalous, because down-slope transport occurs in both warm and cold climatic intervals.

As a consequence, the systematic faunal differences between cold and warm intervals in T80-10 can not be linked to variation in the carbon content caused by differences in sedimentation rate and/or lateral supply. Because taxa such as *E. exigua* 1, *H.elegans* and *N. umboniferus* follow a pattern in T80-10 similar to that in other cores, we assume that effects of those two processes can neither be the main reason for the faunal contrast in the other cores.

Yet, we may postulate that these processes contributed to faunal differences. We suggested earlier that the benthic record in T80-10 combines a local and a regional signal. The benthic signal (fig. 88) shows that the X1 level is more similar to the Z zone than the X3 level. As is readily seen from the frequency diagram (fig. 70), the faunas of the X1 level strongly resemble those of the Z zone, because relative to the other warm intervals they have higher frequencies of *B. inflata, C. carinata, G. translucens* and *O. culter,* and lower frequencies of *B. aculeata.* Percentages of *B. aculeata* drop in the upper part of the core and we surmise that this is to be attributed to the increase in sedimentation rate. By contrast, abundances of *C. carinata* increase in the upper part of this core. This suggests that variation in sedimentation rate determines the local signal in this core.

In summary, we consider it likely that variation in sedimentation rate and lateral flux of organic carbon have contributed to the overall faunal contrast between the warm and cold climatic intervals in the deeper cores.

VII.6.3. Variation in the vertical flux of organic carbon

The vertical flux is essentially determined by the primary production in the photic layer and the degree to which organic matter is consumed on its way down. The planktonic foraminiferal data show that primary production must have changed considerably from cold to warm climatic periods. Low production was concluded for stages Z, Y1 and X1, X2, and X3, whereas primary production was continuously high during cold climatic stages.

Attributing the 'cold' aspect of the benthic faunas in the middle part of the X zone of the deep cores to lowered bottom-water temperatures, we conclude that major changes in the benthic faunas between warm and cold climatic intervals approximately coincide with major changes in surface-water production. We, therefore, suggest that the benthic faunal contrast primarily reflects variation in the vertical flux of organic matter. As to be expected, discrepancies show up, if we compare the benthic signal (see fig. 88) with primary production levels in detail.

In front of the river Zaire, variation in primary production follows a more complicated pattern than in the northern cores, because river induced effects are superimposed on regional variation in primary production. River input of nutrients and river induced upwelling are supposed to have been more significant during stages X1 and X2 and early stage Z than during other warm climatic periods. An effect of river-induced variation in the primary production can, however, not be recognized in the benthic faunas and we, therefore, suggest that the vertical flux is primarily determined by regional variation in primary production.

On a regional scale, primary production was at a mimimum during stage Y1, early stage Z and stage X3. The benthic faunas in the Z zone and at the X3 level are similar, but those in the Y1 zone are transitional between cold and warm climatic intervals. It is likely, in our opinion, that the benthic faunas in the Y1 zone show a transitional aspect, because sedimentation rate and/or lateral supply of organic carbon were higher than in stages Z and X3. In VM29-143 and KW26, the allochthonous category shows higher percentages in the (lower part of the) Y1 zone than at the X3 level and in the Z zone, indicating that the lateral flux was relatively high during the early phase of deglaciation. There is no such evidence in T80-10 and VM19-283, although the probably displaced *C. crassa minima* is relatively abundant in the lowermost part of the Z zone of VM19-283, which interval corresponds to the Y1 zone of other cores. The lengths of the Y1 and Z zones in T80-10, suggest higher average sedimentation rates for the Y1 zone. In addition, we should point out that although the vertical flux was low during the early phase of deglaciation, the carbon content of the underlying sediment was probably high.

VII.7. GLACIAL/INTERGLACIAL CONTRASTS IN THE NW ATLANTIC AND SOUTHERN OCEANS

Deep-sea benthic foraminiferal faunas changed drastically from glacial to interglacial time in various parts of the world ocean and the question arises whether faunal trends are similar from one area to another. Unfortunately, it is difficult to obtain an overview of glacial/interglacial faunal differences in the various areas. Reasons for this are differences in taxonomy and size-fraction investigated and the fact that many authors present merely interpreted data. Nevertheless, literature data strongly suggest that faunal trends similar to those observed in our cores are found in the NW Atlantic and in the sector of the Southern Ocean studied by Corliss (1983a).

The most prominent feature of late glacial faunas at depths between 2000 and 4400 metres in both the marginal and mid-oceanic areas of the N(W) Atlantic is a high abundance of *U. peregrina* (Streeter, 1973; Schnitker, 1979; 1980; Streeter and Shackleton, 1979; Balsam, 1981; Streeter and Lavery, 1982). At present, this species is restricted to depths of less than 3000 metres on the continental margin (e.g. Streeter and Lavery, 1982) and to much shallower depths on the Mid Atlantic Ridge (Streeter, 1973). According to Corliss (1983a), high abundances of *U. peregrina* (see also Corliss et al., 1986) are consistently correlated with glacial intervals in cores from around 3000 metres in the Southern Ocean.

The abundance of *U. peregrina* was initially interpreted in terms of water-mass characteristics, but Corliss et al. (1986) suggested that the high glacial abundances of this species indicate that the carbon content of the sediments was higher at glacial than interglacial time. Although we doubt if the label *U. peregrina* always refers to the same morphology, we think that changes in the distribution of other species are in line with the idea of Corliss et al. (1986).

In the Southern Ocean at depths of around 3000 metres glacial faunas are further characterized by high abundances of *M. barleeanus* and *M. sphaeroides*, both species abounding at high levels of organic carbon in the Angola Basin. These faunas are replaced in interglacials by associations dominated by *E. exigua* and *G. subglobosa*, two species flourishing at much lower food levels in the Angola Basin.

In the NW Atlantic, detailed faunal records are available only for three cores, located between 33° and 37°N. Two sites are on the continental margin (3031, 3942 m) and one at great distance from the continent (4583 m) (Schnitker, 1979). *M. barleeanus* (*M. parkerae* of Schnitker) is the secondmost important species in the late glacial faunas at a depth of 3031 metres and is practically absent in the late Holocene. The late Holocene faunas at 3031 metres are rather diverse and the most characteristic element is *H. elegans* (Schnitker, 1979; see

also Streeter and Lavery, 1982), a species that flourishes at much lower organic carbon levels in the present day Angola Basin than *M. barleeanus.*

The species most characteristic of the late Holocene faunas from below 3500 metres is *N. umboniferus.* In the late Holocene, this species is frequent at depths between 3500 and 4000 metres (Schnitker, 1979; Streeter and Lavery, 1982) and dominant in the faunas at 4583 metres. Late glacial faunas in the core from 4583 metres are not dominated by *U. peregrina,* but by *E. exigua* with *M. sphaeroides* as an additional element. In the Angola Basin *E. exigua* abounds at higher organic carbon levels than *N. umboniferus,* which strongly suggests that the organic carbon content of the sediments was higher at late glacial than at late Holocene time at great depth as well.

Although we surmise that glacial/interglacial differences in bottom water temperature play some role, it seems inevitable to suggest that glacial/interglacial faunal differences in the NW Atlantic and Southern oceans signify primarily that the sediments contained more organic matter in late glacial than in (late) Holocene time.

A higher carbon content of glacial sediments on the continental margin of the NW Atlantic may be controlled mainly by higher sedimentation rates and an increased lateral flux of organic carbon, whereas changes in the vertical flux seem a more plausible explanation for the glacial/interglacial faunal differences at great distance from the continent. By analogy, we may suggest that the vertical flux of organic matter has not changed significantly in those deep-sea areas, where glacial/ interglacial faunal differences seem absent (SW Atlantic (e.g. Gofas, 1978); SE Indian Ocean (Corliss, 1979)).

As diatoms are more abundant in glacial than in interglacial sediments in the Southern Ocean (Corliss, 1983a), we may attribute the increased vertical flux of organic matter at glacial time to enhanced primary production.

It is, however, far from certain, whether glacial/interglacial changes in the vertical flux of organic matter in the NW Atlantic are also to be attributed to variations in primary production. The deep-waters of the world ocean and especially those of the North Atlantic contained more mineralized organic matter at glacial than at interglacial times (e.g. Broecker, 1982; Boyle and Keigwin, 1982; 1987; Shackleton et al., 1983a, b; Mix and Fairbanks, 1985). The glacial increase in the deep-water reservoir is thought to be due to both a land to ocean transfer of organic carbon (Shackleton, 1977) and a surface to deep-water transfer of organic matter (e.g. Broecker, 1982; Boyle and Keigwin, 1982). A higher average primary production of the surface-waters during glacials is a very attractive explanation for the increase in the deep-water reservoir relative to that of the surface waters (e.g. Broecker, 1982; Shackleton, 1983a, b; Sarmiento and Toggweiler, 1984; Siegenthaler and Wenk, 1984). However, most

authors assume that the glacial deep-waters of the North Atlantic were particularly rich in mineralized organic matter because reduced formation of NADW during glacials led to an increased residence time of the deep-water (e.g. Boyle and Keigwin, 1982; 1987; Shackleton et al., 1983b; Mix and Fairbanks, 1985). An increased residence time of the North Atlantic deep waters during glacials may have reduced the oxygen concentration of the deep waters. Lowered oxygen concentrations during glacials could have reduced the proportion of organic matter that is mineralized in the water column, thus resulting in an larger vertical flux of organic matter at glacial than at interglacial time.

Notwithstanding a more sluggish deep-water circulation in the North Atlantic during glacials has been accepted widely, the opposite was defended by Olausson (1985). In addition, Sarnthein et al. (1987) showed that the large glacial/interglacial differences in the amount of mineralized organic carbon stored in the deep-sea of the NE Atlantic could well be caused by differences in primary production. Because estimates on glacial/interglacial differences in the NW Atlantic primary production are lacking, the cause of the larger glacial vertical flux of organic matter must remain uncertain.

VII.8. CONCLUDING REMARKS

Deep-sea benthic foraminiferal faunas from the marginal part of the tropical eastern South Atlantic underwent significant changes during the Late Quaternary. Dissolution and down-slope contamination affected the composition of the faunas to a varying degree and down-core faunal changes are, therefore, only partially the expression of variation in the environmental parameters that determine the distribution of the living foraminifers. In an attempt to simplify the faunal information, we have focused on climate-related faunal changes.

Considerable down-slope transport occurs in the four most shallow cores (1988-3442 m), but this process seems less significant in the deeper KW25 (3994 m). Faunas show that redeposition periodically increased during glacials between 2776 and 3442 metres depth. This fits in with Damuth's model (1975), which predicts intensified down-slope transport during periods of low sea-level stand. Variation in the percentage of allochthonous elements in T80-10 (1988 m) did not show an obvious relation to climate. This is probably connected with the position of this site which is close to the submarine canyon. The canyon may have acted as a major pathway of shallow-water sediments during both cold and warm periods.

Climate-related changes in the autochthonous faunas are thought to be due primarily to variation in the organic carbon levels of the benthic environment, in which cold climatic periods are characterized by the higher carbon levels.

This assertion is supported by literature data on the carbon content of cores from the area. We suggest that the faunas primarily respond to variations in the vertical flux of organic carbon, which is governed by regional changes in the primary production of the overlying surface waters. Effects of changes in the vertical flux are partially accentuated, partially masked by variations in lateral flux and preservation of organic carbon. Independently of changes in the organic carbon content, the temperature of the bottom waters has varied at least at depths below 3000 metres. Cold bottom waters reached the area during isotope stages 2 and 4 and the middle of stage 5. Maximum influence is suggested for stage 4, during which cold bottom waters rose to depths of 3000 metres. During the middle of stage 5, cold bottom waters were below 3500 metres.

Furthermore, we suggest that glacial/interglacial differences in the NW Atlantic and Southern oceans published in the literature may also be attributed to an increase in the vertical flux of organic matter during glacials (cf. Corliss et al., 1986). The larger glacial flux may be due to an increased primary production, but with regard to the NW Atlantic lowered oxygen concentrations in the deep waters may also offer an explanation.

Chapter VIII

TAXONOMIC REMARKS

VIII.1. PLANKTONIC SPECIES

Globigerina bulloides d'Orbigny
Pl. 1, figs. 1-3

Globigerina bulloides d'Orbigny, 1826, Tabl. méth. Céph., Ann. Sci. Nat., sér. 1, vol. 7, p. 277, list no.1, modèles 17, 76; Malmgren and Kennett, 1976, Jour. For. Res., vol. 7(2), pl. 1, figs. 1, 2.

Remarks: Apart from the geographically controlled difference in size discussed in chapter three, variation mainly concerns the aperture.

Intergradation between *Globigerina bulloides* and *G. falconensis* is said to occur (e.g. Bé and Tolderlund, 1971; Bé and Hamlin, 1977), but Malmgren and Kennett (1976) considered them as distinct species. We found both morphologies generally also well distinguishable and consider them as distinct species.

Globigerina falconensis Blow
Pl. 1, figs. 4-5

Globigerina falconensis Blow, 1959, Bull. Amer. Pal., vol. 39, no. 178, p. 177, pl. 9, figs. 40, 41; Malmgren and Kennett, 1976, Jour. For. Res., vol. 7(2), pl. 1, figs. 3-6.

Remarks: This species has a lower and more restricted aperture and a less umbilicate test than *G. bulloides*. The intercameral sutures are generally more incised and the chambers tend to be slightly elongated. A rim-like apertural lip is frequently present, in particular in kummerforms, but it is not as characteristic as suggested by Malmgren and Kennett.

Globigerinella siphonifera (d'Orbigny)
Pl. 1, figs. 7, 8

Globigerina siphonifera d'Orbigny, 1839, In: De la Sagra, Hist. Phys. Nat. Cuba, vol. 8, p. 83, pl. 4, figs. 15-18.
Globigerina aequilateralis Brady, 1879, Quart. Jour. Micr. Sci., vol. 19, p. 285; 1884, Rept. Voy. Chall., pl. 80, figs. 18-21.

Remarks: The arrangement of the chambers is variable, ranging from a low trochospire in small-sized specimens to generally incomplete planispiral coiling in larger individuals. The aperture changes accordingly from a low-arched umbilical-extraumbilical opening, to a broad slit, which extends across the periphery.

It may be difficult to distinguish between *G. siphonifera* and both *G. bulloides* and *G. falconensis* among small-sized specimens. A low-arched umbilical-extraumbilical aperture is considered typical of *G. siphonifera*. In addition, this species has more globular chambers and a more coarsely hispid wall.

Globigerinita glutinata (Egger)
Pl. 1, figs. 6, 9

Globigerina glutinata Egger, 1893, Abh. K. Bayer. Akad. Wiss., Math.-Natw., vol. 18, p. 371, pl. 13, figs. 19-21.

Globigerinita glutinata (Egger), Saito, Thompson and Breger, 1981, Index Rec. Pleistoc. Plankt., p. 77, pl. 22, figs. 1-7.

Globigerinoides ruber (d'Orbigny)
Pl. 2, figs. 1-3

Globigerina rubra d'Orbigny, 1839, In: De la Sagra, Hist. Phys. Nat. Cuba, p. 82; ibid., vol. 8, pl. 4, figs. 5, 12-14.

Globigerinoides ruber (d'Orbigny), Saito, Thompson and Breger, 1981, Index Rec. Pleist. Plankt., p. 59, pl. 15, fig. 1.

Remarks: Considerable variation is observed in chamber form, size of the aperture, height of the trochospire, and in pigmentation of the test, and several morphotypes can be distinguished.

The *ruber* type has rather globular, loosely arranged chambers with deeply incised sutures and the primary aperture is a wide and relatively high arch.

More compact forms, with a much smaller and almost circular opening, are often classified as *G. cyclostoma* (Galloway and Wissler). A similar primary opening is found in the compact *elongatus* type, which is further characterized by laterally and in general slightly obliquely compressed chambers.

No attempt was made to evaluate the distribution of the different morphotypes, but we noted that the *ruber* type tends to become rare towards the fringes of the distribution area.

The colour of the test ranges from white to reddish pink. Specimens with at least one pink chamber were classified as pink varieties.

According to the rules of nomenclature, *G. elongatus* would be the proper name for this species. Because the usage of *G. ruber* is so well established in the literature, we prefer to use this name.

Globigerinoides trilobus (Reuss)
Pl. 2, fig. 4

Globigerina triloba Reuss, 1850, K. Akad. Wiss. Wien, Math-Natw., vol. 1, p. 374, pl. 47, fig. 11.

Remarks: This species includes specimens with a sac-like ultimate chamber (*sacculiferus* type).

Globorotalia crassaformis (Galloway and Wissler)
Pl. 2, figs. 7-9

Globigerina crassaformis Galloway and Wissler, 1927, Jour. Pal., vol. 1, p. 41, pl. 7, fig. 12.

Remarks: Populations are predominantly sinistrally coiled. The periphery varies from narrowly rounded to indistinctly keeled.

Globorotalia hirsuta (d'Orbigny)
Pl. 3, figs. 1-3

Rotalina hirsuta d'Orbigny, 1839, In: Barker-Webb and Berthelot, Hist. Nat. Iles Canaries, vol. 2(2), p. 131, pl. 1, figs. 37-39.

Remarks: Considerable variation was observed in the convexity of the spiral side. The specimens are almost exclusively dextrally coiled.

Globorotalia inflata (d'Orbigny)
Pl. 3, figs. 4-6

Globigerina inflata d'Orbigny, 1839, In: Barker-Webb and Berthelot, Hist. Nat. Iles Canaries, vol. 2(2), p. 134, pl. 2, figs. 7-9.

Remarks: This species is almost exclusively sinistrally coiled.

Globorotalia menardii (d'Orbigny)
Pl. 4, figs. 1-6

Rotalia (Rotalie) menardii d'Orbigny, 1826, Tabl. méth. Céph., Ann. Sci. Nat., sér. 1, vol. 7, p. 273, no. 26.
Pulvinulina menardii (d'Orbigny) var. *tumida* Brady, 1877, Geol. Mag., London, vol. 4, no. 12, p. 535 (no figures)
Pulvinulina tumida Brady, 1884, Rept. Voy. Chall., p. 692, pl. 103, figs. 4-6.

Remarks: Continuous variation occurs between *Globorotalia menardii* and *G. tumida,* which are often treated as different species in the literature (e.g. Bé and Hamlin, 1977; Pujol, 1980). Although we initially tried to distinguish between both morphotypes, their distribution patterns appeared to be very similar.

G. ungulata Bermudez, which is characterized by a relatively high umbilical side and a thin and shiny tests occurs sparsely and has been included in *G. menardii.*

G. flexuosa (Koch), which is characterized by a twisted final part of the test, has been included in *G. menardii.* This type occurs sporadically in the X zone of the cores.

Globorotalia scitula (Brady)
Pl. 3, figs. 7-9

Pulvinulina scitula Brady, 1881, Proc. Roy. Soc. Edinburgh, vol. 11, p. 716; 1884, Rept. Voy. Chall., pl. 103, fig. 7.
Globorotalia scitula (Brady), Saito, Thompson and Breger, 1981, Index Rec. Pleist. Plankt., p. 137, pl. 46, fig. 2.

Remarks: Coiling is predominantly dextral.

Globorotalia truncatulinoides (d'Orbigny)
Pl. 4, figs. 7-9

Rotalina truncatulinoides d'Orbigny, 1839, In: Barker-Webb and Berthelot, Hist. Nat. Iles Canaries, vol 2(2), p. 132, pl. 2, figs. 25-27.

Remarks: Dextral and sinistral forms have been taken separately in the quantitative analyses.

Globorotaloides hexagonus (Natland)
Pl. 6, figs. 3-5

Globigerina hexagona Natland, 1938, Univ. Calif., Scripps Inst. Oceanogr., Bull., Tech. ser., vol. 3(10), p. 149, pl. 7, fig. 1.

Neogloboquadrinids

Continuous variation was observed between two morphotypes, which are mainly distinguished by a difference in size.

Neogloboquadrina dutertrei (d'Orbigny)
Pl. 5, figs. 9, 10; pl. 6, figs. 1, 2

Globigerina dutertrei d'Orbigny, 1839, In: De la Sagra, Hist. Phys. Nat. Cuba, p. 84, pl. 4, figs. 19-21.
Globigerina eggeri Rhumbler, 1901, In: Brandt, Nordisches Plankton, Kiel, pt.1, pp. 12-20., textfig. 20.

Remarks: Test medium to large in size, largest diameter measured roughly parallel to the suture between the ultimate and penultimate chamber, generally more than 0.30 mm. Chambers are coiled in a low to moderately high trochospire and their number in the last whorl varies between four and seven. Aperture is umbilical to umbilical-extraumbilical and a toothplate may be present. Coiling is almost exclusively dextral.

Neogloboquadrina pachyderma (Ehrenberg)
Pl. 5, figs. 1-8

Aristerospira pachyderma Ehrenberg, 1861, K. Preuss. Akad. Wiss. Berlin, Monatsber., pp. 276, 277, 303; 1872, K. Preuss. Akad. Wiss. Berlin, Abh., pl. 1, fig. 4
Globigerina incompta Cifelli, 1961, Cushm. Found. Foram. Res., Contr., vol. 12(3), p. 83, pl. 4, figs. 1-7.

Remarks: Test small-sized, largest diameter measured roughly parallel to the suture between the ultimate and penultimate chamber, generally less than 0.30 mm. Low trochospire, four to five chambers in the last whorl. Umbilical to umbilical/extraumbilical aperture, which is usually bordered by a rimlike lip.

Compact, four-chambered and sinistrally coiled specimens are scarce. Specimens are mostly dextrally and relatively loosely coiled.

Orbulina universa d'Orbigny
Pl. 6, figs. 6,7

Orbulina universa d'Orbigny, 1839, In: De la Sagra, Hist. Phys. Nat. Cuba, p. 2; ibid., vol. 8, pl. 1, fig. 1; Saito, Thompson and Breger, 1981, Index Rec. Pleist. Plankt., p. 70, pl. 19, figs. 1-6.

Pulleniatina obliquiloculata (Parker and Jones)
Pl. 2, fig. 6

Pullenia sphaeroides (d'Orbigny) var. *obliquiloculata* Parker and Jones, 1865, Roy. Soc. London, Philos. Trans., vol. 155, pp. 365, 368, pl. 19, fig. 4.

Sphaeroidinella dehiscens (Parker and Jones)
Pl. 2, fig. 5

Sphaeroidina bulloides d'Orbigny var. *dehiscens* Parker and Jones, 1865, Roy. Soc. London, Philos. Trans., vol. 155, p. 369, pl. 19, fig. 5.

Remarks: Specimens with extremely deep and wide sutures (*excavata* type) were not found.

VIII.2. BENTHIC SPECIES

The selection of benthic species consists of the relevant deep-sea species and some of the species from the shallower depth range (74-1070 m). The shallow-water species are included to elucidate the concept of morphologically related deep-sea species. The distribution of a species on the ocean floor will briefly be discussed, if we have not yet commented upon it.

Anomalinoides minimus Schilling and Parisi
Pl. 7, figs. 1-3

Anomalinoides minimus Schilling and Parisi, 1981, Riv. Ital. Paleont., vol. 87(2), pp. 284-286, pl. 23, figs. 1-5, pl. 24, figs. 1-6.

Remarks: Very small-sized species with six to ten chambers in the final whorl, occurring only in the 63-150 μm fraction.

Astrononion sp.
Pl. 7, figs. 4,5

Astrononion echolsi Kennett, Corliss, 1979, Micropal., vol. 35(1), p. 8, pl. 3, figs. 16,17 (non Kennett, 1967).

Description: Test moderately compressed and small, maximum diameter generally less than 0.32 mm. The last whorl is composed of seven or eight chambers, which increase gradually in size. The periphery is (broadly) rounded and slightly lobulate. The aperture is a low opening at the base of the last chamber and extends from umbilicus to umbilicus; the apertural face is broader than high and distinctly convex. The complex of chamberflaps and secondary chamberlets is indistinctly developed. The secondary openings are pits in the sutures, which are placed closer to the periphery than to the centre of the test. The sutural areas in between these openings and the centre are covered by imperforate umbilical flaps. Beyond the openings, the sutures are somewhat depressed, broad and imperforate.

Remarks: The secondary openings of *A. echolsi* Kennett are closer to the umbilicus than to the periphery.

Bulimina aculeata d'Orbigny
Pl. 7, figs. 7-9

Bulimina aculeata d'Orbigny, 1826, Tabl. méth. Céph., Ann. Sci. Nat., sér. 1, vol. 7, p. 269; Fornasini, 1902, Mem. R. Accad. Sci. Ist., ser. 5, vol. 9, p. 153, fig. 4; Zobel and Ranke, 1978, Meteor Forsch. Ergeb., C, vol. 29, p. 32, pl. 1, figs. 4,5.

Remarks: This species shows wide variation in shape and ornamentation of the test. The one end-member morphology is conical and regularly triserial showing a rapid increase in chamber-size. This morphology shows well-developed spines and the chambers of the final whorl are covered at their base with blunt tubercles. The other end-member is more cylindrical, tordated triserial with more equal-sized and almost smooth chambers in the last whorl.

Occasionally, chambers have weakly developed shoulders. In this respect, they resemble *B. marginata* but actual intergradation between the two species was not observed.

Bulimina costata d'Orbigny
Pl. 8, figs. 2, 3

Bulimina costata d'Orbigny, 1826, Tabl. méth. Céph., Ann. Sci. Nat., sér. 1, vol. 7, p. 269; Fornasini, 1901, Boll. Soc. Geol. Ital., vol. 20, p. 174, pl. 1.
Bulimina striata d'Orbigny, 1826, op. cit., p. 269; Fornasini, 1902, Mem. R. Accad. Sci. Bologna, ser.5, vol. 9, p. 372, pl. 1.
Bulimina costata d'Orbigny s.l., Haake, 1980, Meteor Forsch. Ergeb., C, vol. 32, p. 12, pl. 2, figs. 19-20.

Remarks: Variation ranges from relatively stout forms, with a length/width ratio of approximately 1.2 to more slender types that have a length/width ratio of 1.8. In comparison with both *B. inflata* and *B. subacuminata,* the costae are sharper, finer and more continuous, often extending to the chambers of the previous whorl.

Bulimina exilis Brady

Bulimina elegans d'Orbigny var. *exilis* Brady, 1884, Rept. Voy. Chall., p. 339, pl. 50, figs. 5,6.
Bulimina exilis Brady, Phleger, Parker and Peirson, 1953, Swed. Deep-Sea Exped., vol. 7(1), p. 32, pl. 6, fig. 24.

Distribution: Very sparse (maximum 1 %) in the 150-595 μm fraction at depths between 605 and 1760 metres. Equally rare in the 63-595 μm fraction, and UDL is at a depth of 225 metres

Bulimina gibba Fornasini
Pl. 7, fig. 6

Bulimina gibba Fornasini, 1902, Mem. R. Accad. Sci. Bologna, ser. 5, vol. 9, p. 378, pl. O, figs. 32,34; Parker, 1958, Swed. Deep-Sea Exped., vol. 8, p. 261, pl. 2, figs. 21,22; Haake, 1980, Meteor Forsch. Ergeb., C, vol. 32, p. 11, pl.2, figs. 15,16.

Remarks: Small and slender test, reaching in length up to 0.35 mm. Chambers are less inflated and higher than in *B. aculeata,* but the ornamentation can be similar in both species.

Distribution: Shallow-water species, occurring between 74 and 225 metres depth. Maximum relative abundance is six per cent in the 150-595 μm fraction.

Bulimina inflata Seguenza
Pl. 8, fig. 4

Bulimina inflata Seguenza, 1862, Accad. Gioenia Sci. Nat. Catania, ser. 2, vol. 18, p. 109, pl. 1, fig. 10.
Bulimina inflata Seguenza var. *mexicana* Cushman, 1922, U.S. Nat. Mus., Bull. 104(3), p. 95, pl. 21, fig. 2.
Bulimina mexicana Cushman, Phleger, Parker and Peirson, 1953, Swed. Deep-Sea Exped., vol. 7(1), p. 33, pl. 6, fig. 27.

Remarks: A stout *Bulimina* with a length/width ratio between 1.0 and 1.25. Chambers are inflated and increase rapidly in size. Last whorl covers about half of the test. The costae are stout and may develop into short spines. They are limited to the lower part of the chambers and do not continue on the previous whorl.

This species is distinguished from *B. costata* by its ornamentation and from *B. subacuminata* by its shape.

Bulimina marginata d'Orbigny
Pl. 8, fig. 6

Bulimina marginata d'Orbigny, 1826, Tabl. méth. Céph., Ann. Sci. Nat., sér. 1, vol. 7, p. 269, pl. 12, figs. 10-12.; Murray, 1971, Atlas Brit. Rec. Foram., p. 119, pl. 49.

Remarks: Chambers have distinctly developed shoulders; they can be broad as in *B. costata*, or relatively high as in *B. gibba*. Some specimens tend to biseriality.

Bulimina rostrata Brady
Pl. 8, fig. 1

Bulimina rostrata Brady, 1884, Rept. Voy. Chall., p. 408, pl. 51, figs. 14,15.
Bulimina alazanenis Cushman, 1927, Jour. Pal., vol. 1, p. 161, pl. 25, fig. 4; Phleger, Parker and Peirson, 1953, Swedish Deep-Sea Exped., vol. 7(1), p. 32, pl. 6, fig. 23.

Bulimina subacuminata Cushman and R.E. Stewart
Pl. 8, fig. 5

Bulimina subacuminata Cushman and R.E. Stewart, 1930. In: Cushman, R.E. and K.C. Stewart, San Diego Soc. Nat. Hist., vol 56, p. 65, pl. 5, figs. 2,3; Haake, 1980, Meteor Forsch. Ergeb, C, vol. 32, p. 12, pl. 2, figs. 21,22.

Remarks: Ornamentation is similar to that of *B. inflata*, but the test is more slender showing a length/width ratio between 1.3 and 1.8.

Bulimina translucens Parker
Pl. 8, fig. 7

Bulimina translucens Parker, 1953. In: Phleger, Parker and Peirson, Swed. Deep-Sea Exped., vol. 7(1), p. 33, pl. 6, figs., 30,31.

Remarks: Very small-sized species attaining a maximum length of 0.32 mm. Striae are absent or only weakly developed.

Cassidulina carinata Silvestri
Pl. 8, fig. 8

Cassidulina laevigata d'Orbigny var. *carinata* Silvestri, 1896, Accad. Pont. Nuovi Lincei, Mem., vol. 12, p. 104, pl. 2, fig. 10.
Cassidulina carinata Silvestri, Zobel and Ranke, 1978, Meteor Forsch. Ergeb., C, vol. 29, p. 35, pl. 2, figs. 1,2.

Remarks: Carinate specimens predominate in all our assemblages.

Cassidulina crassa minima Boltovskoy
Pl. 8, figs. 9, 10

Cassidulina crassa d'Orbigny forma *minima* Boltovskoy, 1959, Serv. Hidr. Nav., H 1005, p. 100, pl. 14, fig. 12; Boltovskoy, 1978, Mar. Geol., vol. 26, p. 154, pl. 2, fig. 19.
Cassidulina sp. 1 Phleger, Parker and Peirson, 1953, Swed. Deep-Sea Exped., vol. 7(1), p. 45, pl. 10, fig. 5.

Remarks: Chambers are rather inflated, particularly in small-sized specimens. Aperture a simple slit, which may be obscured by a large triangular lip. Small specimens are difficult to separate from small *Globocassidulina subglobosa,* but the latter is characterized by a small, loop-shaped aperture, which is perpendicular to the base of the last chamber.

Chilostomella oolina Schwager

Chilostomella oolina Schwager, 1878, Uff. Geol., Boll., vol. 9, p. 527, pl. 1, fig. 16; Phleger, Parker and Peirson, 1953, Swed. Deep-Sea Exped., vol. 7(1), p. 47, pl. 10, fig. 18.

Distribution: Apart from a single occurrence in VM29-136 (2270 m), this species is absent on the ocean floor.

Cibicides kullenbergi Parker
Pl. 9, figs. 1-3

Cibicides kullenbergi Parker, 1953, In: Phleger, Parker and Peirson, Swed. Deep-Sea Exped., vol. 7(1), p. 49, pl. 11, figs. 7,8; Parker, 1958, Swed. Deep-Sea Exped., vol. 8, p. 275, pl. 4, figs., 34,35,40.
Cibicidoides kullenbergi (Parker), Lohmann, 1978, Jour. Foram. Res., vol. 8, p. 29, pl. 2, figs. 5-7.

Remarks: Test is large and biconvex, the spiral side being generally less elevated. The periphery is formed by a thickened imperforate rim, which is bluntly angled or rounded.

Sutures are slightly depressed or flush with the surface. At the spiral side, they run obliquely and are nearly straight; at the umbilical side, they are radial, somewhat curved and meet in the centre of the test in an imperforate area.

The last whorl is composed of ten to seventeen chambers, but in the smallest specimens there may be as few as eight.

Cibicides robertsonianus (Brady)

As observed by both Phleger et al. (1953) and Pflum and Frerichs (1976), continuous variation occurs between *C. bradyi* and *C. robertsonianus*. Typical representatives of *C. robertsonianus* are, however, absent in our material and we classified the morphology that comes near to *C. robertsonianus* s.s. as *C.* cf. *robertsonianus*. The distinction between *C. bradyi* and *C.* cf. *robertsonianus* is based on the position of the aperture.

Cibicides sp. cf. **C. robertsonianus** (Brady)
Pl. 9, figs. 4-6

cf. *Truncatulina robertsoniana* Brady, 1881, Quart. Jour. Micr. Sci., vol. 21, p. 65; 1884, Rept. Voy. Chall., p. 664, pl. 95, fig. 4.
Cibicides robertsonianus (Brady), Phleger, Parker and Peirson (partim), 1953, Swed. Deep-Sea Exped., vol. 7(1), p. 50, pl. 11, fig. 17 (non figs. 15, 16).

Remarks: Almost planoconvex test, which tends to become evolute at the umbilical side. The aperture extends over the periphery and may continue along the spiral side. The number of chambers in the last whorl ranges from seven to nine and a half. Chambers are more inflated and, at the spiral side, the sutures are more radial than in *bradyi* types.

C. robertsonianus s.s. has more chambers in the final whorl, a non-lobulate periphery and the chambers are not inflated.

Cibicides robertsonianus bradyi (Trauth)
Pl. 9, figs. 7-9

Truncatulina bradyi Trauth, 1918, Denkschr. K. Akad. Wiss. Wien, Math. Nat. Cl., vol. 95, p. 205.
Cibicides bradyi (Trauth), Barker, 1960, Tax. Notes, S.E.P.M., Spec. Publ., nr. 9, pl. 95, fig. 5.

Remarks: Both planoconvex and biconvex specimens with a very inflated umbilical side are present. The periphery is always broadly rounded. Aperture is a small opening at the umbilical side and generally extends just to the periphery. The opening is located closer to the umbilicus in convex individuals. The number of chambers in the final whorl varies between five and seven.

Cibicides wuellerstorfi (Schwager)

Continuous variation occurs between two morphotypes *C. wuellerstorfi* s.s. and *C. wuellerstorfi* var. Typical *C. wuellerstorfi* dominate at depths of less than 5000 metres, whereas in deeper water forms intermediate between *C. wuellerstorfi* s.s. and *C. wuellerstorfi* var. dominate. Being unable to separate these intermediate forms from typical *C. wuellerstorfi*, we included all intermediate forms in *C. wuellerstorfi* s.s.

Cibicides wuellerstorfi (Schwager) s.s.
Pl. 10, figs. 1-6

Anomalina wuellerstorfi Schwager, 1866, Kar Nicobar, Novara Exped., Geol. Pt., vol. 2, p. 258, pl. 7, figs. 105,107.
Planulina wuellerstorfi (Schwager), Phleger, Parker and Peirson, 1953, Swed. Deep-Sea Exped., vol. 7(1), p. 49, pl. 11, figs. 1,2; Lohmann, 1978, Jour. Foram. Res., vol. 8, p. 26, pl. 4, figs. 1-4.

Remarks: Test is planoconvex. The height of the umbilical side varies largely but is typically very low. The periphery is formed by a thickened imperforate rim, which may be rounded or bluntly angled. Equatorial outline varies between not and distinctly lobulate.

Sutures are curved and chambers are lunate or sickle-shaped. The sutures at the spiral side are broadened and generally raised. At the umbilical side they are flush, raised or depressed.

Number of chambers in the last whorl varies between seven and twelve and is normally nine.

Cibicides wuellerstorfi var.
Pl. 10, figs. 7-9

Cibicidoides cf. *C. kullenbergi* Wright, 1978, Rept. DSDP, vol. 42(1), p. 713, pl. 4, fig. 8.

Remarks: Test biconvex with a relatively low spiral side. Periphery is broadly rounded and may be distinctly lobulate.

The sutures on the spiral side are broadened and generally flush. They are slightly curved or straight, and radial to somewhat oblique. Umbilical sutures are flush with the surface or depressed, radial, and only slightly curved. The last whorl is composed of seven to ten chambers.

Distribution: This morphotype never predominates but is present as a minor constituent. The UDL is 1988 metres and the maximum frequency in the 150-595 μm fraction is four per cent.

Epistominella exigua (Brady)
Pl. 11, figs. 1-6

Pulvinulina exigua Brady, 1884, Rept. Voy. Chall., p. 696, pl. 103, figs. 13,14.
Epistominella exigua (Brady), Phleger, Parker and Peirson, 1953, Swed. Deep-Sea Exped, vol. 7(1), p. 43, pl. 9, figs. 35,36; Todd, 1965, U.S. Nat. Mus., Bull., vol. 161, p. 30, pl. 10, fig. 1.

Remarks: Variation includes two end-member morphologies, viz. *E. exigua* 1 and 2. *E. exigua* 1 is the well-known form to which all the references cited refer. It varies between convexoplan and planoconvex, and the periphery is bluntly angled to sharp. It counts five or six chambers in the final whorl and measures up to 0.38 mm.

E. exigua 2 is more biconvex and has a rounded periphery. This type is smaller (largest diameter up to 0.25 mm), and the number of chambers in the last whorl ranges from four to six. The test is usually vitreous.

Epistominella smithi (R.E. and K.C. Stewart)

Pulvinulina smithi R.E. and K.C. Stewart, 1930, Jour. Pal., vol. 4, p. 70, pl. 9, fig.4.
Epistominella smithi Bandy, 1953, Jour. Pal., vol. 27, p. 177, pl. 23, fig. 7.

Distribution: In the 150-595 μm fraction only at 719 metres depth. In the 63-595 μm fraction, at depths between 605 and 719 metres reaching a maximum frequency of five per cent.

Eponides tumidulus (Brady)
Pl. 11, figs. 7-9

Truncatulina tumidula Brady, 1884, Rept. Voy. Chall., p. 666, pl. 95, fig. 8a-d.
Eponides tumidulus (Brady), Phleger, Parker and Peirson, 1953, Swed. Deep-Sea Exped., vol. 7(1), p. 42, pl. 9, figs. 7,8.

Remarks: Test is always biconvex, and the spiral side can be extremely inflated. The number of chambers in the last whorl varies from five to six. The aperture is a small slit at the base of the last chamber close to the umbilicus and bordered by a distinct lip. Designation to *Eponides* is tentative.

Fursenkoina bradyi (Cushman)
Pl. 11, fig. 10

Virgulina bradyi Cushman, 1922, U.S. Nat. Mus., Bull. 104(3), p. 115, pl. 24, fig. 1; Phleger, Parker and Peirson, 1953, Swed. Deep-Sea Exped., vol. 7(1), p. 34, pl. 7, figs. 4,5.

Remarks: Two morphotypes can be distinguished, which differ in the size of the proloculus. The macrospheric form, which usually predominates, has a cylindrical test, whereas the type that starts with a small proloculus has a tapering test.

Distribution: Low frequent (less than 3%) throughout the area in the 150-595 μm fraction. The UDL is 2675 metres in the 150-595 μm fraction, but this species occurs as shallow as 719 metres in the 63-150 μm fraction.

Gavelinopsis translucens (Phleger and Parker)

'Rotalia' translucens Phleger and Parker, 1951, Geol. Soc. Am., Mem., vol. 46(2), p. 24, pl. 12, figs. 11,12; Phleger, Parker and Peirson, 1953, Swed. Deep-Sea Exped., vol. 7(1), p. 42, pl. 9, figs. 22,23.

Globobulimina spp.

Notwithstanding the presence of species such as *G. affinis, G. glabra, G. hoeglundi,* and *G. turgida,* we lumped all globobuliminids, because intraspecific variation in this genus can cover a wide range (see also van der Zwaan, 1982).

Globocassidulina subglobosa (Brady)
Pl. 8, fig. 11

Cassidulina subglobosa Brady, 1881, Quarl. Jour. Micro. Soc., vol. 21, p. 605; 1884, Rept. Voy. Chall., pl. 54, fig. 17; Phleger, Parker and Peirson, 1953, Swed. Deep-Sea Exped., vol. 7(1), p. 45, pl. 10, fig. 4
Globocassidulina subglobosa (Brady), Lohmann, 1978, Jour. Foram. Res., vol. 8, p. 26, pl. 2, figs. 8,9.

Remarks: Extremely large-sized specimens, up to 0.70 mm long, occur in the area of maximum abundance.

Gyroidina sp. cf. **G. altiformis** R.E. and K.C. Stewart
Pl. 12, figs. 1-3

cf. *Gyroidina altiformis* d'Orbigny var. *altiformis* R.E. and K.C. Stewart, 1930, Jour. Pal., vol. 4(1), p. 67, pl. 9, fig. 2.
Gyroidina soldanii d'Orbigny variants, Phleger, Parker and Peirson, 1953, Swed. Deep-Sea Exped., vol 7(1), p. 41, pl. 9, figs. 1,2 (non d'Orbigny, 1826).
Gyroidina altiformis Stewart and Stewart, Gofas, 1978, Thèse Univ. Bret. Occ., pl. 14, fig. 1.

Remarks: This species differs in a number of characteristics from *G. altiformis.* The test is less deeply umbilicate and the sutures are not depressed around the umbilicus. The number of chambers in the last whorl varies between seven and eight and a half, whereas *G. altiformis* has eight to eleven. Maximum diameter up to 0.5 mm.

In two samples from the extreme SW of the region (4295, 4525 m) specimens were found, which have only three to five chambers and an extremely large proloculus (0.2 mm in diameter).

The difference between *Gyroidina* and *Gyroidinoides* is not accepted, because both types of aperture are found in the assemblages.

Distribution: A minor element of the faunas at depths between 1760 and 5410 metres and virtually absent in the area of the Zaire deep-sea fan. Maximum frequency in the 150-595 μm fraction is four per cent.

Gyroidina polia (Phleger and Parker)
Pl. 12, figs. 4-6

Eponides polius Phleger and Parker, 1951, Geol. Soc. Am., Mem., vol. 46 (2), p. 21, pl. 11, figs. 1,2; Phleger, Parker and Peirson, 1953, Swed. Deep-Sea Exped., vol. 7(1), p. 41, pl. 9, figs. 3,4.

Remarks: This species is distinctly smaller than *G.* cf. *altiformis* and counts more chambers, i.e. eight to eleven, in the final whorl. In addition, this species is less umbilicate and the umbilical side is comparatively low. The overall morphology of the two taxa is, however, very similar and intergradation can not be excluded. Maximum diameter 0.30 mm.

Gyroidina sp. 1
Pl. 12, figs.7-9

Description: Small-sized species showing a planoconvex test and a broadly rounded periphery. Sutures are radial, fairly straight and depressed or flush. On the spiral side they are narrow, on the umbilical side slightly broadened. The number of whorls reaches up to two and a half, and each whorl is composed of six or seven, occasionally eight, chambers. The test is slightly umbilicate and the *Gyroidina* type of aperture predominates. The wall is very finely perforate. The largest diameter reaches up to 0.3 mm, but usually measures between 0.2 and 0.25 mm.

Hoeglundina elegans (d'Orbigny)
Pl. 12, figs. 10-12

Rotalia (Turbuline) elegans d'Orbigny, 1826, Tabl. méth. Céph., Ann. Sci. Nat., sér. 1, vol. 7, p. 276; Parker, Jones and Brady, 1871, Ann. Mag. Nat. Hist., ser. 4a, vol. 8, pl. 12, fig. 14.
Hoeglundina elegans (d'Orbigny), Phleger, Parker and Peirson, 1953, Swed. Deep-Sea Exped., vol. 7(1), p. 43, pl. 9, figs. 24,25.

Melonis barleeanus (Williamson)
Pl. 13, figs. 1,2

Nonionina barleeana Williamson, 1858, Rec. Foram. G.B., p. 32, pl. 3, figs. 68,69.
Nonion barleeanum (Williamson), Phleger, Parker and Peirson, 1953, Swed. Deep-Sea Exped., vol. 7(1), p. 30, pl. 6, fig. 4.
Melonis barleeanus (Williamson), Haake, 1980, Meteor Forsch. Ergeb., C., vol. 32, p. 17, pl. 3, fig. 23.

Remarks: Test very compressed. Periphery rounded to subangular and provided with a pseudocarina. Sutures are straight or slightly curved, relatively broad and generally raised. They coalesce at the centre of the test and form a rim of imperforate shell material around the umbilicus. The number of chambers per whorl ranges from ten to fourteen.

In samples from core KW25 and in samples from relatively deep water in the fan-area, specimens are atypical and tend to resemble *M. formosus.*

Melonis formosus (Seguenza)
Pl. 13, figs. 3,4

Nonionina formosa Seguenza, 1880, R. Accad. Lincei, Roma, Cl. Sci. Fis., Mat., Nat., Mem., vol. 6, p. 63, pl. 7, fig. 6.
Nonion formosum (Seguenza), Phleger, Parker and Peirson, 1953, Swed. Deep-Sea Exped., vol. 7(1), p. 30, pl. 6, fig. 5.

Remarks: In being moderately compressed, the species is intermediate between *M. barleeanus* and compressed types of *M. sphaeroides.* In contrast to those species, *M. formosus* is generally finely perforate and only slightly umbilicate. Sutures are broad or narrow but never raised. The number of chambers in the final whorl ranges from seven to ten.

Melonis sphaeroides Voloshinova
Pl. 13, figs. 5-8

Nonionina pompilioides (Von Fichtel and Von Moll), Brady, 1884, Rept. Voy. Chall., p. 727, pl. 109, figs. 10,11 (non *Nautilus pompilioides* Von Fichtel and Von Moll, 1798).
Melonis sphaeroides Voloshinova, 1958, Microfauna USSR, vol. 115, p. 9, pl. 3, figs. 8,9; Hasegawa, 1984, Benthos'83, Proc., p. 302, pl. 1, figs. 1-3.

Remarks: This species shows conspicuous variation in the flatness of the test. Whorls are invariably composed of six to eight chambers. This feature makes it easy to distinguish this species from *M. pompilioides,* which has ten or more chambers (Hasegawa, op. cit.).

Nuttallides pusillus (Parr)

The number of chambers in the last whorl changes with depth and on that basis we distinguished three morphotypes. The test is very small and the largest diameter measures usually less than 150 μm.

The generic position of the species assigned to *Nuttallides* has been matter of some discussion. Confusion seems to be caused by the apparent variability of the apertural characteristics (see pl. 16, figs. 4-7). In our material, the aperture is always located at the base of the chamber in a depression, which is hooded by the periphery. In some specimens, the opening appears as a simple and low slit which extends from the periphery to near the centre of the test. In other specimens, the aperture is a very small restricted opening or it may be split into two separate openings. Removal of the last chamber shows always two septal foramina separated by a modified lip that extends into the next chamber as an internal plate. The presence of this feature, which can generally be observed only by SEM photography, renders it likely that these species belong to *Nuttallides.*

Nuttallides pusillus pusillus (Parr)
Pl. 14, figs. 4-12

Eponides pusillus Parr, 1950, Antarct. Res. Exped., Repts., ser. B, vol 5(6), p. 360, pl. 14, fig. 16; Phleger, Parker and Peirson, 1953, Swed. Deep-Sea Exped., vol. 7(1), p. 41, pl. 9, figs. 5,6.

Remarks: Test is biconvex but both sides vary considerably in convexity. The number of chambers in the last whorl, which is best determined in spiral view, varies between four and a half and eight. This subspecies is split into two morphotypes, viz. *pusillus* 1 with less than five and a half chambers in the last whorl, and *pusillus* 2 which has more chambers.

Nuttallides pusillus turgidus (Phleger and Parker)
Pl. 14, figs. 1-3

Eponides turgidus Phleger and Parker, 1951, Geol. Soc. Am., Mem., vol. 46(2), p. 22, pl. 11, fig. 9; Parker, 1954, Bull. Mus. Comp. Zool., Harv. Coll., vol. 111, p. 530, pl. 9, figs. 22,23.

Remarks: The number of chambers in the last whorl ranges from four to four and a half and this type is distictly more inflated than *N. pusillus pusillus.*

Nuttallides rugosus (Phleger and Parker)
Pl. 16, figs. 8-10

Pseudoparrella (?) rugosa Phleger and Parker, 1951, Geol. Soc. Am., Mem., vol. 46(2), p. 28, pl. 15, figs. 8,9.
Osangularia rugosa (Phleger and Parker), Pflum and Frerichs, 1976, Cushm. Found. Foram. Res., Spec. Publ., vol. 14, pl. 7, figs. 2-4.

Remarks: Test planoconvex amd medium-sized, maximum diameter up to 0.3 mm. Surface rugosity hides the older part of the test. The number of chambers in the last whorl varies between six and ten and is usually eight. The periphery is a sharp rim.

This taxon can easily be distinguished from *N. umboniferus convexus,* because it is invariably planoconvex, the wall is more rugose and the periphery is sharp. Unclear is whether there is any relationship with *N. umboniferus* s.l.

Distribution: Relatively shallow-water species, intermittently present in low numbers between 267 and 1017 metres. Maximum abundance in the 150-595 μm fraction is five per cent.

Nuttallides umboniferus (Cushman)

Also within this species a number of characteristics change with depth. The most conspicuous change toward deeper water is an increase in test-size and the development of a distinct umbo. Three morphotypes are distinguished, viz. *N. umboniferus* s.s., *N. umboniferus convexus,* and *N. umboniferus decoratus.*

Nuttallides umboniferus decoratus (Phleger and Parker)
Pl. 15, figs. 1-4

Pseudoparrella (?) decorata Phleger and Parker, 1951, Geol. Soc. Am., Mem., vol. 46(2), p. 28, pl. 15, figs. 4,5.
Alabamina decorata (Phleger and Parker), Pflum and Frerichs, 1976, Cushm. Found. Foram. Res., Spec. Publ., vol. 14, pl. 6, figs. 8,9, pl. 7, fig. 1.
Nuttallides decorata (Phleger and Parker), Poag, 1981, Ecol. Atlas Gulf Mex., p. 74, pl. 5, fig. 2, pl. 6, fig. 2.

Remarks: Test biconvex and small. Largest diameter is less than 0.20 mm and this type occurs only in the 63-150 μm fraction. The diameter of the proloculus is less than 10 μm. The number of whorls varies between one and a half and three and the last whorl is composed of five or six chambers. The periphery is more or less rounded and the equatorial outline is (slightly) lobulate. The centre of the spiral side is rugose in the largest specimens.

Nuttallides umboniferus convexus (Parker)
Pl. 15, figs. 5-10

Epistominella rugosa convexa Parker, 1958, Swed. Deep-Sea Exped., vol. 8, p. 273, pl. 4, figs. 21-23.

Remarks: This type is distinctly larger than the *decoratus* type and reaches a maximum diameter of up to 0.38 mm. The proloculus diameter usually measures approximately 20 μm. The test is planoconvex or biconvex with a relatively low spiral side and counts up to three whorls. The final whorl is composed of six or seven chambers. The periphery is angular and is formed by a thickened rim; the equatorial outline is generally distinctly lobulate. Sutures are occasionally raised on the spiral side. The sutures do not meet at the centre of the umbilical side, but an umbo is absent or weakly developed. The surface is rugose, especially in the centre of the spiral side and near the aperture.

Nuttallides umboniferus (Cushman) s.s.
Pl. 15, figs. 11-13; pl. 16, figs. 1-7

Pulvinulinella umbonifera Cushman, 1933, Cushm. Lab. Foram. Res., Contr., vol. 9(4), p. 90, pl. 9, fig. 9.
Epistominella? umbonifera (Cushman), Phleger, Parker and Peirson, 1953, Swed. Deep-Sea Exped., vol 7(1), p. 43, pl. 9, figs. 33,34.
Nuttallides umboniferus (Cushman), Todd, 1965, U.S. Nat. Mus., Bull., vol. 161, p. 29, pl. 11, fig. 1.

Remarks: This form is the largest one within *N. umboniferus* s.l. and measures up to more than 0.50 mm. The proloculus is usually larger than 20 μm. The test is planoconvex or biconvex, and the umbilical side is much more elevated than in the other two types. The test counts maximally two and a half whorls, and the number of chambers in the last whorl ranges usually from seven to eight and a half, but occasionally six or nine chambers occur. The periphery

is rounded and formed by a thickened rim; the test is rarely lobulate. A distinct umbo is present, which measures up to 100 μm. This umbo is very prominent in small specimens. The surface is generally rather smooth, except near the aperture where it is often rugose.

Oridorsalis umbonatus (Reuss)

This ubiquitous species shows an almost bewildering variation, particularly with respect to the peripheral characteristics and the size of the proloculus. The first feature enables to distinguish two morphotypes, viz. a carinate type 1 and a deeper living non-carinate type 2. Discrimination between the types is difficult in the case of small-sized specimens having a small proloculus.

Variation in the size of the first chamber is described by three size-classes. Class A shows a diameter of less than 0.03 mm; in class C the diameter is larger than 0.07 mm, whereas class B occupies an intermediate position.

Oridorsalis umbonatus (Reuss) 1
Pl. 17, figs. 1-3

Rotalina umbonata Reuss, 1851, Deutsch. Geol. Ges., Zeitschr., vol. 3, p. 75, pl. 5, fig. 35.
Truncatulina tenera Brady, 1884, Rept. Voy. Chall., p. 665, pl. 95, fig. 11.

Remarks: Test biconvex, the spiral side less inflated. Periphery is sharp, keeled, and in equatorial view not or only slightly lobulate. The number of chambers in the last whorl is six or seven. We found only specimens with a proloculus size-class A or B. Type A dominates in the assemblages of *O. umbonatus* 1, except in core VM29-136 (2270 m). Assemblages dominated by type 1B include very small specimens with a rounded periphery. Largest dimension up to 0.4 mm.

Oridorsalis umbonatus (Reuss) 2
Pl. 17, figs. 4-13

Eponides umbonatus (Reuss), Phleger, Parker and Peirson, 1953, Swed. Deep-Sea Exped., vol. 7(1), p. 42, pl. 9, figs. 9,10 (non Reuss, 1851).
Oridorsalis umbonatus (Reuss), Lohmann, 1978, Jour. Foram. Res., vol. 8, p. 26, pl. 4, figs. 1-3 (non Reuss, 1851).
Oridorsalis tener (Brady), Lohmann, 1978, Jour. Foram. Res., vol. 8, p. 26, pl. 4, figs. 5-7 (non Brady, 1884).

Remarks: Test variably biconvex. Periphery is broadly rounded to subangular and an imperforate band is sometimes present. Equatorial outline not or slightly lobulate. The number of chambers in the last whorl varies from four in the smallest specimens to about seven in larger ones. Maximum diameter up to 0.65 mm. Type 2 shows more variation in the size of the proloculus than type 1.

Specimens of proloculus size-class A have a small and very inflated test with a broadly rounded periphery. This type is usually the most abundant form in the 63-150 μm fraction.

Type 2B generally dominates the assemblages in the 150-595 μm fraction and usually has a moderately inflated test and a rounded periphery. The width of the chambers increases gradually and the test is almost circular in equatorial view. This type resembles *O. umbonatus* sensu Lohmann (1978).

Type 2C is generally large-sized and is less inflated than the other types. The periphery is subangular. The equatorial outline is rather elliptical, because the chambers steadily increase in both length and width. Type 2C is virtually restricted to the 150-595 μm fraction and similar to *O. tener* sensu Lohmann (1978).

Osangularia culter (Parker and Jones)
Pl. 19, figs. 1-3

Planorbulina culter Parker and Jones, 1865, Roy. Soc. London, Philos. Trans., p. 421, pl. 19, fig. 1.
Osangularia cultur (Parker and Jones), Phleger, Parker and Peirson, 1953, Swed. Deep-Sea Exped., vol 7(1), p. 42, pl. 9, figs. 11, 16.
Osangularia culter (Parker and Jones), Todd, 1965, U.S. Nat. Mus., Bull., vol. 161, p. 25, pl. 15, fig. 1.

Pullenia bulloides (d'Orbigny)

This species comprises two morphotypes viz. *P. bulloides* s.s. and *P. bulloides osloensis.* The latter being asymmetrical and more compressed. Actually, this distribution may be valid only in the 150-595 μm fraction. Samples that yield only *P. bulloides* in the 150-595 μm fraction, may predominantly contain very small, slightly asymmetrical specimens in the finer fraction. Phleger et al. (1953) and Corliss (1979) interpreted such specimens as immature *P. bulloides.*

Pullenia bulloides (d'Orbigny) s.s.
Pl. 18, figs. 1, 4

Nonionina bulloides d'Orbigny, 1846, Foram. Foss. Bass. Tert. Vienne, p. 107, pl. 5, figs. 9,10.
Pullenia bulloides Phleger, Parker and Peirson, 1953, Swed. Deep-Sea Exped., vol. 7(1), p. 47, pl. 10, fig. 19.

Remarks: The number of chambers in the last whorl varies between four and five. Largest diameter up to 0.40 mm.

Pullenia bulloides osloensis Feyling-Hansen
Pl. 18, figs. 2, 3, 5, 6

Pullenia quinqueloba (Reuss) subsp. *minuta* Feyling-Hansen, 1954, Norsk Geol. Tidsskr., vol 33, p. 133, pl. 2, fig. 3, p. 119, pl. 4.
Pullenia osloensis Feyling-Hansen, 1954, Norsk Geol. Tidsskr., vol 33, p. 194, figs. 33-35; Boltovskoy, 1978, Mar. Geol., vol. 26, p. 166, pl. 6, figs. 15-18.

Remarks: Apart from being asymmetrical and somewhat more compressed, this type differs from *P. bulloides* s.s. in having a more restricted aperture. Largest diameter generally less than 0.25 mm.

Pullenia sp. 1
Pl. 18, figs. 7, 8

Description: Test almost circular, non-umbilicate and relatively compressed, i.e. in peripheral view about half as broad as long. Periphery is broadly rounded and not lobulate. Sutures are radial, slightly curved and hardly if at all depressed. The last whorl is composed of four and a half to five and a half, hardly or not inflated chambers, which gradually increase in size. Aperture is a low umbilical/umbilical slit, and the apertural face is relatively low and narrow and almost parallel sided. The wall is hyaline and very finely perforate. Largest diameter ranges from 0.12 to 0.32 mm.

Remarks: This species is probably labelled in many studies as *P. quinqueloba* (Reuss). That name is, however, used for so many different morphologies, that it can practically stand for any compressed *Pullenia* with about five chambers per whorl.

Pyrgo murrhina (Schwager)
Pl. 18, figs. 9-12

Biloculina murrhina Schwager, 1866, Kar Nicobar, Novara Exped., Geol. Pt., vol. 2, p. 203, pl. 4, fig. 15.
Pyrgo oblonga (d'Orbigny), Phleger, Parker and Peirson, 1953, Swed. Deep-Sea Exped., vol. 7(1), p. 28, pl. 5, figs. 25, 26. (non *Biloculina oblonga* d'Orbigny, 1839).
Pyrgo murrhina (Schwager), Phleger, Parker and Peirson, 1953, Swed. Deep-Sea Exped., vol. 7(1), p. 28, pl. 5, figs. 22-24.

Remarks: Variation includes two end-member morphologies. The smallest one (largest dimension about 0.30 mm), has an elongate and inflated test with a subangular periphery. The aperture is situated on a neck-like extension and possesses a simple tooth. This type resembles *P. oblonga* (d'Orbigny), but that species has more inflated chambers and a rounded periphery.

The larger type (usually about 0.50 mm) is more circular and has a distinct keel with a characteristic sinus at the aboral side. The aperture is rather broad, does generally not protrude and has a large bifid tooth. The keel is often lost in specimens from samples that suffered from severe dissolution.

Uvigerina auberiana d'Orbigny
Pl. 19, fig. 4

Uvigerina auberiana d'Orbigny, 1839, In: De la Sagra, Hist. Phys. Nat. Cuba, vol. 8, p. 106, pl. 2, figs. 23-24; Van Leeuwen, 1986, Utrecht Micropal. Bull., vol. 35, p. 64, pl. 4, figs. 3-5.

Remarks: A very finely hispid form, spines never showing alignment (see Van Leeuwen, 1986).

Uvigerina peregrina group

The variation in this group has been discussed and illustrated by Van Leeuwen (1986). Both on the ocean floor and downcore, there is a continuous variation between two morphotypes, viz. the predominantly costate *U. peregrina* s.s. and the hispidocostate *dirupta* type.

Intergradation between *dirupta* types and the completely hispid *U. hispida* was found only downcore. The latter type is, however, always a rather subordinate element in the downcore assemblages of *U. peregrina.*

On the ocean floor completely hispid forms co-occur with *U. peregrina* without any morphologic overlap; on the MAR monotypic completely hispid assemblages are found. This, of course, does not preclude that the three types belong to one and the same species, but we considered it more convenient to gather them in a more informal category, i.e. the *U. peregrina* group.

Uvigerina hispida Schwager
Pl. 19, fig. 8

Uvigerina hispida Schwager, 1866, Kar Nicobar, Novara Exped., Geol. pt., vol. 2, p. 258, pl. 7, figs. 105-107; Van Leeuwen, 1986, Utrecht Micropal. Bull., vol. 35, p. 62, pl. 3, figs. 1-3.

Remarks: A coarsely and fully hispid form with spines placed at random.

Uvigerina peregrina Cushman s.s.
Pl. 19, figs. 5, 6

Uvigerina peregrina Cushman, 1923, U.S. Nat. Mus., Bull., vol. 104(4), p. 166, pl. 42, figs. 7-10; Van Leeuwen, 1986, Utrecht Micropal. Bull., vol. 35, p. 58, pl. 1, figs. 1-5.

Remarks: Fully costate form, at least if the last formed chamber and the oldest one are disregarded.

Uvigerina peregrina dirupta Todd
Pl. 19, fig. 7

Uvigerina peregrina Cushman var. *dirupta* Todd, 1948, A. Hancock Pacif. Exped., vol 6(5), p. 267, pl. 34, fig. 3.
Uvigerina dirupta Todd, Van Leeuwen, 1986, Utrecht Micropal. Bull., vol. 35, p. 60, pl. 2, figs. 1-5.

Remarks: Variation ranges from hispidocostate forms to hispid forms showing alignment of spines.

REFERENCES

Adelseck, C.G. (1978). Dissolution of deep-sea carbonate: preliminary calibration of preservational and morphologic aspects. Deep-Sea Res., vol. 25, pp. 1167-1185.

Almogi-Labin, A. (1984). Population dynamics of planktic foraminifera and pteropoda: Gulf of Aqaba, Red Sea. Proc. Kon. Ned. Ak. Wetensch., ser. B, vol. 87, pp. 481-511.

Bainbridge, A.E. (1976). GEOSECS Atlantic final hydrographic data report. GEOSECS Operation Group, Scripps Inst. Oceanogr., La Jolla.

Balsam, W.L. (1981). Late Quaternary sedimentation in the western North Atlantic: stratigraphy and paleoceanography. Palaeogeogr., -clim., -ecol., vol. 35, pp. 215-240.

Balsam, W.L. and F.W. McCoy (1987). Atlantic sediments: glacial/interglacial comparisons. Paleoceanogr., vol. 2, pp. 531-542.

Bandy, O.L. (1953). Ecology and paleoecology of some California foraminifera (1): the frequency distribution of recent foraminifera off California. Jour. Pal., vol. 27, pp. 161-182.

Barker, P.F., R.L. Carlson, D.A. Johnson, P. Cepek, W. Coulbourn, L.A. Gamboa, N. Hamilton, U. Melo, C. Pujol, A.N. Shor, A.E. Suzyumov, L.R.C. Tjalsma, W.H. Walton and W. Weiss (1981). Deep-Sea Drilling Project leg 72: Southwest Atlantic paleocirculation and Rio Grande rise tectonics, Geol. Soc. Am. Bull., vol. 92, pp. 294-309.

Barmawidjaja, D.M., K. Van der Borg, A.F.M. De Jong, W.A. Van der Kaars and W.J. Zachariasse (1988). Kau Basin, Halmahera, a Late Quaternary paleoenvironmental record in a poorly ventilated basin. In: J.E. van Hinte, Tj. C.E. Van Weering and A.R. Fortuin (Eds.). Proc. Int. Symp. Results Snellius II Exp., Jakarta 1987. Neth. Jour. Sea Res. (in press).

Bé, A.W.H. (1969). Planktonic Foraminifera. In: Distribution of selected groups of marine invertebrates in waters south of 35°S latitude. Antarctic Folio Ser., fol. 11, Am. Geogr. Soc., pp. 9-12.

Bé, A.W.H. (1977). An ecological, zoogeographic and taxonomic review of recent planktonic foraminifera. In: A.T.S. Ramsey (Ed.): Oceanic micropaleontology. Academic Press, pp. 1-101.

Bé, A.W.H., J.K.B. Bishop, M.S. Sverdlove and W.D. Gardner (1985). Standing stock, vertical distribution and flux of planktonic foraminifera in the Panama Basin. Marine Micropal., vol. 9, pp. 307-333.

Bé, A.W.H., J.E. Damuth, L. Lott and R. Free (1976). Late Quaternary climatic record in western Equatorial Atlantic sediment. Mem. Geol. Soc. Am., vol. 145, pp. 165-200.

Bé, A.W.H. and W.H. Hamlin (1967). Ecology of recent planktonic foraminifera (pt. 3). Distribution in the North Atlantic during the summer of 1962. Micropal., vol. 13, pp. 87-106.

Bé, A.W.H. and W.H. Hutson (1977). Ecology of planktonic foraminifera and biogeographic patterns of life and fossil assemblages in the Indian Ocean. Micropal., vol. 23, pp. 369-414.

Bé, A.W.H. and D.S. Tolderlund (1971). Distribution and ecology of living planktonic foraminifera in surface waters of the Atlantic and Indian oceans. In: B.M. Funnell and W.R. Riedel (Eds.): The micropaleontology of oceans. Cambridge Univ. Press, pp. 105-149.

Belanger, P.E. (1982). Paleo-oceanography of the Norwegian Sea during the past 130,000 years: coccolithophorid and foraminiferal data. Boreas, vol 11, pp. 29-36.

Berger, W.H. (1969). Ecologic patterns of living planktonic Foraminifera. Deep-Sea Res., vol. 16, pp. 1-24.

Berger, W.H. (1970). Planktonic foraminifera: selective solution and the lysocline. Mar. Geol., vol. 8, pp. 111-138.

Berger, W.H. (1979). Preservation of foraminifera. SEPM Short Course, no. 6, Soc. Ec. Pal. & Min., pp. 105-155.

Berger, W.H. (1982). On the definition of the Pleistocene/Holocene boundary in deep-sea sediments. In: E. Olausson (Ed.): The Pleistocene/Holocene boundary in the southwestern Sweden. Sver. Geol. Unders. Afh. (Ser. C), vol. 794. Uppsala, pp. 270-280.

Berger, W.H. and A. Soutar (1970). Preservation of plankton shells in an aerobic basin off California. Geol. Soc. Am. Bull., vol. 81, pp. 275-282.

Berger, W.H., J.S. Killingley and E. Vincent (1985). Timing of deglaciation from an oxygen isotope curve for Atlantic deep-sea sediments. Nature, vol. 314, pp. 156-158.

Berner, R.A. (1982). Chemistry of biogenic matter at the deep-sea floor. In: W.G. Ernst and J.G. Morrin (Eds.): The environment of the deep sea, Prentice-Hall, pp. 154-176.

Berner, R.A., M.R. Scott and C. Thomlinson (1970). Carbonate alkalinity in the pore waters of anoxic marine sediments. Limnol. Oceanogr., vol. 15, pp. 544-549.
Berrit, G.R. (1976). Les eaux froides côtières du Gabon à l'Angola sont-elles dues à un upwelling d'Ekman. Cah. ORSTOM, sér. Océanogr., vol. 14, pp. 273-278.
Biscaye, P.E., V. Kolla and K.K. Turekian (1976). Distribution of calcium carbonate in surface sediments of the Atlantic Ocean. Jour. Geoph. Res., vol. 81, pp. 2595-2603.
Boltovskoy, E. and R. Wright (1976). Recent Foraminifera. Dr. W. Junk, The Hague, 515 pp.
Bornhold, B.D. (1973). Late Quaternary sedimentation in the eastern Angola Basin. Tech. Rep. Woods Hole Oceanogr. Instn., vol 73 (8), pp. 1-213.
Boyle, E.A. and L.D. Keigwin (1982). Deep circulation of the North Atlantic over the last 200,000 years: geochemical evidence. Science, vol. 218, pp. 784-787
Boyle, E.A. and L.D. Keigwin (1987). North Atlantic thermohaline circulation during the past 20,000 years linked to high-latitude surface temperature. Nature, vol. 330, pp. 35-40.
Bradshaw, J.S. (1959) Ecology of living planktonic foraminifera of the North and Equatorial Pacific Ocean. Cushm. Found. Foram. Res., Contr., vol. 10, pp. 25-64.
Bremer, M.L. and G.P. Lohmann (1982). Evidence for primary control of the distribution of certain Atlantic Ocean benthonic foraminifera by degree of carbonate saturation. Deep-Sea Res., vol 29, pp. 987-998.
Broecker, W.S. (1982). Glacial to interglacial changes in ocean chemistry. Prog. Oceanog., vol. 11, pp. 151-197.
Broecker, W.S. (1986). Oxygen isotope constraints on surface ocean temperatures. Quat. Res., vol. 26, pp. 121-134.
Broecker, W.S. and T.-H. Peng (1982). Tracers in the sea. Eldigio Press, pp. 1-690.
Broecker, W.S. and T. Takahashi (1978). The relationship between lysocline depth and *in situ* carbonate ion concentration. Deep-Sea Res., vol. 25, pp. 65-95.
Broecker, W.S. and T. Takahashi (1980). Hydrography of the Central Atlantic-III. The North Atlantic deep-water complex. Deep-Sea Res., vol. 27A, pp. 591-613.
Broecker, W.S. and J. Van Donk (1970). Insolation changes, ice volumes, and the 18O record in deep-sea cores. Rev. Geophys. Space Phys., vol. 8, pp. 169-198.
Bubnov, V.A. (1972). Structure and characteristics of the oxygen minimum layer in the southeastern Atlantic. Oceanology, vol. 12, pp. 193-201.
Buzas, M.A. and S.J. Culver (1980). Foraminifera: distribution of provinces in the western North Atlantic. Science, vol. 209, pp. 687-689.
Cadée, G.C. (1978). Primary production and chlorophyll in the Zaire river, estuary and plume. Neth. Jour. Sea Res., vol. 12, pp. 368-381.
Cadée, G.C. (1984). Particulate and dissolved organic carbon and chlorophyll a in the Zaire river, estuary and plume. Neth. Jour. Sea Res., vol. 17, pp. 426-440.
Chappell, J. and N.J. Shackleton (1986). Oxygen isotopes and sea level. Nature, vol. 324, pp. 137-140.
Cifelli, R. (1967). Distributional analysis of North Atlantic foraminifera collected in 1961 during cruises 17 and 21 of the R/V Chain. Cushm. Found. Foram. Res., Contr., vol. 18, pp. 118-127.
Cifelli, R. (1971). On the temperature relationships of planktonic foraminifera. Jour. Foram. Res., vol. 1, pp. 170-177.
Cifelli, R. (1974). Planktonic foraminifera from the Mediterranean and adjacent Atlantic waters (cruise 49 of the Atlantis II, 1969). Jour. Foram. Res., vol. 4, pp. 171-183.
Cifelli, R. and C.S. Bénier (1976). Planktonic foraminifera from near the West African coast and a consideration of faunal parcelling in the North Atlantic. Jour. Foram. Res., vol. 6, pp. 258-273.
Cifelli, R. and R.K. Smith (1974). Distributional patterns of planktonic foraminifera in the western North Atlantic. Jour. Foram. Res., vol. 4, pp. 112-125.
CLIMAP Project Members (1976). The surface of the Ice-Age earth. Science, vol. 191, pp. 1131-1136.
CLIMAP Project Members (1984). The last interglacial Ocean. Quat. Res., vol. 21, pp. 123-224.
Connary, S.D. and M. Ewing (1974). Penetration of Antarctic bottom water from the Cape Basin into the Angola Basin. Jour. Geoph. Res., vol. 79, pp. 463-469.
Corcoran, E.F. and C.V.W. Mahnken (1969). Productivity of the tropical Atlantic Ocean. Proc. Symp. Oceanogr. Fish. Res. Trop. Atlantic, UNESCO, pp. 57-67.

Corliss, B.H. (1979a). Recent deep-sea benthonic foraminiferal distributions in the Southeast Indian Ocean: inferred bottom-water routes and ecological implications. Mar. Geol., vol. 31, pp. 115-138.
Corliss, B.H. (1979b). Quaternary Antarctic Bottom-Water history: deep-sea benthonic foraminiferal evidence from the Southeast Indian Ocean. Quat. Res., vol. 12, pp. 271-289.
Corliss, B.H. (1983a). Quaternary circulation of the Antarctic Circumpolar Current. Deep-Sea Res., vol. 30, pp. 47-61.
Corliss, B.H. (1983b). Distribution of Holocene deep-sea benthonic foraminifera in the southwest Indian Ocean. Deep-Sea Res., vol. 30, pp. 95-117.
Corliss, B.H. (1985). Microhabitats of benthic foraminifera within deep-sea sediments. Nature, vol. 314, pp. 435-438.
Corliss, B.H. and S. Honjo (1981). Dissolution of deep-sea benthonic foraminifera. Micropal., vol. 27, pp. 356-378.
Corliss, B.H., D.G. Martinson and T. Keffer (1986). Late Quaternary deep-ocean circulation. Geol. Soc. Am. Bull., vol. 97, pp. 1106-1121.
Coulbourn, W.T., F.L. Parker and W.H. Berger (1980). Faunal and solution patterns of planktonic foraminifera in surface sediments of the North Pacific. Marine Micropal., vol. 5, pp. 329-399.
Culver, S.J. and M.A. Buzas (1981). Foraminifera distribution of provinces in the Gulf of Mexico. Nature, vol. 290, pp. 328-329.
Damuth, J.E. (1975). Quaternary climate change as revaled by calcium carbonate fluctuations in western Equatorial Atlantic sediments. Deep-Sea Res., vol. 22, pp. 725-743.
Davis, J.C. (1973). Statistics and data analysis in geology. Wiley and Sons, New York, 550 pp.
Dean, W. and J. Gardner (1985). Cyclic variation in calcium carbonate and organic carbon in Miocene to Holocene sediments, Walvis Ridge, South Atlantic Ocean. In: K.J. Hsü and H.J. Weissert (Eds.): South Atlantic Paleoceanography. Cambridge, Cambridge Univ. Press, pp. 61-78.
Demaison, G.J. and G.T. Moore (1980). Anoxic environments and oil source bed genesis. Org. Geochem., vol. 2, pp. 9-31.
Deuser, W.G., E.H. Ross, C. Hemleben and M. Spindler (1981). Seasonal changes in species composition, numbers, mass, size, and isotopic composition of planktonic foraminifera settling into the deep Sargasso Sea. Palaeogeogr., -clim., -ecol., vol. 33, pp. 103-127.
Diester-Haass, L. and P.J. Müller (1979). Processes influencing sand fraction composition and organic matter content in surface sediments off W. Africa (12-19°N). Meteor Forsch. Ergeb., ser. C, vol. 31, pp. 21-48.
Douglas, R.G. (1979). Benthic foraminiferal ecology and paleoecology. A review of concepts and methods. SEPM Short Course, no. 6, Soc. Ec. Pal. and Min., pp. 21-53.
Douglas, R.G. and F. Woodruff (1981). Deep-sea benthic foraminifera. In: C. Emiliani (Ed.): The oceanic lithosphere, the sea, vol. 7. Wiley-Interscience, New York, pp. 1233-1327.
Drooger, M.M. (1982). Quantitative range chart analyses. Utr. Micropal. Bull., vol. 26, 227 pp.
Dufour, P. and J.-M. Stretta (1973). Production primaire, biomasses du phytoplankton et du zooplankton dans l'Atlantique tropical sud le long du meridien 4°W. Cah. ORSTOM, sér. Océanogr., vol. 11, pp. 419-429.
Duplessy, J.-C., A.W.H. Bé and P.L. Blanc (1981a). Oxygen and carbon isotope composition and biogeographic distribution of planktonic foraminifera in the Indian Ocean. Palaeogeogr., -clim., -ecol., vol. 33, pp. 9-46.
Duplessy, J.-C., G. Delibrias, J.L. Turon, C. Pujol and J, Duprat (1981b). Deglacial warming of the northeastern Atlantic Ocean: correlation with the paleoclimatic evolution of the European continent. Palaeogeogr., -clim., -ecol., vol. 35, pp. 121-144.
Duplessy, J.-C., J. Moyes and C. Pujol (1980). Deep water formation in the North Atlantic Ocean during the last ice age. Nature, vol. 286, pp. 479-482.
Duplessy, J.-C. and N. J. Shackleton (1985). Response of global deep-water circulation to Earth's climatic change 135,000-107,000 years ago. Nature, vol. 316, pp. 500-507.
Eckert, H.-R. (1965). Une station d'observation sur les foraminifères planktoniques actuels dans le Golfe de Guinée. Eclogae Geol. Helv., vol. 58, pp. 1039-1058.
Eisma, D. and J. Kalf (1984). Dispersal of Zaire river suspended matter in the estuary and the Angola Basin. Neth. Jour. Sea Res., vol. 17, pp. 385-411.

Eisma, D., J. Kalf and S.J. van der Gaast (1978). Suspended matter in the Zaire estuary and the adjacent Atlantic Ocean. Neth. Jour. Sea Res., vol. 12, pp. 382-402.
Eisma, D. and A.J. van Bennekom (1978). The Zaire river and estuary and the Zaire outflow in the Atlantic Ocean. Neth. Jour. Sea Res., vol. 12, pp. 255-272.
Ellis, D.B. and T.C. Moore (1973). Calcium carbonate, opal, and quartz in Holocene pelagic sediments and the calcite compensation level in the South Atlantic Ocean. Jour. Mar. Res., vol. 31, pp. 210-227.
Embley, R.W. and J.J. Morley (1980). Quaternary sedimentation and paleoenvironmental studies off Namibia (South-West Africa). Mar. Geol., vol. 36, pp. 183-204.
Emerson, S. and M. Bender (1981). Carbon fluxes at the sediment-water interface of the deep-sea: calcium carbonate preservation. Jour. Mar. Sc., vol. 39, pp. 139-162.
Emery, K.O. (1972). Eastern Atlantic continental margin: some results of the 1972 cruise of the R.V. Atlantic II. Science, vol. 178, pp. 298-301.
Emiliani, C. (1955). Pleistocene temperatures. Jour. Geol., vol. 63, pp. 538-578.
Emiliani, C. (1966). Paleotemperature analysis of the Caribbean cores P6304-8 and P6304-9 and a generalized temperature curve for the last 425,000 year. Jour. Geol., vol. 74, pp. 109-126.
Ericson, D.B., M. Ewing, G. Wollin and B.C. Heezen (1961). Atlantic deep-sea sediment cores. Geol. Soc. Am. Bull., vol. 72, pp. 193-286.
Fairbanks, R.G., M. Sverdlove, R. Free, P.H. Wiebe and A.W.H. Bé (1982). Vertical distribution and isotopic fractionation of living planktonic foraminifera from the Panama Basin. Nature, vol. 298, pp. 841-844.
Fairbanks, R.G., P.H. Wiebe and A.W.H. Bé (1980). Vertical distribution and isotope composition of living planktonic foraminifera in the western North Atlantic. Science, vol. 207, pp. 61-63.
Fairbanks, R.G. and P.H. Wiebe (1979). Foraminifera and chlorophyll maximum: vertical distribution, seasonal succession, and paleoceanographic significance. Science, vol. 209, pp. 1524-1526.
Froelich, P.N., G.P. Klinkhammer, M.L. Bender, N.A. Luedtle, G.R. Heath, D. Cullen and P. Dauphin (1979). Early oxidation of organic matter in pelagic sediments of the eastern equatorial Atlantic: suboxic diagenesis. Geochim. Cosmochim. Acta, vol. 43, pp. 1075-1090.
Fuglister F.C. (1960). Atlantic Ocean Atlas. Woods Hole Oceanogr Inst., Woods Hole.
Gaby, M.L. and B.K. Sen Gupta (1985). Late Quaternary benthic foraminifera of the Venezuela Basin. Mar. Geol., vol. 68, pp. 125-144.
Gallardo, Y. (1981). Océanographie physique. In: A. Fontana (Ed.): Milieus marins et ressources halieutiques de la République Populaire du Congo. Trav. Doc. de l'ORSTOM, no. 138, pp. 47-73.
Ganssen, G. and G.F. Lutze (1982). The aragonite compensation depth at the northeastern Atlantic continental margin. Meteor Forsch. Ergeb, ser. C, vol. 36, pp. 57-59.
Gardner, J.V. (1975). Late Pleistocene carbonate dissolution cycles in the eastern Equatorial Atlantic. Cushm. Found. Foram. Res., Spec. Publ., vol. 13, pp. 129-141.
Gardner, J.V. and J.D. Hays (1976). Responses of sea-surface temperature and circulation to global climatic change during the past 200,000 years in the eastern Equatorial Atlantic Ocean. Mem. Geol. Soc. Am., vol. 145, pp. 221-246.
Gevirtz, J.L., R.A. Park and G.M. Friedman (1971). Paraecology of benthonic foraminifera and associated micro-organisms of the continental shelf off Long Island, New York. Jour. Pal., vol. 45, pp. 153-177.
Giresse, P., F. Jansen, G. Kouyoumontzakis and G. Moquedet (1981). Les fonds du plateau continental congolais et le delta sous-marin du fleuve Congo. In: A. Fontana (Ed.): Milieus marins et ressources halieutiques de la République Populaire du Congo, Trav. Doc. de l'ORSTOM, no. 138, pp. 13-45.
Gofas, S. (1978). Une approche du paléoenvironnement océanique: les foraminifères benthiques calcaires, traceurs de la circulation abyssale. Thèse Univ. Bret. Occ., Brest, 107 pp.
Goll, R.M. and K.R. Bjørklund (1974). Radiolaria in surface sediments of the South Atlantic. Micropal., vol. 20, pp. 38-75.
Haake, F.-W. (1980). Benthische Foraminiferen in Oberflachen-Sedimenten und Kernen des Ostatlantiks vor Senegal/Gambia (Westafrika). Meteor Forsch. Ergeb., ser. C, vol. 32, pp. 1-29.
Hagen, E., R. Schemainda, N. Mikkelsen, L. Postel, S. Schulz and M. Below. (1981). Zur küstensenkrechten Struktur des Kaltwasserauftriebs vor der Küste Namibias. Geodat. Geophys. Veroff., ser. 4, vol. 36, pp. 1-99.
Halicz, E. and Z. Reiss (1981). Paleoecological relations of foraminifera in a desert-enclosed sea: the Gulf of Aqaba (Elat), Red Sea. Mar. Ecol., vol. 2, pp. 15-34.

Hastenrath, S. and P.J. Lamb (1977). Climatic atlas of the tropical Atlantic and eastern Pacific Ocean. Univ. Wisconsin Press, Michigan, 133 pp.
Hays, J.D., J. Imbrie and N.J. Shackleton (1976). Variations in the earth's orbit: pacemaker of the ice ages. Science, vol. 194, pp. 1121-1132.
Hays, J.D. and A. Perruzza (1972). The significance of calcium carbonate oscillations in eastern Equatorial Atlantic deep-sea sediments for the end of the Holocene warm interval. Quat. Res., vol. 2, pp. 355-362.
Heath, G.R., T.C. Moore and J.P. Dauphin (1977). Organic carbon in deep-sea sediments. In: N.R. Andersen and A. Malahoff (Eds.): The fate of fossil fuel CO2 in the oceans, Plenum Press, pp. 605-625.
Hecht, A.D. (1976). An ecologic model for test size variation in recent planktonic foraminifera: applications to the fossil record. Jour. Foram. Res., vol. 6, pp. 295-311.
Heezen, B.C., R.J. Menzies, E.D. Schneider, W.M. Ewing and N.C.L. Granelli (1964). Congo submarine canyon. Bull. Am. Ass. Petrol. Geol., vol. 48, pp. 1126-1149.
Herbland, A., R. Le Borgne, A. Le Bouteiller and B. Voituriez (1983). Structure hydrologique et production primaire dans l'Atlantique tropical oriental. Océanogr. Trop., vol. 18, pp. 223-248.
Herbland, A. and B. Voituriez (1979). Hydrological structure analysis for estimating the primary production in the tropical Atlantic Ocean. Jour. Mar. Res., vol. 37, pp. 87-101.
Honjo, S., S.J. Manganini and J.J. Cole (1982). Sedimentation of biogenic matter in the deep ocean. Deep-Sea Res., vol. 29, pp. 609-625.
Imbrie, J., J.D. Hays, D.G. Martinson, A. McIntyre, A.C. Mix, J.J. Morley, N.G. Pisias, W.L. Prell, and N.J. Shackleton (1984). The orbital theory of Pleistocene climate: support from a revised chronology of the marine d18O record. In: A.L. Berger, J. Imbrie, J. Hays, G. Kukla and B. Salzman: Milankovitch and climate, pt. I. NATO ASI series, C, vol. 126, pp. 269-305.
Jansen, J.H.F., T.C.E. van Weering, R. Gieles and J. van Iperen (1984). Middle and Late Quaternary oceanography and climatology of the Zaire-Congo fan and the adjacent eastern Angola Basin. Neth. Jour. Sea Res., vol. 17, pp. 201-249.
Jones, J.I. (1967). Significance of distribution of planktonic foraminifera in the Equatorial Atlantic Undercurrent. Micropal., vol. 13, pp. 489-501.
Kahn, M.I. (1981). Ecological and paleoecological implications of the phenotypic variation in three species of living planktonic foraminifera from the northeastern Pacific Ocean (50°N, 145°W). Jour. Foram. Res., vol. 11, pp. 203-211.
Keller, G. (1977). Morphologic variation of *Neogloboquadrina pachyderma* (Ehrenberg) in sediments of the marginal central northeast Pacific Ocean and paleoclimatic interpretation. Jour. Foram. Res., vol. 8, pp. 208-224.
Kellogg, T.B., J.C. Duplessy and N.J. Shackleton (1978). Planktonic foraminiferal and oxygen isotopic stratigraphy of Norwegian Sea deep-sea cores. Boreas, vol. 7, pp. 61-73.
Kennett, J.P. (1968). Latitudinal variation in *Globigerina pachyderma* (Ehrenberg) in surface sediments of the southwest Pacific Ocean. Micropal., vol. 14, pp. 305-318.
Kennett, J.P. and P. Huddlestun (1972). Late Pleistocene paleoclimatology, foraminiferal biostratigraphy and tephrochronology, western Gulf of Mexico. Quat. Res., vol.2, pp. 38-69.
Kerr, R.A. (1983). An early glacial two-step? Science, vol. 221, pp. 143-144.
Koblentz-Mishke, O.J., V.V. Volkovinsky and J.G. Kabanova (1970). Plankton primary production of the world ocean. In: W.S. Wooster (Ed.): Symp. Sci. Explor. South Pacific. Scripps Inst. Oceanogr., pp. 183-193.
Kouyoumontzakis, G. (1979). La microfauna bènthique du plateau congolais invèntaire, répartition, stratigraphie du Quaternaire supérieur, rapports avec le milieu sédimentaire. Thèse Univ. Provence, Marseille, 141 pp.
Leventer, A., D.F. Williams and J.P. Kennett (1983). Relationships between anoxia, glacial meltwater and microfossil preservation in the Orca Basin, Gulf of Mexico. Mar. Geol., vol. 53, pp. 23-40.
Lohmann, G.P. (1978). Abyssal benthonic foraminifera as hydrographic indicators in the western South Atlantic Ocean. Jour. Foram. Res., vol. 8, pp. 6-34.
Loubere, P. (1981). Oceanographic parameters reflected in the seabed distribution of planktic foraminifera from the North Atlantic and Mediterranean Sea. Jour. Foram. Res., vol. 11, pp. 137-158.
Lutze, G.F. (1977). Neogene benthonic foraminifera from Site 369, Leg 41, Deep Sea Drilling Project. In:

Y. Lancelot, E. Siebold et al. (Eds.): Init. Repts. DSDP, Leg 41. U.S. Govt. Printing Office, Washington, pp. 659-666.
Lutze, G.F. (1979). Benthic foraminifera at Site 397: faunal fluctuations and ranges in the Quaternary. In: U. von Rad, W.B.F. Ryan et al. (Eds.): Init. Repts. DSDP, Leg 47. U.S. Govt. Printing Office, Washington, pp. 419-425.
Lutze, G.F. (1980). Depth distribution of benthic foraminifera on the continental margin off NW Africa. Meteor Forsch. Ergeb., ser. C, vol. 32, pp. 31-80.
Lutze, G.F. and W.T. Coulbourn (1984). Recent benthic foraminifera from the continental margin of Northwest Africa: community structure and distribution. Marine Micropal., vol. 8, pp. 361-401.
Lutze, G.F. (1986). *Uvigerina* species of the eastern North Atlantic. In: G.J. van der Zwaan, F.J. Jorissen, P.J.J.M. Verhallen and C.H. von Daniels (Eds.): Atlantic-European Oligocene to Recent Uvigerina. Utr. Micropal. Bull., vol. 35, pp. 47-66.
Lutze, G.F., U. Pflaumann and P. Weinholz (1986). Late Pleistocene faunal fluctuation of deep sea benthic foraminifera: a response to fertility changes in the surface water. Abstr. 3d Intern. Symp. on benthic foraminifera, Geneva, p. 46.
Lutze, G.F., M. Sarnthein, B. Koopmann and U. Pflaumann (1979). Meteor cores 12309: Late Pleistocene reference section for interpretation of the Neogene of Site 397. In: U. von Rad, W.B.F. Ryan et al. (Eds.): Init. Repts. DSDP, Leg 47. U.S. Govt. Printing Office, Washington, pp. 727-739.
Mackensen, A., H.P. Sejrup and E. Jansen (1985). The distribution of living benthic foraminifera on the continental slope and rise off southwest Norway. Marine Micropal., vol. 9, pp. 275-306.
Malmgren, B and J.P. Kennett (1972). Biometric analysis of phenotypic variation: *Globigerina pachyderma* (Ehrenberg) in the South Pacific Ocean. Micropal., vol. 18, pp. 241-248.
Malmgren, B and J.P. Kennett (1977). Biometric differentiation between recent *Globigerina bulloides* and *Globigerina falconensis* in the southern Indian Ocean. Jour. Foram. Res., vol. 7, pp. 130-148.
Mantyla, A.W. and J.L. Reid (1983). Abyssal characteristics of the world ocean waters. Deep-Sea Res., vol. 30, pp. 805-833.
Mazeika, P.A. (1968). Mean monthly sea surface temperatures and zonal anomalies of the tropical Atlantic. Serial atlas of the marine environment, folio 16, Am. Geogr. Soc.
Mayr, E. (1976). Populations, species and evolution. Harvard Univ. Press, Cambridge, Mass., 453 pp.
Mellor, G.L., C.R. Mechoso and E. Keto (1982). A diagnostic calculation of the general circulation of the Atlantic Ocean. Deep-Sea Res., vol. 29, pp. 1171-1192.
Metzler, C.V., C.R. Wenkam and W.H. Berger (1982). Dissolution in the eastern Equatorial Pacific: an *in situ* experiment. Jour. Foram. Res., vol. 12, pp. 362-368.
Miller, K.G. and G.P. Lohmann (1982). Environmental distribution of recent benthic foraminifera on the northeast United States continental slope. Geol. Soc. Am. Bull., vol. 93, pp. 200-206.
Mix, A.C. and R.G. Fairbanks (1985). North Atlantic surface-ocean control of Pleistocene deep-ocean circulation. Earth Plan. Sc. Lett., vol. 73, pp. 231-243.
Mix, A.C. and W.F. Ruddiman (1985). Structure and timing of the last deglaciation: oxygen-isotope evidence. Quat. Sc. Rev., vol. 4, pp. 59-108.
Mix, A.C., W.F. Ruddiman and A. McIntyre (1986a). Late Quaternary paleoceanography of the tropical Atlantic, 1: spatial variability of annual mean sea-surface temperatures, 0-20,000 years B.P.. Paleoceanogr., vol. 1, pp. 43-66.
Mix, A.C., W.F. Ruddiman and A. McIntyre (1986b). Late Quaternary paleoceanography of the tropical Atlantic, 2: the seasonal cycle of sea surface temperatures, 0-20,000 years B.P.. Paleoceanogr., vol. 1, pp. 339-353.
Moroshkin, K.V., V.A. Bubnov and R.P. Bulatov (1970). Water circulation in the eastern South Atlantic Ocean. Oceanology, vol. 10, pp. 27-34.
Müller, P.J. and E. Suess (1979). Productivity, sedimentation rate, and sedimentary organic matter in the oceans (1): Organic carbon preservation. Deep-Sea Res., vol. 26, pp. 1347-1362.
Murray, J.W. (1973). Distribution and ecology of living benthic foraminiferids. Heinemann, London, 274 pp.
Ninkovich, D. and N.J. Shackleton (1975). Distribution, stratigraphic position and age of ash-layer 'L', in the Panama Basin regio. Earth. Plan. Sc. Lett., vol. 27, pp. 20-34.

Olausson, E. (1960). Description of sediment cores from the North Atlantic. Rept. Swedish Deep-Sea Exped. 1947-1948, vol. 7, pp. 229-286.
Olausson, E. (1965). Evidence of climatic changes in North Atlantic deep-sea cores, with remarks on isotopic paleotemperature analysis. Progr. Oceanog., vol. 3, pp. 221-252.
Olausson, E. (1982). General comments on the Pleistocene/Holocene boundary. In: E. Olausson (Ed.): The Pleistocene/Holocene boundary in southwestern Sweden. Sver. Geol. Unders., Afh. (ser. C), vol. 794, pp. 10-15.
Olausson, E. (1984). Oxygen and carbon isotope analysis of a Late Quaternary core in the Zaire (Congo) fan. Neth. Jour. Sea. Res., vol. 17, pp. 276-279.
Olausson, E. (1985). The glacial oceans. Palaeogeogr., -clim, -ecol., vol. 50, pp. 291-301.
Orr, W.N. (1969). Variation and distribution of *Globigerinoides ruber* in the Gulf of Mexico. Micropal., vol. 15, pp. 373-379.
Oyama, M. and H. Takehara (1970). Revised standard soil color charts.
Parker, F.L. (1971). Distribution of planktonic foraminifera in recent deep-sea sediments. In: B.M. Funnell and W.R. Riedel (Eds.): The micropaleontology of oceans. Cambridge Univ. Press, pp. 289-307.
Parker, F.L. and W.H. Berger (1971). Faunal and solution patterns of planktonic foraminifera in surface sediments of the South Pacific. Deep-Sea Res., vol. 18, pp. 73-107.
Peterson, L.C. and G.P. Lohmann (1982). Major change in Atlantic deep and bottom waters 700,000 yr ago: benthonic foraminiferal evidence from the South Atlantic. Quat. Res., vol. 17, pp. 26-38.
Peterson, L.C. and W.L. Prell (1985). Carbonate dissolution in recent sediments of the eastern Equatorial Indian Ocean: preservation patterns and carbonate loss above the lysocline. Mar. Geol., vol. 64, pp. 259-290.
Pflum, C.E. and W.E. Frerichs (1976). Gulf of Mexico deep-water foraminifers. Cushm. Found. Foram. Res., Spec. Publ., vol 14, 125 pp.
Phleger, F.B. (1960). Ecology and distribution of recent foraminifera. John Hopkins Press, Baltimore, 297 pp.
Phleger, F.B., F.L. Parker and J.F. Peirson (1953). North Atlantic foraminifera. Repts. Swed. Deep-Sea Exped., vol. 7(1), pp. 1-122.
Phleger, F.B. and A. Soutar (1973). Production of benthonic foraminifera in the eastern Pacific. In: M. Sears (Ed.): Progress in oceanography, vol. 3, Pergamon Press, pp. 273-287.
Piton, B., Y. Montel and J.P. Gausi (1978). Compte-rendue des campagnes par le N.O. Nizery effectuées de mars à septembre dans le sud-est du Golfe de Guinée. Doc. Scient. Centre Rech. Océanogr. Pointe Noire, vol. 623, pp. 1-9.
Poag, C.W. (1981). Ecologic atlas of benthic foraminifera of the Gulf of Mexico. Marine Science Intern., Woods Hole, 162 pp.
Pokras, E. (1987). Diatom record of Late Quaternary climatic change in the eastern equatorial Atlantic and tropical Africa. Paleoceanogr., vol. 2, pp. 273-286.
Prell, W.L. and W.B. Curry (1981). Faunal and isotopic indices of monsoonal upwelling: western Arabian Sea. Oceanol. Acta, vol. 4, pp. 91-98.
Prell, W.L. and J.E. Damuth (1978). The climate-related diachronous disappearance of *Pulleniatina obliquiloculata* in Late Quaternary sediments of the Atlantic and Caribbean. Marine Micropal., vol. 3, pp. 267-277.
Prell, W.L. and J.D. Hays (1976). Late Pleistocene faunal and temperature patterns in the Colombia Basin, Caribbean Sea. Mem. Geol. Soc. Am., vol. 145, pp. 201-220.
Pujol, C. (1980). Les foraminifères planctoniques de l'Atlantique Nord au Quaternaire. Ecologie-stratigraphie-environnement. Mém. Inst. Geol. Bassin Aquitaine, vol 10, pp. 1-254.
Reiss, Z., E. Halicz and L. Perelis (1974). Planktonic foraminifera from recent sediments in the Gulf of Elat. Isr. Jour. Earth Sc., vol. 23, pp. 69-105.
Rex, M.A. (1976). Biological accommodation in the deep-sea benthos: comparative evidence on the importance of predation and productivity. Deep-Sea Res., vol. 23, pp. 975-987.
Rowe, G.T. (1981). The deep-sea ecosystem. In: A.R. Longhurst (Ed.): Analysis of marine ecosystems, Academic Press, New York, pp. 235-267.
Ruddiman, W.F. and J.-C. Duplessy (1985). Conference on the last deglaciation: timing and mechanism. Quat. Res., vol. 23, pp. 1-17.

Ruddiman, W.F. and A. McIntyre (1976). Northeast Atlantic paleoclimatic changes over the past 600,000 years. Mem. Geol. Soc. Am., vol 145, pp. 111-146.
Sarmiento, J.L. and J.R. Toggweiler (1984). A new model for the role of the oceans in determining atmospheric pCO2. Nature, vol. 308, pp. 621-624.
Sarnthein, M., J. Thiede, U. Pflaumann, H. Erlenkeuser, D. Fütterer, B. Koopmann, H. Lange and E. Siebold (1982). Atmospheric and oceanic circulation patterns off northwest Africa during the past 25 million years. In: U. von Rad, K. Hinz, M. Sarnthein and E. Siebold (Eds.): Geology of the northwest African continental margin, Springer Verlag, pp. 545-604.
Sarnthein, M., K. Winn and R. Zahn (1987). Paleoproductivity of oceanic upwelling and the effect on atmospheric CO2 and climatic change during deglaciation times. In: W.H. Berger and L.D. Labeyrie (Eds.): Abrupt climatic change, Reidel Publ. Co., pp. 311-337.
Schott, W. (1935). Die Foraminiferen in dem aequatorialen Teil des Atlantischen Ozeans. Deutsch. Atl. Exped. 'Meteor' 1925-1927, Wiss. Ergeb., vol. 3, pp. 43-134.
Schnitker, D. (1974). West Atlantic abyssal circulation during the past 120,000 years. Nature, vol. 248, pp. 385-387.
Schnitker, D. (1979). The deep waters of the western North Atlantic during the past 24,000 years, and the re-initiation of the western boundary undercurrent. Marine Micropal., vol. 4, pp. 265-280.
Schnitker, D. (1980). Quaternary deep-sea benthic foraminifers and bottom water masses. An. Rev. Earth. Planet. Sci., vol. 8, pp. 343-370.
Schrader, H., Guangfen Cheng and R. Mahood (1983). Preservation and dissolution of foraminiferal carbonate in an anoxic slope environment, southern Gulf of California. In: J.E. Meulenkamp (Ed.): Reconstruction of marine paleoenvironments. Utr. Micropal. Bull., vol. 30, pp. 205-228.
Sen Gupta, B.K., T.J. Temples and M.D. Gilmore Dallmeyer (1982). Late Quaternary benthic foraminifera of the Grenada Basin: stratigraphy and paleoceanography. Marine Micropal., vol. 7, pp. 297-309.
Shackleton, N.J. (1977). Carbon-13 in Uvigerina: tropical rainforest history and the Equatorial Pacific carbonate dissolution cycles. In: N.R. Andersen and A. Malakoff (Eds.): Fate of fossil fuel CO2 in the oceans, Plenum Press, pp. 401-427.
Shackleton, N.J., M.A. Hall, J. Line and Cang Shuzi (1983a). Carbon isotope data in core V19-30 confirm reduced carbon dioxide concentration in the ice age atmosphere. Nature, vol. 306, pp. 319-322.
Shackleton, N.J., J. Imbrie and M.A. Hall (1983b). Oxygen and carbon isotope record of East Pacific core V19-30: implications for the formation of deep water in the late Pleistocene North Atlantic., Earth Plan. Sc. Lett., vol. 65, pp. 233-244.
Shepard, F.P. and K.O. Emery (1973) Congo submarine canyon and fan valley. Bull. Am. Ass. Petrol. Geol., vol. 57, pp. 1679-1691.
Siegenthaler, U. and T. Wenk (1984). Rapid atmospheric CO2 variations and ocean circulation. Nature, vol. 308, pp. 624-626.
Smith, K.L. Jr. and G.A. White (1982). Ecological energetic studies in the deep-sea benthic boundary layer: *in situ* respiration studies. In: W.G. Ernst and J.G. Morrin (Eds.): The environment of the deep sea, Prentice-Hall, pp. 279-300.
Srinivasan, M.S. and J.P. Kennett (1976). Evolution and phenotypic variation in the Late Cenozoic *Neogloboquadrina dutertrei* plexus. Progress in Micropaleontology, pp. 329-355.
Steemann Nielsen, E. and E. Aabye Jensen (1957). Primary oceanic production. The autotrophic production of organic matter in the oceans. Galathea Rept., vol. 1, pp. 49-124.
Streeter, S.S. (1973). Bottom water and benthonic foraminifera in the North Atlantic: glacial-interglacial contrasts. Quat. Res., vol. 3, pp. 131-141.
Streeter, S.S., P.E. Belanger, T.B. Kellogg and J.-C. Duplessy (1982). Late Pleistocene paleo-oceanography of the Norwegian-Greenland Sea: benthic foraminiferal evidence. Quat. Res., vol. 18, pp. 72-90.
Streeter, S.S. and S.A. Lavery (1982). Holocene and latest glacial benthic foraminifera from the slope and rise off eastern North America. Geol. Soc. Am. Bull., vol. 93, p. 190-199.
Streeter, S.S. and N.J. Shackleton (1979). Paleocirculation of the deep North Atlantic: 150,000-year record of benthic foraminifera and oxygen-18. Science, vol. 203, pp. 168-171.
Tchernia, P. (1980). Descriptive regional oceanography. Pergamon Press, 253 pp.
Thiede, J. (1975). Distribution of foraminifera in surface waters of a coastal upwelling area. Nature, vol. 253, pp. 712-714.

Thiede, J. (1983). Skeletal plankton and nekton in upwelling water masses off northwestern South America and northwest Africa. In: E. Suess and J. Thiede (Eds.): Coastal Upwelling, pt. A., Plenum Publishing Corp., pp. 183-207.

Thunell, R.C. (1978). Distribution of recent foraminifera in surface sediments of the Mediterranean Sea. Marine Micropal., vol. 3, pp. 147-173.

Thunell, R.C. (1982). Carbonate dissolution and abyssal hydrography in the Atlantic Ocean. Mar. Geol., vol. 47, pp. 165-180.

Thunell, R.C. and L.A. Reynolds (1984). Sedimentation of planktonic foraminifera: seasonal changes in species flux in the Panama Basin. Micropal., vol. 30, pp. 243-262.

Troelstra, S.R. (1984). Foraminiferal studies on cores from the Madeira Abyssal Plain, eastern North Atlantic. In: A. Kuijpers, R.T.E. Schüttenhelm and J.W. Verbeek (Eds.): Geological studies in the eastern North Atlantic, Meded. Geol. Dienst, vol. 38, pp. 153-168.

Van Bennekom, A.J. and G.W. Berger (1984). Hydrography and silica budget of the Angola Basin. Neth. Jour. Sea Res., vol. 17, pp. 149-200.

Van Bennekom, A.J., G.W. Berger, W. Helder and R.T.P. de Vries (1978). Nutrient distribution in the Zaire estuary and river plume. Neth. Jour. Sea Res., vol. 12, pp. 296-323.

Van der Gaast, S.J. and J.H.F. Jansen (1984). Mineralogy, opal, and manganese of Middle and Late Quaternary sediments of the Zaire (Congo) deep-sea fan: origin and climatic variation. Neth. Jour. Sea Res., vol. 17, pp. 313-341.

Van der Zwaan, G.J. (1982). Paleoecology of Late Miocene Mediterranean foraminifera. Utr. Micropal. Bull., vol. 25, 202 pp.

Van Donk, J. (1976). O18 record of the Atlantic Ocean for the entire Pleistocene Epoch. Mem. Geol. Soc. Am., vol. 145, pp. 201-220.

Van Leeuwen, R.J.W. (1986). The distribution of *Uvigerina* in the Late Quaternary sediments of the deep eastern South Atlantic. In: G.J. van der Zwaan, F.J. Jorissen, P.J.J.M. Verhallen and C.H. von Daniels (Eds.): Atlantic-European Oligocene to Recent Uvigerina. Utr. Micropal. Bull., vol. 35, pp. 47-66.

Van Weering, T.C.E. and J. van Iperen (1984). Fine-grained sediments of the Zaire deep-sea fan, southern Atlantic Ocean. In: D.A.V. Stow and D.J.W. Piper (Eds.): Fine-grained sediments, deep water processes and facies. Geol. Soc. Spec. Publ., vol. 15, pp. 95-113.

Van Zinderen Bakker, E.M. (1976). The evolution of late Quaternary palaeoclimates of southern Africa. In: E.M. van Zinderen Bakker (Ed.): Palaeoecology of Africa, the surrounding islands and Antarctica, vol. 9, Balkema, Cape Town, pp. 160-202.

Voituriez, B. and A. Herbland (1981). Primary production in the tropical Atlantic Ocean mapped from oxygen values of Equalant 1 and 2 (1963). Bull. Mar. Sc., vol. 31, pp. 853-863.

Voituriez, B. and A. Herbland (1982). Comparaison des systèmes productifs de l'Atlantique Tropical Est: domes thermiques, upwellings côtiers et upwelling équatorial. Rapp. P.-v. Réun. Cons. Int. Explor. Mer, vol. 180, pp. 114-130.

Voituriez, B. and A. Herbland (1984). Signification de la relation nitrate/temperature dans l'upwelling équatorial du Golfe de Guinée. Oceanol. Acta, vol. 7, pp. 169-174.

Voituriez, B., A. Herbland and R. Le Borgne (1982). L'upwelling équatorial de l'Atlantique est pendant l'expérience météorologique mondiale (PEMG). Oceanol. Acta, vol 5, pp. 301-314.

Volat, J.-L., L. Pastouret and C. Vergnaud-Grazzini (1980). Dissolution and carbonate fluctuations in Pleistocene deep-sea cores: a review. Mar. Geol., vol. 34, pp. 1-28.

Walsh, J.J. (1976). Herbivory as a factor in patterns of nutrient utilization in the sea. Limnol. Oceanogr., vol. 21, pp. 1-13.

Wauthy, B. (1977). Révision de la classification des eaux de surface du Golfe de Guinée (Berrit, 1961). Cah. ORSTOM, sér. Océanogr., vol. 15, pp. 279-295.

Weston, J. F. and J.W. Murray (1984). Benthic foraminifera as deep-sea water-mass indicators. In: H.J. Oertli (Ed.): Benthos '83, 2nd Int. Symp. on benthic foraminifera (Pau, April 1983), Elf Aquitaine, Esso REP and Total CFP, Pau and Bordeaux, pp. 605-610.

Williams, D.F. (1984). Correlation of Pleistocene marine sediments in the Gulf of Mexico and other basins using oxygen isotope stratigraphy. In: N. Healy-Williams (Ed.): Principles of Pleistocene stratigraphy applied to the Gulf of Mexico. Reidel Publ. Co., pp. 65-118.

Williams, D.F., A.W.H. Bé and R.G. Fairbanks (1981). Seasonal stable isotopic variation in living planktonic foraminifera from Bermuda plankton tows. Palaeogeogr., -clim., -ecol., vol. 38, pp. 71-102.
Wooster, W.S., A. Bakun and D.R. McLain (1976). The seasonal upwelling cycle along the eastern boundary of the North Atlantic. J. Mar. Res., vol. 34, pp. 131-141.
Wright, S.H. and G.C. Stephens (1982). Transepidermal transport of amino acids in the nutrition of marine invertebrates. In: W.G. Ernst and J.G. Morrin (Eds.): The environment of the deep sea, Prentice-Hall, pp. 301-323.
Zachariasse, W.J. (1975). Planktonic foraminiferal biostratigraphy of the Late Neogene of Crete (Greece). Utr. Micropal. Bull., vol. 11, 171 pp.
Zachariasse, W.J., R.R. Schmidt and R.J.W. van Leeuwen (1984). Distribution of foraminifera and calcareous nannoplankton in Quaternary sediments of the eastern Angola Basin in response to climatic and oceanic fluctuations. Neth. Jour. Sea Res., vol. 17, pp. 250-275.
Zhang, J. (1985). Living planktonic foraminifera from the eastern Arabian Sea. Deep-Sea Res., vol. 32, pp. 789-798.
Zobel, B. and U. Ranke (1978). Zusammensetzung, Stratigraphie und Bildungsbedingungen der Sedimente am Kontinentalabhang vor Sierra Leone (Westafrika). Meteor Forsch. Ergeb., ser. C, vol. 29, pp. 21-74.

Plate 1

Fig. 1 *Globigerina bulloides*, sample T80-27/top.
Fig. 2 *Globigerina bulloides*, sample VM19-260/top.
Fig. 3 *Globigerina bulloides*, sample CHN99-33/top.
Fig. 4 *Globigerina falconensis*, sample T80-25/top.
Fig. 5 *Globigerina falconensis*, sample T80-25/top.
Fig. 6 *Globigerinita glutinata*, sample VM22-174/top.
Fig. 7 *Globigerinella siphonifera*, sample T80-24/top.
Fig. 8 *Globigerinella siphonifera*, sample T80-24/top.
Fig. 9 *Globigerinita glutinata*, sample VM22-174/top.

All magnifications x100.

Plate 1

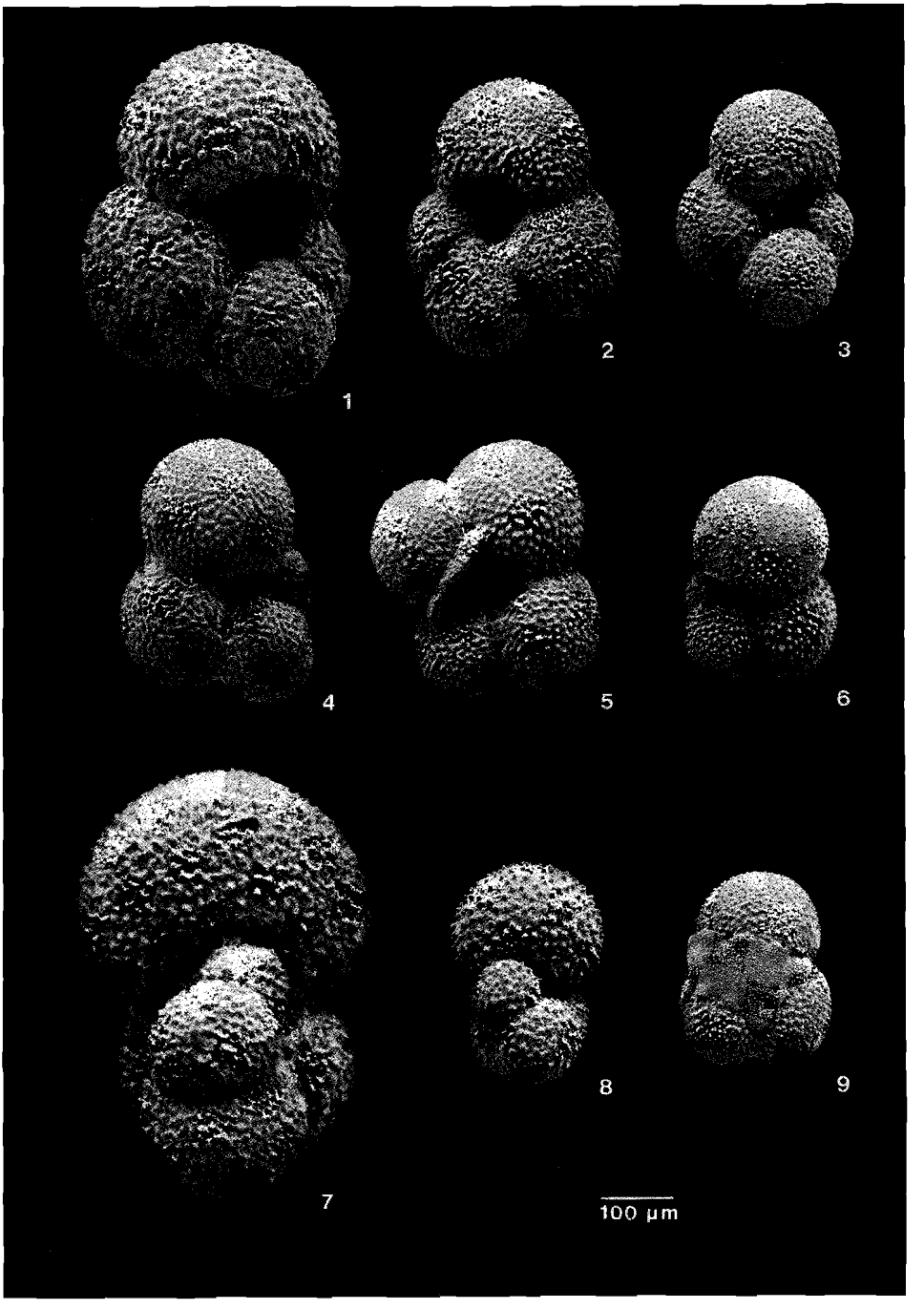

Plate 2

Fig. 1 *Globigerinoides ruber, ruber* type, sample VM22-174/top.
Fig. 2 *Globigerinoides ruber, ruber* type, sample VM22-174/top.
Fig. 3 *Globigerinoides ruber, elongatus* type, sample T80-24/top.
Fig. 4 *Globigerinoides trilobus*, sample VM22-174/top.
Fig. 5 *Sphaeroidinella dehiscens*, sample VM22-174/top.
Fig. 6 *Pulleniatina obliquiloculata*, sample VM22-174/top.
Fig. 7-9 *Globorotalia crassaformis*, sample CHN99-32/top.

All magnifications x50, except figs. 1-3 (x100)

Plate 2

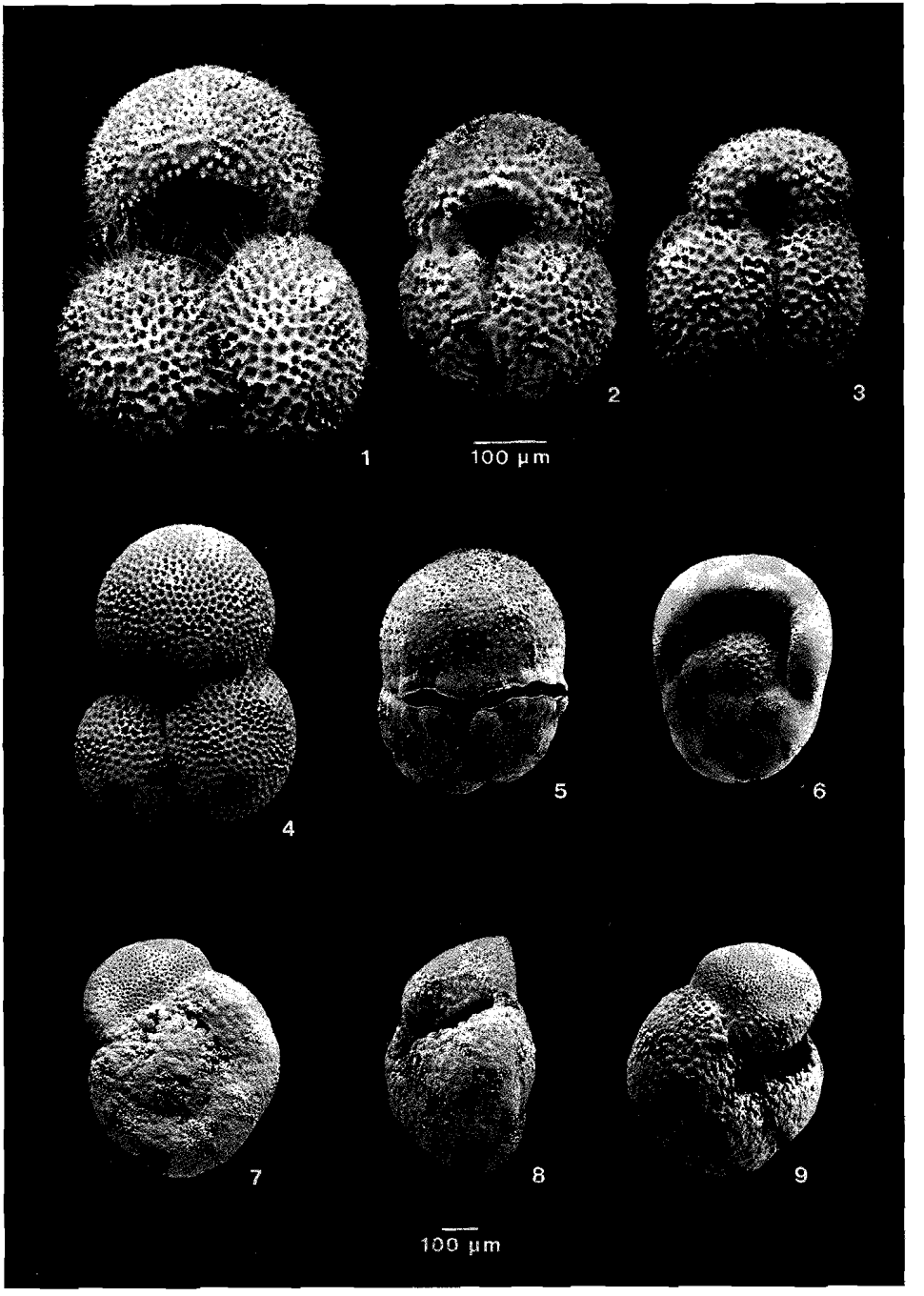

Plate 3

Figs. 1-3 *Globorotalia hirsuta,* sample T80-24/top.
Figs. 4-6 *Globorotalia inflata,* sample T80-27/top.
Figs. 7-9 *Globorotalia scitula,* sample T80-24/top.

All magnifications x100, except figs. 1-3 (x50)

Plate 3

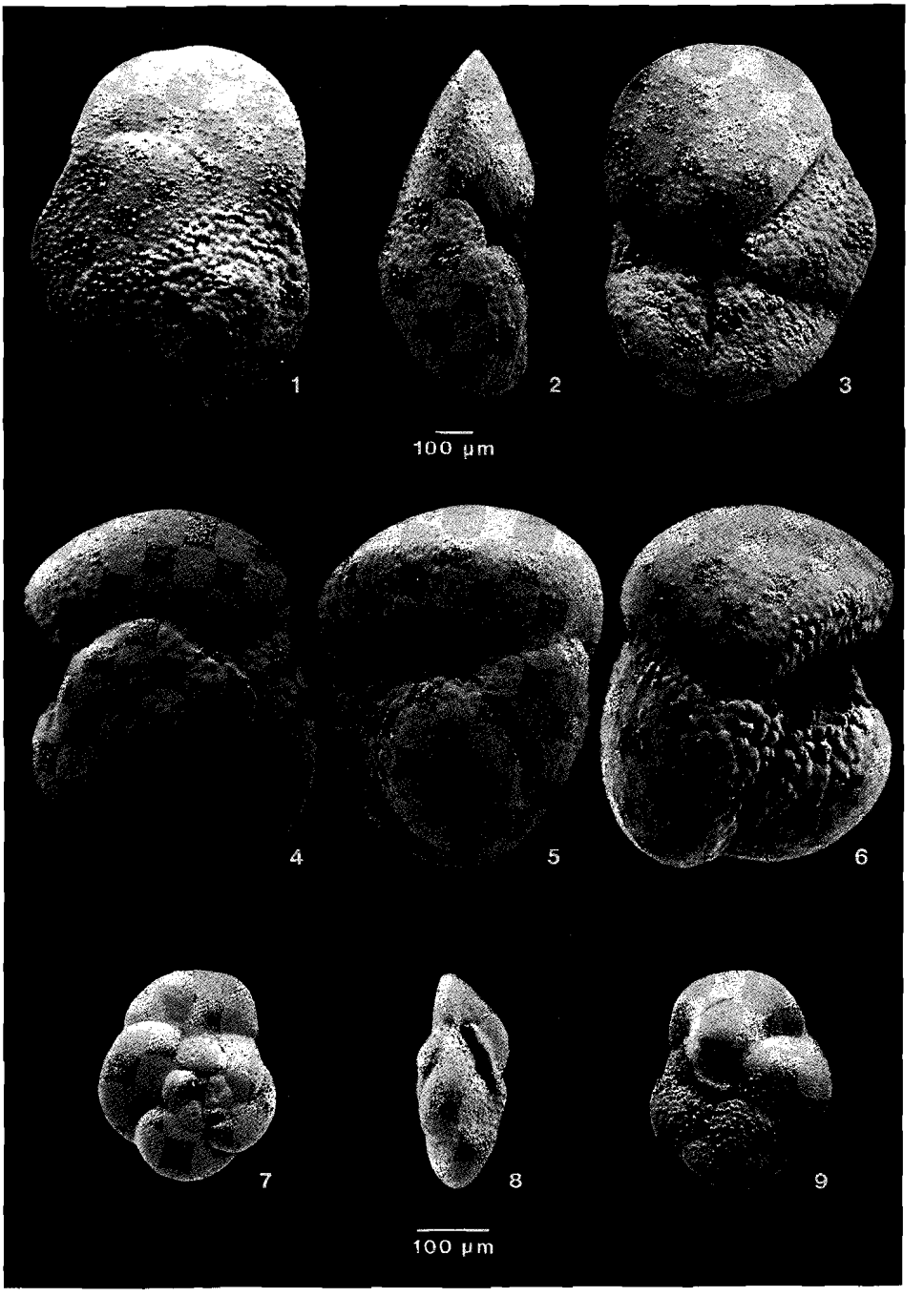

Plate 4

Figs. 1,4 *Globorotalia menardii, menardii* type, sample RC13-212/top.
Figs. 2,5 *Globorotalia menardii, tumida* type, sample RC13-212/top.
Figs. 3,6 *Globorotalia menardii, flexuosa* type, sample VM29-143/26.
Figs. 7-9 *Globorotalia truncatulinoides*, right-coiling type, sample T80-24/top.

All magnifications x50

Plate 4

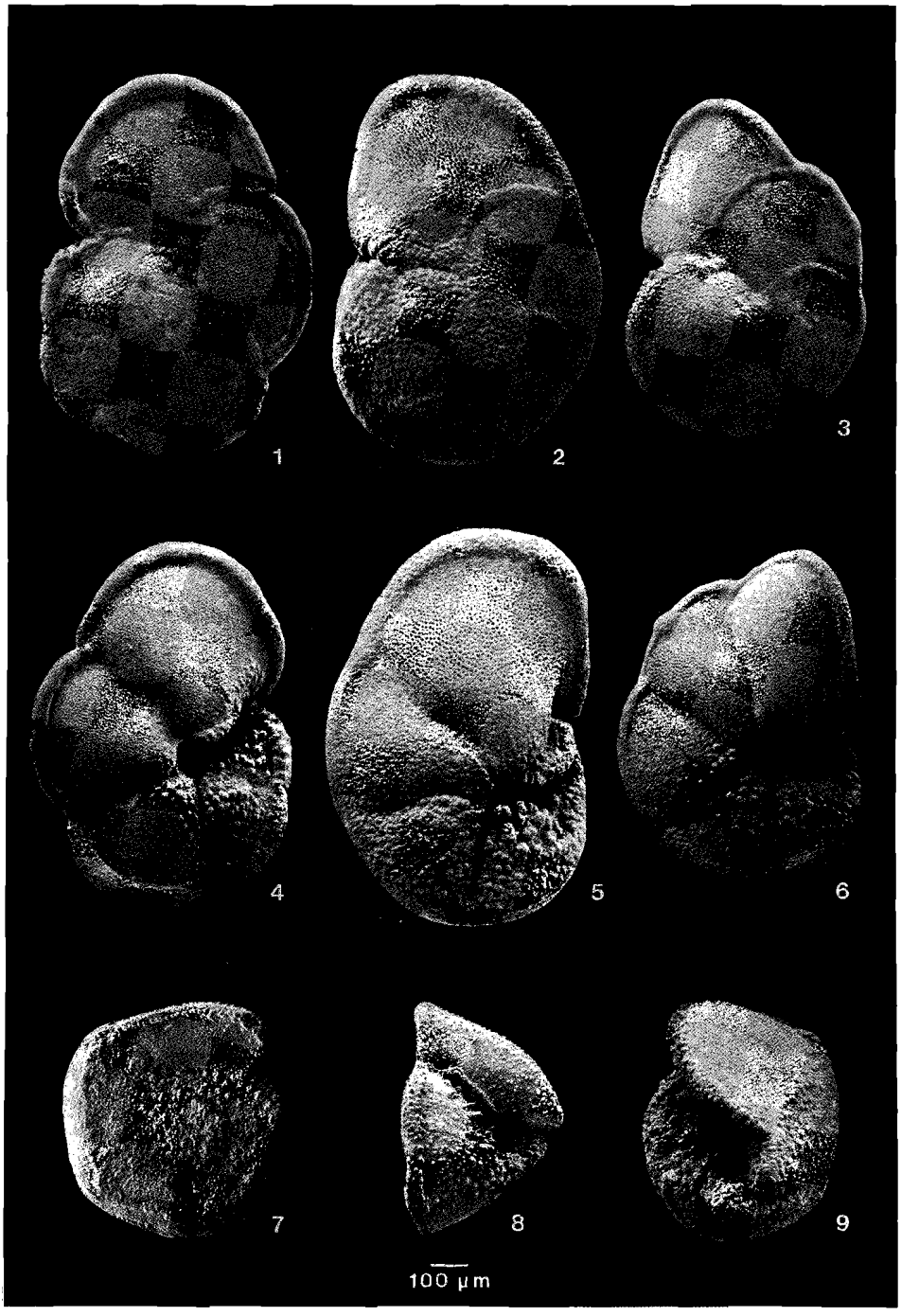

Plate 5

Figs. 1,2 *Neogloboquadrina pachyderma*, left-coiling type, sample T80-10/26.
Figs. 3,4 *Neogloboquadrina pachyderma*, left-coiling type, sample T80-10/26.
Figs. 5,6 *Neogloboquadrina pachyderma*, right-coiling type, sample T80-25/top.
Figs. 7,8 *Neogloboquadrina pachyderma*, right-coiling type, sample T80-25/top.
Figs. 9,10 *Neogloboquadrina dutertrei*, sample CHN99-30/top.

All magnifications x100

Plate 5

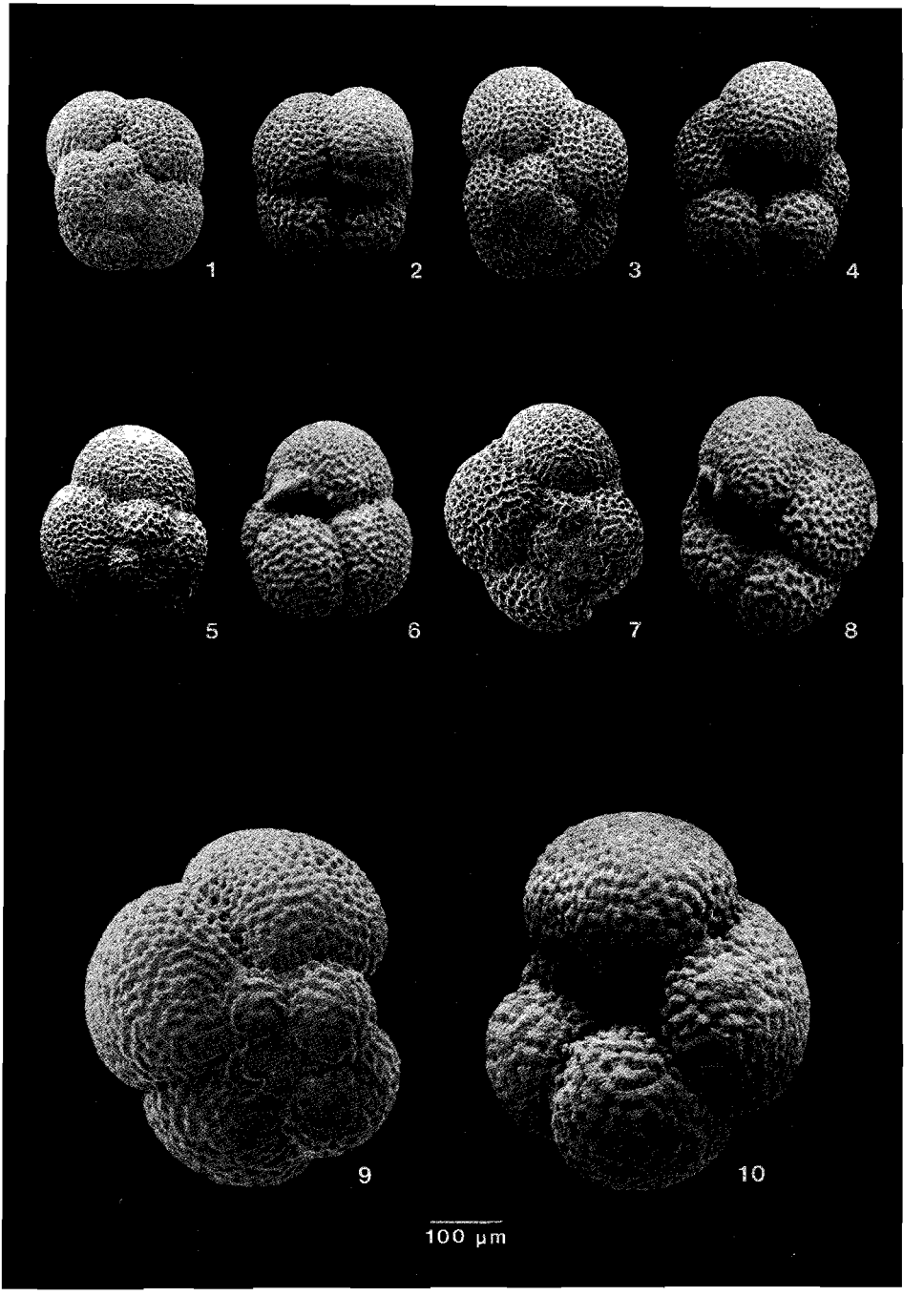

Plate 6

Figs. 1,2 *Neogloboquadrina dutertrei*, sample CHN99-30/top.
Figs. 3-5 *Globorotaloides hexagonus*, sample T80-10/40.
Fig. 6 *Orbulina universa*, sample VM22-174/top.
Fig. 7 *Orbulina universa*, sample T80-10/20.

All magnifications x100

Plate 6

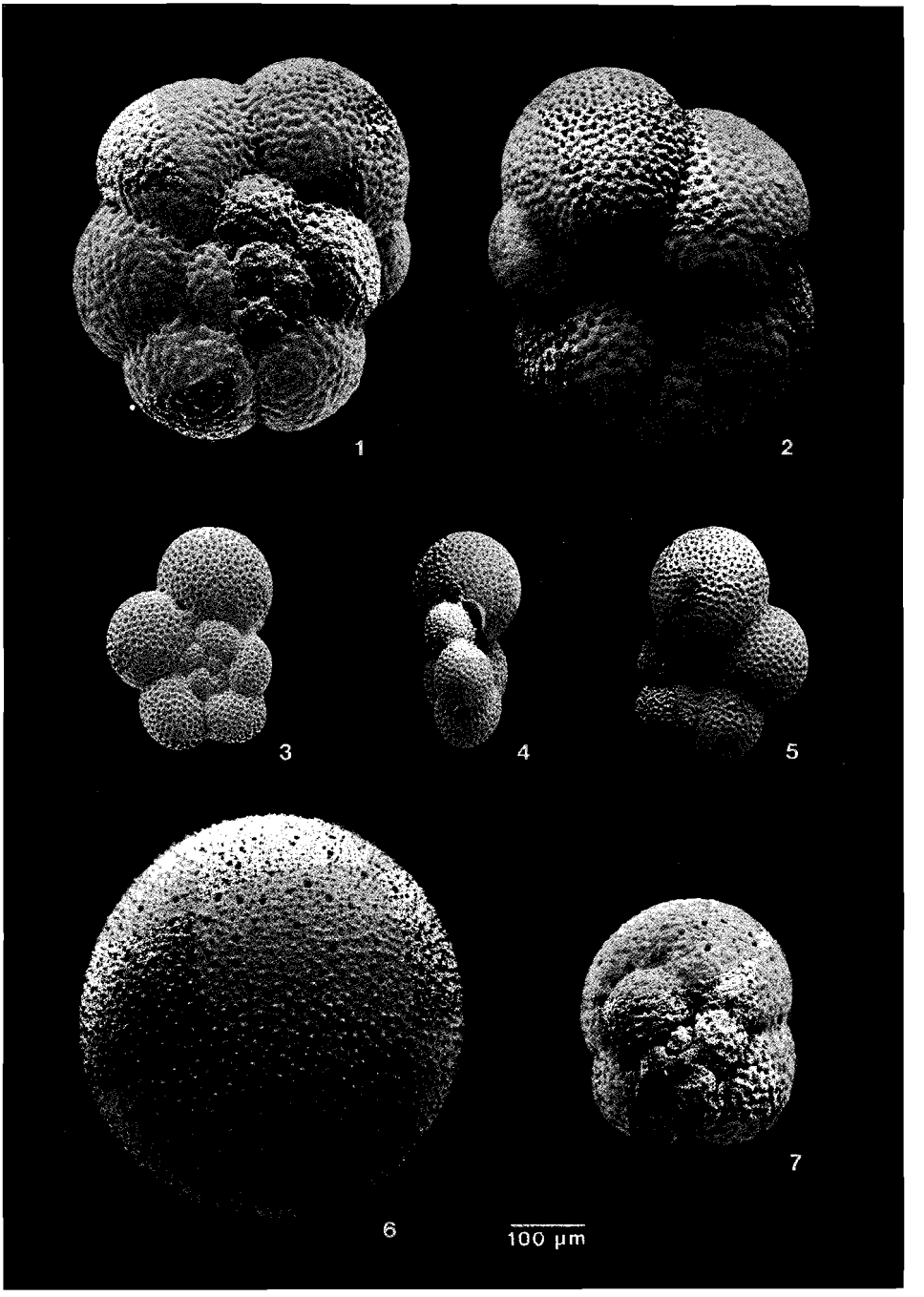

Plate 7

Figs. 1-3 *Anomalinoides minimus*, sample KW26/25.
Figs. 4,5 *Astrononion* sp., sample T80-34/top.
Fig. 6 *Bulimina gibba*, sample T78-23/top.
Fig. 7 *Bulimina aculeata*, sample T80-10/26.
Fig. 8 *Bulimina aculeata*, sample T80-10/26.
Fig. 9 *Bulimina aculeata*, sample T80-10/26.

All magnifications x100, except figs. 1-3 (x200)

Plate 7

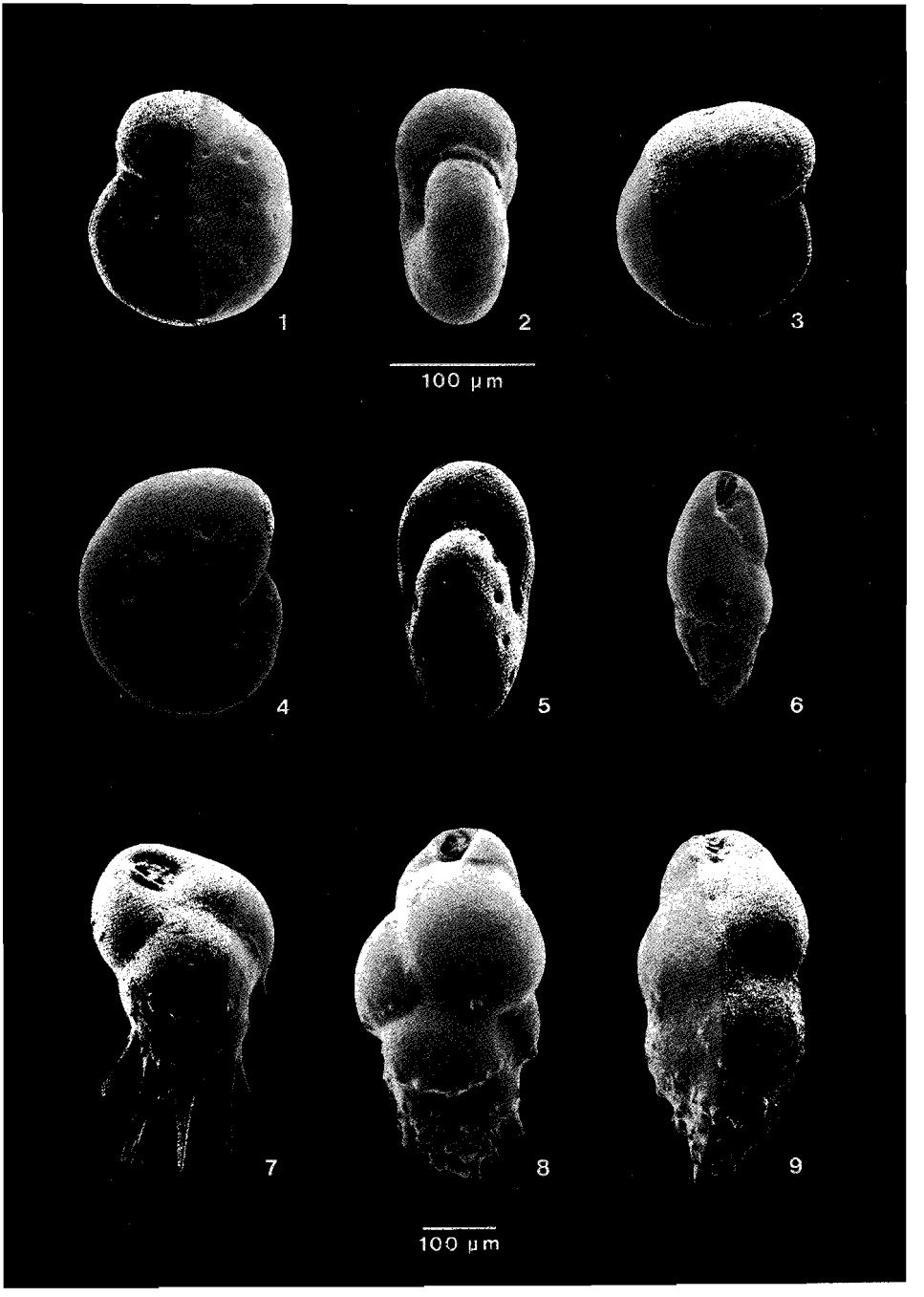

Plate 8

Fig. 1 *Bulimina rostrata,* sample T80-34/top.
Fig. 2 *Bulimina costata,* sample T78-25/top.
Fig. 3 *Bulimina costata,* sample T78-26/top.
Fig. 4 *Bulimina inflata,* sample RC13-220/top.
Fig. 5 *Bulimina subacuminata,* sample RC13-225/top.
Fig. 6 *Bulimina marginata,* sample T78-23/top.
Fig. 7 *Bulimina translucens,* sample RC17-034/top.
Fig. 8 *Cassidulina carinata,* sample T78-25/top.
Fig. 9 *Cassidulina crassa minima,* sample VM19-283/5.
Fig. 10 *Cassidulina crassa minima,* sample VM19-283/5.
Fig. 11 *Globocassidulina subglobosa,* sample T80-34/top.

All magnifications x100, except fig. 7 (x200)

Plate 8

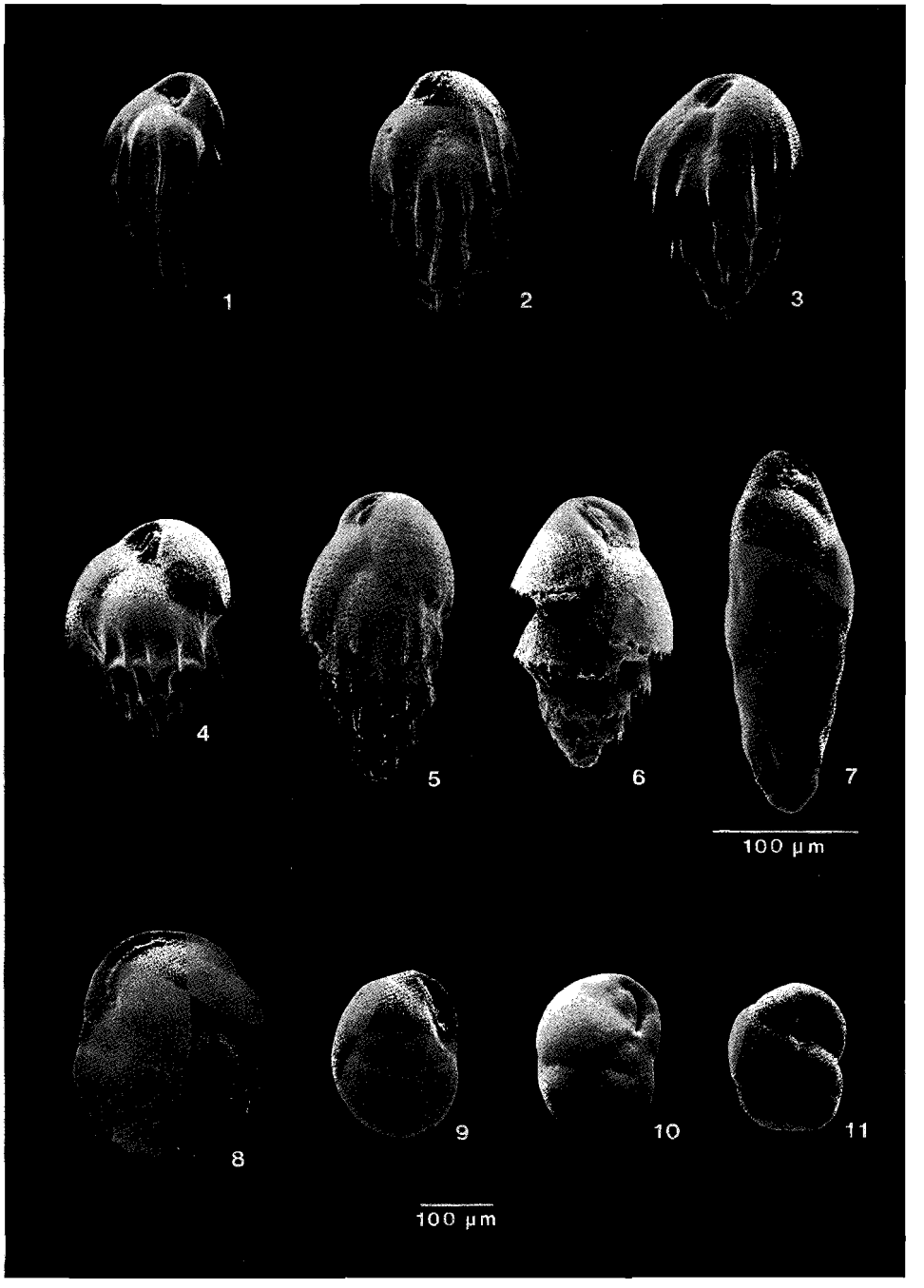

Plate 9

Figs. 1-3 *Cibicides kullenbergi*, sample RC13-074/top.
Figs. 4-6 *Cibicides* cf. *robertsonianus*, sample T80-3/top.
Figs. 7-9 *Cibicides robertsonianus bradyi*, sample RC17-033/top.

All magnifications x100

Plate 9

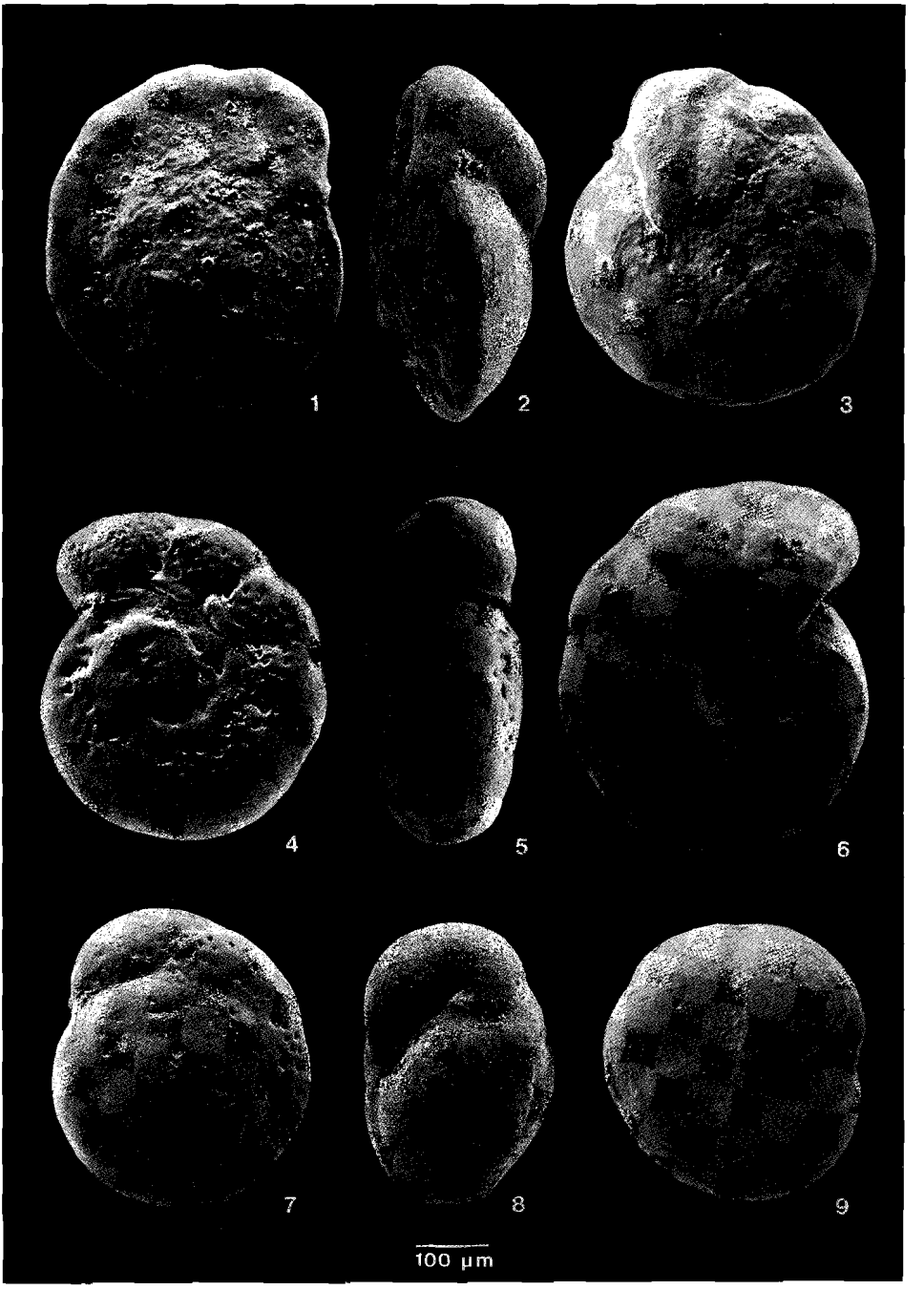

Plate 10

Figs. 1-3 *Cibicides wuellerstorfi* s.s., sample RC13-209/top.
Figs. 4-6 *Cibicides wuellerstorfi* s.s., sample VM27-239/top.
Figs. 7-9 *Cibicides wuellerstorfi* var., sample VM27-239/top.

All magnifications x50

Plate 10

Plate 11

Figs. 1-3 *Epistominella exigua* 1, sample T80-24/top. Magnification x100.
Figs. 4,5 *Epistominella exigua* 2, sample T80-24/top. Magnification x200.
Fig. 6 *Epistominella exigua* 2, sample T80-28/top. Magnification x200.
Figs. 7-9 *Eponides tumidulus*, sample VM19-283/24. Magnification x200.
Fig. 10 *Fursenkoina bradyi*, sample VM19-283/7. Magnification x50.

Plate 11

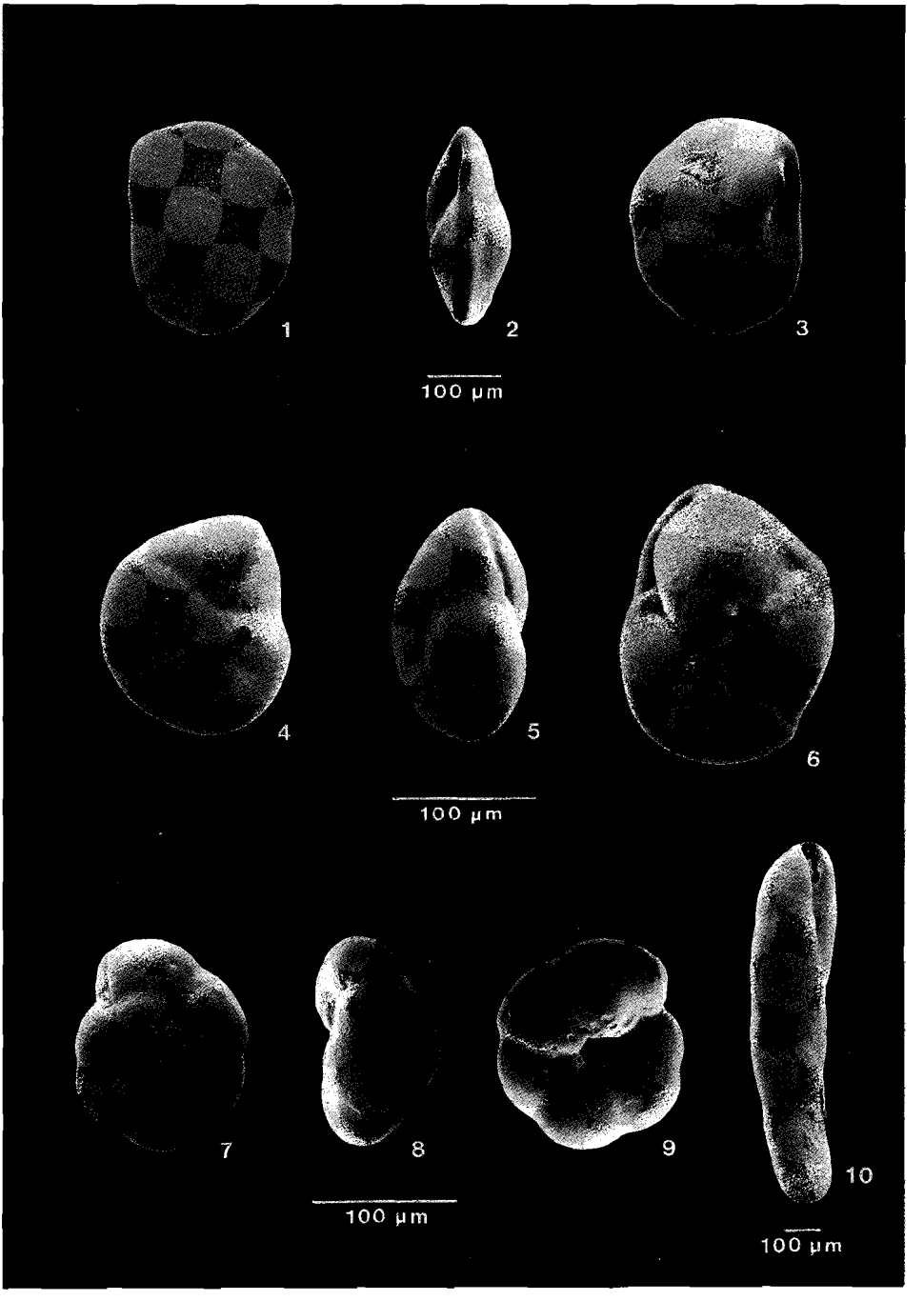

Plate 12

Figs. 1-3 *Gyroidina* cf. *altiformis,* sample VM22-168/top.
Figs. 4-6 *Gyroidina polia,* sample T80-25/top.
Figs. 7-9 *Gyroidina* sp. 1, sample T80-24/top.
Figs. 10-12 *Hoeglundina elegans,* sample VM29-143/4.

All magnifications x100

Plate 12

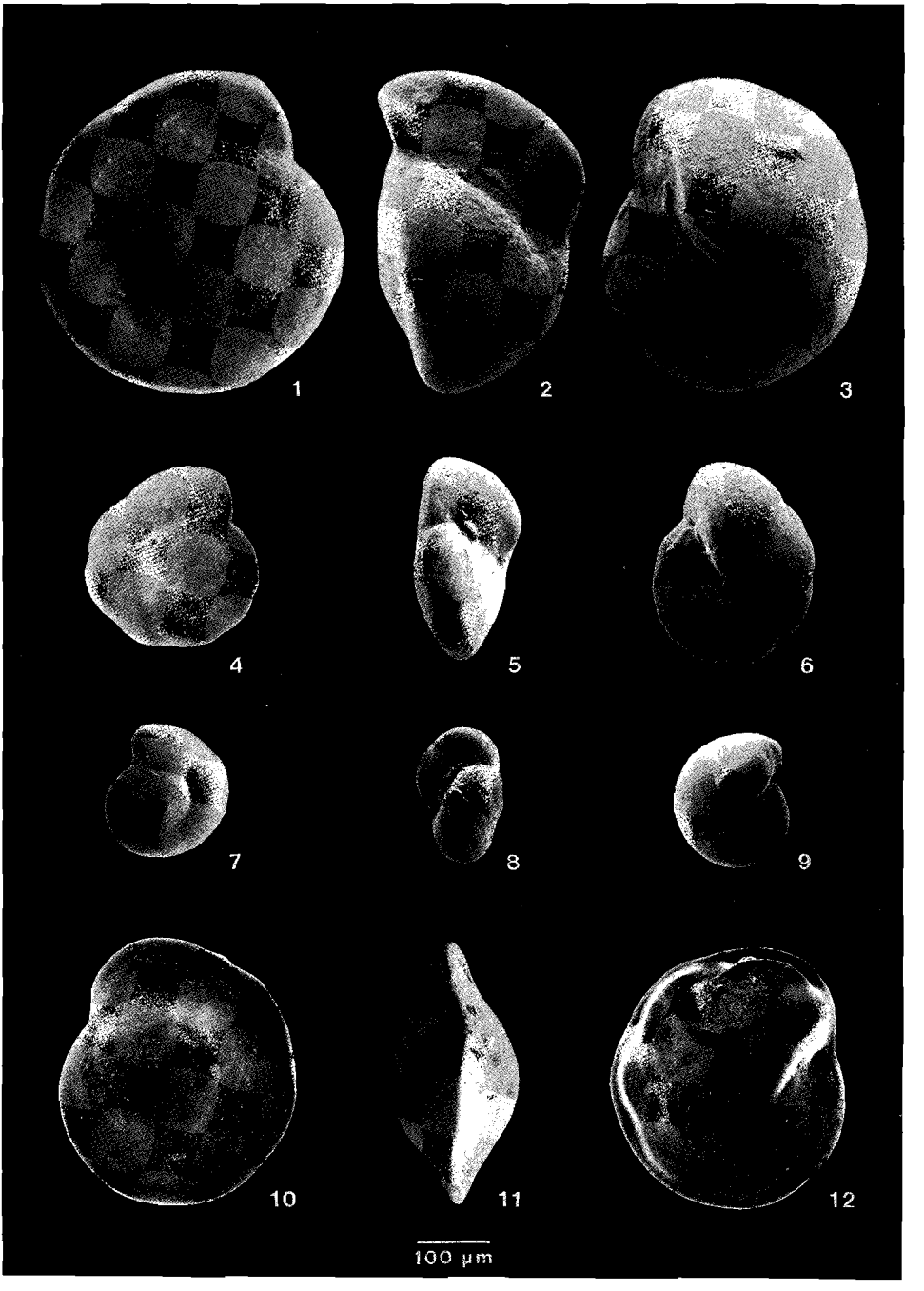

Plate 13

Figs. 1,2 *Melonis barleeanus*, sample KW23/top.
Figs. 3,4 *Melonis formosus*, sample T80-25/top.
Figs. 5,6 *Melonis sphaeroides*, sample VM29-143/6.
Figs. 7,8 *Melonis sphaeroides*, sample T80-28/top.

All magnifications x100

Plate 13

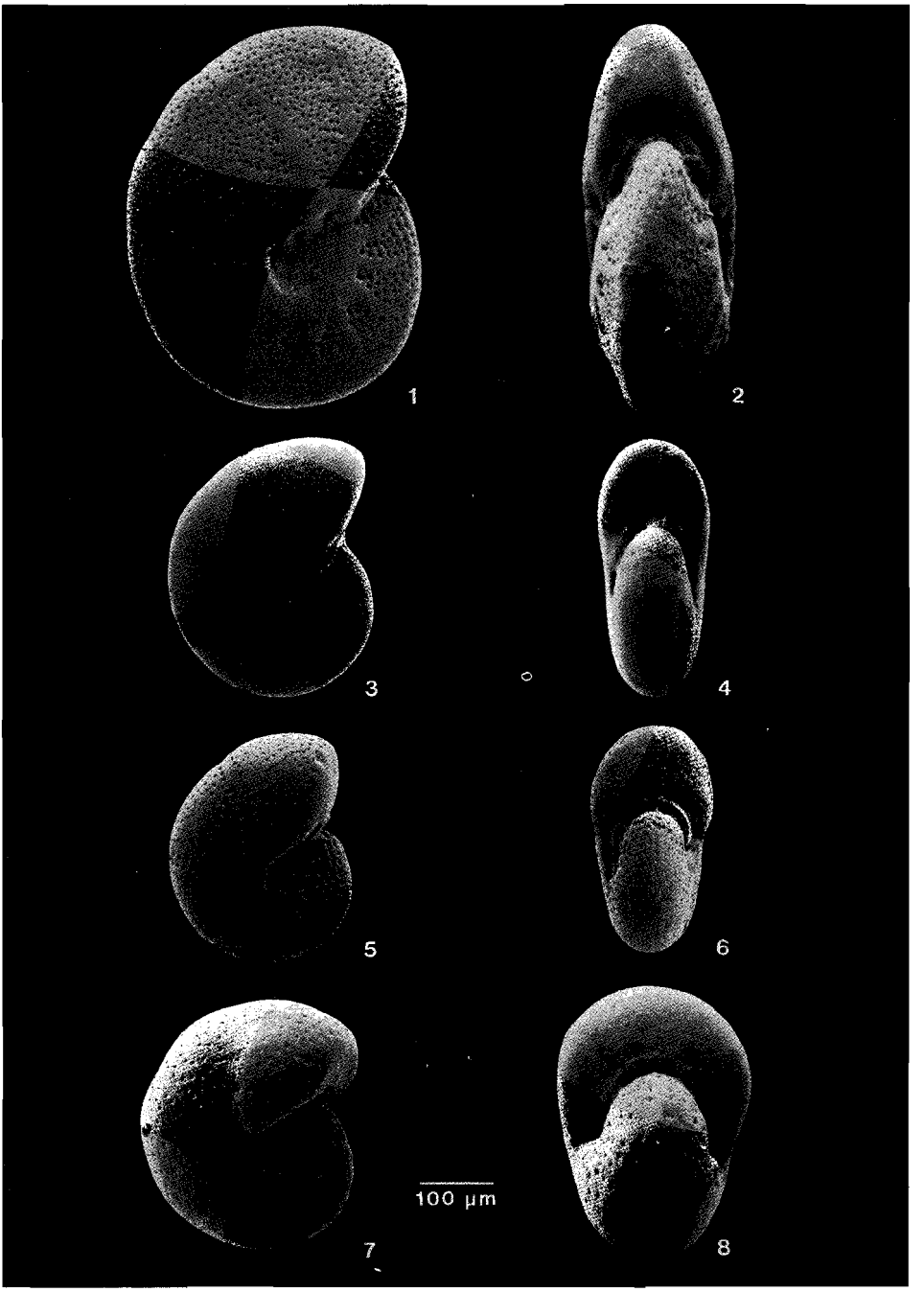

Plate 14

Figs. 1-3 *Nuttallides pusillus turgidus*, sample RC13-220/top.
Figs. 4-6 *Nuttallides pusillus pusillus* 1, sample T80-10/12.
Figs. 7-9 *Nuttallides pusillus pusillus* 1, sample KW25/7.
Figs. 10-12 *Nuttallides pusillus pusillus* 2, sample RC13-208/top.

All magnifications x200

Plate 14

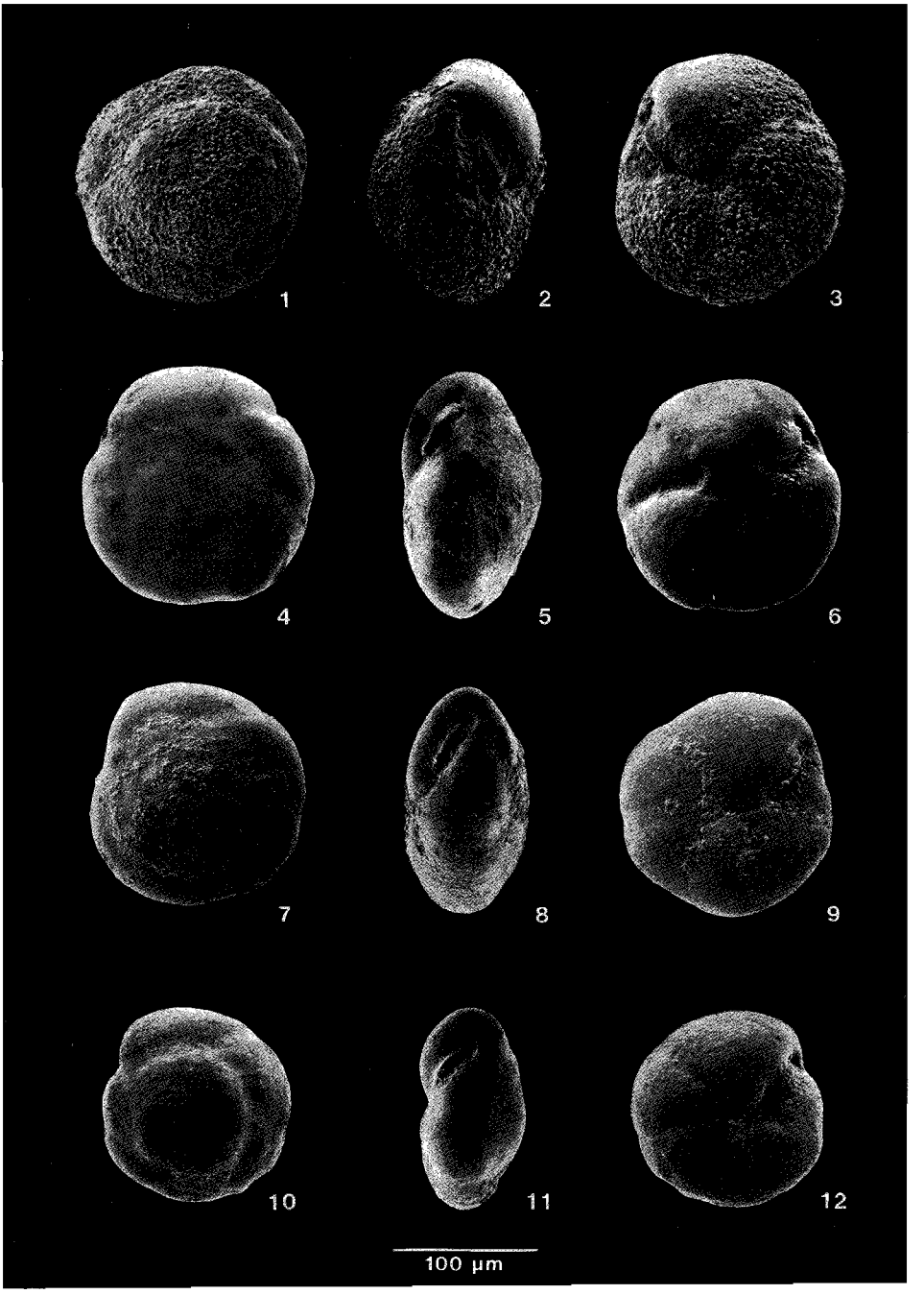

Plate 15

Fig. 1 *Nuttallides umboniferus decoratus*, sample T80-10/9.
Figs. 2,3 *Nuttallides umboniferus decoratus*, sample T80-10/39.
Fig. 4 *Nuttallides umboniferus decoratus*, sample T80-10/8.
Figs. 5-7 *Nuttallides umboniferus convexus*, sample T80-34/top.
Figs. 8-10 *Nuttallides umboniferus convexus*, sample RC13-205/top.
Figs. 11-13 *Nuttallides umboniferus umboniferus*, sample T80-25/top.

Magnifications figs. 1-7 x200
Magnifications figs. 8-13 x100

Plate 15

Plate 16

Figs. 1-3 *Nuttallides umboniferus umboniferus*, sample T80-25/top. Magnification x50.
Fig. 4 *Nuttallides umboniferus umboniferus*, aperture; detail of fig. 12, pl. 15. Magnification x400.
Fig. 5 *Nuttallides umboniferus umboniferus*, aperture; sample T80-24/top. Magnification x450
Fig. 6 *Nuttallides umboniferus umboniferus*, aperture; detail of fig. 2. Magnification x150.
Fig. 7 *Nuttallides umboniferus umboniferus*, sample T80-23/top. Magnification x200.
Figs. 8-10 *Nuttallides rugosus*, sample T80-25/top. Magnification x100.

Plate 16

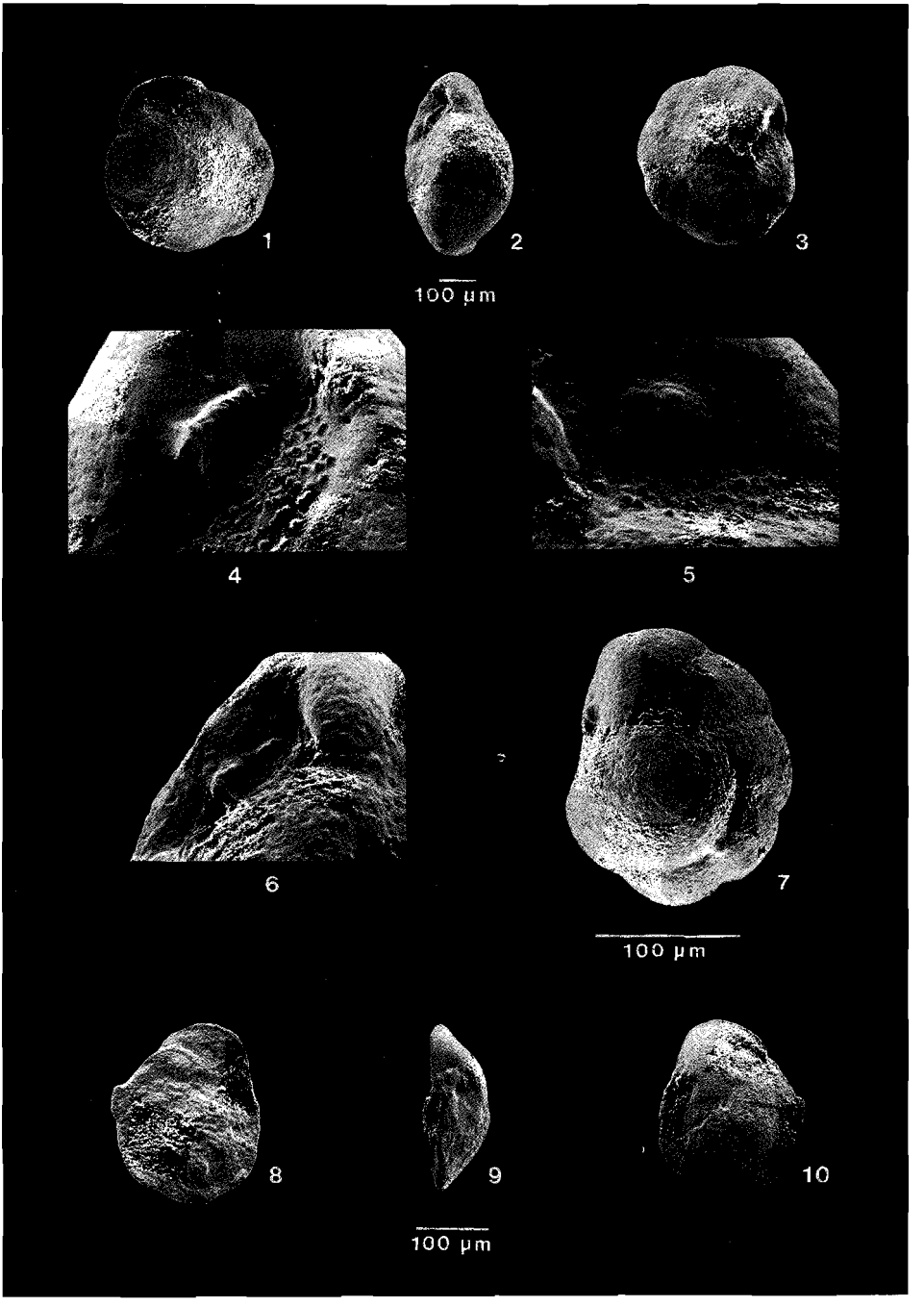

Plate 17

Figs. 1-3 *Oridorsalis umbonatus* 1, type A, sample VM29-136/top. Magnification x100.
Figs. 4-6 *Oridorsalis umbonatus* 2, type A, sample VM19-283/2. Magnification x200.
Figs. 7-9 *Oridorsalis umbonatus* 2, type B, sample KW25/30. Magnification x100.
Figs. 10-12 *Oridorsalis umbonatus* 2, type C, sample KW25/6. Magnification x50.
Fig. 13 *Oridorsalis umbonatus* 2, type C, sample VM19-283/2. Magnification x100.

Plate 17

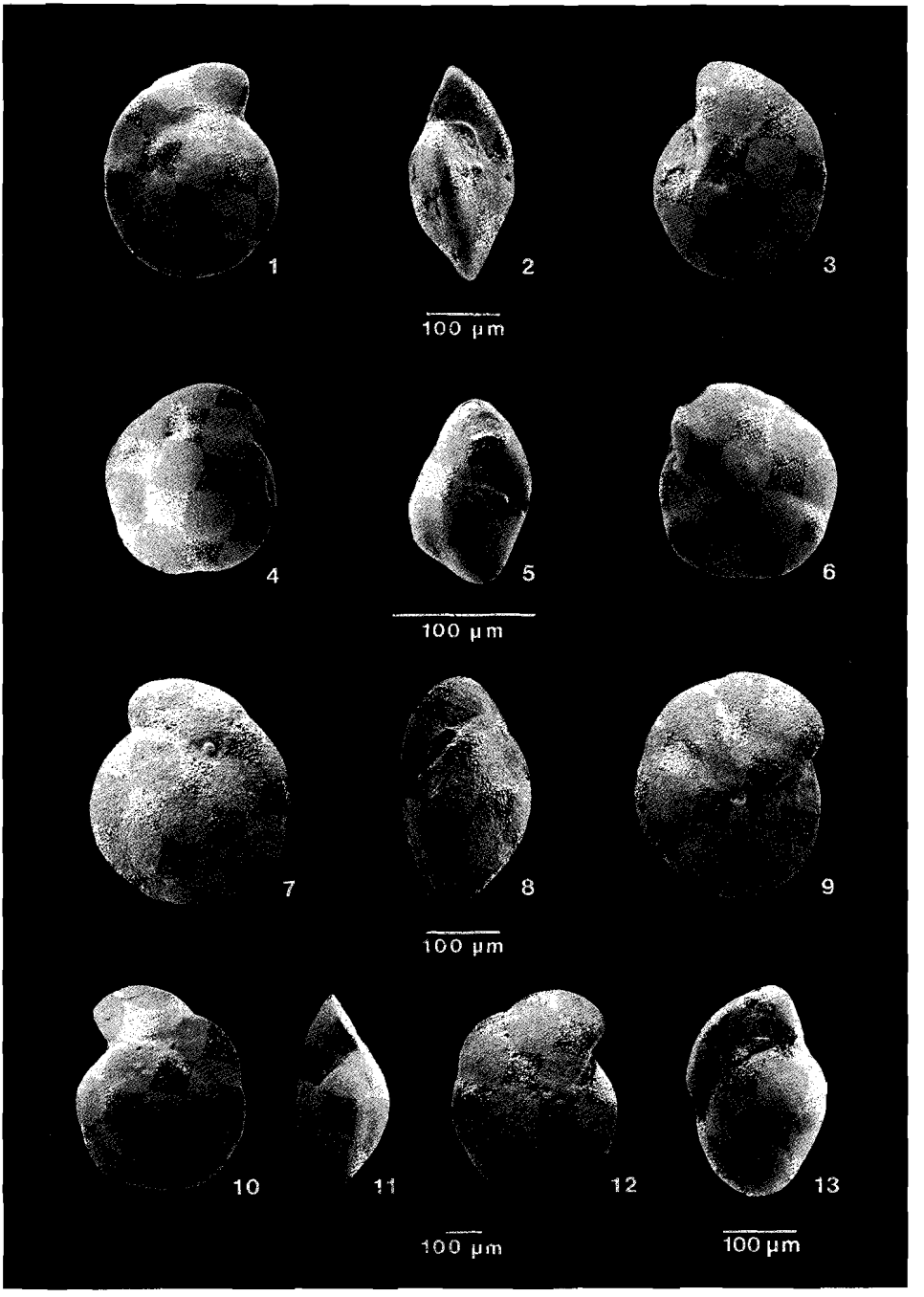

Plate 18

Figs. 1,4 *Pullenia bulloides bulloides*, sample KW26/7.
Figs. 2,5 *Pullenia bulloides osloensis*, sample RC13-208.
Figs. 3,6 *Pullenia bulloides osloensis*, sample T80-27.
Figs. 7,8 *Pullenia* sp. 1, sample T80-27.
Fig. 9 *Pyrgo murrhina*, sample VM29-143/7.
Fig. 10 *Pyrgo murrhina*, sample VM29-143/8.
Fig. 11 *Pyrgo murrhina*, sample VM29-143/7.
Fig. 12 *Pyrgo murrhina*, sample VM29-143/7.

All magnifications x100

Plate 18

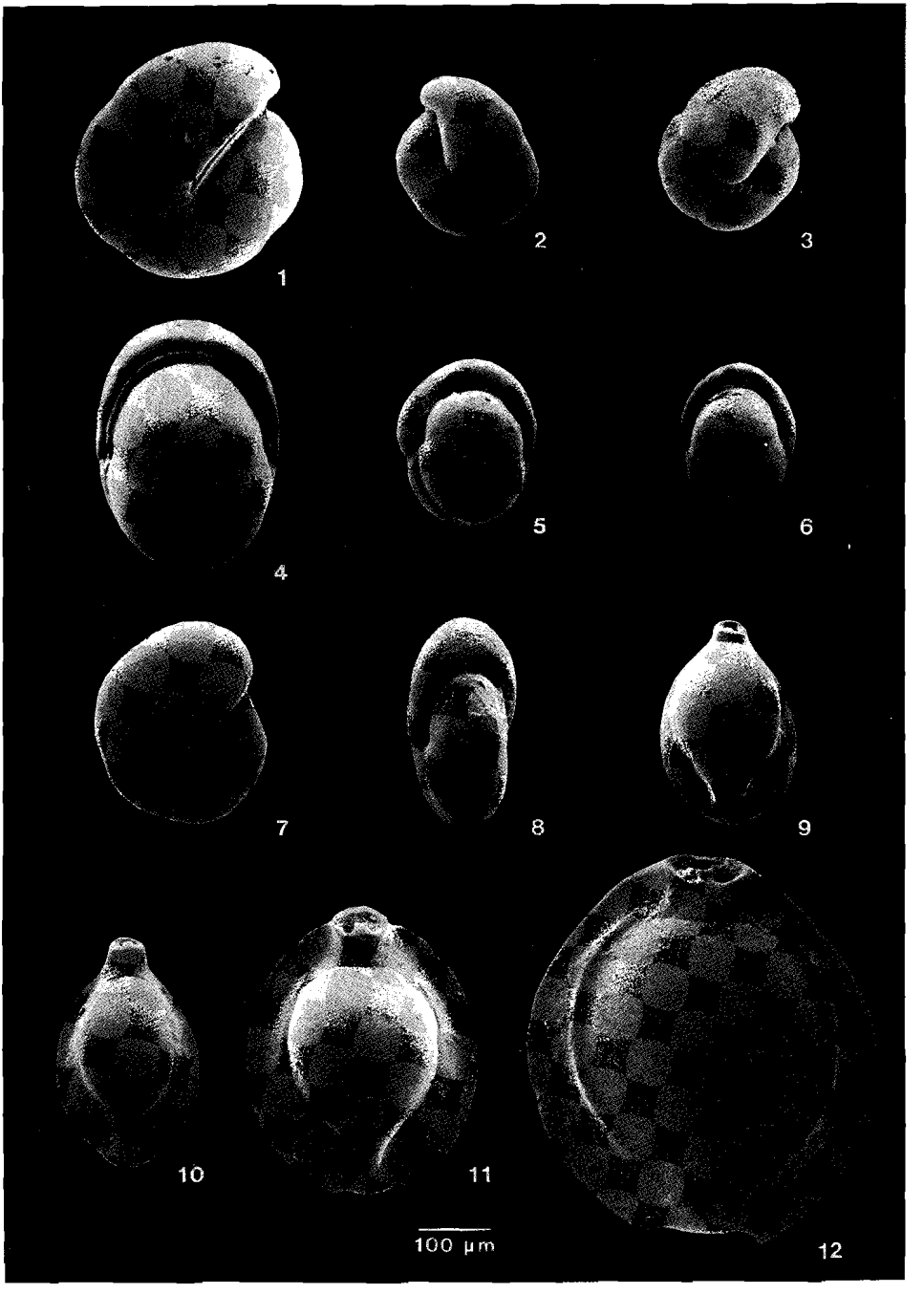

Plate 19

Figs. 1-3 *Osangularia culter*, sample T80-10/top.
Fig. 4 *Uvigerina auberiana*, sample RC13-225/top.
Fig. 5 *Uvigerina peregrina peregrina*, sample RC13-220/top.
Fig. 6 *Uvigerina peregrina peregrina*, sample KW23/top.
Fig. 7 *Uvigerina peregrina dirupta*, sample KW25/8.
Fig. 8 *Uvigerina hispida*, sample VM22-174/top.

All magnifications x50, except figs. 1-3 x100

Plate 19

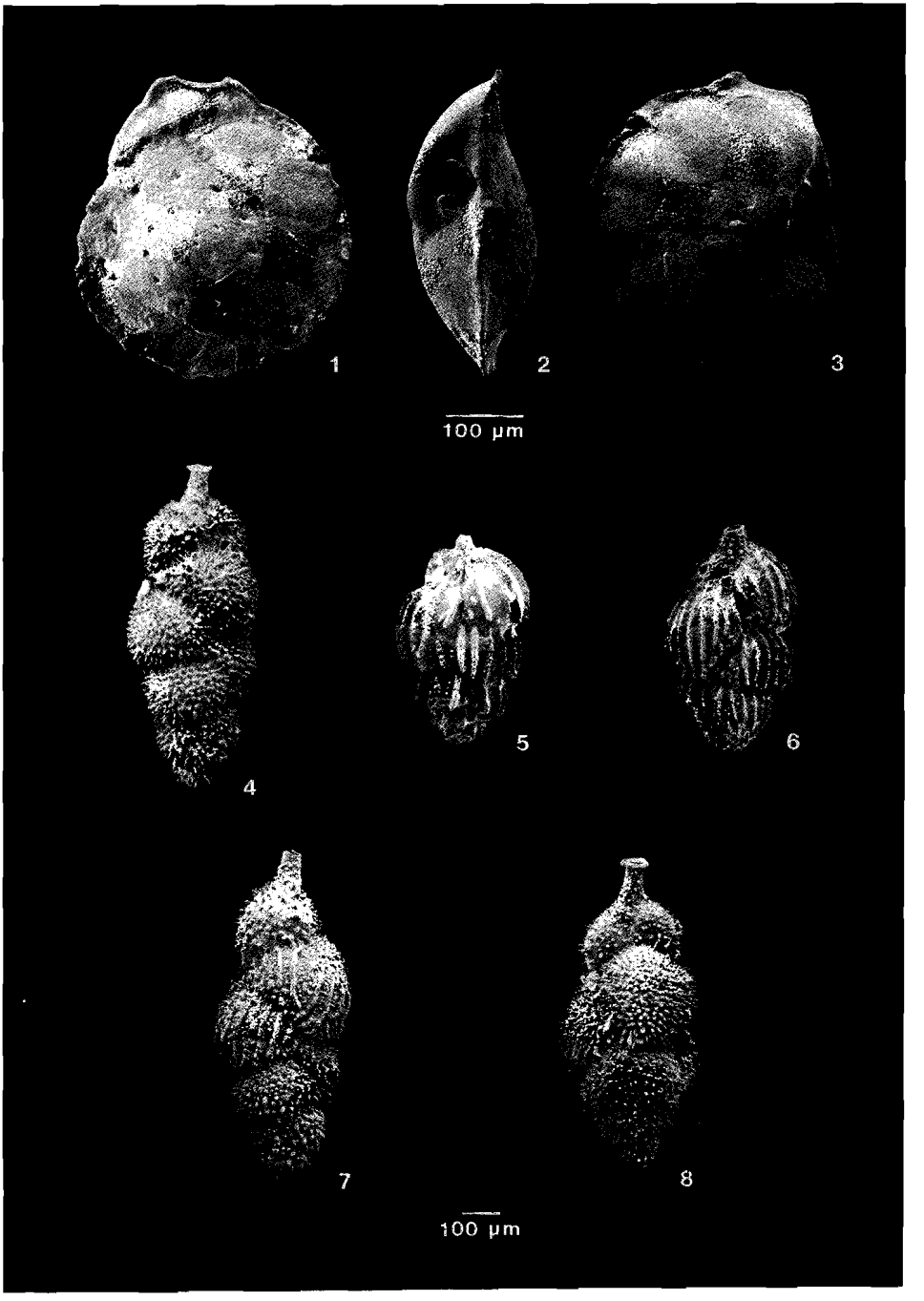

nr	core	type	depth m	latitude	longitude	interval cm below top	P/P+B x100	FN-P	FN-B	FN-b	CaCO3 %
1	T78-23	P	75	5°58.0′ S	11°51.0′ E	0-3	-	-	62	665	-
2	T78-24	P	230	5°54.5′ S	11°37.0′ E	0-3	56.3	52	41	465	-
3	T78-25	P	270	6°03.5′ S	11°28.1′ E	0-3	54.3	460	390	655	-
4	T78-26	P	605	6°05.0′ S	11°16.6′ E	0-3	-	-	41	285	-
5	VM29-140	P	719	3°07.′ S	9°19.′ E	0-2	38.0	4020	6550	13100	26.1
6	VM29-142	P	1017	2°05.′ S	6°23.′ E	2-3	90.8	9970	650	6725	85.8
7	RC13-220	P	1760	12°12.′ S	12°36.′ E	3-4.5	67.8	78	37	160	-
8	T80-10	P	1988	6°13.1′ S	10°34.5′ E	0-4	86.3	57	9	21	-
9	RC13-225	P	2078	17°36.′ S	11°02.′ E	1-3	3.5	10	290	380	-
10	T78-46	P	2100	6°50.1′ S	10°45.3′ E	0-3	-	-	11	145	-
11	VM29-136	P	2270	19°02.′ S	10°20.′ E	0-2	94.6	9360	840	2190	64.3
12	KW23	P	2330	3°46.5′ S	9°17.3′ E	2.5-4.5	87.8	270	32	190	6.9
13	VM27-228	T	2392	10°04.′ S	11°27.′ E	0-2	87.6	390	48	190	14.2
14	VM22-174	P	2630	10°04.′ S	12°49.′ W	0-2	99.5	11150	97	630	90.4
15	VM29-135	P	2675	19°42.′ S	8°53.′ E	0-2	99.2	36500	270	2200	-
16	VM29-144	P	2685	0°12.′ S	6°03.′ E	0-2	98.4	6460	135	1300	63.7
17	VM29-143	P	2756	0°45.′ S	7°15.′ E	0-2	88.1	1050	145	610	43.8
18	RC13-219	P	2770	11°15.′ S	11°53.′ E	2.5-4	77.8	460	125	810	-
19	KW26	P	3038	0°31.0′ S	6°50.0′ E	0-2	93.9	2080	120	680	-
20	RC13-204	P	3096	1°22.′ S	6°53.′ E	0-2	87.9	1450	200	890	-
21	VM22-177	P	3290	7°45.′ S	14°36.3′ W	0-2	99.5	18300	110	1350	68.5
22	VM19-283	P	3442	1°17.′ S	5°32.′ E	2-3	97.5	4650	89	1300	70.2
23	VM29-137	P	3486	6°31.′ S	10°04.′ E	0-3	94.1	210	8	27	3.5
24	RC17-034	T	3537	21°26.′ S	6°18.′ E	0-2	99.5	20100	110	610	-
25	VM19-260	P	3585	19°20.′ S	9°37.′ E	0-2	87.7	685	86	540	55.0
26	T80-8	T	3678	6°48.3′ S	9°52.8′ E	0-2	98.5	550	7	11	-
27	RC13-205	P	3731	2°17.3′ S	5°11.′ E	0-2	95.4	8600	280	2050	-
28	RC17-033	T	3857	5°18.′ S	0°13.′ W	0-2	97.7	15300	130	940	-
29	VM27-229	P	3908	7°27.′ S	9°36.′ E	0-2	89.8	260	14	36	-
30	T80-7	P	3946	7°00.0′ S	9°01.9′ E	0-3	82.1	67	15	95	-
31	RC13-212	P	3952	9°30.′ S	7°54.′ W	0-2	99.6	13500	66	320	-
32	RC13-222	P	3988	13°34.′ S	9°55.′ E	2-3.5	68.5	350	180	1250	22.8
33	T78-44	P	3990	7°24.2′ S	9°25.8′ E	0-3	94.6	1200	63	180	-
34	VM29-141	P	3993	2°38.′ S	6°29.′ E	0-2	75.8	245	143	960	47.9
35	VM12-075	P	4021	6°19.′ S	8°19.′ E	0-2	92.2	115	10	44	12.5
36	T78-45	P	4070	7°47.8′ S	10°07.0′ E	0-3	-	-	16	55	-
37	T78-33	P	4120	5°11.0′ S	7°58.0′ E	0-3	92.1	220	19	71	-
38	T80-26	T	4115	36°39.′ S	4°11.′ W	0-5	99.1	10600	125	490	80.5
39	RC13-218	P	4145	10°38.′ S	9°33.′ E	0-2	8.3	14	160	870	28.0
40	T80-34	T	4195	0°52.′ N	14°07.′ W	0-3.5	99.2	15100	150	1400	81.2
41	VM12-078	P	4232	4°23.′ S	0°11.′ W	0-1	98.7	7500	205	2180	86.4
42	T80-25	T	4235	33°29.′ S	5°33.5′ W	0-5	99.3	20600	130	430	72.5
43	VM27-231	T	4252	3°28.′ S	7°27.′ E	0-3	91.2	390	34	170	19.1
44	T78-34	P	4270	6°49.5′ S	7°47.7′ E	0-3	15.4	4	24	50	-
45	T80-28	T	4295	32°38.′ S	8°27.5′ W	0-7.5	99.2	14100	93	380	87.6
46	RC13-209	P	4296	8°12.′ S	8°13′ W	0-1.5	99.7	18200	59	300	-
47	T80-3	T	4310	3°14.5′ S	2°23.5′ E	2-5	96.8	5350	210	1170	72.7
48	T80-27	T	4325	35°51.′ S	6°44.′ W	0-5	98.0	7200	195	850	73.4

Table I. Location and sample-interval of cores used for the analyses of foraminiferal distribution on the sea-floor. Included type of core (P refers to piston-core, T to trigger-core), calcium carbonate content (weight percentage), P/P+B-ratios, planktonic foraminiferal number (FN-P), benthic foraminiferal number in the 150-595 μm fraction (FN-B) and benthic foraminiferal number in the 63-150 μm fraction (FN-b).

Bull. 34. B. STAM – Quantitative analysis of Middle and Late Jurassic foraminifera from Portugal and its implications for the Grand Banks of Newfoundland. 168 p., 14 pl., 50 figs. (1986) *f* 54,–

Bull. 35. G. J. VAN DER ZWAAN, F. J. JORISSEN, P. J. J. M. VERHALLEN and C. H. VON DANIELS (ed.) – Atlantic-European Oligocene to Recent *Uvigerina*. 237 p., 69 pl., 25 figs. (1986) *f* 66,–

Bull. 36. B. W. M. DRIEVER – Calcareous nannofossil biostratigraphy and paleoenvironmental interpretation of the Mediterranean Pliocene. 245 p., 13 pl., 56 figs. (1988) *f* 63,–

Bull. 37. F. J. JORSISSEN – Benthic foraminifera from the Adriatic Sea; Principles of phenotypic variation. 176 p., 25 pl., 46 figs. (1988) *f* 57,–

Bull. 38. R. J. W. VAN LEEUWEN – Sea-floor distribution and Late Quaternary faunal patterns of planktonic and benthic foraminifera in the Angola Basin. 287 p., 19 pl., 91 figs. (1989) *f* 69,–

Spec. Publ. 1. A. A. BOSMA – Rodent biostratigraphy of the Eocene-Oligocene transitional strata of the Isle of Wight. 128 p., 7 pl., 38 figs. (1974) *f* 43,–

Spec. Publ. 2. A. VAN DE WEERD – Rodent faunas of the Mio-Pliocene continental sediments of the Teruel – Alfambra region, Spain. 217 p., 16 pl., 30 figs. (1976) *f* 63,–

Spec. Publ. 3. R. DAAMS – The dental pattern of the dormice *Dryomys, Myomimus, Microdyromys* and *Peridyromys*. 115 p., 5 pl., 42 figs. (1981) *f* 41,–

Spec. Publ. 4. C. G. RÜMKE – A review of fossil and recent Desmaninae (Talpidae, Insectivora). 241 p., 4 pl., 88 figs. (1985) *f* 71,–

Spec. Publ. 5. E. ÜNAY-BAYRAKTAR–Rodents from the Middle Oligocene of Turkish Thrace. 120 p., 11 pl., 11 figs. (1989) *f* 39,–

nr	core	type	depth m	latitude	longitude	interval cm below top	P/P+B x100	FN-P	FN-B	FN-b	CaCO3 %
49	T78-49	P	4340	3°57.8' S	8°03.7' E	0-3	95.8	1330	47	115	-
50	VM19-282	P	4356	2°45.' S	4°35.' E	0-2	92.2	1930	150	1140	63.2
51	CHN99-32	P	4404	8°43.0' S	4°58.7' W	4-6	94.3	2250	125	530	88.7
52	CHN99-33	P	4414	8°41.8' S	3°32.5' W	7-9	97.9	11600	165	615	97.0
53	T80-33	T	4360	0°36.' S	13°08.' W	0-3.5	96.9	2550	185	270	78.6
54	T80-6	T	4457	8°00.2' S	7°59.3' E	0-2	56.9	160	125	730	-
55	T78-42	P	4470	8°36.4' S	8°47.8' E	0-3	74.0	490	170	1070	-
56	VM27-239	T	4464	7°50.' S	1°31.' W	0-1	98.8	16400	115	840	-
57	T80-35	T	4505	0°28.' N	14°20.' W	3-6	94.4	2170	79	450	76.5
58	T80-24	T	4525	30°04.' S	3°02.' W	0-5	99.5	12800	92	530	89.3
59	RC13-208	P	4625	6°56.' S	5°10.' W	0.5-2	99.8	16100	70	415	-
60	VM22-168	P	4625	17°28.' S	5°11.' W	0-2	99.3	9800	75	525	82.2
61	CHN99-31	P	4660	8°42.8' S	6°25.5' W	3-5	99.5	1860	13	54	34.1
62	RC13-217	P	4759	10°24.' S	8°28.' E	0-2	13.3	20	135	625	24.5
63	T78-41	P	4810	8°45.1' S	7°08.1' E	0-3	47.9	190	270	950	-
64	VM27-238	P	4813	6°27.9 S	3°43.2' W	0-1	98.0	8550	92	660	89.8
65	CHN99-34	P	4896	8°44.2' S	1°52.5' W	2-4	99.2	14600	98	340	98.4
66	CHN99-36	P	4914	8°44.5' S	0°11.6' W	2-3.5	39.0	150	225	1620	17.5
67	T78-36	P	4980	7°35.2' S	6°29.5' E	0-3	33.6	78	135	400	-
68	RC13-207	P	4971	5°02.' S	1°23.' E	1.5-2.5	90.8	2000	195	1120	-
69	T80-29	T	5015	24°17.5' S	6°57.' W	0-5	96.8	3140	72	250	71.8
70	T78-39	P	5070	8°49.7' S	6°01.9' E	0-3	65.4	-	-	-	-
71	T80-30	T	5180	18°40.' S	5°10.' W	0-5	90.3	1200	115	490	80.8
72	RC13-206	P	5194	4°28.' S	2°54.' E	1.5-2	87.3	1100	155	730	-
73	VM22-165	P	5198	23°08.' S	0°31.' E	0-2	90.5	1450	155	700	66.0
74	RC13-233	P	5205	23°32.' S	1°01.' W	0-1	91.4	1540	115	440	67.8
75	VM12-077	P	5212	4°48.' S	2°45.' E	0-2	74.8	880	150	730	-
76	VM12-077	T	5212	4°48.' S	2°45.' E	0-2	74.0	325	110	700	12.5
77	VM19-276	P	5282	8°58.' S	2°52.' E	0-5	69.2	975	370	1000	60.9
78	VM27-220	P	5360	24°28.' S	0°27.' W	0-3	91.0	1260	100	690	62.1
79	T80-21	T	5400	16°45.' S	6°28.' E	0-5	46.7	56	64	220	40.3
80	T80-23	T	5410	23°47.' S	1°21.' E	0-5	95.9	1510	83	480	63.5
81	VM27-225	P	5495	16°32.' S	3°54.' E	0-2	80.4	720	155	1020	69.2
82	VM27-224	P	5513	18°31.' S	1°37.' E	0-2	77.3	380	115	440	39.4
83	VM27-224	T	5513	18°31.' S	1°37.' E	0-2	91.6	2470	135	470	56.6
84	RC13-214	P	5608	11°01.' S	0°30.' E	3-4.5	54.4	60	49	215	59.0

Table II. Location and sample-interval of cores excluded from the analyses of foraminiferal distribution on the sea-floor. P refers to piston-core and T to trigger-core.

Bull. 15. Z. REISS, S. LEUTENEGGER, L. HOTTINGER, W. J. J. FERMONT, J. E. MEULENKAMP, E. THOMAS, H. J. HANSEN, B. BUCHARDT, A. R. LARSEN and C. W. DROOGER – Depth-relations of Recent larger foraminifera in the Gulf of Aqaba-Elat. 244 p., 3 pl., 117 figs. (1977) *f* 53,–

Bull. 16. J. W. VERBEEK – Calcareous nannoplankton biostratigraphy of Middle and Upper Cretaceous deposits in Tunisia, Southern Spain and France. 157 p., 12 pl., 22 figs. (1977) *f* 51,–

Bull. 17. W. J. ZACHARIASSE, W. R. RIEDEL, A. SANFILIPPO, R. R. SCHMIDT, M. J. BROLSMA, H. J. SCHRADER, R. GERSONDE, M. M. DROOGER and J. A. BROEKMAN – Micropaleontological counting methods and techniques – an exercise on an eight metres section of the Lower Pliocene of Capo Rossello, Sicily. 265 p., 23 pl., 95 figs. (1978) *f* 59,–

Bull. 18. M. J. BROLSMA – Quantitative foraminiferal analysis and environmental interpretation of the Pliocene and topmost Miocene on the south coast of Sicily. 159 p., 8 pl., 50 figs. (1978) *f* 49,–

Bull. 19. E. J. VAN VESSEM – Study of Lepidocyclinidae from South-East Asia, particularly from Java and Borneo. 163 p., 10 pl., 84 figs. (1978) *f* 53,–

Bull. 20. J. HAGEMAN – Benthic foraminiferal assemblages from the Plio-Pleistocene open bay to lagoonal sediments of the Western Peloponnesus (Greece). 171 p., 10 pl., 28 figs. (1979) *f* 54,–

Bull. 21. C. W. DROOGER, J. E. MEULENKAMP, C. G. LANGEREIS, A. A. H. WONDERS, G. J. VAN DER ZWAAN, M. M. DROOGER, D. S. N. RAJU, P. H. DOEVEN, W. J. ZACHARIASSE, R. R. SCHMIDT and J. D. A. ZIJDERVELD – Problems of detailed biostratigraphic and magnetostratigraphic correlations in the Potamidha and Apostoli sections of the Cretan Miocene. 222 p., 7 pl., 74 figs. (1979) *f* 57,–

Bull. 22. A. J. T. ROMEIN – Evolutionary lineages in Early Paleogene calcareous nannoplankton. 231 p., 10 pl., 50 figs. (1979) *f* 64,–

Bull. 23. E. THOMAS – Details of *Uvigerina* development in the Cretan Mio-Pliocene. 168 p., 5 pl., 65 figs. (1980) *f* 50,–

Bull. 24. A. A. H. WONDERS – Planktonic foraminifera of the Middle and Late Cretaceous of the Western Mediterranean area. 158 p., 10 pl., 44 figs. (1980) *f* 52,–

Bull. 25. G. J. VAN DER ZWAAN – Paleoecology of Late Miocene Mediterranean foraminifera. 202 p., 15 pl., 65 figs. (1982) *f* 57,–

Bull. 26, M. M. DROOGER – Quantitative range chart analyses. 227 p., 3 pl., 3 figs. (1982) *f* 59,–

Bull. 27. W. J. J. FERMONT – Discocyclinidae from Ein Avedat (Israel). 173 p., 11 pl., 58 figs. (1982) *f* 51,–

Bull. 28. P. SPAAK – Accuracy in correlation and ecological aspects of the planktonic foraminiferal zonation of the Mediterranean Pliocene. 160 p., 10 pl., 51 figs. (1983) *f* 52,–

Bull. 29. J. R. SETIAWAN – Foraminifera and microfacies of the type Priabonian. 173 p., 18 pl., 35 figs. (1983) *f* 55,–

Bull. 30. J. E. MEULENKAMP (ed.) – Reconstruction of marine paleoenvironments. 298 p., 5 pl., 112 figs. (1983) *f* 69,–

Bull. 31. H. A. JONKERS – Pliocene benthonic foraminifera from homogeneous and laminated marls on Crete. 179 p., 12 pl., 46 figs. (1984) *f* 56,–

Bull. 32. S. THEODORIDIS – Calcareous nannofossil biozonation of the Miocene and revision of the Helicoliths and Discoasters. 272 p., 37 pl., 67 figs. (1984) *f* 68,–

Bull. 33. C. W. DROOGER and J. C. DE KLERK – The punctuation in the evolution of *Orbitoides* in the Campanian of South-West France. 144 p., 5 pl., 63 figs. (1985) *f* 48,–